ROLES OF THE NUCLEOSOME ACIDIC PATCH IN REGULATING HISTONE MODIFICATIONS AND TRANSCRIPTION

by

Christine Elizabeth Cucinotta

B.S., The University of Texas at Austin, 2011

Submitted to the Graduate Faculty of the

Kenneth P. Dietrich School of Arts & Sciences in partial fulfillment

of the requirements for the degree of

Doctor of Philosophy

University of Pittsburgh

2017

UNIVERSITY OF PITTSBURGH

KENNETH P. DIETRICH SCHOOL OF ARTS & SCIENCES

This dissertation was presented

by

Christine Elizabeth Cucinotta

It was defended on

July 12, 2017

and approved by

Mark Rebeiz, PhD, Associate Professor, Dept. of Biological Sciences

Anthony Schwacha, PhD, Associate Professor, Dept. of Biological Sciences

Andrew VanDemark, PhD, Associate Professor, Dept. of Biological Sciences

C. Joel McManus, PhD Assistant Professor, Dept. of Biological Sciences, Carnegie Mellon University

Thesis Advisor: Karen Arndt, PhD, Professor, Dept. of Biological Sciences

ROLES OF THE NUCLEOSOME ACIDIC PATCH IN REGULATING HISTONE MODIFICATIONS AND TRANSCRIPTION

Christine Elizabeth Cucinotta, PhD

University of Pittsburgh, 2017

Proper transcription elongation is critical for all eukaryotes. One regulatory mechanism cells employ is modification of nucleosomes during transcription. H2B K123 monoubiquitylation (H2Bub) is a key histone posttranslational modification that correlates with transcription elongation, promotes downstream histone marks, and regulates chromatin architecture. The E2 and E3 enzymes, Rad6 and Bre1, catalyze H2Bub in collaboration with the Paf1 complex member Rtf1. Additionally, H2Bub and the histone chaperone complex FACT appear to be interdependent. While it is known that these factors promote and catalyze the modification, how these proteins interface with the nucleosome to promote transcription is still unclear. However, reports show that the nucleosome acidic patch is an important regulatory region that binds many different factors. This dissertation describes roles for the nucleosome acidic patch regulates the H2Bub modification cascade and transcription elongation efficiency in *Saccharomyces cerevisiae*. As the acidic patch is a hub for chromatin-binding proteins, I hypothesize that transcription elongation factors interface with the acidic patch to properly regulate gene expression. To determine whether the acidic patch may function directly in promoting H2Bub, I measured H2Bub levels in a minimal *in vitro* assay, and found that the acidic patch is required for proper H2Bub. To identify factors that bind to the nucleosome acidic patch *in vivo*, I implemented a proteomics approach that utilized site-specific crosslinking with which I uncovered an interaction between transcription elongation factors and the nucleosome acidic patch. These data, and that of others, show that the acidic patch can dynamically interact with chromatin-binding proteins to control gene expression.

TABLE OF CONTENTS

LIST OF TABLES

LIST OF FIGURES

PREFACE

Words cannot describe how grateful I am to have had Karen Arndt as my mentor and scientific role model. Karen has not only been a phenomenal scientist to look up to, but she has been extraordinarily supportive throughout my entire graduate career. She taught me how to think like a scientist – to always seek the truth, no matter what the answer is. She taught me persistence and strength, important abilities to navigate academia. Discussing ideas and experimental plans with Karen is always fun and exciting. In times where I was frustrated with my data, I could always go to Karen's office to discuss my trajectory, and I'd leave feeling reinvigorated to attack problems at the bench. A strong passion for science has been instilled in me, thanks to Karen.

Peggy Shirra is another key figure in my scientific development. Peggy has been long-revered in our department as the "go-to" person with all the answers. If Peggy doesn't know the answer, she will help you find it. Whenever I was about to walk off a cliff, Peggy would be the one to say something along the lines of "Okay, let's step back and figure out how to fix the problem." Peggy's pragmatism has been a lifesaver numerous times during my graduate career. Peggy has also been supportive throughout the years in helping me manage both life and science.

I thank members of the Arndt lab, past and present for being wonderful mentors and friends. I especially thank Kristin Klucevsek, Ally Young, Brett Tomson, Manasi Mayekar, Beth Raupach, Branden Van Oss, Elizabeth Hildreth, Mitch Ellison, Ellie Kerr, Rachel Schusteff, Alex Lederer, Rachel Kocik, and my fantastic undergraduate mentees Logan Russell and Chelsea Guan. I'd like to give extra thanks to Brett Tomson who continued to check up on me and mentor me after she left the lab – thank you! I would also like to thank Joe Martens for being my first mentor

in Pittsburgh and Sarah Hainer, who was incredibly helpful during my rotation in the Martens lab and toward the end of my graduate career as I planned my next steps.

I want to thank my thesis committee for helping to shape me into the scientist that I am today. Andy VanDemark was very generous with his time and in allowing me to purify some proteins in his lab. Andy's general science and career advice has also been invaluable to me. I thank members of Andy's lab who have helped me with purifying proteins, learning Pymol, and having fun scientific discussions: Jenna Zalewski, Joel Rosenbaum, and Adam Wier.

Mark Rebeiz has been supportive from the very beginning when I rotated in his lab. I always appreciate his big picture questions and insights. Mark has been very kind to make time to give valuable career advice as well. I appreciate Tony Schwacha's expertise in both yeast genetics and biochemistry. I was fortunate to also have Joel McManus as my outside committee member who provided fascinating ideas and questions. I thank Andrea Berman and Miler Lee for being generous with their time in giving insightful career advice. I want to thank members of the Berman lab: Roni Lahr, Hiba Al-Ashtal, and Daniel Totten for their friendship and scientific discussions.

I wouldn't have survived graduate school without my friends Swarna Mohan, Adam Wier and Greg Wier, Bill Glassford, Beth Raupach, Branden and Dana Van Oss. I especially thank my classmates and close friends Elise English and Lynley Doonan for always being there for me and helping me survive graduate school, particularly through ridiculous bouts of laughter. I thank my brother, Max Cucinotta. I also thank my other half, Ryan Johnson, for always supporting my career endeavors and for keeping me alive for the past six years.

I dedicate this dissertation to the memory of my grandparents Santo Dominic Cucinotta (1919 – 2014) and Suzanne Cucinotta (1934 – 2017).

1.0 INTRODUCTION

The term “chromatin” was first coined by German biologist Walther Flemming in the 1880s. Flemming was studying cell division; and when staining cells, he observed a structure that was amenable to staining and thus darker in color – hence the term chromatin, which was borrowed from the Greek *khrôma*, or “color” (OLINS AND OLINS 2003). The chromatin field has come a long way since the late 19th century. 1974 brought us the discovery of the nucleosome, the lowest order repeating unit of chromatin (KORNBERG 1974; OLINS AND OLINS 1974). The high-resolution X-ray crystal structure of the nucleosome was solved twenty years ago at the time of writing this dissertation (LUGER *et al.* 1997). Since then, the field has exploded over the years and scientists can now map genome-wide locations of proteins on DNA at the single nucleotide level (RHEE AND PUGH 2011). Structures of proteins in complex with the nucleosome are now being solved relatively frequently (MCGINTY AND TAN 2015). We are aware of specific mutations within the nucleosome protein coding sequences that can cause devastating cancers, which will help in developing treatments (YUEN AND KNOEPFLER 2013). And we are gaining insights into how viruses can directly high-jack human chromatin for self-propagation, as several of the solved structures of proteins bound to the nucleosome are viral proteins (BARBERA *et al.* 2006) (FANG *et al.* 2016) (LESBATS *et al.* 2017).

It was previously thought that the proteins that package DNA were simply there to serve as barriers to DNA-templated processes and to compact DNA. We know now that these proteins are not inert – they are instead dynamic structures that are a key force in regulating all DNA-templated processes. Indeed it was recently proposed that chromatin can even enhance

transcription (NAGAI *et al.* 2017). We can see that the nucleosome plays major roles in modifying chromatin architecture and activating and repressing transcription. The information in this thesis demonstrates just how important the nucleosome itself is in promoting and repressing chromatin transactions.

1.1 DNA IS PACKAGED INTO CHROMATIN

1.1.1 The structure of the nucleosome

All eukaryotic genomes are packaged into chromatin. The basic unit of chromatin is the nucleosome, which is repeated throughout the genome, and contains ~145-147 base pairs of DNA spooled around an octamer of histone proteins (KORNBERG 1974; LUGER *et al.* 1997). Histones are highly conserved among eukaryotes and are small, basic DNA binding proteins that form the nucleosome. Generally, within each nucleosome there are two copies of each of the four core histones: H2A, H2B, H3, and H4. The two copies of H2A and H2B bind to form dimers, and the two copies of H3 and H4 form a tetramer (Fig. 1B). However, it was recently revealed that a large portion of the yeast genome has variability in histone occupancy in one half of the nucleosomes (RHEE *et al.* 2014). Histone chaperones help to properly assemble the histones to form the complete nucleosome, which is held together via protein-protein interactions, electrostatic interactions, and hydrogen bonds with the DNA (Fig. 1C) (LUGER *et al.* 1997). The secondary structure of histones can be described by a globular region and two unstructured tails on each end of the protein. The structured region is called the "histone fold," which is defined by three α helices connected by two loops (Fig. 1) (LUGER *et al.* 1997; MCGINTY AND TAN 2015). The unstructured tail regions are rich

in lysines and arginines, making them amenable to a plethora of posttranslational modifications, and are important for interactions with DNA, proteins, and neighboring nucleosomes (DU PREEZ AND PATTERTON 2013). All four histones have unstructured N-terminal tail regions, although H2A also has a long C-terminal tail. The H2A C-terminal tail is a part of the docking domain, which is important for stabilizing nucleosomes and binding to the chromatin remodeling enzyme RSC and the linker histone H1 (VOGLER *et al.* 2010; SHUKLA *et al.* 2011). The histone chaperone complex FACT, which is responsible for disassembling and reassembling nucleosomes in the wake of transcribing Pol II, has also shown to interact with the docking domain (VANDEMARK *et al.* 2008). Thus, the docking domain is a critical region for maintaining chromatin integrity during DNA-templated processes.

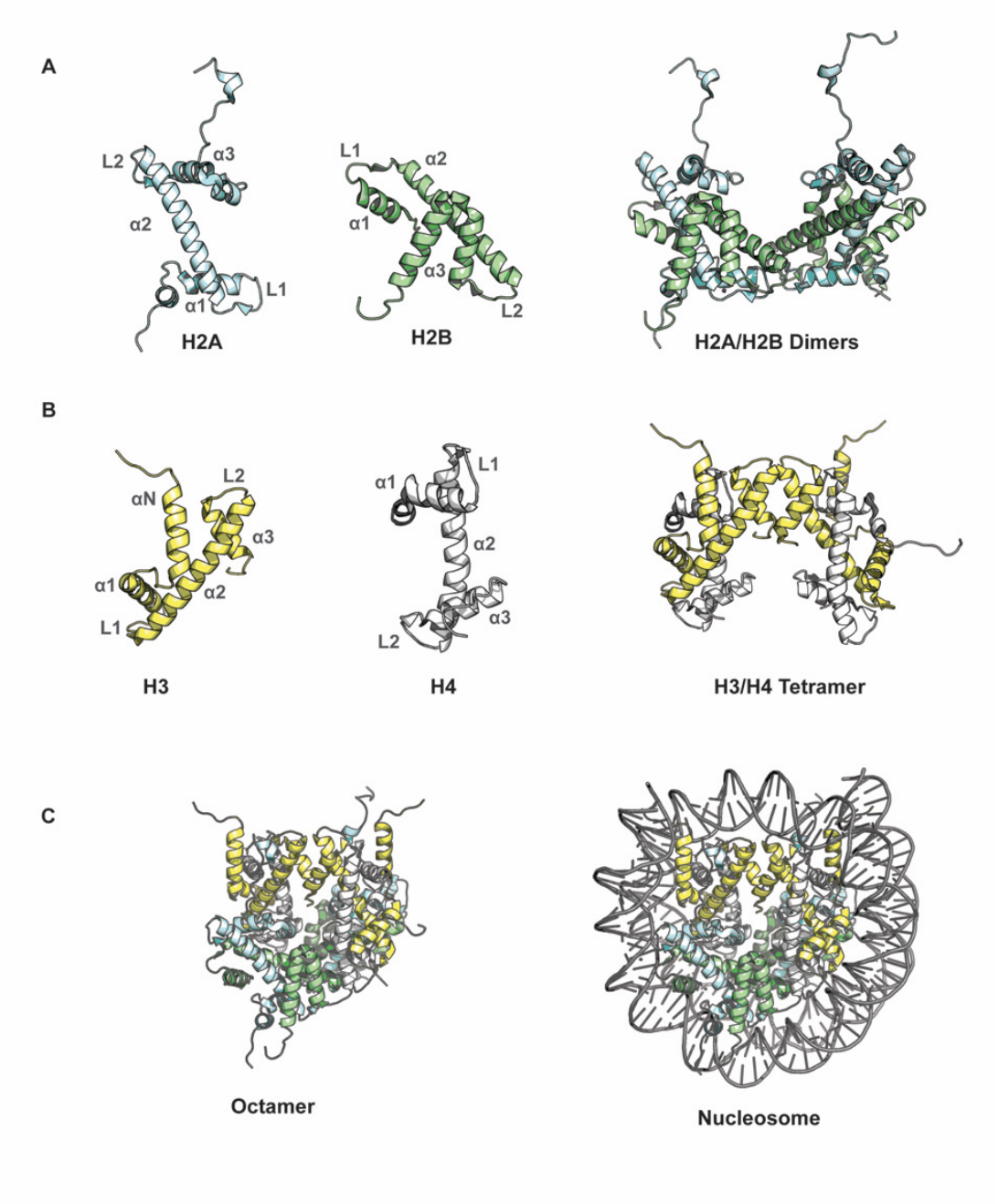

Figure 1. Histone and nucleosome structure

(A) H2A and H2B form two dimers within the X-ray crystal structure of the nucleosome (LUGER *et al.* 1997). **(B)** Two copies of H3 and H4 form one tetramer. Loops (L) and α helices (α) of the canonical histone fold are marked in grey. **(C)** Full nucleosome structure. This figure was generated in PyMol using PDB ID: 1ID3 from (WHITE *et al.* 2001).

The nucleosome face (Fig. 2A) is a disc-shaped structure that contains several furrows for proteins to bind to and alter chromatin. The orientation of the histones binding to DNA gives rise to two-fold symmetry, which can be observed when rotating the nucleosome along the dyad axis. While this two-fold symmetry exists *in vitro*, in many cases nucleosomes are asymmetrically arranged throughout the genome, which can range from subnucleosomal structures, histone variants, and histone posttranslational modifications (VOIGT *et al.* 2012; RHEE *et al.* 2014). We are just starting to understand the biological relevance of nucleosome asymmetry. For example, a long-held hypothesis has been that combinatorial modifications, which can occur asymmetrically, to the nucleosome can "poise" genes for activation (BERNSTEIN *et al.* 2006). A recent study showed that nucleosomes can be asymmetrically modified by isolating single nucleosomes and assessing modifications at the single molecule level using TIRF microscopy (SHEMA *et al.* 2016). In this study, the authors were further able to sequence DNA from single nucleosomes and measure histone modifications at the single molecule level as well as map the marks to the genome, where they observed asymmetrical, bivalent histone marks at promoters (SHEMA *et al.* 2016).

The DNA entry/exit sites allow for proteins to slide nucleosomes along DNA for nucleosome repositioning, which is important during gene expression and other DNA-templated processes (KASSABOV *et al.* 2003). The DNA entry/exit site is emerging as a key region of the nucleosome for regulating gene expression. A surface along the DNA entry/exit site has also been shown to be important for promoting the histone modification, H3 K36 methylation, which is involved in transcription elongation and termination (ENDO *et al.* 2012). A recent study also showed that TBP can bind to TATA box DNA in the nucleosome DNA entry/exit site (HIEB *et al.* 2014). Thus, the conformation of the nucleosome can determine access of TBP to DNA.

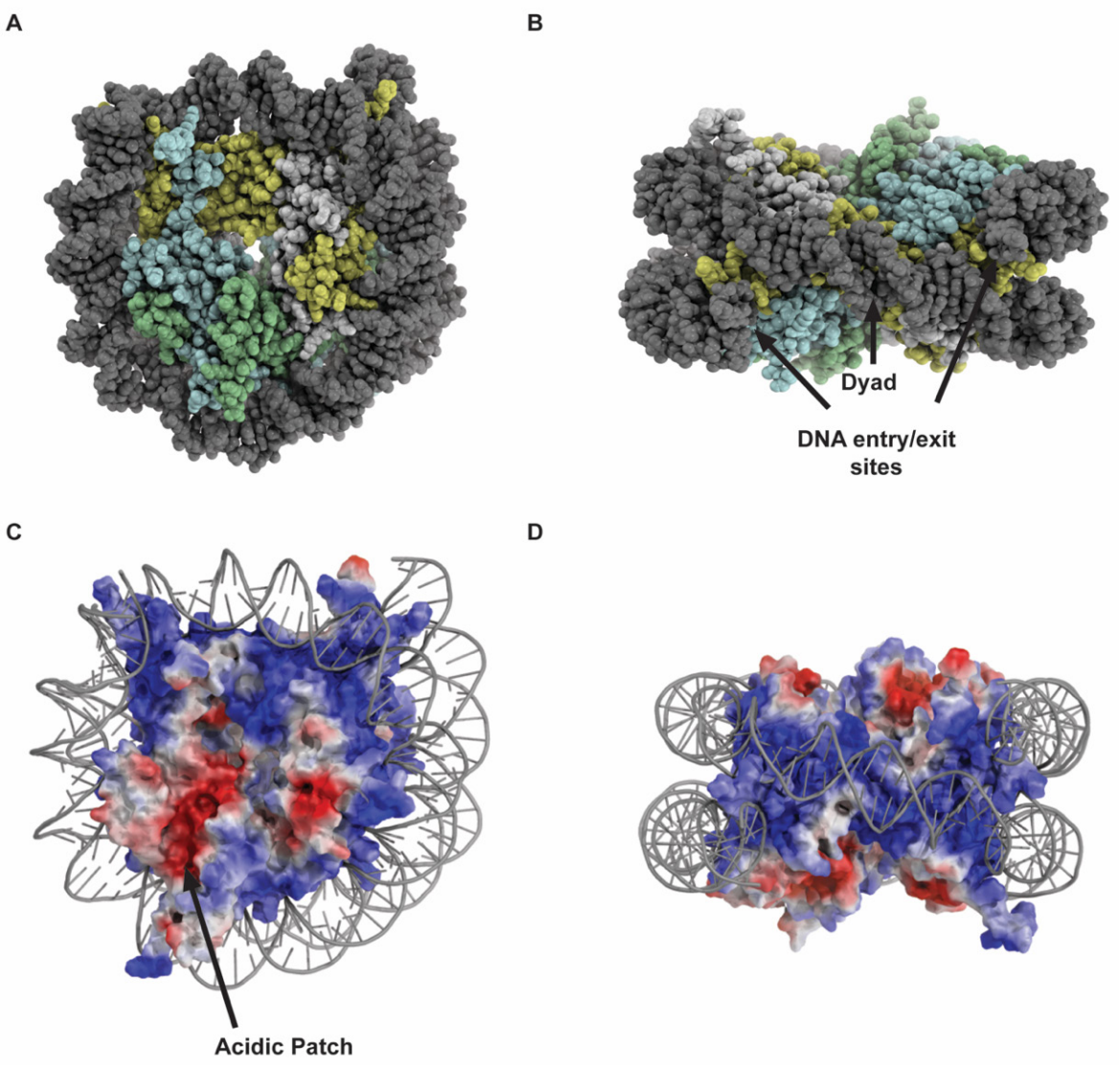

Figure 2. Nucleosome surface and DNA interactions

(A) Topology of the yeast nucleosome. **(B)** Side view of the nucleosome showing the dyad axis of the nucleosome and the DNA entry/exit sites. **(A, B)** H2A is cyan, H2B is green, H3 is yellow, and H4 is white. **(C, D)** Electrostatic potential of the nucleosome surface. Red residues are acidic and blue residues are basic. The arrow signifies the nucleosome acidic patch. This figure was generated in PyMol using PDB ID: 1ID3 from (WHITE *et al.* 2001).

1.1.2 The nucleosome acidic patch is an interaction hub for chromatin factors

As expected for proteins that bind to DNA, histones have a large number of positively charged amino acids (Fig. 2D). However, there is a prominent region of the nucleosome that is enriched for negatively charged amino acids. This region is known as the "nucleosome acidic patch," and it is defined by the cavity of negatively charged residues at the H2A/H2B interface (Fig. 2C). There is a smaller acidic region to the right of the acidic patch on H2B, though it is not concave and little is known about the function of this region. The nucleosome acidic patch has become known as an interaction "hot spot" for chromatin factors, which range from the H4 tail of neighboring nucleosomes to viral proteins that tether the viral genome to host chromatin (KALASHNIKOVA *et al.* 2013; MCGINTY AND TAN 2015).

One of the defining characteristics of acidic patch interactions is the "arginine anchor," which consists of three arginines on the chromatin binding proteins that interact with acidic residues in the nucleosome. The list of proteins that bind to the acidic patch continues to grow; to date, ten structures have been solved with proteins bound to the nucleosome acidic patch (Table 1). Among these proteins, the only common motif for binding to the acidic patch is through the arginine anchor. The reason so many proteins localize to the acidic patch could be because the acidic patch is involved in forming higher order chromatin structures by interacting with neighboring nucleosomes (discussed in more detail below). It is thus plausible that in order to prevent nucleosome-nucleosome interactions that give rise to chromatin compaction, proteins involved in chromatin transactions could "protect" the acidic patch by binding to it and preventing interactions with neighboring nucleosomes, allowing chromatin to be more open. A more simple, obvious rationale for the abundance of proteins interacting with the acidic patch is because the acidic patch is relatively unique within the nucleosome: it is very acidic, while the rest of the

nucleosome is basic, and it forms a cavity that allows for proteins to lock into the nucleosome for binding. Thus, the acidic patch is inherently amenable to protein-protein interactions.

Protein	Function	Method
H4 Tail	Promotes nucleosome-nucleosome interactions for higher order chromatin folding (LUGER *et al.* 1997; DORIGO *et al.* 2003) (WILKINS *et al.* 2014)	X-ray crystallography; crosslinking *in vivo*
LANA	Latent nuclear antigen peptide of Kaposi's sarcoma virus; tethers viral genome to host chromatin (BARBERA *et al.* 2006)	X-ray crystallography
RCC1	Guanine exchange factor for Ran; important for chromatin condensation (MAKDE *et al.* 2010)	X-ray crystallography
Sir3	Promotes telomeric silencing (ARMACHE *et al.* 2011)	X-ray crystallography
CENP-C	Centromeric protein (KATO *et al.* 2013)	X-ray crystallography
PRC1	Ubiquitylates H2A K119 to silence chromatin (MCGINTY *et al.* 2014)	X-ray crystallography
HMGN2	Regulates chromatin structure during transcription and DNA repair (KATO *et al.* 2011)	NMR
IE1	Immediate early protein from human cytomegalovirus; unfolds host chromatin during viral infection (FANG *et al.* 2016)	X-ray crystallography
Sgf11	Member of SAGA deubiquitylation module; deubiquitylates H2B K123 (MORGAN *et al.* 2016)	X-ray crystallography
Set8	H4K20me1; involved in genome integrity (GIRISH *et al.* 2016)	Structural modeling
Bre1	E3 ligase for H2B K123 ubiquitylation during transcription elongation (GALLEGO *et al.* 2016)	Crosslinking and mass spectrometry
GAG	Spumavirus tethering protein; functions similar to LANA (LESBATS *et al.* 2017)	X-ray crystallography

Table 1. List of proteins that bind to the nucleosome acidic patch

One well-characterized interaction is between Sgf11 and the nucleosome acidic patch. Sgf11 is a component of the deubiquitylation (DUB) module of the SAGA complex, which associates with elongating Pol II and removes ubiquitin from H2B K123 (HENRY *et al.* 2003; POWELL *et al.* 2004; EMRE *et al.* 2005; LEE *et al.* 2005; SCHULZE *et al.* 2011). The Wolberger lab

recently solved the X-ray crystal structure of Sgf11 bound to the nucleosome (MORGAN *et al.* 2016). In this structure, we can see the three arginines in Sgf11 (R84, R91, and R78) interacting with glutamic acids on H2A (E57, E62, and E65) (Fig. 3, PDB ID: 4ZUX). Interestingly, as described in this thesis, several residues within the acidic patch have been shown to be important for the addition of ubiquitin to H2B K123 as well (Fig. 3, red residues) (CUCINOTTA *et al.* 2015).

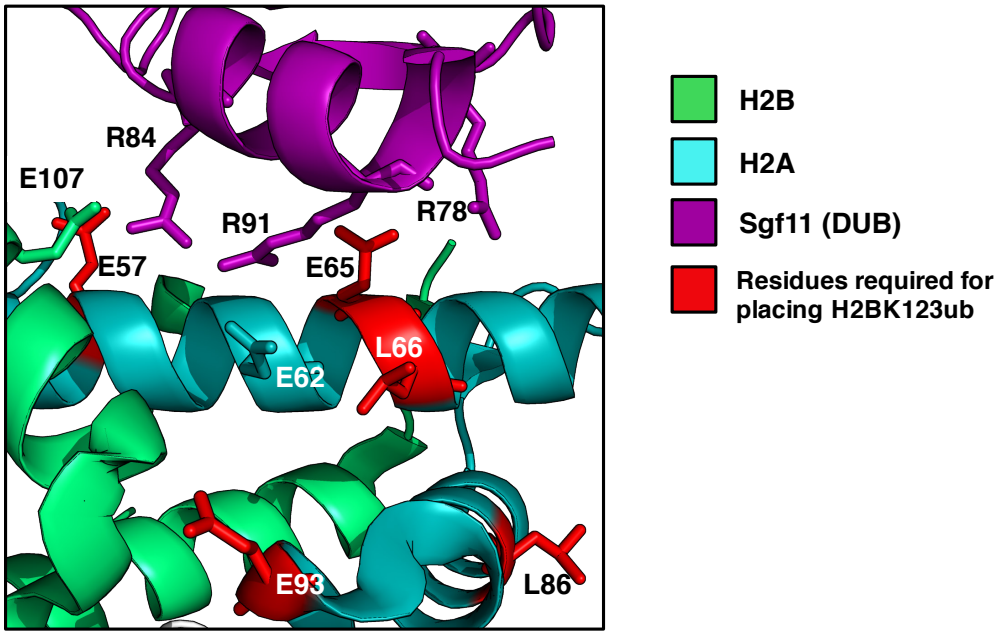

Figure 3. Detailed view of Sgf11 bound to the nucleosome

Sgf11 binds to the acidic patch using an arginine anchor. Sgf11 is shown in purple, H2B in green, and H2A in cyan. Residues highlighted in red are those required for installing ubiquitin on H2B K123 (CUCINOTTA *et al.* 2015). This figure was created in PyMol using PDB ID: 4ZUX from (MORGAN *et al.* 2016).

1.1.3 Nucleosome-nucleosome interactions and higher-order chromatin folding

Nucleosomes can compact into arrays *in vitro* under different ionic conditions (BEDNAR *et al.* 1995; ARYA AND SCHLICK 2009). Removal of histone tails can impede this compaction, as the histone tails are important for inter-nucleosome contacts. The nucleosome acidic patch was shown to bind to the H4 tail of neighboring nucleosomes in the X-ray crystal structure and later by *in vivo* site-specific crosslinking (LUGER *et al.* 1997; WILKINS *et al.* 2014). In the original 2.8Å structure of the nucleosome, H4 residues 16-25 were shown to bind to H2A at the acidic patch. Interestingly, H4 K16 acetylation is a prevalent histone posttranslational modification involved in transcription elongation. It was later shown that H4 K16 acetylation is important for altering chromatin structure, in that formation of the 30-nm fiber, the next level of chromatin folding, was impeded by H4 K16 acetylation *in vitro* (SHOGREN-KNAAK *et al.* 2006).

The 30-nm fiber is a higher-order chromatin structure observed *in vitro* in which nucleosome arrays are compacted by the linker histone H1 (diagrammed as a cartoon in Fig. 4) (FINCH AND KLUG 1976). In a recent cryo-EM structure, Song and colleagues showed that a 12-nucleosome array forms a double-helical 30-nm fiber in which H1 binds asymmetrically in the chromatin fiber (SONG *et al.* 2014). The biological role of the 30-nm fiber is hypothesized to help package the roughly 2-meters of DNA into a 10μm cell. Identifying the 30-nm fiber *in vivo* has been elusive, however. Though there are some indications that the 30-nm fiber is present in certain cell types (LANGMORE AND SCHUTT 1980), there is mounting evidence that the 30-nm fiber is in fact rare *in vivo* and chromatin takes on a more irregular higher-order structure (NISHINO *et al.* 2012; CAI *et al.* 2017). How chromatin is compacted is nevertheless still dependent on histone tails (ARYA AND SCHLICK 2009), histone modifications (SHOGREN-KNAAK *et al.* 2006; FIERZ *et al.*

2011), and the recently identified heterochromatin sequestration by HP1 via liquid phase separation (LARSON *et al.* 2017; STROM *et al.* 2017).

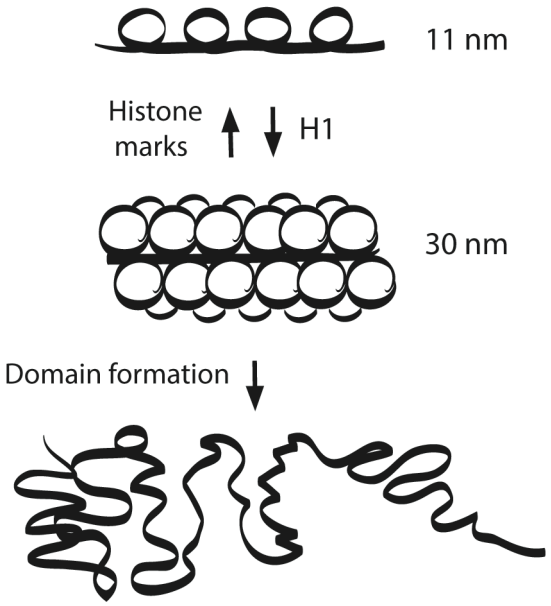

Figure 4. Diagram of chromatin compaction

Given that the genome can be tightly compacted into chromatin and nucleosomes can block proteins from binding to DNA, cells must employ methods to disrupt chromatin and nucleosome and nucleosome structures. Cells also need to label different portions of the genome for proper spatiotemporal access. Thus, nucleosomes can be modified, moved, and removed during all chromatin transactions. All of these processes are critical to cellular function and defects in these processes can give rise to diseases, such as cancer.

1.2 EUKARYOTIC GENE EXPRESSION OVERVIEW

Transcription of DNA to form RNA is the first level of gene expression. RNA is transcribed from DNA by one of three canonical RNA polymerases: Pol I, II, and III (ROEDER AND RUTTER 1969). The focus of this dissertation is on Pol II-dependent transcription, which can be divided into three stages: initiation, elongation, and termination. Initiation involves loading the polymerase and the transcription of a few nucleotides prior to promoter clearance and the transition to elongation. During elongation, the polymerase must processively polymerize RNA molecules as it transits through nucleosomes. Depending on the type of transcript, termination of RNAs may involve cleavage of the transcript, followed by polyadenylation and further processing for export to the cytoplasm for translation or to the exosome for rapid clearance of the nascent transcript (MISCHO AND PROUDFOOT 2013). All three stages include a host of different accessory factors that coordinate transcriptional regulation with modulation of the chromatin architecture.

1.2.1 Pol II CTD phosphorylation

Central to gene expression is the C-terminal domain (CTD) of Pol II, which is an essential unstructured tail that consists of a consensus heptad repeat containing the amino acids: $Y_1S_2P_3T_4S_5P_6S_7$. In yeast and humans, this sequence is repeated 26 and 52 times, respectively (HSIN AND MANLEY 2012). These amino acids are subject to posttranslational modifications that are critical to regulating transcription. The most studied modifications to the CTD are Ser2-P, Ser5-P, Ser7-P, Thr4-P, and most recently discovered, Tyr1-P (Fig. 7) (ZABOROWSKA *et al.* 2016). These marks are conserved from yeast to humans and are involved in all parts of the transcription cycle and even in posttranscriptional processes. The CTD is dynamically phosphorylated and

dephosphorylated across a gene by various kinases and phosphatases (Fig. 5). A recent study using SAXS analysis suggested that the unmodified CTD is semi-compact and that it extends upon phosphorylation (PORTZ *et al.* 2017).

Recently, two groups created modified versions of the human (SCHULLER *et al.* 2016) and yeast (SCHULLER *et al.* 2016; SUH *et al.* 2016) CTD that made it amenable to mass spectrometry analyses. These two studies addressed the important question of whether multiple repeats are phosphorylated when conventional ChIP analyses could not answer this question. Suh *et al.* found that the predominant CTD modifications are Ser2-P and Ser5-P and that the patterning of CTD phosphorylation is similar among the repeats. Schuller *et al.* showed similar results in mammals and yeast. They found that Thr4-P was also abundant, however little is known of this mark compared to Ser2-P and Ser5-P.

A recent NET-seq analysis followed by quantitative mass spectrometry investigated the roles of the different phosphorylation sites in the CTD (HARLEN *et al.* 2016). In this paper, the investigators found a role for Ser5-P and Thr4-P in splicing. They also showed that Thr4-P along with the termination factor Rtt103 are required for Pol II pausing after Poly(A) sites. This was validated in a recent study showing that Rtt103 binds both Thr4 to terminate snoRNAs and to Ser2-P to terminate mRNAs (NEMEC *et al.* 2017). Thus, the CTD code functions to recruit different factors to the transcription apparatus to regulate transcription and the fate of transcripts.

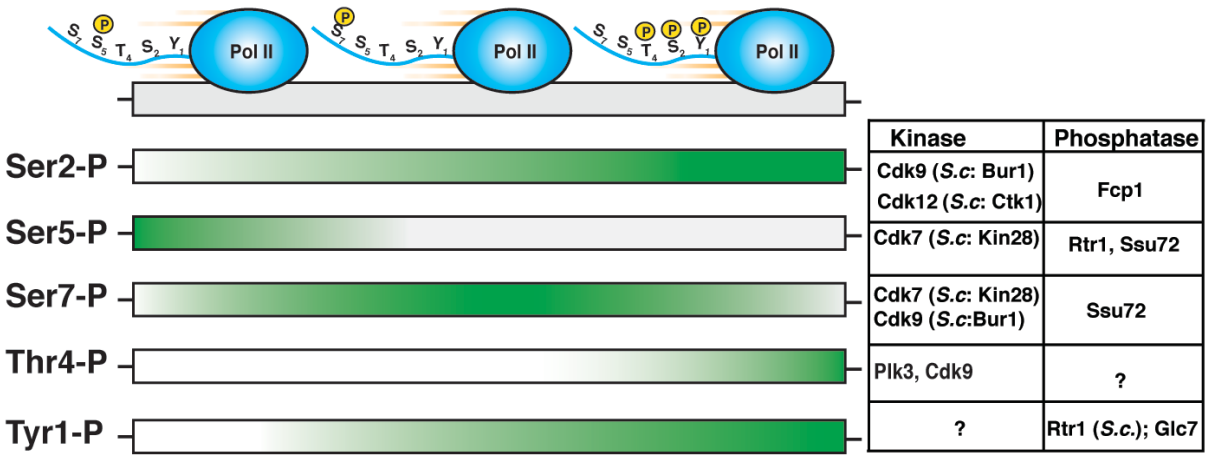

Figure 5. Pol II CTD phosphorylation

The Pol II CTD is phosphorylated during transcription. The green bars indicate enrichment of the corresponding marks from the 5' –end to the 3'-end of a gene. The darker color represents higher levels of the mark. The table on the right lists various kinases and phosphatases for the marks. These have been summarized in (JERONIMO *et al.* 2013)

1.2.2 Initiation

Transition of the apo state to the phospho state of the CTD occurs as Pol II is loaded into the pre-initiation complex (PIC). PIC formation of is a highly regulated process involving various co-activators and co-repressors (Fig. 6) (SHANDILYA AND ROBERTS 2012). Nucleosome positioning helps to dictate where PICs are assembled. On the genome-wide scale, PICs are largely localized to nucleosome-free regions at the 5'-ends of genes (RHEE AND PUGH 2012). The PIC consists of Pol II, the Mediator co-activator complex, and the general transcription factors: TFIIB, TFIID, TFIIE, TFIIF, and TFIIH. The order of factor-binding in PIC formation has been

characterized by many and it is summarized as follows: TFIID with TBP bind to the promoter; TFIIB, Pol II together with TFIIF, TFIIE, and TFIIH (DVIR *et al.* 2001).

TFIID contains TBP, which recognizes a TATA-containing sequence and bends promoter DNA (KIM *et al.* 1993a; KIM *et al.* 1993b). Although few promoters contain TATA sequences, TBP is still required for transcription, as TBP can bind sequences that deviate from the canonical TATA motif (PUGH AND TJIAN 1991; RHEE AND PUGH 2012). In fact, 10% of TATA-containing promoters generally bind the SAGA complex instead of TFIID (BASEHOAR *et al.* 2004), where the majority of the SAGA-dependent genes are those involved in the stress response pathway (HUISINGA AND PUGH 2004). Promoters containing TATA sequences can be transcribed without TFIID if TBP is present.

TBP interacts with a suite of transcription factors (TBP-associated factors, or TAFs) (SHANDILYA AND ROBERTS 2012; ALLEN AND TAATJES 2015). The TAFs are not required for transcription of all promoters, as both TAF dependent and TAF independent promoters have been observed (LI *et al.* 2000). Interestingly, TAFs have histone fold domains and can even form dimers and tetramers similar to H2A/H2B and H3/H4, respectively (XIE *et al.* 1996; GANGLOFF *et al.* 2001; LEURENT *et al.* 2002). TFIIA is a multifunctional complex; its key function is to bind TBP and stabilize the TBP-DNA complex (BURATOWSKI *et al.* 1989; KANG *et al.* 1995). TFIIA also competes with repressors that bind to TBP (OZER *et al.* 1998).

TFIIB interacts with TBP and binds to specific sequences in the promoters of genes called TFIIB recognition sequences (LAGRANGE *et al.* 1998). In turn, TFIIB recruits Pol II to promoters (HA *et al.* 1991; BURATOWSKI AND ZHOU 1993). Post PIC-formation, TFIIB plays roles in transcription start site (TSS) selection (CHO AND BURATOWSKI 1999). This function is likely due to TFIIB interacting with the catalytic core of Pol II (KOSTREWA *et al.* 2009; LIU *et al.* 2010).

Interestingly, it has been suggested that TFIIB and TFIIH are both involved in TSS selection through a gene looping mechanism (GOEL *et al.* 2012). However, one study in *Schizosaccharomyces pombe* suggested that TFIIB does not direct TSS selection, however (YANG AND PONTICELLI 2012).

Photocrosslinking experiments revealed that TFIIF increases wrapping of promoter DNA around the initiation complex (ROBERT *et al.* 1998). TFIIF then recruits TFIIE and TFIIH. TFIIH is a multifunctional complex containing subunits with kinase, ATPase, and helicase domains. It is involved in transcription elongation and even plays roles in DNA repair (COMPE AND EGLY 2012). In initiation, TFIIH is important for unwinding DNA to open the PIC. A recent study used a single molecule strategy to observe initiation of Pol II transcription in real time (FAZAL *et al.* 2015). In this study, the authors found that TFIIH helps to unwind ~85bp to form the transcription bubble. TFIIH is also involved post-initiation, entering the transcription cycle during PIC assembly and affecting early elongation of Pol II (discussed more in detail below) (DVIR *et al.* 1997). TFIIE interacts with Pol II, recruits TFIIH, and is thought to build a bridge between Pol II and TFIIH (SAINSBURY *et al.* 2015).

Mediator is a dynamic complex of 21 (yeast) or 26 (human) subunits that interacts with many components of the PIC, lending stability to the complex. Mediator can regulate the recruitment and activity of general transcription factors TFIIA, TFIIB, TFIIE, TFIIF, and TFIIH. Mediator contains a kinase module that can phosphorylate a number of transcription factors for either negative or positive regulation (ALLEN AND TAATJES 2015). Mediator is suggested to be important for the transition from initiation to elongation, as it stimulates the kinase activity of TFIIH to phosphorylate the CTD at serine 5, causing Pol II to leave the PIC. There is still more to learn about Mediator, however. A recent study using a novel, high resolution genome mapping

technique, ChEC-seq, showed that Mediator localizes to upstream activating sequences rather than core promoters and that Mediator occupancy was not correlated with gene expression levels at most genes. Instead, Mediator's main role could be in PIC assembly, as depletion of a core Mediator subunit resulted in a drastic decrease in TFIID occupancy genome-wide (GRUNBERG *et al.* 2016).

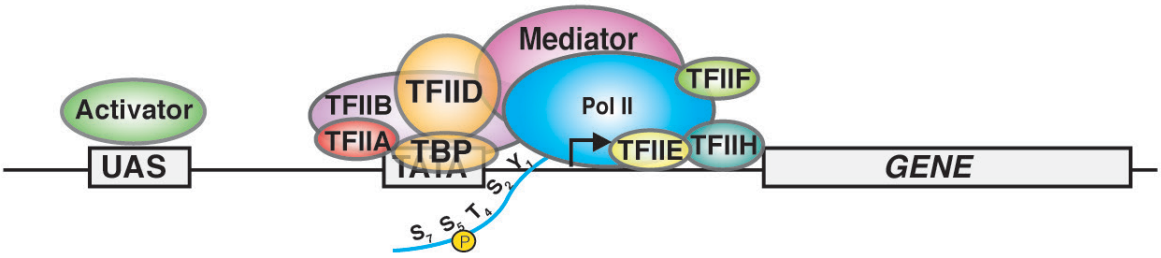

Figure 6. Diagram of factors involved in transcription initiation.

1.2.3 Elongation

Once the PIC is formed and productive initiation is successful, the transcription apparatus can transition into elongation. Until recently, it was thought that initiation was the main level of transcriptional regulation. However, over the years it has come to light that the elongation process has many opportunities for regulation as Pol II tracks along a gene. There are several ways in which a transcribing Pol II complex may be stalled. This includes Pol II arrest and pausing. The resumption of transcription is promoted by different factors, depending on how the elongation complex was halted (SIMS *et al.* 2004).

Pol II arrests when it encounters DNA sequences that cause back tracking, which causes the 3' end of the growing RNA molecule to disengage from the active site of Pol II (NUDLER 2012). TFIIS reverses backtracking by stimulating the weak nuclease activity of Pol II (IZBAN AND LUSE 1992; KETTENBERGER *et al.* 2003), resulting in cleavage of the nascent transcript so that the transcript can be reoriented in the Pol II active site. Pol II backtracking and nascent RNA cleavage are processes that are conserved from prokaryotes to higher eukaryotes (BORUKHOV *et al.* 1993; KOMISSAROVA AND KASHLEV 1997; KORZHEVA *et al.* 1998; CHEUNG AND CRAMER 2011).

In higher eukaryotes, Pol II remains in a paused form near promoters across the genome, which poises genes for expression (MUSE *et al.* 2007). In this system, the first step to productive elongation is release of promoter proximal pausing (ADELMAN AND LIS 2012). Promoter proximal pausing occurs when Pol II is bound to the hypophosphorylated forms of negative elongation factor, NELF and DRB-induced sensitivity factor, DSIF (Fig. 7A). P-TEFb is a cyclin-dependent kinase that phosphorylates NELF, DSIF, and Pol II to regulate transcription (PRICE 2000). NELF is phosphorylated by P-TEFb, which releases NELF from Pol II and allows for transcription elongation. Recently, it was discovered that NELF is also ADP-ribosylated by PARP-1 to release NELF from paused polymerase (Fig. 7B) (GIBSON *et al.* 2016). Another factor that helps promote elongation is DSIF, which is a heterodimeric complex that contains the human homologs of the yeast proteins Spt4-Spt5 (WADA *et al.* 1998). DSIF is also bound to Pol II, however it is stimulated to promote elongation upon phosphorylation by P-TEFb (Fig. 6B).

DSIF in mammals and Spt4-Spt5 in yeast is a universally conserved protein, being present in all three kingdoms. DSIF has been shown to stabilize the pausing complex and enhance transcription elongation. Recent work by Crickard *et al.* showed that Spt5 can prevent Pol II arrest by interacting with the non-coding DNA template strand (CRICKARD *et al.* 2016). Spt5 has roles

in binding to nascent RNA as well (MISSRA AND GILMOUR 2010; VIKTOROVSKAYA *et al.* 2011; BLYTHE *et al.* 2016). A recent study has shown that Spt5 enhances transcription elongation rate, prevents antisense transcription, and promotes proper mRNA splicing (SHETTY *et al.* 2017). As Spt5 plays multiple roles in regulating gene expression, it is apparent why this protein is essential for viability and conserved across kingdoms.

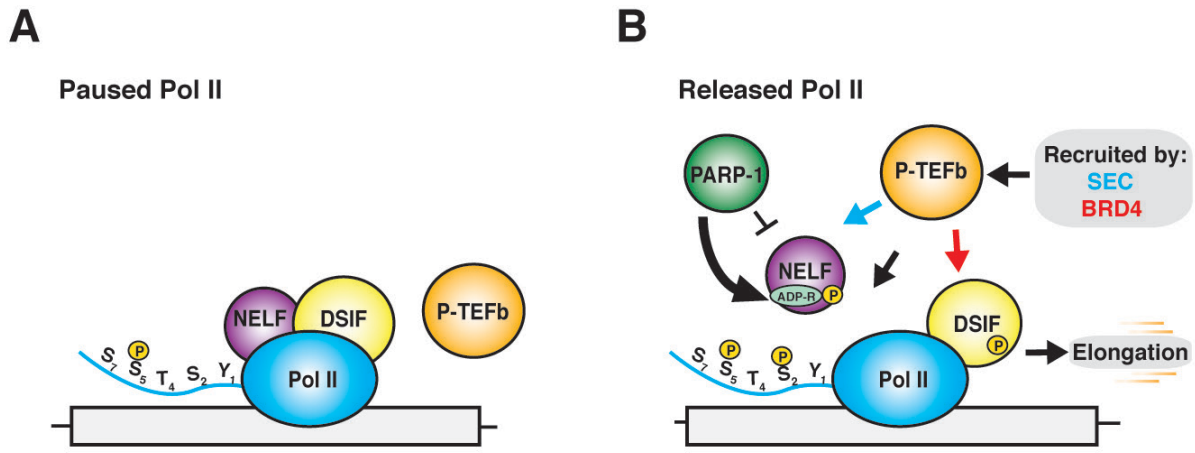

Figure 7. Diagram of Pol II pause and release

Many processes involving RNA synthesis and processing are co-transcriptional (PERALES AND BENTLEY 2009). Thus, the rate of transcription elongation is a major influence on the fate of a transcript. Transcription elongation kinetics can control alternative splicing (DE LA MATA *et al.* 2003; DUJARDIN *et al.* 2014; FONG *et al.* 2014), transcription termination (HAZELBAKER *et al.* 2013), and poly(A) site selection (PINTO *et al.* 2011). Factors that enhance the rate of transcription elongation include the trigger loop domain of Pol II subunit Rpb1 (KAPLAN *et al.* 2012), TFIIF (BENGAL *et al.* 1991; TAN *et al.* 1995), Elongin (ASO *et al.* 1995), ELL (SHILATIFARD *et al.* 1996), Spt6 (ARDEHALI *et al.* 2009), Spt5 (SHETTY *et al.* 2017), and others (KWAK AND LIS 2013). Other factors involved in transcription elongation are summarized in Table 2. Genomic sequences have

also been suggested to impact transcription elongation rates. A genome-wide study assessed Pol II elongation rates and found that high elongation rates correlate with gene length and low complexity DNA sequences (VELOSO *et al.* 2014). The authors also found that genes with rapid elongation rates have high densities of specific histone modifications, H3K79me^2 and H4 K20me^1.

It was recently found that many elongation factors interact with nascent RNA (BATTAGLIA *et al.* 2017). Some of these factors include all members of the Paf1C. This finding was interesting in light of various other studies that have identified the ability of many chromatin binding proteins to also bind RNA (BELTRAN *et al.* 2016; D *et al.* 2016; HE *et al.* 2016; BOSE *et al.* 2017; SAYOU *et al.* 2017). It is likely that the RNA-binding ability of chromatin-associated factors will emerge as an important regulatory mechanism for gene expression (SKALSKA *et al.* 2017).

Protein	Function
P-TEFb/Cdk9/CycT1 (yeast: Bur1/Bur2)	Cyclin-dependent kinase, releases Pol II from pausing and phosphorylates Pol II, NELF, and DSIF
DSIF (yeast: Spt4-Spt5)	Stabilizes Pol II pausing, recruits elongation factors, stimulates elongation
NELF	Negative elongation factor; promotes pausing
PARP-1	Poly[adenosine diphosphate (ADP-ribose)] polymerase, transfers ADP-ribose to NELF to inhibit NELF
BRD4	Recruits and activates P-TEFb
TFIIS	Resumes Pol II elongation from backtracked-arrest
TFIIF	Prevents transient pausing of Pol II
Elongin	Increases transcription rate
Super elongation complex (SEC)	Recruits P-TEFb, increases Pol II elongation rate
Little elongation complex	Required for snRNA expression in metazoans
Paf1C	Associated with Pol II and Spt4-Spt5, recruits chromatin remodeling enzymes, histone chaperones, and modifiers
GDOWN1	Tightly associated with Pol II, stabilizes pausing
RNA processing factors	CCR4-NOT, THO/TREX, Xrn2: mRNA processing and export factors that also regulate elongation

Table 2. Factors involved in Pol II pausing and transcription elongation

Adapted from (CUCINOTTA AND ARNDT 2016)

1.2.4 Termination

To ensure demarcation of the transcriptome and recycling of the transcription apparatus, Pol II implements multiple mechanisms to achieve termination of different types of transcripts (KIM *et al.* 2006; RONDON *et al.* 2009). Two major methods of transcription termination in yeast are the cleavage and polyadenylation pathway and the Nrd1-Nab3-Sen1 pathway.

1.2.4.1 Cleavage and polyadenylation pathway

Most mRNAs in eukaryotes are terminated and processed via the cleavage and polyadenylation pathway (CPF) (PORRUA AND LIBRI 2015). Ser2-P of the Pol II CTD and sequences encoded in the 3' untranslated region (UTR) of transcripts recruit CPF machinery. RNA is cleaved at the poly(A) site by an endonuclease present within the CPF complex. This allows a poly(A) polymerase to generate the poly(A)-tail of a transcript, which is important for preventing transcript degradation and promoting RNA export. Termination arises when an exonuclease complex, Rat1/Rai1, degrades the nascent transcript (KIM *et al.* 2004). This is thought to destabilize the elongation complex and promote termination. The mode of CTD phosphorylation is important for termination decisions. For example, Rtt103, a factor that recruits Rat1/Rai, binds to the CTD at Ser2-P for termination of protein coding genes and Thr4-P for termination of non-coding RNAs (ncRNAs) (HARLEN *et al.* 2016; NEMEC *et al.* 2017).

1.2.4.2 Nrd1-Nab3-Sen1 pathway

In yeast, transcription termination of many ncRNAs is achieved through a separate pathway than that of the polyadenylation pathway used for mRNA transcript termination, and requires the Nrd1-Nab3-Sen1 (NNS) complex (STEINMETZ *et al.* 2006a; ARNDT AND REINES 2015). Sen1 is an RNA helicase that unwinds the RNA-DNA hybrid during transcription (KIM *et al.* 1999; URSIC *et al.* 2004; KIM *et al.* 2006; STEINMETZ *et al.* 2006b). Nrd1 and Nab3 are RNA binding proteins involved in recruitment of Sen1 (YURYEV *et al.* 1996; STEINMETZ *et al.* 2001; ARIGO *et al.* 2006a; VASILJEVA *et al.* 2008). Nrd1 binds the Pol II CTD at Ser5-P, and Sen1 binds Ser2-P (VASILJEVA *et al.* 2008; CHINCHILLA *et al.* 2012). Nrd1, Nab3, and Sen1 are essential for yeast viability. The NNS complex is involved in termination of non-coding RNAs, including cryptic unstable transcripts (CUTs) (ARIGO *et al.* 2006b) and small nucleolar RNAs (snoRNAs), which are critical

for ribosome biogenesis (KIM *et al.* 2006; DIECI *et al.* 2009). Elongation rate and the chromatin environment is important for termination (TERZI *et al.* 2011; TOMSON *et al.* 2011; SUH *et al.* 2013; CASTELNUOVO *et al.* 2014). Chromatin remodeling enzymes Isw1 and Chd1 have been implicated in transcription termination of a set of specific genes, including the NNS-mediated termination of *IMD2* (ALEN *et al.* 2002; MORILLON *et al.* 2003). Histone modifications are also important for termination, including H2B K123ub and H3 K4me^3 (TERZI *et al.* 2011; TOMSON *et al.* 2011; TOMSON *et al.* 2013). Another complex involved in transcription termination of RNAs by NNS is the Paf1 complex (Paf1C) (SHELDON *et al.* 2005; TOMSON *et al.* 2011; TOMSON *et al.* 2013). Paf1C promotes transcription termination, in part, due to its role in promoting histone modifications (see below).

1.2.5 The Paf1 Complex

The Polymerase associated factor 1 complex (Paf1C) is a five-subunit complex that was discovered over twenty years ago using affinity chromatography to isolate factors that bind to Pol II (SHI *et al.* 1996). Since then, Paf1C has been implicated in every step of gene expression (Fig. 8), ranging from chromatin modifications and transcription elongation to cleavage and polyadenylation and RNA export (STOLINSKI *et al.* 1997; CRISUCCI AND ARNDT 2011; TOMSON AND ARNDT 2013; YANG *et al.* 2016b; FISCHL *et al.* 2017).

Paf1C consists of the subunits Rtf1, Cdc73, Leo1, Paf1, and Ctr9 (MUELLER AND JAEHNING 2002). In humans, the subunit Ski8, involved in mRNA decay, also associates with Paf1C (ZHU *et al.* 2005). The human Rtf1 subunit appears to be more loosely associated with the Paf1C and may function independently of Paf1C (CAO *et al.* 2015). Yeast Paf1C associates with chromatin via two major attachment points through Cdc73 and Rtf1. The C-domain of Cdc73

interacts with the CTD of Pol II (AMRICH *et al.* 2012; QIU *et al.* 2012) and the Plus-3 domain of Rtf1 interacts with the phosphorylated C-terminal region (CTR) of Spt5 (LIU *et al.* 2009; MAYEKAR *et al.* 2013; WIER *et al.* 2013). Leo1 has also been implicated in helping to recruit the Paf1C to chromatin via an interaction with RNA (DERMODY AND BURATOWSKI 2010). One structural study showed that human Paf1 and Leo1 form a tightly associated heterodimer and that the binding of Leo1 to Paf1C is mediated by Paf1 (CHU *et al.* 2013). This study also suggested that the Paf1/Leo1 heterodimer can interact with the N-terminus of histone H3.

ChIP-exo analysis has revealed that the Paf1C associates with chromatin at the +2 nucleosome (the second well-positioned nucleosome downstream from the promoter) and nucleosomes further downstream (VAN OSS *et al.* 2016). In this study, all five subunits had similar ChIP-exo profiles; and Spt5 associated with chromatin earlier than the Paf1C, which aligns with previous studies that Spt5 recruits Paf1C (LIU *et al.* 2009; MAYEKAR *et al.* 2013; WIER *et al.* 2013; YANG *et al.* 2016b).

One of the major roles of the Paf1C is its involvement in transcription elongation (COSTA AND ARNDT 2000; SQUAZZO *et al.* 2002a; KIM *et al.* 2010). In the absence of Paf1, transcription elongation is slowed (RONDON *et al.* 2004). In humans, Paf1C has also been suggested to regulate promoter-proximal pausing, however whether it plays a positive or negative role appears to be context-dependent and a unified model for Paf1C's involvement in pausing still needs to be pursued (CHEN *et al.* 2015; YU *et al.* 2015).

The Paf1C is important for proper transcription termination and 3'-end formation of snoRNAs (SHELDON *et al.* 2005; TOMSON *et al.* 2011; TOMSON *et al.* 2013). Additionally, Paf1C has been shown to interact with cleavage and polyadenylation factors and affect poly(A) site

selection (MUELLER *et al.* 2004; PENHEITER *et al.* 2005; NORDICK *et al.* 2008; ROZENBLATT-ROSEN *et al.* 2009; YANG *et al.* 2016b).

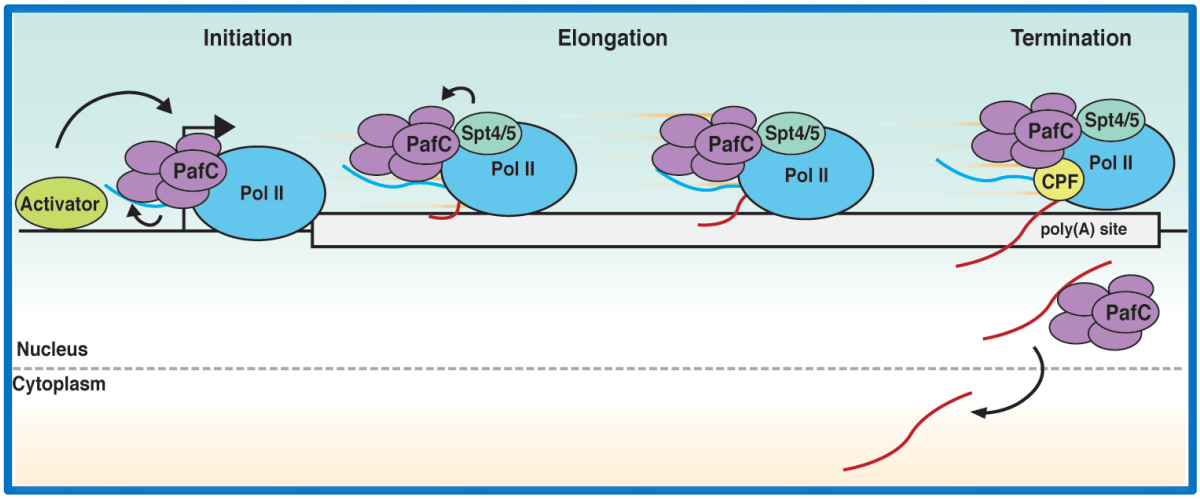

Figure 8. Paf1C is involved in RNA synthesis from beginning to end

Paf1C can be recruited to promoters and enhancers by transcriptional activators in metazoans. Upon the transition to elongation, Paf1C directly binds to the Pol II CTD via the Cdc73 subunit and the elongation factor Spt4-Spt5 (DSIF in humans) through the Rtf1 subunit. In yeast, these methods of recruitment appear to predominate. Pol II is phosphorylated at serine 2 (Ser2) during elongation. As transcription ends, the growing transcript is polyadenylated and cleaved at sites defined in part by Paf1C, which interacts with the cleavage and polyadenylation machinery (CPF). Paf1C then helps determine which transcripts are exported to the cytoplasm. (Summarized in Van Oss et al 2017; submitted for publication).

The most well-characterized role that Paf1C plays in transcription is in promoting histone modifications, which will be discussed in more detail in the following section. Briefly, the Paf1C is necessary for H2B K123 monoubiquitylation through its histone modification domain (HMD), which interacts with one of the catalytic enzymes, Rad6 (KROGAN *et al.* 2003; NG *et al.* 2003;

WOOD *et al.* 2003b; LARIBEE *et al.* 2005; XIAO *et al.* 2005; ZHU *et al.* 2005; WARNER *et al.* 2007; KIM AND ROEDER 2009; PIRO *et al.* 2012; WOZNIAK AND STRAHL 2014; VAN OSS *et al.* 2016). Paf1C is also suggested to be involved in H4 K31ub through an interaction with an H1 histone variant (KIM *et al.* 2013b). Another study identified a role for Paf1C in promoting H2B K34ub (WU *et al.* 2014). Paf1C is also important for H3 K36 tri-methylation, which is likely due to its role in promoting Ser2-P of the Pol II CTD (CHU *et al.* 2007; NORDICK *et al.* 2008; OH *et al.* 2008; ZHANG *et al.* 2013). Together, all of these studies demonstrate how the importance of Paf1C in all levels of gene regulation (Fig. 8).

1.3 HOW THE CHROMATIN LANDSCAPE IS ALTERED FOR GENE EXPRESSION

The nucleosome can act as an obstacle to transcription machinery (KULAEVA *et al.* 2013). Therefore, cells implement a variety of strategies to overcome this barrier, including chromatin remodeling and reorganization (CLAPIER *et al.* 2017; HAMMOND *et al.* 2017). An additional process involves the addition of histone post-translational modifications that affect all stages of transcription (OWEN-HUGHES AND GKIKOPOULOS 2012). These post-translational modifications can impact chromatin structure and the recruitment of proteins (KOUZARIDES 2007; LU *et al.* 2008; FIERZ *et al.* 2011).

1.3.1 Histone posttranslational modifications

Histones are posttranslationally modified to regulate all chromatin transactions. There are hundreds of known histone modifications, while only a subset have been well-characterized. These

modifications can range from the addition of small chemical groups such as phosphorylation, acetylation, and methylation to larger modifications such as the addition of proteins ubiquitin and SUMO. Proline isomerization and ADP ribosylation have also been observed (BANNISTER AND KOUZARIDES 2011). Interestingly, the H3 N-terminal tail can be degraded to regulate gene expression as well (SANTOS-ROSA *et al.* 2009) (see Table 3 for a summary of a set of modifications).

The patterning of histone modifications across a genome has been termed the "histone code" (STRAHL AND ALLIS 2000). In this hypothesis, proteins can "read" the code to bring about changes, such as "writing" other marks. For example, H3 K36me^2, is written by Set2, read by the histone deacetylation complex (HDAC) Rpd3S, and "erased" by the demethylase Jhd1 (SMOLLE AND WORKMAN 2013). However, it is argued that this viewpoint may be too simplistic and that the histone marks are "modified" and "bound" rather than "written" and "read;" and that histone marks mainly function to alter the chromatin environment to allow access to the underlying DNA sequence (HENIKOFF AND SHILATIFARD 2011). One of the arguments described by Henikoff and Shilatifard was the finding that substituting lysines to arginines on the H4 tail changed gene expression. However, it was found out that the number of lysines contributed to the major difference in gene expression, not a specific combination (DION *et al.* 2005). Still, the idea of a "histone code" can be revisited to include the functions of the marks rather than simple "reading" and "writing." It cannot be denied that histone modifications can recruit specific factors, such is the case with the *trans*-histone H2B K123ub modification cascade described in the next section.

Other factors are important for histone modifications and to effect change to the chromatin environment. For example, PRC2, a methyltransferase involved in forming repressive chromatin, binds non-specifically to RNA and methylates histones nearby to generate closed chromatin

(DAVIDOVICH *et al.* 2013). Nevertheless, a recent study suggested that PRC2 binds to RNA in an antagonistic fashion to chromatin, implying that the presence of RNA can prevent PRC2 from binding and methylating chromatin (BELTRAN *et al.* 2016). It will be interesting to see the resolution of these two models; however, it is apparent that RNA can be a key factor in regulating histone modifications, adding a level of complexity to the idea of the "histone code."

Histone acetylation and PRC1 and PRC2 mediated modifications are very well-studied. More recently, the H2B K123ub modification cascade has been intensely investigated (discussed in more detail below).

1.3.1.1 H2B monoubiquitylation

Monoubiquitylation of H2B on lysine 123 occurs both in yeast and in humans (H2B K123ub or K120ub) (THORNE *et al.* 1987; ROBZYK *et al.* 2000). This modification is associated with transcription elongation, DNA repair, DNA replication, and promotes downstream histone histone marks (FUCHS AND OREN 2014). H2B K123 ubiquitylation is achieved by the actions of the ubiquitin conjugating and ligase enzymes Rad6 and Bre1, respectively (SUN AND ALLIS 2002)(ROBZYK *et al.* 2000; NG *et al.* 2002b). H2B K120ub in humans is catalyzed by human homologs to Rad6 and Bre1: RAD6A/RAD6B (KIM *et al.* 2009) and RNF20/RNF40 (KIM *et al.* 2005), respectively.

As mentioned previously, Paf1C member Rtf1 is required for H2B K123ub. A recent study used ChIP-exo analysis to show that the Rtf1 member of the Paf1C is important for recruiting Rad6/Bre1 to chromatin, particularly at highly expressed genes (VAN OSS *et al.* 2016). In this same study, the authors used *in vivo* site-specific photocrosslinking to identify a direct interaction between Rad6 and the HMD of Rtf1 in a manner that was dependent on the E104 residue of the HMD. This study also went on to show that the HMD can stimulate H2B K120ub *in vitro*. The

HMD is important for stabilizing the Bre1 protein in certain conditions (WOZNIAK AND STRAHL 2014).

Another factor required for H2B K123ub *in vivo* is the Lge1 protein (HWANG *et al.* 2003; SONG AND AHN 2010). Little is known about how Lge1 is recruited to chromatin, however a recent study suggested a role for Cdc48 in Lge1 recruitment (BONIZEC *et al.* 2014). How Lge1 stimulates the H2B K123ub is truly understudied, though we know that Lge1 is also required for marks downstream of H2B K123ub *in vivo* (SONG AND AHN 2010). It is not yet known whether Lge1 can stimulate H2B K123ub *in vitro*. A similar protein in humans, WAC, interacts with RNF20/RNF40 through its coiled-coiled region (ZHANG AND YU 2011). Lge1 has a predicted C-terminal coiled-coiled domain so it would be interesting to test if that region is important for H2B K123ub (HWANG *et al.* 2003). Future studies characterizing Lge1 will shed light on the mechanism of H2B K123ub.

H2B K123ub is removed during transcription via the deubiquitylating enzymes Ubp8 and Ubp10 in a locus-specific manner (HENRY *et al.* 2003; DANIEL *et al.* 2004; EMRE *et al.* 2005; SCHULZE *et al.* 2011). As mentioned above, the SAGA DUB module binds to monoubiquitylated nucleosomes through the nucleosome acidic patch (MORGAN *et al.* 2016). Additionally, a recently identified histone modification, phosphorylation of residue Y58 on H2A, prevents deubiquitylation of H2B K123ub (BASNET *et al.* 2014).

Not surprisingly, addition of ubiquitin onto a histone results in a change in chromatin architecture. H2B K123ub disrupts higher order nucleosome structure, as shown in a study that used chemically defined nucleosome arrays (FIERZ *et al.* 2011). An intriguing finding from this study was that a different protein that was similar size to ubiquitin did not interfere with higher order structure formation, suggesting that the effect is specific to ubiquitin. In addition to higher order chromatin structure, local nucleosome density is affected by H2B K123ub. In the absence of

H2B K123ub, nucleosome occupancy is reduced, suggesting that H2B K123ub stabilizes nucleosome structures (BATTA *et al.* 2011). H2B K123ub correlates with nucleosome stability *in vitro* as well (CHANDRASEKHARAN *et al.* 2009). Together, these two studies suggest that H2B K123ub stabilizes nucleosomes to position them over promoters. Furthermore, H2B K123ub can inhibit Pol II occupancy at promoters of inactive genes but can enhance gene expression at active loci (BATTA *et al.* 2011).

H2B K123ub facilitates nucleosome dynamics (XIAO *et al.* 2005; PAVRI *et al.* 2006; FLEMING *et al.* 2008), and collaborates with the histone chaperone FACT in regulating transcription elongation (PAVRI *et al.* 2006). Both H2B K123ub and FACT recruitment promote efficient Pol II transcription elongation through chromatin (FORMOSA *et al.* 2002; PAVRI *et al.* 2006). H2B K123ub is so tightly linked with transcription elongation, it can be used to represent Pol II movement across a gene (FUCHS *et al.* 2014). In addition to promoting other histone marks related to transcription and facilitating elongation, H2B K123ub was shown to have a functional role in transcription termination (TOMSON *et al.* 2011). Therefore, the H2B ubiquitylation pathway is important in multiple facets of gene expression.

1.3.1.2 H3 methylation

Other post-translational histone modifications involved in transcription include methylation of various residues in H3. For example, H3K4 di- and tri-methylation, which is catalyzed by Set1 (KROGAN *et al.* 2002), is associated with active promoters, and this mark is involved in recruitment of histone acetyltransferase and deacetyltransferase complexes (LIU *et al.* 2005; POKHOLOK *et al.* 2005; TAVERNA *et al.* 2006; BARSKI *et al.* 2007; CRISUCCI AND ARNDT 2011). H3K79 di- and tri-methylation, a mark that is correlated with actively transcribed genes, is catalyzed by Dot1 (FENG *et al.* 2002; KOUSKOUTI AND TALIANIDIS 2005). Lysine 79 of H3 is

located in the globular region of H3, and dimethylation of this residue can locally alter the nucleosome surface (LU *et al.* 2008).

Set1 and Dot1 both depend on H2B K123ub for methylation. In a reconstituted system, it was shown that H2B K123ub directly stimulates H3 K4 methylation (KIM *et al.* 2013a). This study also found that the Set1 n-SET domain contains an RXXXRR motif that is critical for H3 K4 methylation. The methyltransferase Dot1 methylates ubiquitylated nucleosomes in a ubiquitin-dependent fashion (NGUYEN AND ZHANG 2011). Specifically, there is a region on ubiquitin that stimulates the methyltransferase activity of Dot1 (HOLT *et al.* 2015). The H4 tail of the nucleosome has a basic stretch of amino acids that stimulate Dot1 methyltransferase activity (FINGERMAN *et al.* 2007). This study also found an acidic set of residues in Dot1 that are required for Dot1 binding to the H4 tail. As mentioned previously, the Paf1C sits at the top of a modification cascade where Paf1C promotes H2B K123ub, which in turn promotes H3 K4me$^{2/3}$ and H3 K79me$^{2/3}$. These methyl marks then lead to histone acetylation and deacetylation (Fig. 9). Thus, one histone mark can result in significant consequences on chromatin architecture and gene expression.

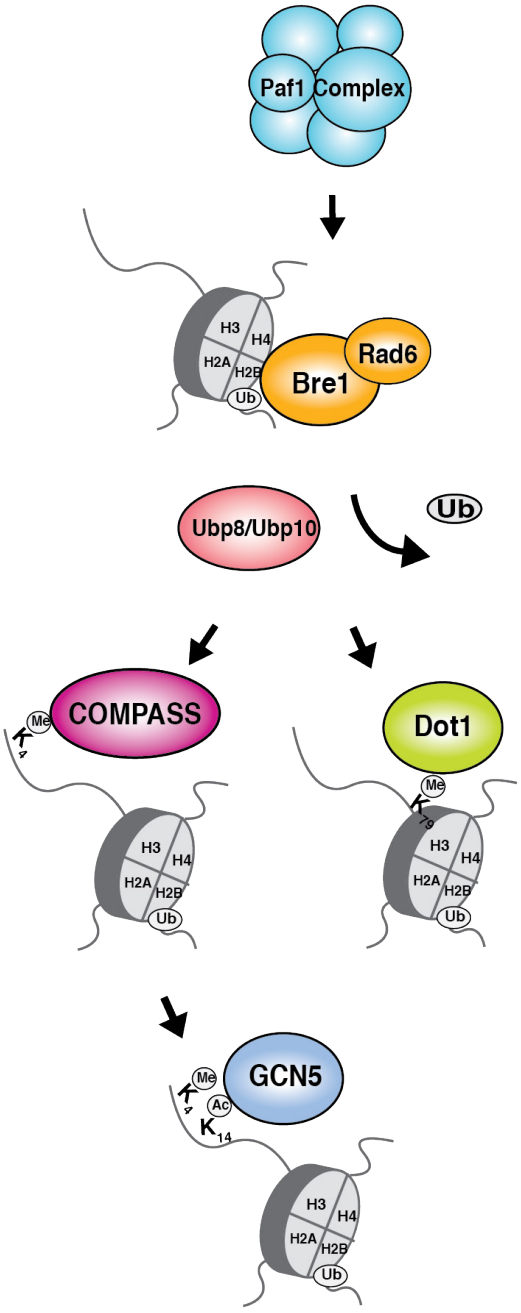

Figure 9. Histone modifications involved in transcription elongation

H2B K123ub cascade promoted by the Paf1C. Rad6/Bre1 are the enzymes that install ubiquitin onto H2B K123. Ubp8/Ubp10 are deubiquitylating enzymes that remove ubiquitin. COMPASS, containing Set1, methylates H3 K4 and Dot1 methylates H3 K79. Downstream acetylation occurs where Gcn5 is an acetyltransferase for H3 K14.

Modification	Modifier	Associated Factors
H2B K120ub (yeast: H2B K123ub)	Rad6, RNF20/40 (yeast: Rad6/Bre1)	WAC (humans), Lge1 (yeast), PAF1C, FACT, COMPASS/MLL, Dot1/Dot1L, SAGA
H2A Y57p (yeast: H2A Y58p)	Ck2	SAGA
H3 K4me$^{2/3}$	COMPASS/MLL	NuA3, Set3, PRMT6
H3 K79me$^{2/3}$	Dot1/Dot1L	
H3 K36me$^{2/3}$	SetD2, Set2 (yeast)	PAF1C, Cdk12, Chd1, Isw1, Rpd3S, Ctk1
H3 K14ac	Elp3, Gcn5, NuA3	
H3 R2me^{2}	PRMT6	MLL
H3 R17me2a	CARM1	hPAF1C

Table 3. Histone modifications involved in transcription elongation

Reviewed in (SMOLLE AND WORKMAN 2013)

1.3.2 Nucleosome dynamics

To allow for proper transcription, nucleosomes can be disassembled ahead of transcribing Pol II and reassembled in its wake. Histone chaperones are responsible for forming and breaking down nucleosomes in an ATP-independent manner (Fig. 10A). Typically, histone chaperones have acidic regions that interact with the basic histone residues. Important functions of histone chaperones are to prevent non-specific interactions between the DNA and the histones and to keep cellular pools of free histones to a minimum (HAMMOND *et al.* 2017). Chaperones are critical for correctly assembling functional nucleosomes by facilitating the stepwise assembly of histone complex intermediates. Structural studies have revealed that chaperones are multivalent proteins, with some chaperones able to bind dimers, tetramers, and assembly intermediates (HAMMOND *et al.* 2017). Many histone chaperones are involved in transcription elongation, such as FACT and

Spt6 (DUINA 2011). Spt6 interacts with Pol II, prevents cryptic initiation, and reorganizes nucleosomes during elongation. Spt6 can also increase the elongation rate on a naked DNA template (KWAK AND LIS 2013).

Chromatin remodeling enzymes can remove nucleosomes as well as slide them along DNA to minimize transcriptional barriers (Fig. 10B). Nucleosome positioning is also controlled by chromatin remodeling enzymes. For genes that are highly transcribed, nucleosomes are well-positioned, meaning that there is little variability in the mapping of these nucleosomes (STRUHL AND SEGAL 2013). Most genes with well positioned nucleosomes have a "+1 nucleosome," which is the first nucleosome downstream of the TSS. There is also a "-1" nucleosome, which is just upstream from the promoter. Between the -1 and +1 nucleosomes is a nucleosome free region, to which transcription factors can bind. Further downstream from the +1 nucleosome, positioning becomes more variable. However, generally the first three nucleosomes are well positioned compared to the 3'-end of the gene.

Until recently, it was difficult to distinguish how different remodeling enzymes position nucleosomes *in vivo*. A recent study (KRIETENSTEIN *et al.* 2016) generated a genome-wide reconstituted system to identify the functions of individual remodeling enzymes. They found that the RSC chromatin remodeling complex removes nucleosomes from promoters, while INO80 and ISW2 position +1 nucleosomes and nucleosomes downstream. ISW1 is required for spacing nucleosomes to previously characterized repeat lengths. These are just some examples of how chromatin remodeling enzymes function to properly maintain nucleosome occupancy across the genome. Here I will be discussing one other chromatin remodeling enzyme, Chd1, which has roles in elongation and interactions with the Paf1C. A summary of histone chaperones and chromatin remodelers involved in transcription elongation is located in Table 4.

1.3.2.1 FACT

The FACT complex is a histone chaperone that consists of Spt16, Pob3, and Nhp6 in yeast. FACT is conserved in humans, and is formed by Spt16 and SSRP1, which are homologous to both Pob3 and Nhp6 (FORMOSA 2012). FACT disassembles and reassembles nucleosomes during transcription (SCHWABISH AND STRUHL 2004), and also has the capability of evicting nucleosomes from inducible promoters (XIN *et al.* 2009). In addition to transcription elongation, FACT is required for histone recycling from the parent strand and nucleosome reassembly during DNA replication (RANSOM *et al.* 2010; YANG *et al.* 2016a).

FACT binds both dimers and tetramers in the nucleosome (WINKLER AND LUGER 2011; HAMMOND *et al.* 2017), and the Spt16 M domain binds to H3/H4 tetramers (TSUNAKA *et al.* 2016). Another study found that the N-domain of Spt16 binds to H3/H4 (STUWE *et al.* 2008). FACT interacts with histone tails, and the H2A docking domain is functionally important for FACT (VANDEMARK *et al.* 2008). However, the detailed interactions between FACT and nucleosomes remain controversial. Spt16 and Pob3 subunits bind to H2A/H2B to disrupt nucleosome structure (HONDELE *et al.* 2013; KEMBLE *et al.* 2015). In a FACT-nucleosome structure solved by the Ladurner lab (HONDELE *et al.* 2013), the M domain of Spt16 was shown to bind H2A/H2B. However, in a separate FACT/nucleosome structure solved by the Hill lab (KEMBLE *et al.* 2015), the acidic C-terminal tails of Spt16 and Pob3 bind the same regions of H2A/H2B. Kemble *et al.* suggest a model in which Spt16 binds one H2A/H2B dimer and Pob3 binds the other within the same nucleosome (KEMBLE *et al.* 2015). In this study, residues H2A R78 H2B Y45, and H2B M62 (located near the DNA binding site near the outside of the docking domain) were shown to be required for Spt16 and Pob3 binding. Hopefully, future studies will reconcile the differences between the structures.

1.3.2.2 Chd1

Chd1 is a chromatin remodeling enzyme that is conserved from yeast to humans and maintains proper nucleosome occupancy in transcriptionally active genes. Chd1 in yeast (yChd1) belongs to the CHD family of chromatin remodeling enzymes, which are characterized by having two tandem chromodomains and a Snf2-like ATPase domain (MARFELLA AND IMBALZANO 2007). Although Chd1 is enriched at nucleosome-free regions, it mainly functions in gene bodies to promote transcription-coupled nucleosome turnover (ZENTNER *et al.* 2013). yChd1 was recently shown to be important for H3 K4me^3 and H3 K36me^3 localization across the yeast genome (LEE *et al.* 2017). Human Chd1 is recruited by H3 K4me$^{2/3}$ but binds monomethylated H3 K4 with lower affinity (SIMS *et al.* 2005). yChd1lacks the ability to bind methylated H3 K4, thus other factors are important in Chd1 recruitment (MURAWSKA AND BREHM 2011). Indeed, in a mutant in which the N-terminal region of Rtf1 is deleted, Chd1 occupancy levels are reduced (WARNER *et al.* 2007). yChd1 also interacts with elongation factors Spt4-Spt5 and the FACT complex (SIMIC *et al.* 2003). An important function of yChd1 is to repress transcription from within gene bodies (CHEUNG *et al.* 2008). Additionally, it was also recently reported that yChd1 can shift hexasomes in a manner dependent on an H2A/H2B dimer (hexasomes are nucleosome structures that lack one H2A/H2B dimer) (LEVENDOSKY *et al.* 2016). Interestingly, this study also showed that H2B K123ub enhanced the sliding of hexasomes by Chd1. This result suggests that Chd1 could be involved in moving (partial) nucleosomes during transcription elongation and provides an additional role for H2B K123ub.

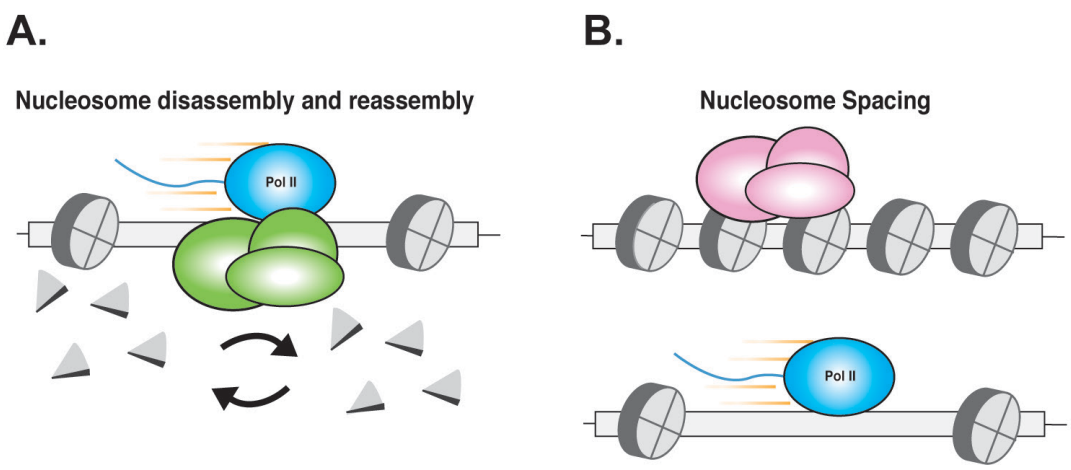

Figure 10. Rearrangement of nucleosomes during transcription

(A) Simplified diagram of nucleosomes being disassembled and reassembled during transcription. These activities are largely carried out by histone chaperones. **(B)** Cartoon depicting altered spacing between nucleosomes, an outcome achieved either by the removing or sliding of nucleosomes by chromatin remodeling enzymes.

Protein	Function	Role in Elongation
FACT	Histone chaperone complex of human: hSpt16, Ssrp1 yeast: Spt16, Nhp6, Pob3	Displaces H2A-H2B dimer in the wake of transcribing Pol II; evicts nucleosome; reassembles nucleosomes; regulates H2BK12oub; prevents cryptic transcription
Spt6	Histone chaperone	Prevents cryptic transcription, required for proper histone occupancy during elongation
Asf1	Histone chaperone	Controls H3 exchange during transcription
Nap1	Histone chaperone	Binds H2A-H2B and forms hexasome structures through RSC, promotes nucleosome assembly
Rtt106	Histone chaperone	Binds H3-H4 and promotes transcription-coupled H3 deposition; prevents cryptic initiation
Chd1	Chromatin remodeler	Controls nucleosome spacing and histone exchange, slides hexasomes, promotes Pol II promoter escape (mammals)
ISW1	Chromatin remodeler	Controls nucleosome spacing and histone exchange
RSC	Chromatin remodeler	Helps Pol II passage through nucleosomes and maintains proper nucleosome occupancy

Table 4. Histone chaperones and chromatin remodeling enzymes involved in transcription elongation

Adapted from (CUCINOTTA AND ARNDT 2016)

1.4 THE IMPORTANCE OF STUDYING CHROMATIN AND TRANSCRIPTION

Understanding the mechanisms that regulate chromatin structure and transcription is fundamental to the study of life. Chromatin regulates transcription at the earliest step and is essential for promoting and maintaining organismal homeostasis. For example, mutations in the

SET-domain containing methyltransferase gene *MLL* (mixed-lineage leukemia) lead to human leukemia (AYTON AND CLEARY 2001).

Telomeric silencing plays a role in regulating cellular life span (AUSTRIACO AND GUARENTE 1997). The non-SET domain containing methyltransferase Dot1 was initially discovered in a screen to identify defects in telomeric silencing in yeast (SINGER *et al.* 1998), and later it was found that the H3K79 methylation mark was required for proper telomeric silencing (NG *et al.* 2002a). Human Dot1 is conserved, and is capable of methylating H3K79 as well, and it is involved in Wnt signaling (MOHAN *et al.* 2010). Human Dot1-mediated H3K79 methylation is also critical in cardiomyocyte function, via its regulation of dystrophin (NGUYEN *et al.* 2011).

Human Bre1 (hBre1/RNF20), the E3 ligase responsible for H2B K120ub, is suggested to be a tumor suppressor, as down regulation of hBre1 results in decreased p53 expression (SHEMA *et al.* 2008).

Histone mutations themselves are associated with disease. Arguably the most intensely studied histone mutation is the mutation of the *H3F3A* gene that encodes the histone variant H3.3 (SCHWARTZENTRUBER *et al.* 2012). One of the mutations results in a lysine 27 substitution with methionine. Mutation of this gene is present in severe forms of adult and pediatric gliomas (SCHWARTZENTRUBER *et al.* 2012). One consequence of this mutation is the inhibition of PRC2 (LEWIS *et al.* 2013), which is a critical in regulating gene expression by methylating the H3 K27, a mark associated with gene repression. Thus, chromatin is more open in cells lacking PRC2 function, allowing for aberrant gene expression and ultimately cancer (MARGUERON AND REINBERG 2011).

Further highlighting the role of chromatin regulation in organismal homeostasis, the Paf1C has been implicated in a variety of diseases, including heart disease and cancer. For example, high

levels of the Paf1 subunit have been detected in a variety of cancers (CHAUDHARY *et al.* 2007). The Paf1C subunit Cdc73, also known as parafibromin in humans, is a tumor suppressor, and mutations in the protein result in hyperparathyroidism-jaw tumor syndrome (NEWEY *et al.* 2009; CASCON *et al.* 2011). Underscoring the importance of Paf1C in organismal homeostasis, the Paf1C is also critical in cardiomyocyte development (NGUYEN *et al.* 2010; LANGENBACHER *et al.* 2011; TOMSON AND ARNDT 2012).

While the function of the Nrd1-Nab3-Sen1 complex in humans remains to be defined, mutations in the human homolog of the yeast Sen1, senataxin, are linked to amyotrophic lateral sclerosis (ALS) (HIRANO *et al.* 2011). Furthermore, down-regulation of senataxin in cell lines resulted in deficient transcription termination (SURAWEERA *et al.* 2009). From these examples, it is apparent that transcriptional control is critical for human health, and control of gene expression at the level of chromatin is one of the first steps in gene regulation that play a role in preventing human disease.

2.0 THE NUCLEOSOME ACIDIC PATCH REGULATES THE H2B K123 MONOUBIQUITYLATION CASCADE AND TRANSCRIPTION ELONGATION

The work in this chapter was published in the open access journal *PLOS Genetics* (CUCINOTTA *et al.* 2015) and is re-printed here in altered form, in accordance with the Creative Commons Attribution (CC BY) license, © Cucinotta et al. 2015.

2.1 INTRODUCTION

In eukaryotes, transcription and other nuclear processes take place in the context of chromatin. The basic unit of chromatin is the nucleosome, which consists of approximately 147 base pairs of DNA wrapped around a histone octamer, containing two copies of each of the four core histone proteins: H2A, H2B, H3, and H4 (LUGER *et al.* 1997). Histones are decorated with posttranslational modifications, which can alter chromatin architecture and recruit a wide range of proteins to the genome, thus regulating all chromatin transactions (ZENTNER AND HENIKOFF 2013). In addition to their intrinsic effects on modulating the chromatin template, certain histone modifications can promote other histone modifications, either on the same histone (*cis*-regulation) or on a different histone (*trans*-regulation) in a process termed "histone crosstalk" (FISCHLE *et al.* 2003).

The monoubiquitylation of H2B on lysine 123 (H2B K123ub) in *S. cerevisiae* is associated with active gene transcription, impacts global nucleosome occupancy and plays important roles in transcription elongation, telomeric silencing, DNA replication, and DNA repair (FUCHS AND OREN

2014). In yeast, this modification is catalyzed by the ubiquitin-protein ligase Bre1 and the ubiquitin-conjugating enzyme Rad6 (ROBZYK *et al.* 2000; HWANG *et al.* 2003; WOOD *et al.* 2003a). In humans, the analogous lysine, H2B K120, is ubiquitylated by RNF20/RNF40 and RAD6A/RAD6B (KIM *et al.* 2005; KIM *et al.* 2009). In one of the best-studied examples of histone crosstalk, H2B K123ub is required for other histone modifications associated with active transcription: H3 K4 and H3 K79 di- and tri-methylation (BRIGGS *et al.* 2002; DOVER *et al.* 2002; SUN AND ALLIS 2002). H3 K4 dimethylation, which is enriched at the 5'-ends of coding regions, and H3 K4 trimethylation, which is associated with active promoters, regulate histone acetylation patterns on genes by directing the recruitment of histone acetyltransferases and histone deacetylases (LATHAM AND DENT 2007). H3 K79 methylation occurs across active genes, and dimethylation of this residue locally alters the nucleosome surface (LIU *et al.* 2005; LU *et al.* 2008). All of these histone modifications are conserved in higher eukaryotes, and disruption of these modifications can result in a range of human diseases, including cancer (PORTELA AND ESTELLER 2010).

In addition to Rad6 and Bre1, several protein complexes that regulate transcription elongation and nucleosome dynamics are required for wild-type levels of H2B K123ub. These include the Bur1-Bur2 cyclin-dependent kinase complex and the FACT histone chaperone complex (WOOD *et al.* 2005; PAVRI *et al.* 2006; FLEMING *et al.* 2008). Additionally, the Polymerase Associated Factor 1 complex (Paf1C), which travels with RNA pol II and Spt5 during transcription elongation, promotes H2B K123ub through the Rtf1 subunit of the complex (NG *et al.* 2003; WOOD *et al.* 2003b; WARNER *et al.* 2007; PIRO *et al.* 2012). While protein complexes that promote H2B K123ub have been identified, little is known about how the nucleosome itself promotes H2B K123ub.

We previously reported that the ubiquitin-protein ligase Rkr1/Ltn1 is required for the viability of yeast cells that lack the *RTF1* gene or harbor an amino acid substitution for H2B K123 that prevents ubiquitylation (H2B-K123R) (BRAUN *et al.* 2007). Rkr1/Ltn1 associates with ribosomes and degrades nonstop proteins (BENGTSON AND JOAZEIRO 2010; BRANDMAN *et al.* 2012). The genetic interactions between *rtf1*Δ*, H2B-K123R*, and *rkr1*Δ suggest a requirement for the quality control functions of Rkr1 in the absence of an intact H2B ubiquitylation pathway. We reasoned that the negative genetic interactions between *rkr1*Δ and H2B-K123R could be exploited to identify histone residues that are required for H2B K123ub. Using a genetic screen, we identified H2A and H2B residues required for proper H2B K123ub and downstream histone modifications. Many of these residues map to the acidic patch on the surface of H2A. We found that amino acid substitutions in the acidic patch cause defects in the recruitment of the H2B K123ub machinery to active genes, an accumulation of read-through transcripts, and altered transcription elongation efficiency *in vivo*. Interestingly, the substitutions differentially impact histone modifications downstream of H2B K123ub. Therefore, while the H2A acidic patch residues functionally converge in regulating H2B K123ub, they diverge in regulating downstream histone modifications. Our data reveal a requirement for the nucleosome acidic patch in H2B K123ub and argue that this exposed nucleosome surface serves as an important protein docking site in which individual residues uniquely contribute to the regulation of histone modifications and gene expression.

2.2 MATERIALS AND METHODS

2.2.1 Yeast strains and media

The *S. cerevisiae* strains used in this study are listed in Table 5 and are isogenic to the strain FY2, which is a *GAL2*$^{+}$ derivative of S288C (WINSTON *et al.* 1995). Yeast transformations were performed as previously described (AUSUBEL FM 1988)). With noted exceptions, experiments were performed using the strain KY943 transformed with histone mutant plasmids. To replace wild-type histone plasmids with *HIS3*-marked mutant histone plasmids, transformants were sequentially passaged three times on SC-His medium containing 2% dextrose and 0.1% 5-FOA. Unless otherwise noted, for all experiments, yeast strains were grown in SC-His medium containing 2% dextrose. HSV-Bre1 and HSV-Set1 strains contain three chromosomally located HSV tags on the N-termini of the proteins (MOQTADERI AND STRUHL 2008). These proteins were checked for proper function and expression.

2.2.2 Dilution growth assays

Cells were grown to saturation at 30°C and washed with sterile water. Beginning with a cell suspension at a concentration of 1 X 10^{8} cells/mL, cells were diluted serially four times by a factor of ten in water. Two microliters of each dilution were spotted on SC-His medium and SC-His medium containing 5-FOA. Plates were incubated at 30°C for three days.

2.2.3 Plasmid construction

Site-directed mutagenesis (Agilent) with the primers AYO12 (5'-ccatacacacatacaatgtctgctaaagccg-3') and AYO13 (5'-cggctttagcagacattgtatgtgtgtatc-3') was performed to remove the sequence encoding the FLAG tag from plasmids obtained from the H2A and H2B mutant library (NAKANISHI *et al.* 2008a). Plasmid sequences were confirmed by DNA sequencing.

2.2.4 Western blot analysis

For western analyses other than those that measure H2B K123ub, yeast cells were grown to log phase (2-3 X 10^7 cells/mL) and lysed by bead beating in trichloroacetic acid (TCA), as described previously (COX *et al.* 1997). To make whole cell extracts for H2B K123ub analysis, cells were lysed in SUTEB buffer (10 mM Tris-HCl, pH 8.0, 1% SDS, 8 M urea, 10 mM EDTA, pH 8.0, and 0.01% bromophenol blue) (TOMSON *et al.* 2011). Proteins were resolved on SDS-polyacrylamide gels (15% polyacrylamide for histone westerns, 10% polyacrylamide for Rtf1 and HSV-Bre1, and 8% polyacrylamide for HSV-Set1, Spt5, and Spt16 westerns) and transferred to nitrocellulose membranes. For H2B K123ub western blot analysis, proteins were transferred to PVDF membranes. Membranes were incubated with primary antibodies and then with anti-mouse or anti-rabbit secondary antibodies (GE Healthcare 1:5,000 dilution). Antibodies that recognize the following proteins or histone modifications were used: total histone H3 (1:30,000 dilution) (TOMSON *et al.* 2011), trimethylated H3 K4 (H3 K4me^3) (Active Motif 39159, 1:2,000 dilution), H3 K4me^2 (Millipore 07-030, 1:2000 dilution), H3 K79me^3 (note: this antibody has been reported by the manufacturer to cross-react with H3 K79me^2, Abcam ab2621, 1:2,000 dilution), H3 K36me^2

(Millipore 07-369, 1:1000 dilution), H3 K36me^3 (Abcam ab9050, 1:1000 dilution), H2A (Active Motif, 39235, 1:5,000 dilution), H2B (Active Motif, 39237, 1:5,000 dilution), HSV (Sigma-Aldrich H6030, 1:350 dilution), Spt5 (gift from Grant Hartzog, 1:1000 dilution), Spt16 (gift from Tim Formosa, 1:500 dilution), Rtf1 (1:5,000 dilution) (SQUAZZO *et al.* 2002a), and glucose-6-phosphate dehydrogenase (G6PDH) (Sigma-Aldrich A9521, 1:30,000 dilution). An antibody against a human H2B K120ub-containing peptide (Cell Signaling 5546, 1:1000 dilution) was used to detect the analogous modification in *S. cerevisiae*, H2B K123ub. Proteins were visualized using enhanced chemiluminescence substrate (PerkinElmer) and either a 440 CF digital imaging station (Kodak) or a ChemiDoc XRS digital imaging station (BioRad). For western blot analysis, signals were quantified using ImageJ software and normalized to the loading control specified in the figure legend. The relative signal from the wild-type strain was set equal to one. Error bars represent standard error of the mean for three biological replicates (SEM).

2.2.5 Chromatin immunoprecipitation (ChIP) and quantitative PCR assays

Chromatin immunoprecipitation (ChIP) assays were performed with 250 mL of log-phase yeast cultures (1-2 X 10^7 cells/mL) as previously described (SHIRRA *et al.* 2005). For histone ChIPs, sheared chromatin was incubated overnight at 4°C with antibodies specific to H2B, (0.5 µl, Active Motif, 39237), human H2B K120ub (2.5 µl, Cell Signaling 5546), H3 K4me^3 (2.5 µl, Abcam ab8580), H3 K79me$^{2/3}$ (2.5 µl, Abcam ab2621), or total H3 (5 µl) (TOMSON *et al.* 2011). Chromatin prepared from an H2B-K123R strain served as a specificity control for the human H2B K120ub antibody (not shown). For other ChIPs, chromatin was incubated overnight at 4°C with antibodies specific to Spt16 (1 µl, gift from Tim Formosa), Spt5 (1 µl, gift from Grant Harzog), or Rpb3 (2.5 µl Neoclone W0012). Following incubation with the primary antibodies, chromatin was

incubated for 2 hours at 4°C with Protein A-conjugated sepharose for all ChIPs, with the exception of Rpb3 ChIPs, for which chromatin was incubated with Protein G-conjugated sepharose (30 µl, GE Healthcare). For ChIP of HSV-Bre1 and HSV-Set1, chromatin was incubated overnight at 4°C with an antibody specific to the HSV epitope (2.5 µl, Sigma-Aldrich H6030), followed by incubation as described above. For ChIP of Rtf1, chromatin was incubated overnight at 4°C with polyclonal antisera that recognizes Rtf1 (SQUAZZO *et al.* 2002a). DNA was purified (Qiagen) and analyzed by qPCR using Maxima SYBR (Thermo) and primers for the 5' coding region of *PYK1* (amplicon: +253 to +346 relative to ATG), the 3' coding region of *PYK1* (amplicon: +1127 to +1270), the 5' coding region of *PMA1* (amplicon: +214 to +319 relative to ATG), the 3' coding region of *PMA1* (amplicon: +2107 to +2194), or a telomeric region of chromosome VI (chromosomal coordinates, 269495 to 269598). Occupancy levels were calculated using the primer efficiency raised to the difference between input and immunoprecipitated Ct values. Presented data are an average of two technical replicates for each of three biological replicates. The error bars indicate the standard error of the mean (SEM).

2.2.6 Northern blot analysis

Total RNA was isolated from log-phase yeast cultures (1-2 X 10^7), and 20 µg of RNA were subjected to northern blot analysis as described previously (SWANSON *et al.* 1991). Radiolabeled DNA probes were generated through random-prime labeling reactions of PCR templates. Membranes (Gene Screen Plus, Perkin Elmer) were incubated with radiolabeled DNA probes from PCR fragments of *SCR1* (amplicon: -163 to +284 relative to the TSS), *SRG1* (amplicon: -454 to -123 relative to *SER3* ATG), *SER3* (amplicon: +111 to +1342 relative to ATG), and *FLO8* (amplicon: +1515 to + 2326 relative to ATG). Signals were quantified using ImageJ software

relative to the *SCR1* loading control, with wild type set to one. For quantification of all northern blot analyses, signals were averaged for three independent biological replicates. Error bars represent standard error of the mean (SEM).

2.2.7 Quantitative real-time reverse transcription-PCR (RT-qPCR)

Total RNA was isolated as described above and then DNase treated using the Turbo DNA-free kit (Ambion, AM1907) and RNase inhibitor (Ambion, AM2682). cDNA was generated using the RETROscript kit (Ambion, AM1710) with random hexamers and oligo(dT) primers. Quantitative PCRs were performed as described above using primers specific for the regions downstream of snoRNAs (Table 3 for primers used). Signals were analyzed using the ΔΔCT method with *ACT1* used as the target gene (LIVAK AND SCHMITTGEN 2001). For controls, reactions lacking reverse transcriptase or template were performed. The graphs show the results of three independent biological replicates.

Strain	*MAT*	Genotype
KY943	**a**	(*hta1-htb1*)Δ::*LEU2* (*hta2-htb2)Δ::TRP1 his3Δ200 lys2-128δ leu2Δ1 ura3-52* [pSAB6 = *URA3/C/A/HTA1-HTB1*]
KY981	**a**	(*hta1-htb1*)Δ::*LEU2 hta2-htb2Δ::TRP1 rkr1ΔKanMX4 his3Δ200 lys2-128δ leu2Δ1 ura3-52* [pSAB6 = *URA3/C/A/HTA1-HTB1*]
KY1599	**a**	*(hta1-htb1)Δ::LEU2 (hta2-htb2)Δ::KanMX6 rtf1ΔKanMX4 his3Δ200 lys2-128δ leu2Δ1 trp1Δ63 ura3-52* [pSAB6 = *URA3/C/A/HTA1-HTB1*]
KY1700	α	*paf1Δ::KanMX4*
KY1715	**a**	*set1Δ::KanMX4*
KY1717	**a**	*dot1Δ::KanMX4*
KY1716	**a**	*set2Δ::KanMX4*
KY2044	**a**	*HTA1-htb1K123R (hta2-htb2*)Δ::*KanMX his3Δ200 leu2Δ1 trp1Δ63 ura3Δ0*
KY2086	α	*(hta1-htb1)Δ::LEU2 (hta2-htb2)Δ::KanMX ubp8Δ::NATMX his3Δ200 lys2-128δ leu2Δ1 trp1Δ63 ura3-52* [pDC92 = *URA3/HTA1-HTB1*/2-micron]
KY2249	**a**	(*hta1-htb1*)Δ::*LEU2* (*hta2-htb2)Δ::TRP1 his3Δ200 lys2-128δ leu2Δ1 ura3-52* [pAY01 = *HIS3/C/A/HTA1-FLAG-HTB1*]
KY2265	**a**	*(hta1-htb1)Δ::LEU2 (hta2-htb2)Δ::TRP1 his3Δ200 lys2-128δ leu2Δ1 trp1Δ63 ura3-52* [pRS313 = *HIS3*/C/A] [pSAB6 = *URA3/C/A/HTA1-HTB1*]
KY2674	**a**	*(hta1-htb1)Δ::LEU2 (hta2-htb2)Δ::TRP1 3XHSV-BRE1 his3Δ200 leu2Δ1 trp1Δ63 ura3-52* [pSAB6 = *URA3/C/A/HTA1-HTB1*]
KY2675	α	*(hta1-htb1)Δ::LEU2 (hta2-htb2)Δ::KanMX6, RAD6-13XMYC::KanMX his3Δ200 leu2Δ1 trp1Δ63 ura3-52* [pSAB6 = *URA3/C/A/HTA1-HTB1*]
KY2676	**a**	(*hta1-htb1*)Δ::*LEU2* (*hta2-htb2Δ)::TRP1 GAL1pr-YLR454W::KanMX6 his3Δ200 lys2-128δ leu2Δ1 ura3-52* [pSAB6 = *URA3/C/A/HTA1-HTB1*]
KY2677	α	wild-type prototroph
KY2678	α	*spt6-1004*
KY2679	α	*spt16-197*
KY2719	**a**	*(hta1-htb1)Δ::LEU2 (hta2-htb2)Δ::KanMX6 3XHSV-SET1 his3Δ200 leu2Δ1 trp1Δ63 ura3-52 arg4-12* [pSAB6 = *URA3/C/A/HTA1-HTB1*]

Table 5. Strains used in this study

Primer	Dir.	Sequence	Ref.
Removal of the FLAG tag	F R	5'-CCATACACACATACAATGTCTGCTAAAGCCG-3' 5'-CGGCTTTAGCAGACATTGTATGTGTGTATGG-3'	This study
PYK1 5' ChIP primer set	F R	5'ACGATCTTCTACAATATCGATTCTACCA-3' 5'-TTCTTACGAATACCACAAGTCTGTCA-3'	(LIU *et al.* 2009)
PYK1 3' ChIP primer set	F R	5'-GCAATGGCCAATGGTCTACCT-3' 5'-AACCTCCACCACCGAAACC-3'	(LIU *et al.* 2009)
PMA1 5' ChIP primer set	F R	5'-GCTAGACCAGTTCCAGAAGAATATTTACA-3' 5'-CAGCCATTTGATTCAAACCGTA-3	(LIU *et al.* 2009)
PMA1 3' ChIP primer set	F R	5'-GAAATCTTCTTGGGTCTATGGATTG-3' 5'-CAACATCAGCGAAAATAGCGAT-3'	(LIU *et al.* 2009)
TELVI ChIP primer set	F R	5'-TGCAAGCGTAACAAAGCCATA-3' 5'-TCCGAACGCTATTCCAGAAAG-3'	(LIU *et al.* 2009)
SER3 Northern probe	F R	5'-TCTGCTAAGATCTCAATTAGATTG-3' 5'-CAAGGATGTCATCGAAGAGGC-3'	(HAINER AND MARTENS 2011)
SRG1 Northern probe	F R	5'-TGGTTAAGCAGTTAGGCTGG-3' 5'-TTTCCTTATCCTCTGCTCCC-3'	(HAINER AND MARTENS 2011)
SCR1 Northern probe	F R	5'-CAACTTAGCCAGGACATCCA-3' 5'-AGAGAGACGGATTCCTCACG-3'	(HAINER AND MARTENS 2011)
FLO8 Northern probe	F R	5'-TGATGCCACTAAGGATGAGA-3' 5'-GGTCTTCAACCATACCAATA-3'	(HAINER AND MARTENS 2011)
SNR47-YDR042C qRT-PCR	F R	5'-CAACAACATGAATTTCTTCGTCCGAATCC-3' 5'-CCGCCTTTCTTCTTGGAAATTGGTAACAGG-3'	(TOMSON *et al.* 2013)

Table 6. Primers used in this study

Plasmid	Histone	Derivation and reference
pAY01	WT untagged	Site directed mutagenesis of pZS145; this study
pCEC01	F26A	This study. Site directed mutagenesis of library plasmid from (NAKANISHI *et al.* 2008a)
pCEC02	E57A	This study. Site directed mutagenesis of library plasmid from (NAKANISHI *et al.* 2008a)
pCEC03	E65A	This study. Site directed mutagenesis of library plasmid from (NAKANISHI *et al.* 2008a)
pCEC04	L66A	This study. Site directed mutagenesis of library plasmid from (NAKANISHI *et al.* 2008a).
pCEC05	L86A	This study. Site directed mutagenesis of library plasmid from (NAKANISHI *et al.* 2008a)
pCEC06	E93A	This study. Site directed mutagenesis of library plasmid from (NAKANISHI *et al.* 2008a)
pCEC07	L94A	This study. Site directed mutagenesis of library plasmid from (NAKANISHI *et al.* 2008a)
pCEC08	H113A	This study. Site directed mutagenesis of library plasmid from (NAKANISHI *et al.* 2008a)
pJH23KR	K123R	Site directed mutagenesis of pJH23 (NG *et al.* 2002b)
pZS145	WT FLAG-H2B	(SUN AND ALLIS 2002)

Table 7. Plasmids used in this study.

2.3 RESULTS

2.3.1 A genetic screen to identify histone residues important for H2B K123ub

To identify histone residues required for H2B K123ub in *S. cerevisiae*, we screened a comprehensive histone mutant library (NAKANISHI *et al.* 2008a) for alanine substitutions in H2A and H2B that cause synthetic lethality or sickness when combined with a deletion of the *RKR1* gene. We previously showed that *rkr1*Δ is synthetically lethal in strains carrying H2B-K123R as the only form of H2B (BRAUN *et al.* 2007). Using a plasmid shuffle strategy, *HIS3*-marked *hta1-HTB1* or *HTA1-htb1* plasmids from the library were transformed into a *rkr1*Δ deletion strain, replacing a *URA3*-marked plasmid carrying wild-type copies of *HTA1* and *HTB1*. The *URA3*-marked wild-type plasmid was counter-selected on medium containing 5-fluoroorotic acid (5-FOA). Relative to their effects on a strain containing a wild-type *RKR1* gene, nine histone mutant plasmids caused enhanced growth defects in the *rkr1*Δ background (Fig. 11A). Eight of the amino acid substitutions were located in H2A, and one was H2B-K123A (Fig. 11A). Identification of H2B-K123A served as a validation of our screen.

Many of the residues identified in our screen cluster within the nucleosome acidic patch (Fig. 11B and 11C). The acidic patch serves as a binding site for several proteins, including the H4 tail of neighboring nucleosomes (LUGER *et al.* 1997; KALASHNIKOVA *et al.* 2013; WILKINS *et al.* 2014; MCGINTY AND TAN 2015). In addition to those in the acidic patch, two residues, L86 and H113, reside near the docking domain of H2A (LUGER *et al.* 1997).

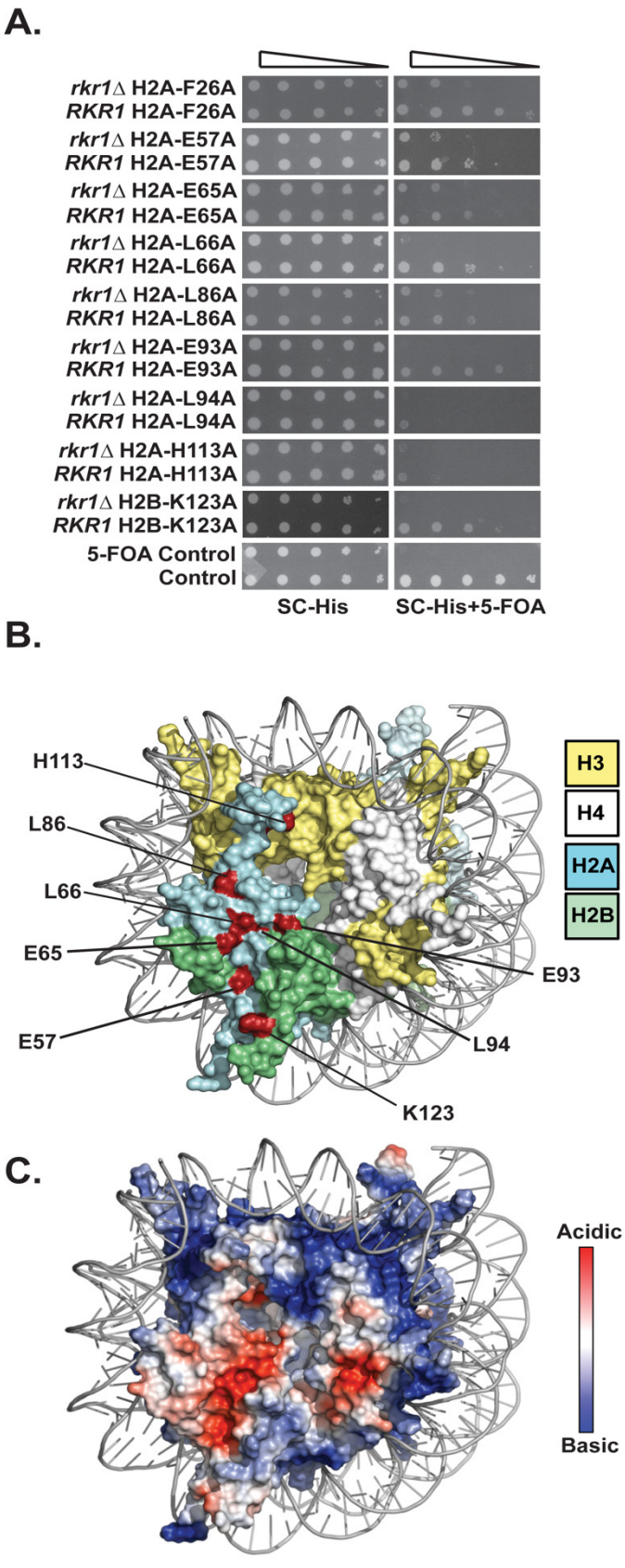
A.
rkr1Δ H2A-F26A
RKR1 H2A-F26A
rkr1Δ H2A-E57A
RKR1 H2A-E57A
rkr1Δ H2A-E65A
RKR1 H2A-E65A
rkr1Δ H2A-L66A
RKR1 H2A-L66A
rkr1Δ H2A-L86A
RKR1 H2A-L86A
rkr1Δ H2A-E93A
RKR1 H2A-E93A
rkr1Δ H2A-L94A
RKR1 H2A-L94A
rkr1Δ H2A-H113A
RKR1 H2A-H113A
rkr1Δ H2B-K123A
RKR1 H2B-K123A
5-FOA Control
Control
SC-His
SC-His+5-FOA
B.
H113
L86
L66
E65
E57
E93
L94
K123
H3
H4
H2A
H2B
C.
Acidic
Basic

Figure 11. Identification of H2A and H2B residues required for growth in the absence of *RKR1*.

(A) Synthetic lethal/sick phenotypes of *rkr1*Δ *hta1* and *rkr1*Δ *htb1* mutants were assessed through ten-fold serial dilution assays. Double mutant cells, as well as control *RKR1 hta1* and *RKR1 htb1* cells, were plated on SC-His medium as a growth control and on SC-His + 5-FOA medium to select for histone mutant plasmids and against the *URA3*-marked *HTA1-HTB1* plasmid. Library plasmids were transformed into the *rkr1*Δ strain KY981 and wild-type strain KY943. KY2676 and KY2265 were used as respective negative and positive growth controls on 5-FOA plates. (**B)** X-ray crystal structure of the nucleosome, denoting histones H2A, H2B, H3, and H4 in cyan, green, yellow, and white, respectively. As depicted in red, the majority of histone residues identified in the *rkr1*Δ synthetic lethality screen form a surface-exposed patch on the nucleosome. **(C)** Electrostatic potential (red is negative, blue is positive) of the nucleosome core particle. This figure was created using Pymol (PDB 1ID3 (WHITE *et al.* 2001)).

To test if the amino acid substitutions in H2A cause H2B K123ub defects, we assessed global H2B K123ub levels by western blot analysis. Because the plasmids in the H2A and H2B mutant libraries encode FLAG-tagged H2B (NAKANISHI *et al.* 2008a), we initially used anti-FLAG western blots to distinguish H2B K123ub from unmodified H2B as a super-shifted band. We subsequently turned to a commercial antibody against human H2B K120ub, which can specifically detect yeast H2B K123ub (WOZNIAK AND STRAHL 2014) (Fig. 12). Surprisingly, this antibody did not recognize FLAG-tagged H2B K123ub to the same degree as untagged H2B K123ub in our strains, raising concerns that the FLAG tag could influence H2B ubiquitylation or our ability to detect this modification (Fig. 7). Therefore, we removed the FLAG tag from all of the plasmids carrying *hta1-HTB1* mutations identified in our screen, and we continued with these constructs for all experiments in this study. The western analysis revealed that all of the H2A mutants have reduced global H2B K123ub levels compared to the wild-type control strain; however, the different substitutions affect H2B K123ub levels to varying degrees (Fig. 13A). For example, there is a striking difference in H2B K123ub levels in strains harboring substitutions of the neighboring residues H2A-E65 and H2A-L66 (Fig. 13A, lanes 4 and 5). Our result reflects the H2B K123ub defect previously observed for an H2A-L66A mutant (NAKANISHI *et al.* 2008a); however, with removal of the FLAG tag, we now detect a defect in H2B K123ub in the H2A-E65A mutant as well.

To measure chromatin-associated levels of H2B K123ub, we performed chromatin immunoprecipitation (ChIP) analysis of H2B K123ub and total H2B at active genes (*PYK1* and *PMA1*) and, as a control, at a non-transcribed region (*TELVI*). We normalized levels of H2B K123ub to levels of total H2B to correct for any defects in H2B occupancy (Fig. 13B). For these ChIP analyses, and most other experiments in this study, we focused our efforts on H2A residues

E57, E65, L66, L86, and E93, because residues F26 and L94 are buried within the protein core of the nucleosome and could be impacting H2B K123ub levels indirectly (Fig. 6A). We also chose not to focus on H113, because it is not conserved in higher eukaryotes. In agreement with the western analyses, the ChIP assays revealed reduced H2B K123ub levels on active genes in the H2A mutant strains (Fig. 8B). However, gene-specific defects are evident. For example, the E57A substitution causes an H2B K123ub defect at *PYK1* but not *ADH1* or *PMA1* (Fig. 13B and 19). Together these data demonstrate that the nucleosome acidic patch promotes H2B K123ub globally and at specific genes.

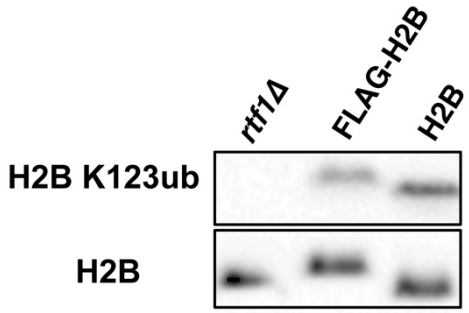

Figure 12. The FLAG epitope tag impacts H2B K123ub detection.

Western analysis of H2B K123ub in yeast strains carrying untagged (lane 1) or FLAG-tagged H2B (lane 2). Western blots were probed with antibodies against human H2B K120ub and total H2B, which served as a loading control.

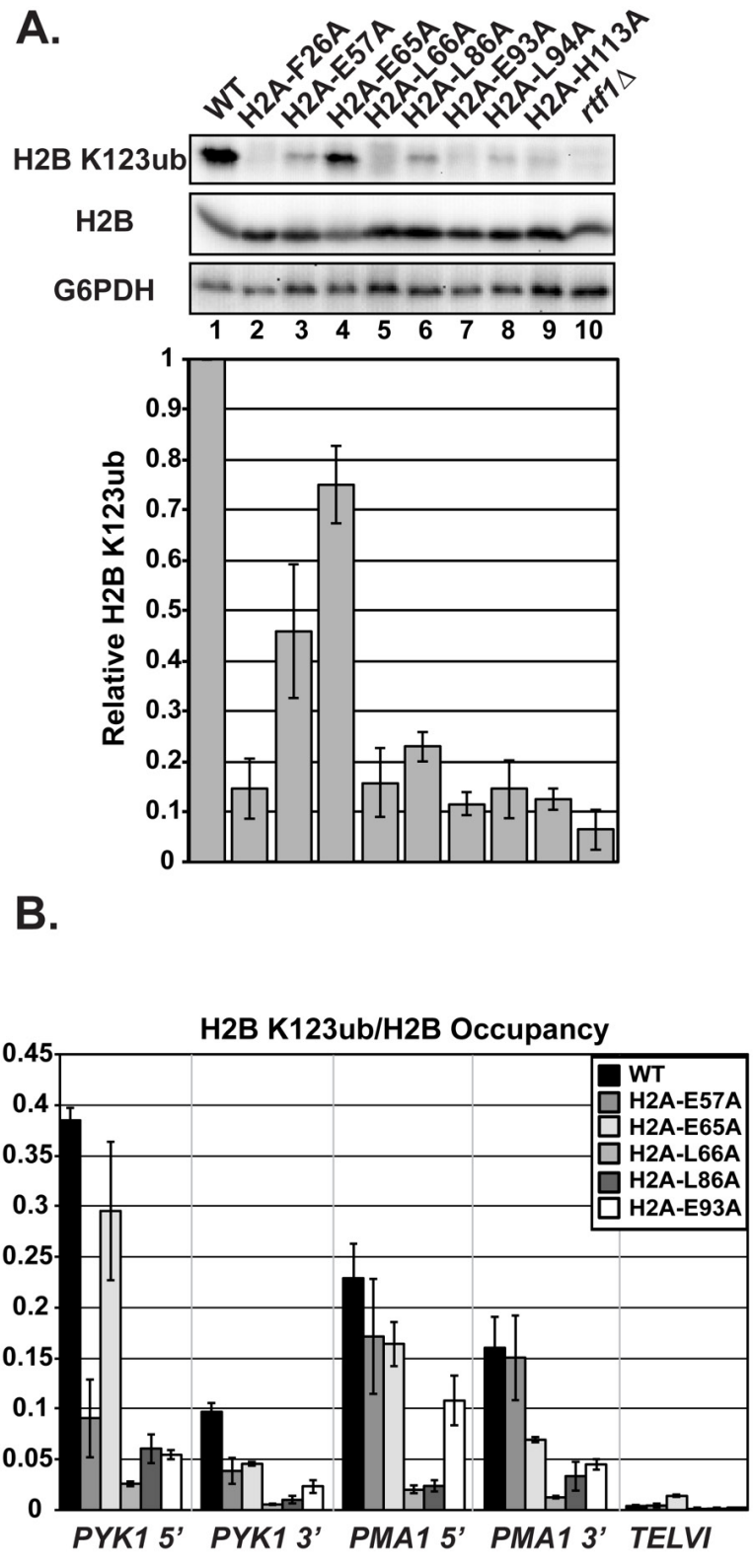

Figure 13. Substitutions in H2A cause H2B K123ub defects.

(A) Western analysis of H2B K123ub, as well as total H2B and G6PDH, both of which served as loading controls. KY1599 (*rtf1*Δ) was used as a negative control. The bar graph shows H2B K123ub levels normalized to total H2B levels. These relative H2B K123ub levels were normalized to the wild-type value. Error bars represent SEM of three independent experiments. **(B)** ChIP analysis of H2B K123ub occupancy at the 5'- and 3'- ends of *PYK1* and *PMA1* and at a nontranscribed region, *TELVI*. H2B K123ub ChIP values were normalized to total H2B ChIP values. The error bars represent SEM of three independent experiments.

2.3.2 The H2A mutants have reduced histone occupancy but do not show dramatic transcriptional changes at loci that are sensitive to chromatin integrity

Previous studies have shown that H2B K123ub is required for proper histone occupancy (CHANDRASEKHARAN *et al.* 2009; BATTA *et al.* 2011), that the docking domain of H2A is important for the association of H2A and H2B with H3 and H4 (WHITE *et al.* 2001; FERREIRA *et al.* 2007; BATTA *et al.* 2011), and that the acidic patch lies at the interface of H2A and H2B (LUGER *et al.* 1997; WHITE *et al.* 2001). Therefore, we examined global and local levels of histones by western analysis and ChIP, respectively (Fig. 14). Global levels of H2B, H3, and H2A were unaffected in the mutants, with two exceptions (Fig. 14A). The two exceptions, H2A-E93A and H2A-L94A, were detected at levels that were lower than wild-type H2A, indicating a potential defect in the expression, stability, or antibody recognition of these H2A mutant proteins. H2B, H2A, and H3 occupancy levels were assessed at both the highly transcribed gene *PYK1* and a non-transcribed telomeric region using ChIP analysis (Fig. 14B-D). Four of the alanine substitutions in H2A resulted in lower occupancy levels of H2B at *PYK1* (Fig. 14B). H2A occupancy was not as drastically affected in the mutant strains; however, the signals for H2A-E57A and H2A-E93A enrichment were reduced at all loci tested (Fig. 14C). For H2A-E93A, this could be due to reduced H2A protein levels or reduced immunoreactivity (Fig. 14A). H3 occupancy levels at *PYK1* were also slightly affected in some of the mutant strains, particularly at the 5' end of the gene (Fig. 14D). Importantly, the reduced histone occupancy levels do not account for the reduced H2B K123ub levels in the H2A mutant strains, as we have normalized the H2B K123ub levels to total histone levels in our assays (Fig. 13).

As an alternative measure of chromatin integrity in the histone mutant strains, we used northern analysis to monitor transcription of the *SER3* and *FLO8* genes, which can serve as

sensitive reporters of defects in chromatin structure (KAPLAN *et al.* 2003; CARROZZA *et al.* 2005; JOSHI AND STRUHL 2005). In rich media, *SER3* expression is repressed by transcription-coupled nucleosome assembly over its promoter via transcription of a noncoding RNA, *SRG1* (HAINER *et al.* 2011; PRUNESKI *et al.* 2011). Mutations in the genes encoding the histone chaperones Spt6 and Spt16 lead to strong derepression of *SER3* without decreasing *SRG1* transcription (HAINER *et al.* 2011). Relative to the temperature-sensitive alleles *spt6-1004* and *spt16-197*, the H2A substitutions identified in our screen do not cause strong derepression of *SER3*, suggesting that transcription-coupled nucleosome occupancy is largely intact over *SRG1* (Fig. 14E).

Cryptic initiation can occur when cryptic promoters within coding regions are unveiled by perturbations in nucleosome occupancy or histone modifications (KAPLAN *et al.* 2003; CARROZZA *et al.* 2005; JOSHI AND STRUHL 2005). To assess cryptic initiation in the H2A mutants, we performed northern analysis of the *FLO8* gene, using *spt6-1004* and *spt16-197* as positive controls for cryptic initiation (Fig. 14E). Relative to these control strains, the H2A mutants generate only very low levels of cryptic transcripts at *FLO8* (Fig. 14E). Together, these data suggest that, although histone occupancy defects can be detected, chromatin structure is not grossly impaired in the H2A mutants.

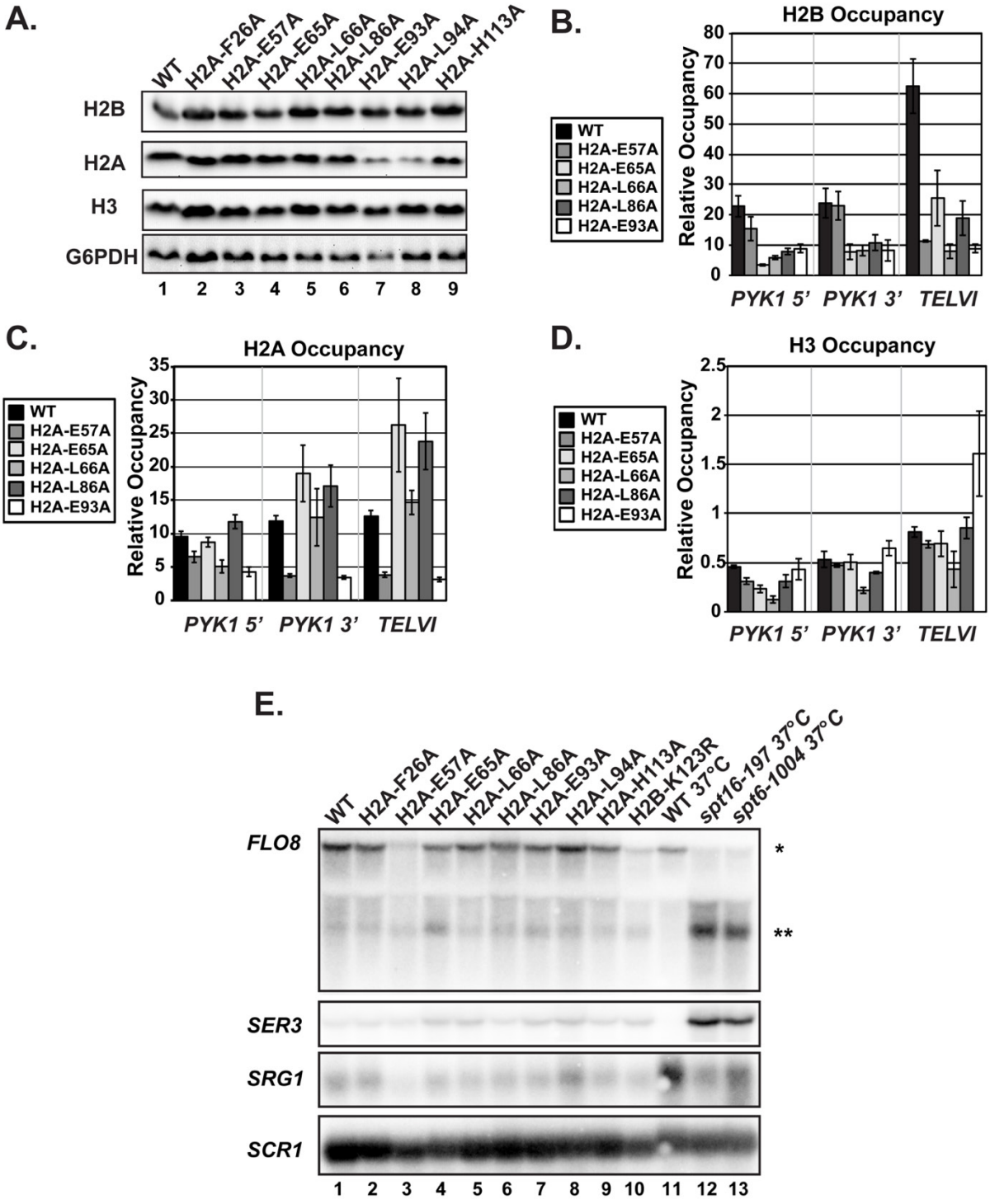

Figure 14. The H2A substitutions affect histone levels on genes but do not greatly affect transcription of genes that are sensitive to nucleosome occupancy.

(A) Western analysis of H2B, H2A**,** and H3 levels in the H2A mutant strains. G6PDH levels served as a loading control. **(B, C, D)** Analysis of H2B (KY2674), H2A (KY2675), and H3 (KY943) occupancy at the 5'- and 3' ends of *PYK1* and at *TELVI* by ChIP. The error bars denote SEM of three independent experiments. **(E)** Northern analysis assessing the effects of the H2A substitutions and H2B-K123R (KY2044) on *SER3, SRG1, FLO8* and *FLO8* cryptic transcript levels. Upper band (*) corresponds to the full-length *FLO8* transcript and the lower band (**) corresponds to the cryptic internally initiated transcript. The *spt6-1004* (KY2678) and *spt16-197* (KY2679) temperature-sensitive alleles serve as positive controls for cryptic initiation and *SER3* derepression and are isogenic to the wild-type strain KY2677. *SCR1* was used as a loading control.

2.3.3 H2A mutants have a range of defects in histone modifications dependent on H2B K123ub

H2B K123ub is required for downstream histone modifications, including H3 K4 di- and tri-methylation (H3 K4me$^{2/3}$), catalyzed by Set1, and H3 K79 di- and tri-methylation (H3 K79me$^{2/3}$), catalyzed by Dot1 (DOVER *et al.* 2002; SUN AND ALLIS 2002; LATHAM AND DENT 2007). We therefore asked whether the H2A substitutions also cause defects in modifications downstream of H2B K123ub, using western analysis. Surprisingly, although all of the H2A mutants identified in our screen have reduced H2B K123ub levels, we observed a range of defects in H3 methylation (Fig. 15). For example, two substitutions, F26A and H113A, cause no apparent defects in global H3 K4 or K79 methylation, despite dramatically reducing H2B K123ub levels (Fig. 13A and 15A). In contrast, the E65A and L66A substitutions greatly reduce H3 K4 methylation and partially reduce H3 K79 methylation even though their effects on H2B K123ub levels are quite different (Fig. 13A and 15A). Substitution of residues E93 and L94 to alanine resulted in a strong H3 K79 methylation defect and only slight defects in H3 K4 methylation (Fig. 15A). Thus, E93 and L94 appear to selectively impact H3 K79 methylation. To determine the levels of H3 methylation on chromatin, we performed ChIP analysis of H3 K79me$^{2/3}$ and H3 K4me^{3} at *PYK1*, *PMA1* and *TELVI* in the H2A mutant cells and normalized the data to total H3 occupancy levels (Fig. 15B). The modification defects observed by ChIP mirror the global H3 methylation defects visualized by western analysis with slight differences being likely due to differences in histone occupancy levels, which were taken into account in the ChIP assay. Our results indicate that the H2A residues play unique roles in regulating histone modifications dependent on H2B K123ub.

To test whether the H2A substitutions confer other histone modification defects potentially through a general change in nucleosome structure, we performed western analysis of Set2-catalyzed H3 K36me^2 and K36me^3, modifications that are not strongly dependent on H2B K123ub (BRIGGS *et al.* 2002; NG *et al.* 2003). None of the H2A mutants exhibited defects in H3 K36 methylation (Fig. 15A). This is in agreement with previous work, which identified a distinct nucleosome surface required for H3 K36 methylation (WYRICK *et al.* 2012), and the idea that the H2A substitutions identified in our screen are largely specific to the H2B K123ub cascade.

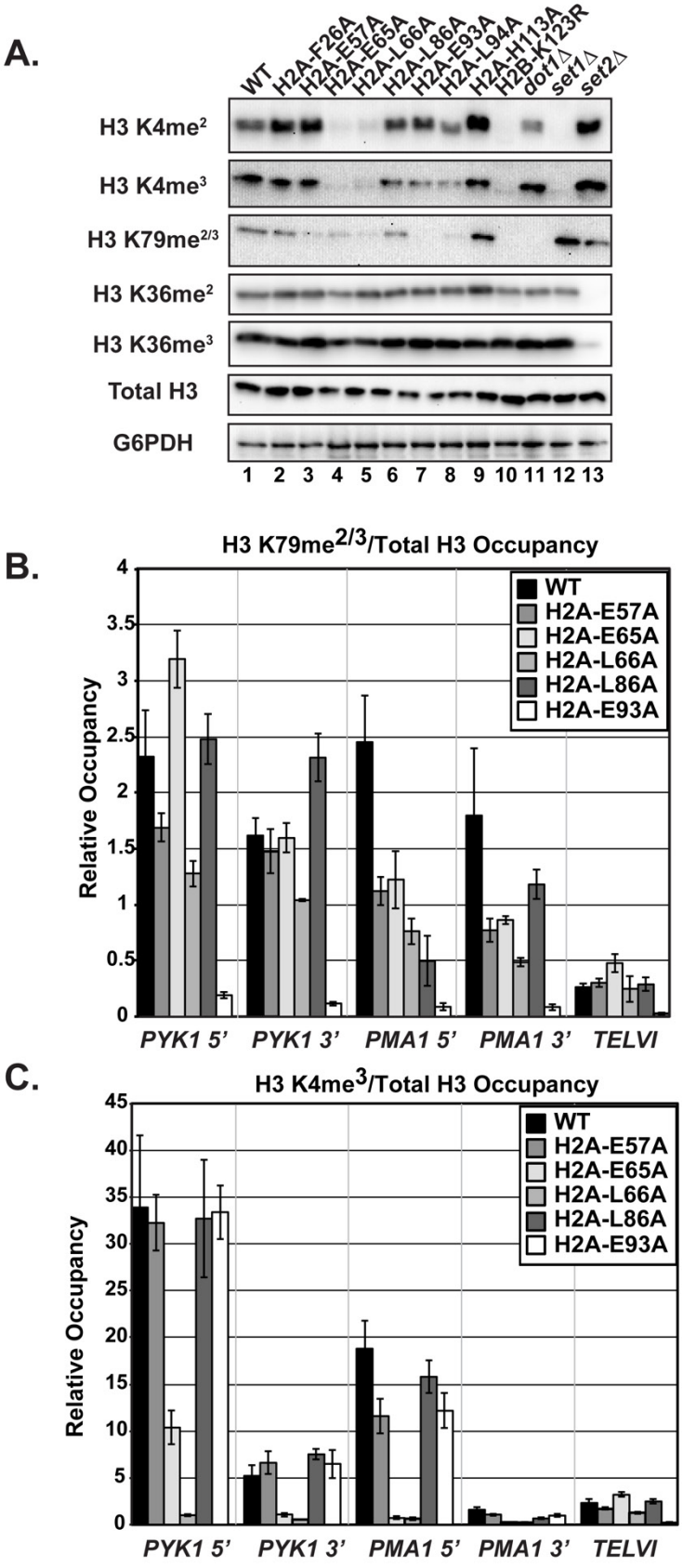
A.
WT
H2A-F26A
H2A-E57A
H2A-E65A
H2A-L66A
H2A-L86A
H2A-E93A
H2A-L94A
H2A-H113A
H2B-K123R
dot1Δ
set1Δ
set2Δ
H3 K4me2
H3 K4me3
H3 K79me2/3
H3 K36me2
H3 K36me3
Total H3
G6PDH
1 2 3 4 5 6 7 8 9 10 11 12 13
B.
H3 K79me2/3/Total H3 Occupancy
Relative Occupancy
WT
H2A-E57A
H2A-E65A
H2A-L66A
H2A-L86A
H2A-E93A
PYK1 5'
PYK1 3'
PMA1 5'
PMA1 3'
TELVI
C.
H3 K4me3/Total H3 Occupancy
Relative Occupancy
WT
H2A-E57A
H2A-E65A
H2A-L66A
H2A-L86A
H2A-E93A
PYK1 5'
PYK1 3'
PMA1 5'
PMA1 3'
TELVI

Figure 15. The H2A substitutions differentially affect H3 methylation

(A) Western blots were probed with antibodies to detect di- and tri-methylation of H3 K4, K36, and K79 as indicated. Total H3 and G6PDH levels were used as loading controls. Strains lacking *SET1* (KY1715), *DOT1* (KY1717), and *SET2* (KY1716) show the specificity of the antibodies used. **(B, C)** ChIP analysis of methylated H3 K79 and K4 at *PYK1*, *PMA1* and *TELVI*. The H3 K79 antibody used in these experiments can detect both the di- and tri-methylated states (Abcam). The error bars represent SEM of three independent experiments.

2.3.4 H2A mutants have transcription termination defects of snoRNAs

Previous studies have shown that H3 K4me^3 and H2B K123ub are required for proper transcription termination of small nucleolar RNAs (snoRNAs) through the Nrd1-Nab3-Sen1 pathway (TERZI *et al.* 2011; TOMSON *et al.* 2011; TOMSON *et al.* 2013). However, little is known about how these histone modifications or other nucleosome residues affect transcription termination. To assess transcription termination in our mutants, we performed RT-qPCR analysis on four snoRNA genes that are affected by histone modifications (TOMSON *et al.* 2013). For these assays, we used probes that hybridize to the intergenic region between the snoRNA gene and the downstream gene. Detection of a PCR product is a measure of transcription in the region downstream of the snoRNA terminator (Fig. 16)**.** The RT-qPCR analysis indicates that the H2A acidic patch residues are required for proper transcription termination at the four snoRNA loci (Fig. 16). Previous work described snoRNA termination to be differentially sensitive to disruption of H2B K123ub: *SNR47* required H2B K123ub for proper termination whereas *SNR48* was relatively insensitive to the absence of this mark (TOMSON *et al.* 2013). The mutants identified in our screen, which all have abrogated H2B K123ub, have termination defects at both loci, indicating that the mechanistic basis for read-through of these terminators could be downstream of H2B K123ub (Fig. 16).

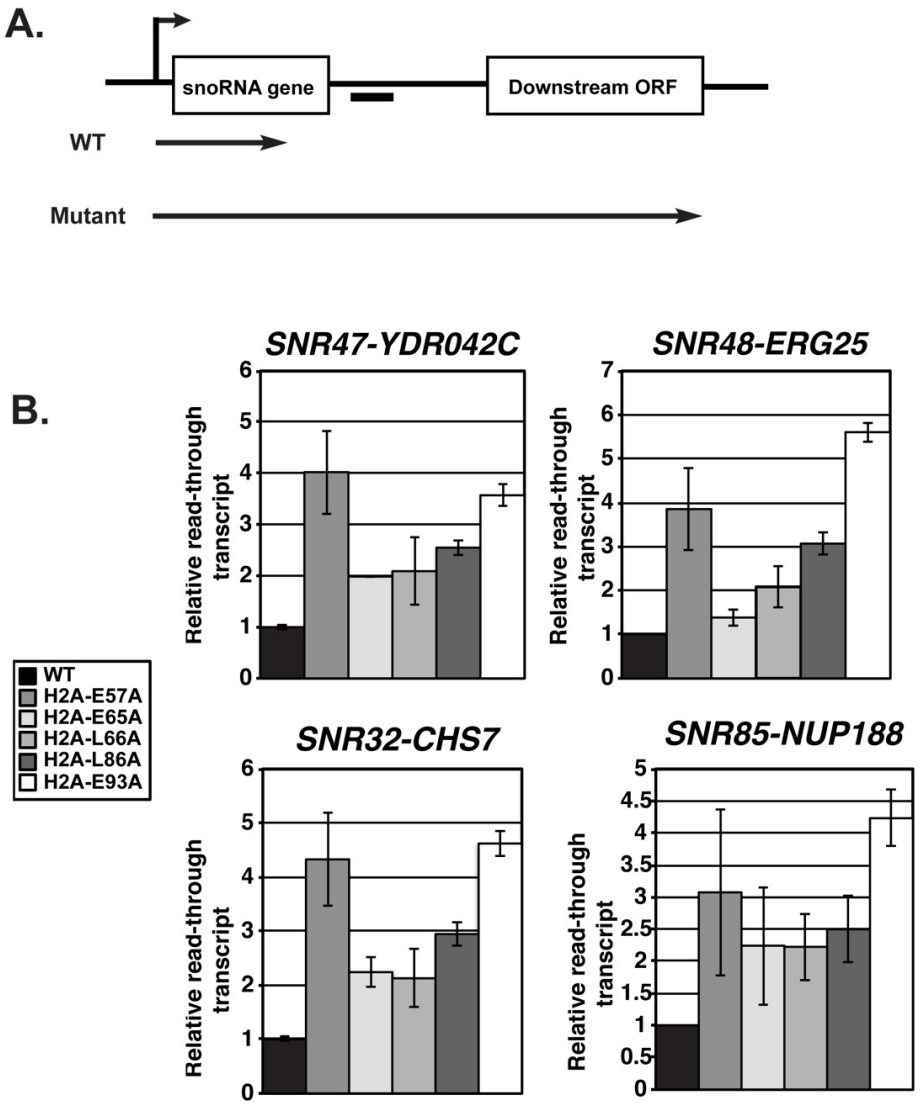

Figure 16. H2A mutants have transcription termination defects.

(A) Diagram of a snoRNA gene and the location of qPCR primers used to assess read-through transcription. **(B)** RT-qPCR analysis of RNA levels downstream of four different snoRNA genes in the H2A mutant strains. Transcript levels in the wild-type control strain were set to 1 and error bars represent SEM of three biological replicates.

2.3.5 Deletion of *UBP8* increases H2B K123ub and H3 methylation in a subset of the mutants

H2B K123ub is a transient histone modification; therefore one possible explanation for reduced H2B K123ub levels in the H2A mutants could be through decreased stability of the mark through the enhanced action of a ubiquitin-specific protease. The removal of H2B K123ub is due to the actions of two ubiquitin-specific proteases Ubp8 and Ubp10 (HENRY *et al.* 2003; DANIEL *et al.* 2004; EMRE *et al.* 2005; SCHULZE *et al.* 2011). To test whether the H2B K123ub deficiency observed in the H2A mutants is through decreased stability of the modification, we performed western blot analysis of H2B K123ub levels in strains that contain the H2A substitutions and are deleted for *UBP8*. Upon deletion of *UBP8*, the fold recovery of H2B K123ub levels was comparable to that of wild-type cells for the H2A-L86A and H2A-E93A mutants, suggesting that the H2B K123ub defect in these mutants is at least partially due to decreased stability of the mark (Fig. 17A-B). For the H2A-E57A, H2A-E65A, and H2A-L66A mutants, deletion of *UBP8* did not fully rescue H2B K123ub levels (Fig. 17A-B). The most drastic effect was that of H2A-L66A, where little to no H2B K123ub was restored. Therefore, for these mutants, and especially H2A-L66A, the defect in H2B K123ub is likely due to a failure of the ubiquitylation machinery to fully establish the mark. An alternative, but not mutually exclusive explanation, is that E57, E65, and L66 could form a surface required for Ubp8 function or recruitment, as these three residues reside near each other on the nucleosome structure (Fig. 11B).

To test the extent to which H2B K123ub and downstream H3 methylation events are coupled in the H2A mutant strains, we measured H3 K4me^3 and H3 K79me$^{2/3}$ levels in the presence and absence of *UBP8*. Upon deletion of *UBP8*, H3 K4me^3 and H3 K79me$^{2/3}$ increased in the wild-type strain and in the H2A-E57A and H2A-L86A mutants. For the H2A-L66A mutant,

no recovery of the methyl marks was observed. This observation is consistent with the idea that the establishment of H2B K123ub is the primary defect in this mutant. For the E65A mutant, H3 K4me^3 levels were extremely low in both the presence and absence of Ubp8, even though H2B K123ub levels were substantially recovered in the *ubp8*Δ background. This observation suggests that the E65A substitution prevents proper H3 methylation possibly by disrupting a functional interaction with the Set1/COMPASS complex. Finally, in agreement with our western and ChIP results (Fig. 15), the E93A mutant appears most defective in supporting H3 K79 methylation, as deleting *UBP8* elevated H3 K4me^3 levels to a greater extent than H3 K79me$^{2/3}$ levels in this strain.

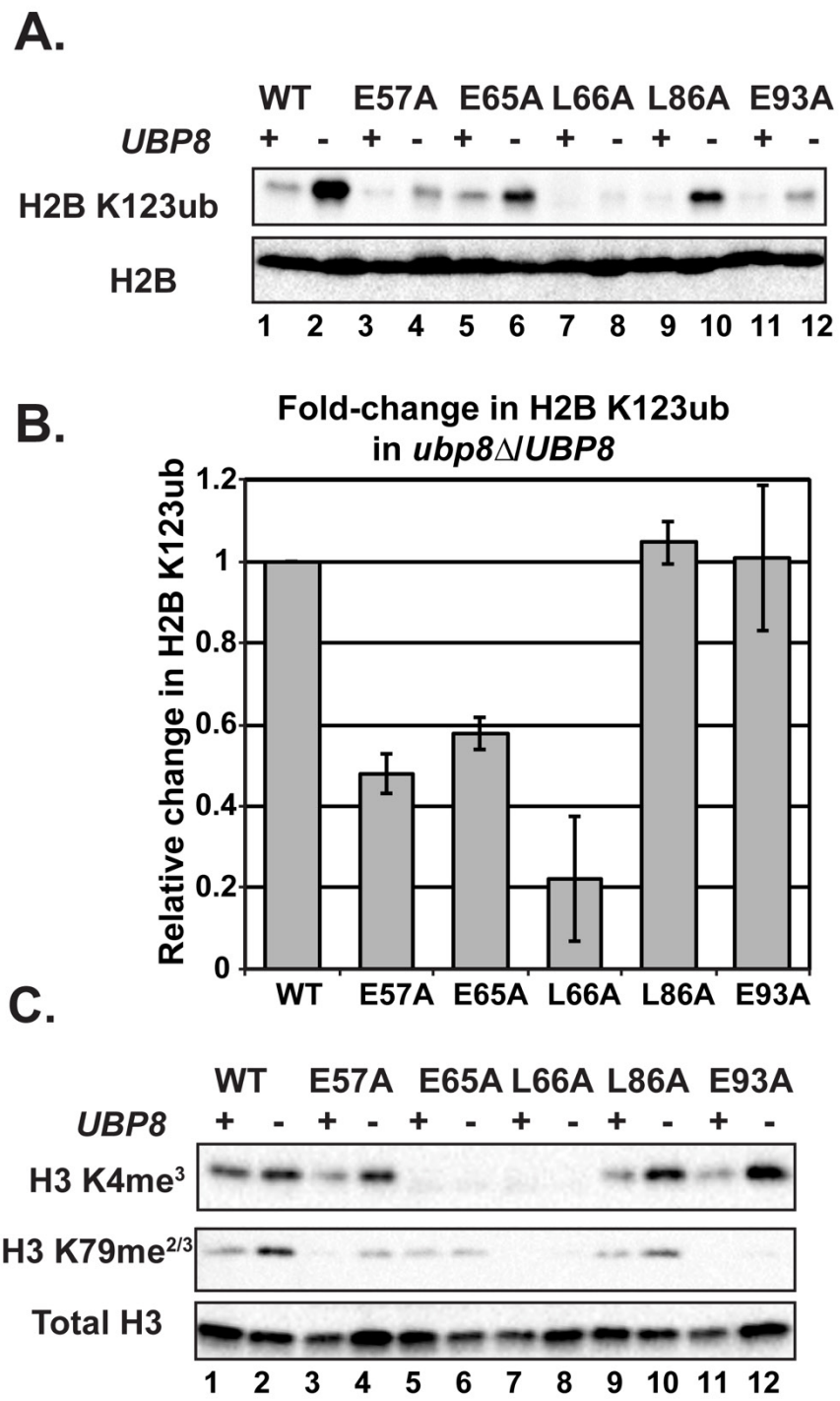

Figure 17. Deletion of *UBP8* variably affects the recovery of H2B K123ub, H3 K4me^3, and H3 K79me$^{2/3}$ in the H2A mutants.

(A) Western analysis of H2B K123ub and total H2B in the indicated wild-type and H2A mutant strains. **(B)** The relative levels of H2B K123ub between *ubp8*Δ (KY2086) and *UBP8* (KY943) backgrounds are shown. The ratio of H2B K123ub in *ubp8*Δ to H2B K123ub in *UBP8* was calculated after normalizing to total H2B levels. To determine the fold change of H2B K123ub levels between H2A mutants, these ratios were normalized to the wild-type H2A background. Error bars represent SEMs of three biological replicates. (C) Western analysis of H3 K4me^{3} and H3 K79me$^{2/3}$ levels in H2A mutants in the presence or absence of *UBP8*. Total H3 served as a loading control.

2.3.6 H2A mutants have defects in recruitment of histone modification and transcription elongation machinery to active genes

In addition to decreased stability of the ubiquitylation mark conferred by Ubp8, the reduction in histone modification levels in the H2A mutants could be due to impaired recruitment of the modification enzymes required for the H2B K123ub cascade, such as the ubiquitin-protein ligase Bre1. To analyze the effects of the H2A substitutions on recruitment of Bre1 to actively transcribed genes, we performed ChIP analysis of HSV-tagged Bre1 (Fig. 18A). All five of the H2A mutants tested showed reduced recruitment of HSV-Bre1 to *PYK1* and *PMA1*, particularly at their 5' ends (Fig. 18A). With the exception of the H2A-E57A mutant, Bre1 occupancy was also reduced at *ADH1* (Fig. 19). As expected, HSV-Bre1 levels at the non-transcribed *TELVI* region were similar to those of the untagged control strain. Also in agreement with previous observations (WOOD *et al.* 2003a), Bre1 levels at the 5' ends of *PMA1* and *PYK1* were higher than those at the 3' ends of the genes. To determine whether reduced levels of HSV-Bre1 could account for the reduced HSV-Bre1 occupancy in the H2A mutant strains, we performed western analysis. Our results show that total HSV-Bre1 levels in the H2A mutants are similar to those in a wild-type strain (Fig. 20). These results indicate that residues in the H2A acidic patch are required for proper Bre1 recruitment to active genes.

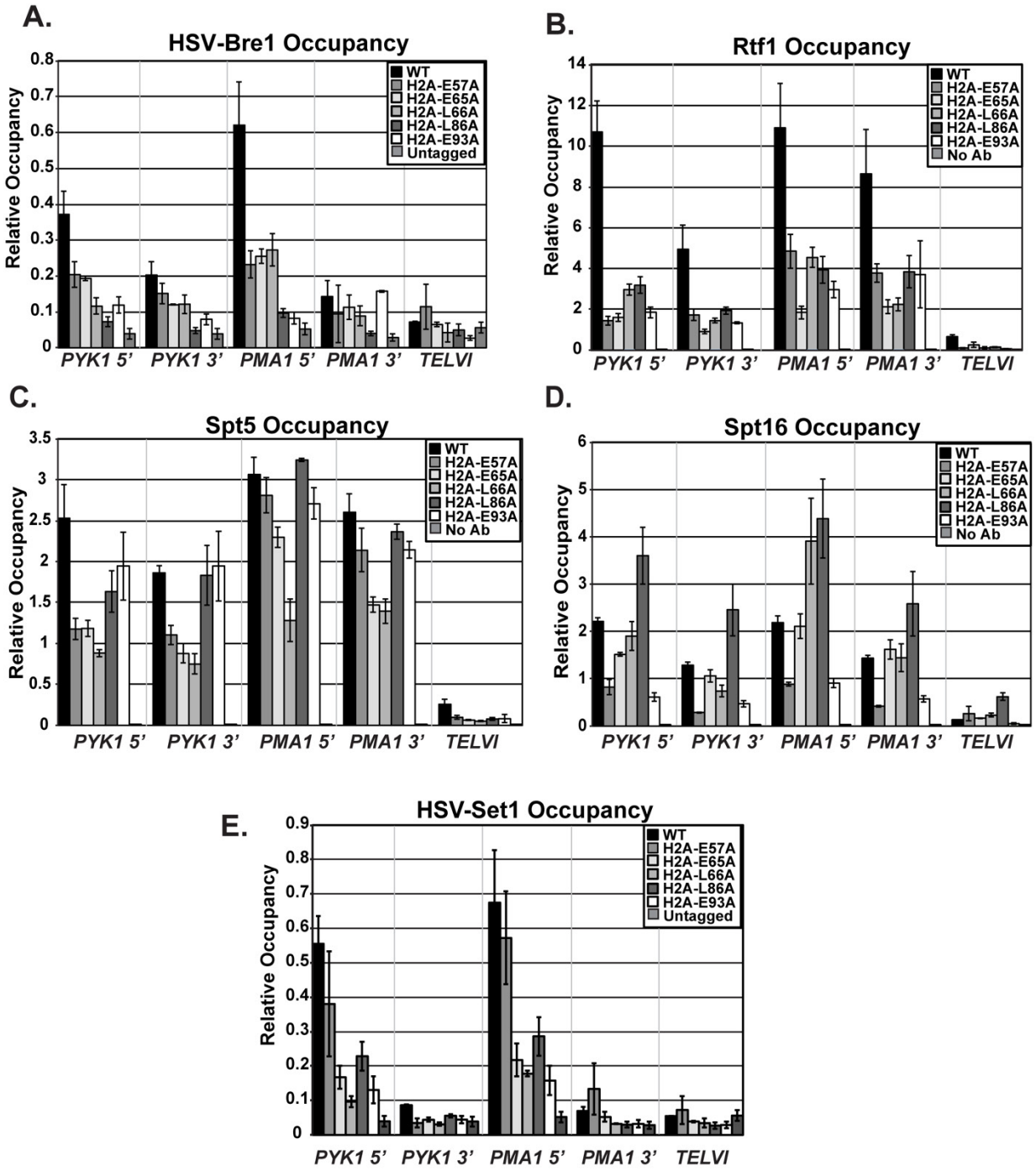

Figure 18. Recruitment of histone modification and elongation machinery is impaired in the H2A mutants.

ChIP analyses of HSV-Bre1 (KY2674) **(A)**, Rtf1 (KY2674) **(B)**, Spt5 (KY943) **(C)**, Spt16 (KY2675) **(D)**, and HSV-Set1 (KY2719) **(E)** at the 5'- and 3'-ends of transcribed loci (*PYK1* and *PMA1*) and at *TELVI*. The error bars represent SEM of three independent experiments.

The Paf1C subunit, Rtf1, has been implicated in the recruitment of the H2B ubiquitylation machinery during transcription (XIAO *et al.* 2005). We therefore used ChIP analysis to test whether the H2A residues that are important for Bre1 recruitment are also important for Rtf1 occupancy on active genes. Our ChIP results demonstrate a significant reduction in Rtf1 levels at *PYK1*, *PMA1*, and *ADH1* in the H2A mutant strains (Fig. 18B, Fig.19). To rule out the possibility that the reduced Rtf1 occupancy is a result of lower protein levels, we measured global Rtf1 levels by western analysis. This analysis showed that Rtf1 levels are unaffected in the H2A mutants, indicating that reduced Rtf1 expression is not the cause of the H2B K123ub defect (Fig. 20). Overall, the occupancy levels of HSV-Bre1 and Rtf1 correlated with H2B K123ub levels in some cases but not others. For example, the H2A-E57A mutant shows reduced HSV-Bre1 and Rtf1 occupancy but normal levels of H2B K123ub at the *PMA1* locus. It is possible that small levels of Bre1/Rad6 and Rtf1 are sufficient to promote H2B K123ub at *PMA1* in this mutant. Alternatively, decreased Ubp8 levels or activity could compensate for reduced Bre1 recruitment. We attempted to test this idea by ChIP but were unable to reliably measure Ubp8 occupancy in our strains.

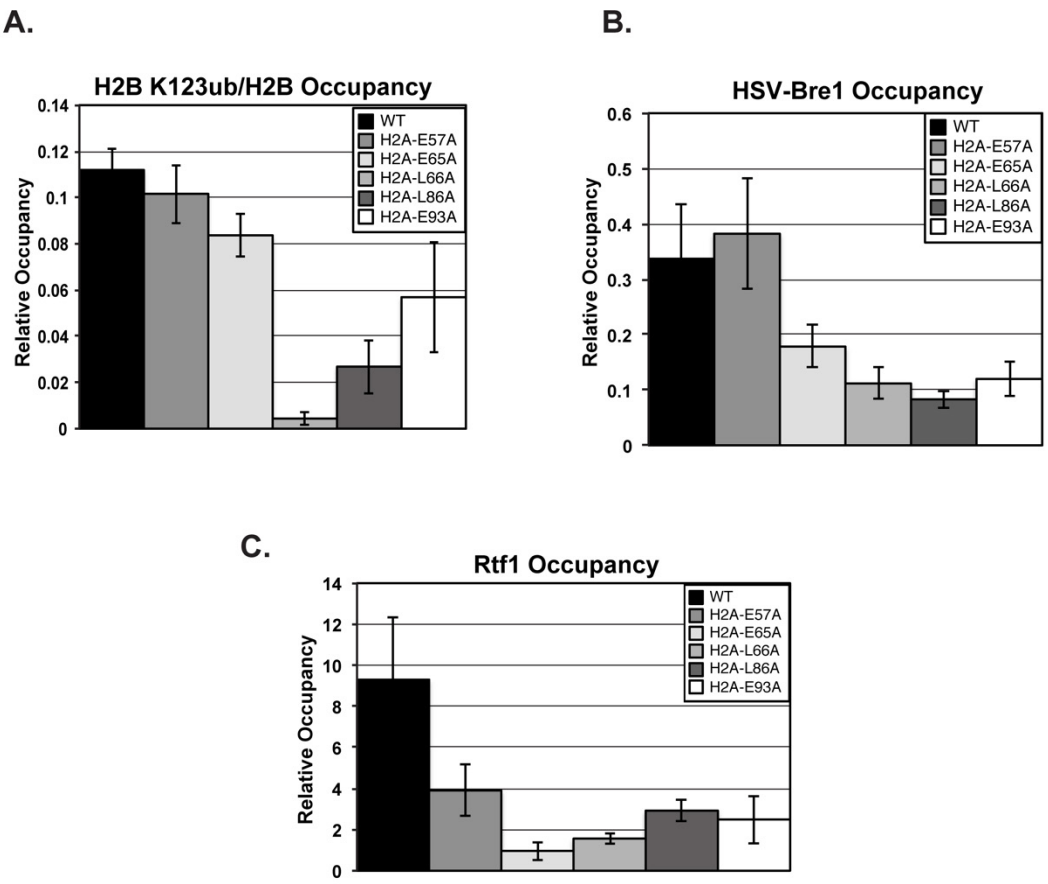

Figure 19. H2B K123ub, HSV-Bre1, and Rtf1 occupancy at *ADH1*.

ChIP analysis of H2B K123ub **(A)**, HSV-Bre1 **(B)**, and Rtf1 **(C)** occupancy at the *ADH1* ORF. The error bars represent SEM of three independent experiments.

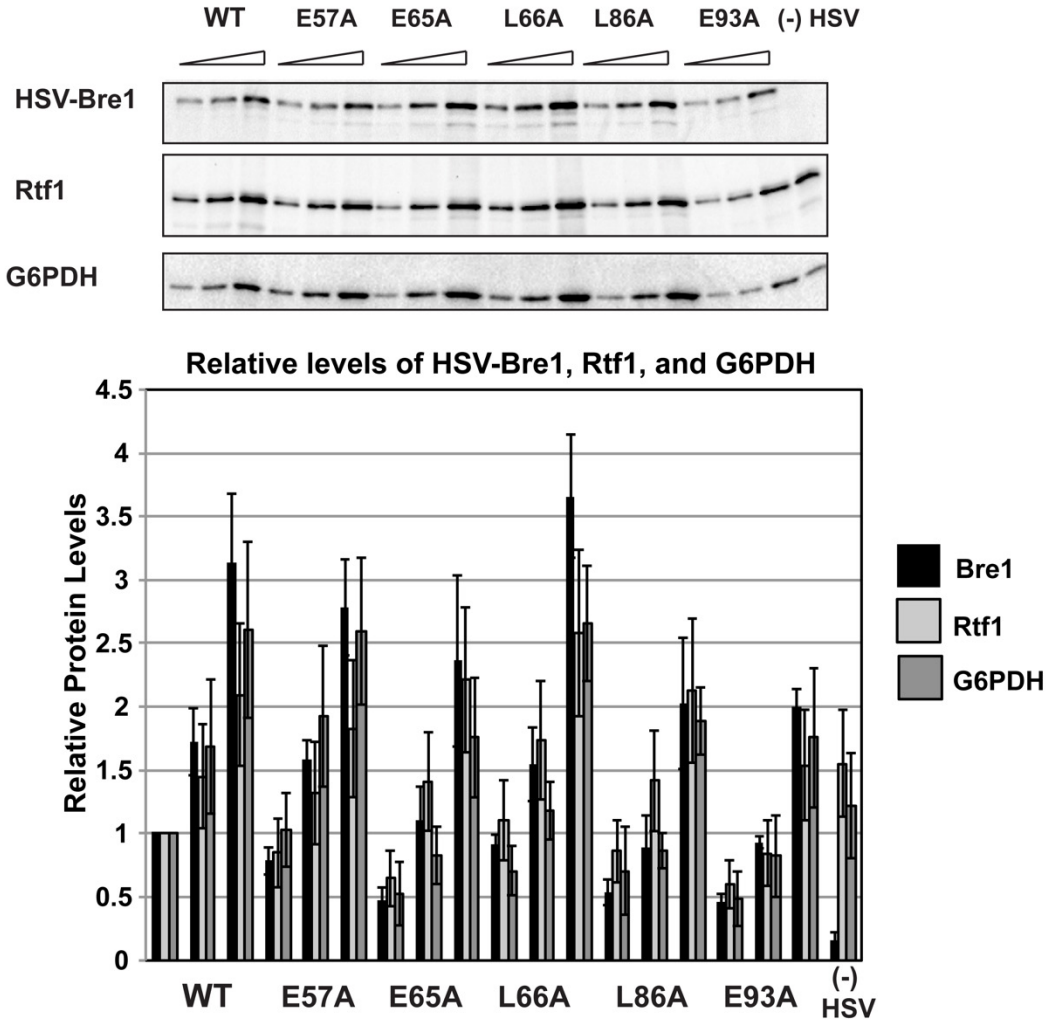

Figure 20. HSV-Bre1 and Rtf1 levels are unaffected in the H2A mutants.

1-fold, 1.5-fold, and 2-fold concentrations of protein extracts were loaded on SDS polyacrylamide gels and analyzed by western blotting using anti-HSV, anti-Rtf1, and anti-G6PDH, as a loading control. Values were normalized to the initial wild-type protein concentration. Mutant strains were transformants of KY2674.

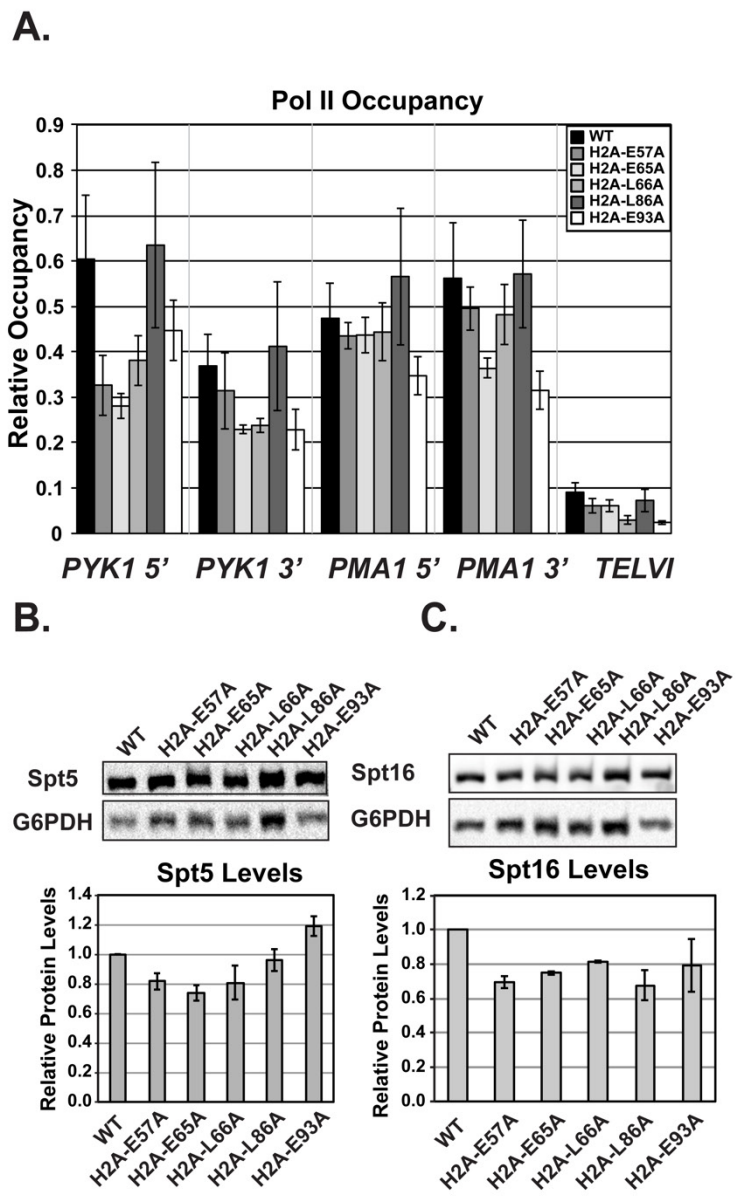

Figure 21. Recruitment of Pol II and levels of Spt5 and Spt16 are modestly affected in the H2A mutants.

(A) ChIP analysis of Pol II (KY943) at the 5'- and 3'-ends of transcribed loci (*PYK1* and *PMA1*) and at *TELVI*. The error bars represent SEM of three independent experiments. Western analyses of Spt5 **(B)**, and Spt16 **(C)** to measure total protein levels in the H2A mutant cells. Values represent protein levels normalized to G6PDH with the wild-type ratio set to one.

We previously demonstrated that recruitment of Paf1C to coding regions is mediated through a direct physical interaction between Rtf1 and the elongation factor Spt5 (MAYEKAR *et al.* 2013; WIER *et al.* 2013). Therefore, it is possible that the lower Rtf1 and Bre1 occupancy levels in the H2A mutant strains reflect impaired recruitment of the transcription elongation machinery. To test this idea, we performed ChIP analysis of Spt5, Spt16, and Pol II occupancy at *PYK1*, *PMA1,* and *TELVI* in the histone mutant strains (Fig. 18C-D, and Fig. 21). We observed gene and allele specific defects in Spt5 occupancy, with the E57A, E65A, and L66A substitutions causing reduced Spt5 occupancy particularly at *PYK1*. However, the levels of Spt5 occupancy largely mirrored Pol II occupancy levels, suggesting that the effects of the H2A substitutions on Spt5 recruitment are likely to be indirect. We also assessed the effects of the H2A substitutions on recruitment of the FACT complex member Spt16 (Fig. 18D), which is required for proper histone occupancy and H2B K123ub (BELOTSERKOVSKAYA *et al.* 2003; PAVRI *et al.* 2006; FLEMING *et al.* 2008). Interestingly the substitution within the docking domain, H2A-L86A, of the nucleosome exhibited increased Spt16 occupancy at all tested loci. In contrast, substitutions E57A and E93A led to reduced Spt16 occupancy, suggesting that, for these H2A mutants, a defect in Spt16 recruitment may be a contributing factor to the reduced H2B K123ub levels and lower histone occupancy levels (Fig. 14B-C). Global levels of Spt5 and Spt16 were not strongly affected, as judged by western analysis (Fig. 21).

Because the histone mutants have defects in H3 K4 methylation (Fig. 15, and 17C), the acidic patch residues may be required for recruitment of the H3 K4 methyltransferase Set1. To test this, we performed ChIP analysis of HSV-tagged Set1 in the H2A mutants (Fig. 18E). With the exception of E57A, all of the substitutions affect occupancy of HSV-Set1. However, after normalizing the H3 K4me^3 occupancy levels to H3 occupancy levels, only the E65A and L66A

substitutions cause a strong defect in H3 K4me^3 (Fig. 15C). We thus conclude that HSV-Set1 recruitment may be impacted by the occupancy levels of H2B K123ub and H3. For the E65A mutant, the severity of the H3 methylation defect and lack of restoration of H3 K4me^3 upon deletion of *UBP8* suggests that E65 may play a more direct role in promoting H3 K4 methylation. We did not observe a reduction in HSV-Set1 levels in the H2A mutants (Fig. 22), as has been reported to occur when H3 K4 cannot be methylated (SOARES *et al.* 2014; THORNTON *et al.* 2014). It is possible that the H2A mutants lack the ability to regulate Set1 levels.

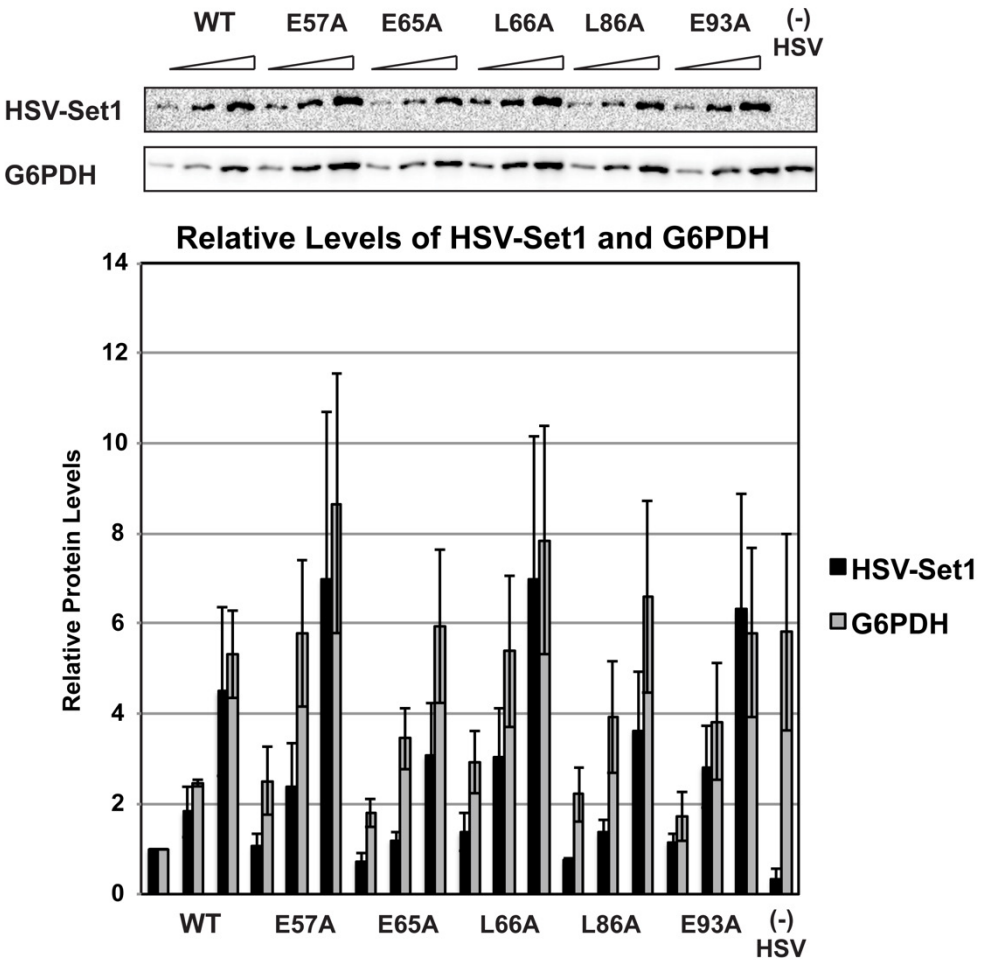

Figure 22. Set1 levels are unaffected in the H2A mutants.

1-fold, 1.5-fold, and 2-fold concentrations of protein extracts were loaded on SDS polyacrylamide gels and analyzed by western blotting using anti-HSV and anti-G6PDH, as a loading control. Values were normalized to the initial wild-type protein concentration.

2.3.7 The H2A substitutions reduce the efficiency of Pol II elongation

Because the H2A mutants exhibit reduced levels of transcription elongation-coupled histone modifications, we asked whether the acidic patch substitutions alter the efficiency of transcription elongation. To assess transcription elongation efficiency *in vivo* we used a well-established galactose-controlled system to shut off transcription of a gene and measure occupancy of Pol II during the last wave of transcription (MASON AND STRUHL 2003; SCHWABISH AND STRUHL 2004; MASON AND STRUHL 2005). This system incorporates the *GAL1* promoter upstream of the non-essential gene *YLR454W*. Cells were grown in 2% galactose to activate the gene and 2% glucose was added to the cultures to prevent further initiation events. Samples were taken at different time points to determine "snap-shots" of Pol II density at four regions of *YLR454W* by ChIP (Fig. 23A). In wild-type cells, Pol II rapidly cleared the *YLR454W* coding region, as previously described (MASON AND STRUHL 2003; SCHWABISH AND STRUHL 2004; MASON AND STRUHL 2005) (Fig. 23B). In the H2A mutants, however, the rate and/or processivity of Pol II elongation was reduced. The most dramatic effect was observed with the H2A-L66A mutant, where Pol II density persisted at the 4 Kb and 8 Kb locations relative to the wild-type kinetics (Fig. 23C). The H2A-E65A mutant also exhibited a delay in Pol II passage, with occupancy persisting at multiple locations throughout the time course (Fig. 23D). The H2A-E93A mutant exhibited a slightly different and more modest elongation defect (Fig. 23E). Collectively these data reveal an important role for the nucleosome acidic patch in promoting efficient transcription elongation.

Because the H2A acidic patch mutants have defects in H2B K123ub, we wanted to determine whether the *in vivo* elongation defects correlated with the loss of H2B K123ub. To begin to address this, we performed a similar analysis on H2B-K123R cells (Fig. 23F). Interestingly, Pol II elongation efficiency was reduced in the H2B-K123R mutant, as indicated by persistent

enrichment toward the 3’ end of the gene. These data indicate that residues within the acidic patch, at least partly through their role in promoting H2B K123ub, are important for transcription elongation efficiency *in vivo*.

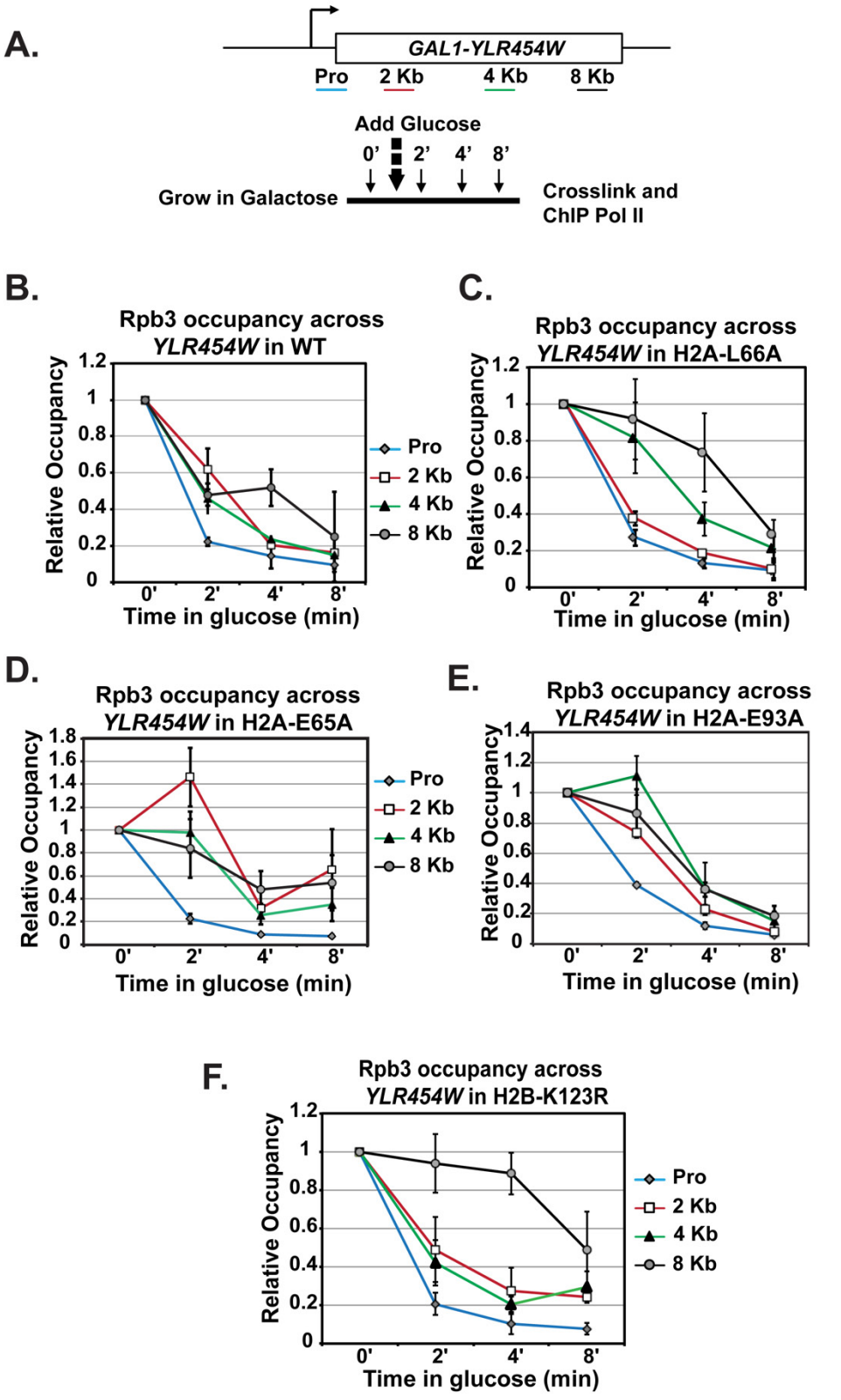

Figure 23. Transcription elongation is affected by substitutions in the nucleosome acidic patch

(A) Diagram of experimental procedure. Cells were grown in medium containing 2% galactose (zero time point) and then 2% glucose was added to shut off transcription. Samples were taken at zero, two, four, and eight-minute time points for cross-linking. ChIP of the Rpb3 subunit of Pol II across *YLR454W* was performed in **(B)** wild type (WT), **(C)** H2A-E65A, **(D)** H2A-L66A**, (E)** H2A-E93A**,** and **(F)** H2B-K123R strains, which were transformants of KY2676. Values were normalized to the zero time point for each locus. Error bars represent SEM of three biological replicates.

2.4 DISCUSSION

In this study, we exploited a genetic interaction between the H2B ubiquitylation pathway and the protein quality control factor Rkr1 to identify residues in H2A and H2B that are required for H2B K123ub. We identified eight residues in H2A that, when changed to alanine, cause defects in H2B K123ub (Fig. 13). Most of these residues map to the acidic patch on the nucleosome (Fig. 11B), which plays critical roles in several important nuclear processes. Indeed, as shown through structural studies, the acidic patch serves as a direct binding platform on the nucleosome for a variety of proteins that affect transcription, chromatin structure, and chromosome segregation. These proteins include the Latency-Associated Nuclear Antigen (LANA) peptide from Kaposi's sarcoma virus, the Regulator of Chromatin Condensation 1 protein (RCC1), the Bromo-Associated Homology (BAH) domain of Sir3, and the centromere binding protein CENP-C (KALASHNIKOVA *et al.* 2013; MCGINTY AND TAN 2015). Additionally, as shown through functional studies and a recently published structure of the Polycomb Repressive Complex 1 ubiquitylation module in complex with a nucleosome, the acidic patch interacts with ubiquitin-protein ligases that target H2A (LEUNG *et al.* 2014; MATTIROLI *et al.* 2014; MCGINTY *et al.* 2014).

Despite the importance of H2B K123ub in regulating gene expression, nucleosome stability, and genic patterns of histone methylation and acetylation, little is known about how the enzymatic machinery for H2B K123ub interfaces with the nucleosome. In a recent study, a basic region of the RING domain of Bre1 was shown to be important for interacting with the nucleosome (TURCO *et al.* 2015). Here, we show that nucleosome acidic patch mutants have impaired chromatin occupancy of the ubiquitin-protein ligase Bre1 and the Paf1C subunit Rtf1. The mechanism by which Rtf1 is required for H2B K123ub is largely undefined, although a recent study indicated a role for Rtf1 in stabilizing Bre1 protein levels (WOZNIAK AND STRAHL 2014). In

our H2A mutant strains, global protein levels of Bre1 are similar to those in a wild-type strain. This observation, together with our ChIP studies on Bre1 and Rtf1, suggests that the nucleosome acidic patch plays an active role in promoting H2B K123ub. A previous study found that the N-terminus of H2A, the H2A repression (HAR) domain, is also required for H2B K123ub. However, recruitment of the H2B K123ub machinery was not affected in the H2A N-terminal tail mutant (ZHENG *et al.* 2010). It is possible, then, that the acidic patch could recruit the H2B K123ub machinery to chromatin, potentially through a direct interaction with Bre1 and/or Rtf1, while the HAR domain stimulates enzyme activity.

In light of previous work showing that Paf1C recruitment is governed by a direct physical interaction between Rtf1 and the phosphorylated C-terminal region of the elongation factor Spt5 (LIU *et al.* 2009; ZHOU *et al.* 2009; MAYEKAR *et al.* 2013; WIER *et al.* 2013), we were surprised that the H2A substitutions identified in our screen caused a loss in Rtf1 occupancy without a corresponding loss in Spt5 recruitment. However, it was recently shown that the human homolog of Bre1, RNF20/40, promotes recruitment of PAF1 to chromatin in human cells (WU *et al.* 2014). In addition, binding of human Paf1 to histone-like proteins and nucleosomes has been reported (MARAZZI *et al.* 2012; CHU *et al.* 2013). These observations align with our results and indicate that multiple interactions can mediate or stabilize the interaction between Paf1C and chromatin. Alternatively, given the importance of Spt5 phosphorylation in mediating the interaction between Rtf1 and Spt5 (LIU *et al.* 2009; ZHOU *et al.* 2009; MAYEKAR *et al.* 2013; WIER *et al.* 2013), it is also possible that the H2A mutants are indirectly affecting Spt5 phosphorylation. Finally, we also note that Rtf1 recruitment defects could be due to the combined effect of the individual, and relatively modest, defects in Pol II, Spt5, and Spt16 occupancy (Fig. 18, 21).

The function of the ubiquitin-specific protease Ubp8 also appears to be affected by substitutions within the acidic patch (Fig. 17). A recent study suggested that the acidic patch residue H2A-Y58 promotes H2B K123ub through regulating Ubp8, as deletion of *UBP8* rescued H2B K123ub in an H2A-Y58F mutant (BASNET *et al.* 2014). The H2A-Y58A is a lethal substitution in yeast and could not be isolated in our screen (NAKANISHI *et al.* 2008a). In our study, deletion of *UBP8* rescued H2B K123ub to some degree in most of our mutants, which suggests that these mutants have defects in both ubiquitylating H2B-K123 and in stabilizing the mark (Fig. 17A). For the H2A-L66A mutant, the nearly complete absence of H2B K123ub in the presence or absence of *UBP8* suggests that little ubiquitin is placed on H2B-K123 such that removal of *UBP8* makes little to no difference in this mutant.

The H2A residues we identified are required for H2B K123ub-dependent H3 methylation (Fig. 15). Interestingly, some mutants exhibited defects in only H3 K4 methylation or H3 K79 methylation, while others had defects in both, despite all having reduced H2B K123ub levels. These data suggest that individual residues within the acidic patch promote methylation through separate mechanisms. Substitution of neighboring residues, H2A-E65A and H2A-L66A, differentially impacted H2B K123ub levels, but both mutants had undetectable levels of H3 K4 methylation (Fig. 15) (NAKANISHI *et al.* 2008a). It is possible that the methylation defects caused by the L66A substitution are largely due to a severe defect in the establishment of H2B K123ub in this mutant, similar to the effect of the H2B K123R mutant (NAKANISHI *et al.* 2009). In contrast, the H3 K4 methylation defect of the H2A-E65A mutant may stem primarily from the reduced recruitment and/or activation of Set1. For the H2A-E65A mutant, we noted a lack of recovery of H3 K4me^{3} and H3 K79me$^{2/3}$ when H2B K123ub levels were increased through the deletion of *UBP8* (Fig. 17C). This observation suggests that E65 is important for coupling H2B K123ub to

downstream H3 methylation events. Interestingly, substitution of other residues near H2B K123 has been shown to uncouple H3 methylation from H2B K123ub. For example, H2B R119 and T112, when mutated, increase H2B K123ub levels but decrease H3 K4me^3 levels (CHANDRASEKHARAN *et al.* 2010).

The severe deficiency in H3 K79me$^{2/3}$ observed in the H2A-E93A mutant (Fig. 15, Fig. 17C) presents the intriguing possibility that this residue may interact with Dot1 to promote H3 K79 methylation. It is unlikely that the H3 K79 methylation defect detected in the H2A-E93A mutant is solely due to its defect in H2B K123ub, because when H2B K123ub levels are increased in the absence of *UBP8*, the increase in H3 K79 methylation is very slight (Fig. 17C). Interestingly, the basic patch in the H4 tail is required for Dot1 methylase activity, but not for Dot1 recruitment (FINGERMAN *et al.* 2007). Since the H4 tail interacts with the acidic patch of the nucleosome (LUGER *et al.* 1997; WILKINS *et al.* 2014), one explanation for the H3 K79me$^{2/3}$ defect could be that E93 is required for recruitment of Dot1, while the H4 tail stimulates Dot1 activity.

Further supporting growing indications that chromatin structure is important for proper transcription termination through the NNS pathway, the H2A mutants tested exhibited transcriptional readthrough at four *SNR* genes (Fig. 16). The magnitude of the transcriptional defect does not correlate strictly with the loss of any particular histone modification, suggesting that this phenotype may be sensitive to the combinatorial loss of several modifications and possibly other factors, such as histone occupancy and Spt16 recruitment (Fig. 14 and 18D). Regardless of the mechanism, the increased levels of aberrant transcripts in the H2A mutants could provide a rationale for the synthetic growth defects observed in H2A mutants lacking *RKR1*. Rkr1 is a protein quality control factor that is involved in the degradation of aberrant proteins, including those that extend past stop codons (BENGTSON AND JOAZEIRO 2010; BRANDMAN *et al.* 2012). The elevated

synthesis of aberrant proteins, potentially as a consequence of improper transcription in the H2A mutants, could have lethal consequences for the cell (KLUCEVSEK *et al.* 2012). The negative genetic interaction between *rkr1*Δ and the histone mutants suggests that the consequences of disrupting the acidic patch extend beyond chromatin and transcription.

We assayed the effects of the H2A substitutions on transcription elongation through analysis of Pol II density during the last wave of transcription across *GAL1-YLR454W*. In this assay, the H2A-L66A mutant exhibited a strong defect in elongation efficiency and most closely mimicked the behavior of the H2B-K123R mutant. These data support the view that H2A-L66A phenocopies H2B-K123R for loss of H2B K123ub and its consequences. The H2A-E93A and H2A-E65A mutants also exhibited impaired elongation, although not to the same degree as the H2A-L66A and H2B-K123R mutants. Given the differential effects of the H2A substitutions on the histone modification levels in the cells, differences in Pol II elongation efficiency were not unexpected. Taken together, these data indicate that H2B K123ub and its effects on downstream histone modifications and nucleosome stability are important for efficient Pol II passage through chromatin.

Combined, our data support a new role for the nucleosome acidic patch in transcription, specifically through the proper recruitment and/or activation of proteins that control H2B K123ub and downstream methylation events on H3. The mutations that disrupt this patch impair several transcription-related processes, including the modification of histones, recruitment of transcriptional machinery, the efficient passage of Pol II through chromatin, and transcription termination (Fig. 24). Many of these transcriptional defects likely stem from the pleiotropic effects of losing the critical H2B K123ub mark. Together with recent structural studies, our results strongly suggest that the acidic patch is an interaction platform for proteins that modulate

numerous chromatin transactions in eukaryotic cells. An exciting goal for future studies will be to understand how cells regulate access to this important region of the nucleosome.

	WT	H2A-F26A	H2A-E57A	H2A-E65A	H2A-L66A	H2A-L86A	H2A-E93A	H2A-L94A	H2A-H113A	Control	
H2B K123ub (western)	+	-	-/+	-/+	-	-	-	-	-	-	Control: *rtf1*Δ, *set1*Δ, *dot1*Δ, or *set2*Δ
H3 K4me2 (western)	+	+	+	-	-	+	+	-/+	+	-	
H3 K4me3 (western)	+	+	+	-	-	-/+	-/+	-/+	+	-	
H3 K79me2/3 (western)	+	+	-/+	-/+	-/+	+	-	-/+	+	-	
H3 K36me2 (western)	+	+	+	+	+	+	+	+	+	-	
H3 K36me3 (western)	+	+	+	+	+	+	+	+	+	-	
SER3 Derepression	-	-	-	-	-	-	-	-	-	+	Control: *spt16-197* or *spt6-1004*
FLO8 Cryptic Initiation	-	-	-	-/+	-	-	-	-	-	+	
H2B K123ub increase in *ubp8*Δ cells	+	N.D.	-/+	-/+	-	+	+	N.D.	N.D.	N.D.	Control: WT histone with *ubp8*Δ vs *UBP8*
H3 K4me3 increase in *ubp8*Δ cells	+	N.D.	-	-	-	+	+	N.D.	N.D.	N.D.	
H3 K79me2/3 increase in *ubp8*Δ cells	+	N.D.	-	-	-	+	-	N.D.	N.D.	N.D.	
Bre1 Occupancy	+	N.D.	-/+	-/+	-/+	-	-/+	N.D.	N.D.	-	Control: Telomeric loci, untagged protein, or no antibody control *Note: some gene-specific differences*
Rtf1 Occupancy	+	N.D.	-/+	-/+	-/+	-/+	-/+	N.D.	N.D.	-	
Spt5 Occupancy	+	N.D.	-/+	-/+	-/+	+	+	N.D.	N.D.	-	
Spt16 Occupancy	+	N.D.	-/+	+	+	+	-/+	N.D.	N.D.	-	
Set1 Occupancy	+	N.D.	+	-/+	-/+	-/+	-/+	N.D.	N.D.	-	
Pol II Occupancy	+	N.D.	-/+	-/+	-/+	+	-/+	N.D.	N.D.	-	
Elongation Rate	+	N.D.	N.D.	-/+	-	N.D.	-/+	N.D.	N.D.	N.D.	
Transcription termination	+	N.D.	-	-/+	-/+	-/+	-	N.D.	N.D.	N.D.	

Figure 24. Summary of molecular defects tested.

Phenotypes of histone mutants rated relative to WT and additional controls that are defined in the figure. Molecular defects not determined for specific mutants are denoted by "N.D."

3.0 PROBING THE NUCLEOSOME ACIDIC PATCH FOR DIRECT INTERACTIONS

The data in this chapter are all unpublished. I performed all the experiments within the chapter (except for mass spectrometry, which was performed by the University of Indiana proteomics core facility). Additionally, the following reagents for the biochemical assays were not purified by me: reconstituted nucleosomes (Song Tan lab), ubiquitin (M. Shirra), Rad6 (S.B. Van Oss), Bre1 (Jaehoon Kim lab), human E1 (Jaehoon Kim lab), and HMD (S.B. Van Oss).

3.1 INTRODUCTION

The nucleosome has long-been regarded as a barrier to transcription in eukaryotes. However, evidence that the nucleosome serves as a functional platform for chromatin-binding factors has emerged over recent years. Knowledge of the nucleosome's functional landscape has been greatly aided by histone mutant libraries and X-ray crystallography (MATSUBARA *et al.* 2007; DAI *et al.* 2008; NAKANISHI *et al.* 2008a; MCGINTY AND TAN 2015). While the histone tails have been acknowledged as the major regulatory components of the nucleosome, the globular domains can also serve as binding platforms to effect change within the chromatin environment. Notably, the nucleosome acidic patch, a highly negatively charged cavity shared between H2A and H2B, has been found to be an anchor point for a myriad of different chromatin factors. Such factors range from the Latent Nuclear Antigen peptide of Kaposi's sarcoma virus to the ubiquitylation module of PRC1 as well as the SAGA deubiquitylation module (LUGER *et al.* 1997; BARBERA *et*

al. 2006; KALASHNIKOVA *et al.* 2013; MCGINTY *et al.* 2014; MORGAN *et al.* 2016). Typically, proteins that bind to the acidic patch do so via a trio of arginines termed the "arginine anchor." This arginine anchor is the only motif that is conserved among acidic patch binding proteins.

One important process that is regulated by the acidic patch is the monoubiquitylation of H2B lysine 123 (H2B K123ub1), which is conserved from yeast to humans (BASNET *et al.* 2014; CUCINOTTA *et al.* 2015; GALLEGO *et al.* 2016; MORGAN *et al.* 2016). In humans, H2B K123ub promotes p53 transcription and stem cell differentiation (SHEMA *et al.* 2008; FUCHS *et al.* 2012). H2B K123ub corresponds with FACT and Pol II chromatin occupancy during transcription elongation. It is also required for proper histone occupancy. H2B K123ub also promotes di- and tri-methylation of H3 at lysines 4 and 79 (BRIGGS *et al.* 2002; DOVER *et al.* 2002; SUN AND ALLIS 2002; PAVRI *et al.* 2006; BATTA *et al.* 2011; FUCHS *et al.* 2014). New evidence that H2B K123ub modulates chromatin by additional means has emerged. H2B K123ub can block eviction of the histone variant H2A.Z from enhancers (SEGALA *et al.* 2016). H2B K120ub in humans is mutually regulated by another histone modification, H2B K34 (WU *et al.* 2011). Additionally, *in vitro* experiments show that H2B K123ub can disrupt higher order chromatin structure (FIERZ *et al.* 2011).

H2B K123ub is catalyzed by the ubiquitin conjugase Rad6 and ligase Bre1 and is co-transcriptionally removed by the deubiquitylating enzymes Ubp8 and Ubp10 (ROBZYK *et al.* 2000; HENRY *et al.* 2003; HWANG *et al.* 2003; WOOD *et al.* 2003a; DANIEL *et al.* 2004; EMRE *et al.* 2005; SCHULZE *et al.* 2011). In addition to the enzymes, the Polymerase Associated Factor 1 Complex (Paf1C) is required for H2B K123ub. Specifically, the Rtf1 subunit activates H2B K123ub through its Histone Modification Domain (HMD), which directly contacts Rad6 (NG *et al.* 2003; WOOD *et al.* 2003b; WARNER *et al.* 2007; PIRO *et al.* 2012; VAN OSS *et al.* 2016).

We previously reported that the nucleosome acidic patch is required for H2B K123ub and downstream modifications, transcription elongation efficiency and termination, and recruitment of Rtf1, Bre1, and Spt16 to chromatin (CUCINOTTA *et al.* 2015). What was not identified however, was whether the acidic patch was interacting directly with Rtf1, Bre1, or Spt16 to execute proper gene expression. A recent study unveiled a direct interaction between the RING domain of Bre1 and the nucleosome acidic patch (GALLEGO *et al.* 2016), which supports our previous recruitment data. Still, what was left to discover was whether the acidic patch could also directly bind Rtf1 and Spt16, or if its interaction with Bre1 was promoting recruitment of Rtf1 and Spt16 to chromatin.

In this study, we exploited a photoactivatable, unnatural amino acid to identify proteins that directly bind to the nucleosome acidic patch through site-specific crosslinking. We found that the nucleosome acidic patch binds additional transcription elongation factors: Rtf1 and Spt16. We performed *in vitro* ubiquitylation assays using recombinant acidic patch mutant nucleosomes and purified HMD. In these assays, the acidic patch mutants did not have any H2B K123ub levels above the levels in a reaction lacking Bre1. This suggests that the nucleosome acidic patch plays a direct role in promoting H2Bub a manner that that supersedes the role of Rtf1. This requirement is likely through interaction between the nucleosome acidic patch and Bre1. Using *in vivo* site-specific crosslinking, we found that the H2A-Rtf1 interaction occurs independently of Bre1 and Rad6, suggesting that this interaction occurs before H2B K123ub. We also found that the N-terminus of Rtf1 and a portion of the HMD are necessary for the H2A-Rtf1 interaction. Together, our data show that the nucleosome acidic patch plays dynamic roles during transcription elongation, as it is an important interaction hub for a variety of elongation factors.

3.2 MATERIALS AND METHODS

3.2.1 Yeast strains and media

The *S. cerevisiae* strains used in this study are listed in Table 8 and are isogenic to the strain FY2, which is a *GAL2*$^{+}$ derivative of S288C (WINSTON *et al.* 1995). Yeast transformations were performed as previously described (AUSUBEL FM 1988). For the BPA strains, log phase yeast cultures were co-transformed with the tRNA/tRNA synthetase plasmid, pLH157/*LEU2*, and the H2A derivative plasmid. Cells were grown on SC-Leu-Ura +2% glucose. For BPA experiments cells were grown in the presence of 1mM BPA.

3.2.1 Plasmid construction

H2A was cloned into pRS426 as described in (WILKINS *et al.* 2014). Gibson assembly and site-directed mutagenesis were used to generate the HBH-tagged BPA constructs. Primers and plasmids are described in Tables 9 and 10, respectively.

3.2.2 Western blot analysis

For western analyses of whole cell extracts, yeast cells were grown to log phase (0.5-1.0 OD_{600}) and 12.5 OD were lysed by bead beating in trichloroacetic acid (TCA), as described previously (COX *et al.* 1997). Proteins were resolved on SDS-polyacrylamide tris-glycine gels (15% polyacrylamide) for anti-histidine westerns and transferred to nitrocellulose membranes. For the HA-Rtf1-H2A-HBH interaction westerns, proteins were resolved for 4 hours at 100V on 4%

- 8% polyacrylamide gradient Tris-Acetate denaturing gels (Novex, Life Technologies) and transferred to PVDF membranes. For IP western blots, proteins were resolved on 4% - 20% polyacrylamide gradient Tris-Glycine denaturing gels (BioRad) and transferred to nitrocellulose membranes. Membranes were incubated with primary antibodies and then with anti-mouse or anti-rabbit secondary antibodies (GE Healthcare 1:5,000 dilution in 5% dry milk and 1X TBST). Proteins were visualized using enhanced chemiluminescence substrate (PerkinElmer) and a ChemiDoc XRS digital imaging station (BioRad).

3.2.3 Photocrosslinking

50 mL of cells were grown to log phase (between 0.5 and 1.0 OD_{600}) in SC-Leu-Ura + 2% dextrose and 1mM BPA. For each culture, two sets of 12.5 OD units were pelleted and separately resuspended in 1 mL ddH_2O. One half was placed in the center of a 50-mL falcon tube lid 2 cm below a UVGL-55 lamp, which UV-irradiated the cells at 365 nm. Cells were exposed to UV light for 10 minutes. All cells were then subjected to TCA extraction, as described above.

3.2.4 Protein purification

WT and mutant LANA were purified as described in (ENGLAND *et al.* 2010). Briefly, BL21 (DE3)pLysS cells expressed the HisTrxN-LANA constructs. 1L of cells were grown at 37°C to an OD_{600} of 0.5. Protein expression was induced by incubating the culture with 0.2 mM IPTG for one hour. Cells were lysed and HisTrxN-LANA protein was purified via nickel affinity chromatography followed by Q anion-exchange HPLC.

3.2.5 *In vitro* ubiquitylation assay

For the LANA peptide competition, either WT or mutant LANA was pre-incubated with 2.5 µg of reconstituted *Xenopus laevis* nucleosomes in thin-walled PCR tubes for 30 minutes in a 30°C water bath. Following pre-incubation, 10 µl reactions were set up in the presence of 1X reaction buffer containing: 50 mM Tris HCl, 7.9, 5 mM $MgCl_2$, 2 mM NaF, 0.4 mM DTT, 4 mM ATP. In the following order, these factors were added to the reaction: 1.4 µg His-pK-HA-Ubiquitin, 50 ng FLAG-hE1, 100ng FLAG-yBre1, and 100ng yRad6. For the HMD experiment, instead of pre-incubation with nucleosomes, 15 pmol of purified HMD was added prior to the ubiquitin and same procedure was followed. All reactions were immediately stopped by adding 1X SDS loading buffer and boiling for 3 minutes in a thermocycler and flash freezing the samples in liquid nitrogen.

3.2.6 Immunoprecipitation

100 mL of cells were grown to OD_{600} 1.0. Cells were pelleted and resuspended in 4mL of ddH_2O. Cells were UV-irradiated 1mL at a time for 10 minutes each. Cells were pelleted together and lysed by hand vortexing the pellets with ~500 µl glass beads in 500 µl lysis buffer: 50 mM Tris 8, 300 mM NaCl, 20 mM imidazole, 0.1% NP-40, and 8M urea for 30s at a time, 7 times with one minute on ice in between vortexing. Lysates were separated from glass beads and then cleared by centrifugation at 15000 X g for 10 min at 4°C. 50 µl of lysate was saved for the input sample. ~450 µl was incubated with 100 µL pre-equilibrated (in lysis buffer) magnetic nickel beads (Qiagen) overnight at 4°C. The beads were washed four times with wash buffer: 50 mM Tris 8, 300 mM NaCl, 25 mM NaCl, 25 mM imidazole, 0.1% NP-40, and 8M urea. Proteins were eluted

in 50 mM Tris 8, 300 mM NaCl, 1 M imidazole, and 8 M urea. All buffers contained 1X HALT protease inhibitors (Thermo Fisher).

Strain	***MAT***	**Genotype**
KY2808	α	*his3Δ200 lys2-128δ leu2Δ1 ura3-52 3XHA-RTF1*
KY860	a	*his3Δ200 lys2-128δ leu2Δ0 ura3Δ0*
KY2788	α	*his4-912δ lys2-128δ ura3-52 trp1Δ63 3XHA-RTF1 bre1Δ::kanmx*
KY3019	a	*his3Δ200 lys2-128δ leu2Δ1 ura3-52 3XHA-RTF1 rad6Δ::kanmx*
KY680	α	*his4-912δ lys2-173R2 leu2Δ1 ura3-52 trp1Δ63 3XHA-rtf1Δ1*
KY2032	a	*his4-912δ lys2-128δ leu2Δ1 trp1Δ63 ura3-52 3XHA-rtf1Δ3*
KY2033	a	*his4-912δ lys2-128δ leu2Δ1 trp1Δ63 ura3-52 3XHA- rtf1Δ4*
KY1155	a	*his3Δ200 leu2Δ1 ura3-52 trp1Δ63 3XHA- rtf1Δ5*
KY1157	a	*his3Δ200 leu2Δ1 ura3-52 trp1Δ63 3XHA- rtf1Δ7*
KY2423	a	*his4-912δ lys2-128δ leu2Δ1 ura3-52 trp1Δ63 3XHA-rtf1-R251E-R273E-K299E*
KY2424	a	*his4-912δ lys2-128δ leu2Δ1 ura3-52 trp1Δ63 3XHA-rtf1 -R273E-R288E*
KY1159	a	*his3Δ200 leu2Δ1 ura3-52 trp1Δ63 3XHA- rtf1*Δ12
KY1420	α	*his3Δ200 leu2Δ1 ura3-52 trp1Δ63 3XHA- rtf1Δ13*

Table 8. Strains used in this study

Primer	Dir.	Sequence 5' → 3'	Ref.
Amplify *HTA1* 450 bp up and down ATG	F R	ATCAGAGCTCGCGCTGTTCCAAAATTTTCGCC ATCACTCGAGGCGTATATATATATACAAATATGCG	(WILKINS *et al.* 2014)
Back bone for gibson assembly to add HBH tag	F R	TAAGATCGGTTCTGGTATTTTAAAG TAATTCTTGAGAAGCCTTGG	This study
Insert for Gibson assembly to add HBH tag to H2A	F R	AAGGCTTCTCAAGAATTATTAATTAACAGGGGTTCACATC TACCAGAACCGATCTTAAGATCTATATTACCCTGTTATCC	This study
Y58TAG SDM	F R	ACTTGACTGCTGTCTTGGAATAGTTGGCCGCTGAAATT TCTAAAATTTCAGCGGCCAACTATTCCAAGACAGCAGTC	This study
A61TAG SDM	F R	CTTGGAATATTTGGCCTAGGAAATTTTAGAATTAGC CAGCTAATTCTAAAATTTCCTAGGCCAAATATTCCAAGAC	This study

Table 9. Primers used in this study

Plasmid	Purpose	Derivation and reference
pCEC09	Untagged H2A	This study; (WILKINS *et al.* 2014)
pCEC21	WT H2A-HBH	Gibson assembly of pCEC09
pCEC23	H2A-AY58$_{BPA}$-HBH	Site-directed mutagenesis of pCEC09
pCEC23	H2A-A61$_{BPA}$-HBH	Site-directed mutagenesis of pCEC09
pST50Tr-LANA	WT LANA	(ENGLAND *et al.* 2010)
pST50Tr-LANA8LRS	8LRS mutant LANA	(ENGLAND *et al.* 2010)
pLH157/*LEU2*	tRNA/tRNA synthetase containing plasmid	(VAN OSS *et al.* 2016)

Table 10. Plasmids used in this study

3.3 RESULTS

3.3.1 The nucleosome acidic patch directly promotes H2B K120ub

Previous studies have shown that the nucleosome acidic patch is a central regulator of histone modifications associated with transcription elongation (BASNET *et al.* 2014; CUCINOTTA *et al.* 2015; GALLEGO *et al.* 2016; MORGAN *et al.* 2016). Our goal was to identify previously unknown chromatin-associated factors that bind the nucleosome acidic patch. One process we focused on was H2B K123ub, as the acidic patch was recently found to be directly involved in promoting H2B K123ub (GALLEGO *et al.* 2016). Using a minimal *in vitro* ubiquitylation system (KIM AND ROEDER 2009; VAN OSS *et al.* 2016), we blocked the nucleosome acidic patch using the LANA peptide of Kaposi's sarcoma virus, which was previously co-crystallized with the nucleosome (BARBERA *et al.* 2006). In the presence of LANA, H2B K120ub levels were decreased (Fig. 25A, lanes 6-8). This reduction was not observed when a mutated form of LANA that cannot bind to the acidic patch was added to the reaction (Fig. 25A, lanes 4 and 5). This result confirmed that the acidic patch plays a direct role in promoting H2B K120ub, which was previously shown for H2B K123ub using yeast nucleosomes in (GALLEGO *et al.* 2016).

3.3.2 Site-specific crosslinking experiments indicate that multiple proteins bind to the nucleosome acidic patch

To identify proteins that bind to the acidic patch *in vivo*, particularly those that might play a role in H2B K123ub, we employed site-specific crosslinking using a photoactivatable, unnatural amino acid, ρ-benzoyl-phenylalanine (BPA). This amino acid can be incorporated at specific

locations within a protein of interest via amber suppression (CHIN *et al.* 2003). Others have successfully used this system to identify nucleosome-nucleosome interactions during mitosis (WILKINS *et al.* 2014). We adapted this system for use in targeted western blot screening and mass spectrometry analysis. Wild-type yeast expressed the engineered tRNA and tRNA synthetase, as well as a C-terminally tagged H2A with or without the amber codon. Two plasmids were generated, each carrying a mutant form of *hta1*: a plasmid encoding H2A-Y58BPA or H2A-A61BPA. We chose these locations (Fig. 25B; orange and blue residues) because they are located near amino acids we previously described to be required for H2B K123ub (Fig. 25B; red residues) (CUCINOTTA *et al.* 2015). We hypothesized that we would be able to capture proteins that bind to the acidic patch using site-specific crosslinking at these sites. For the C-terminal tag, we utilized a 6XHis-Biotin-6XHis-tag for use in denaturing conditions. Thus, we can detect H2A and any H2A-crosslinked species using an anti-His antibody. Placing the tag at the C-terminus was also advantageous because we would not detect or purify truncated H2A proteins in which BPA was not incorporated. When cells were exposed to long-wave UV radiation, and the resulting whole-cell extracts were subjected to western blot analysis, we observed several UV-specific bands for cells expressing the two H2A BPA derivatives (Fig. 25C). These UV-specific bands are indicative of interactions between unknown proteins and H2A residues Y58BPA and A61BPA. Based on the crystal structure of the nucleosome (Fig. 25B), we performed western blot analysis with an H2B antibody and detected the H2A-H2B interaction in the A61BPA mutant, which confirmed that the BPA crosslinking experiments could detect known interactions (Fig. 25D, lane 5).

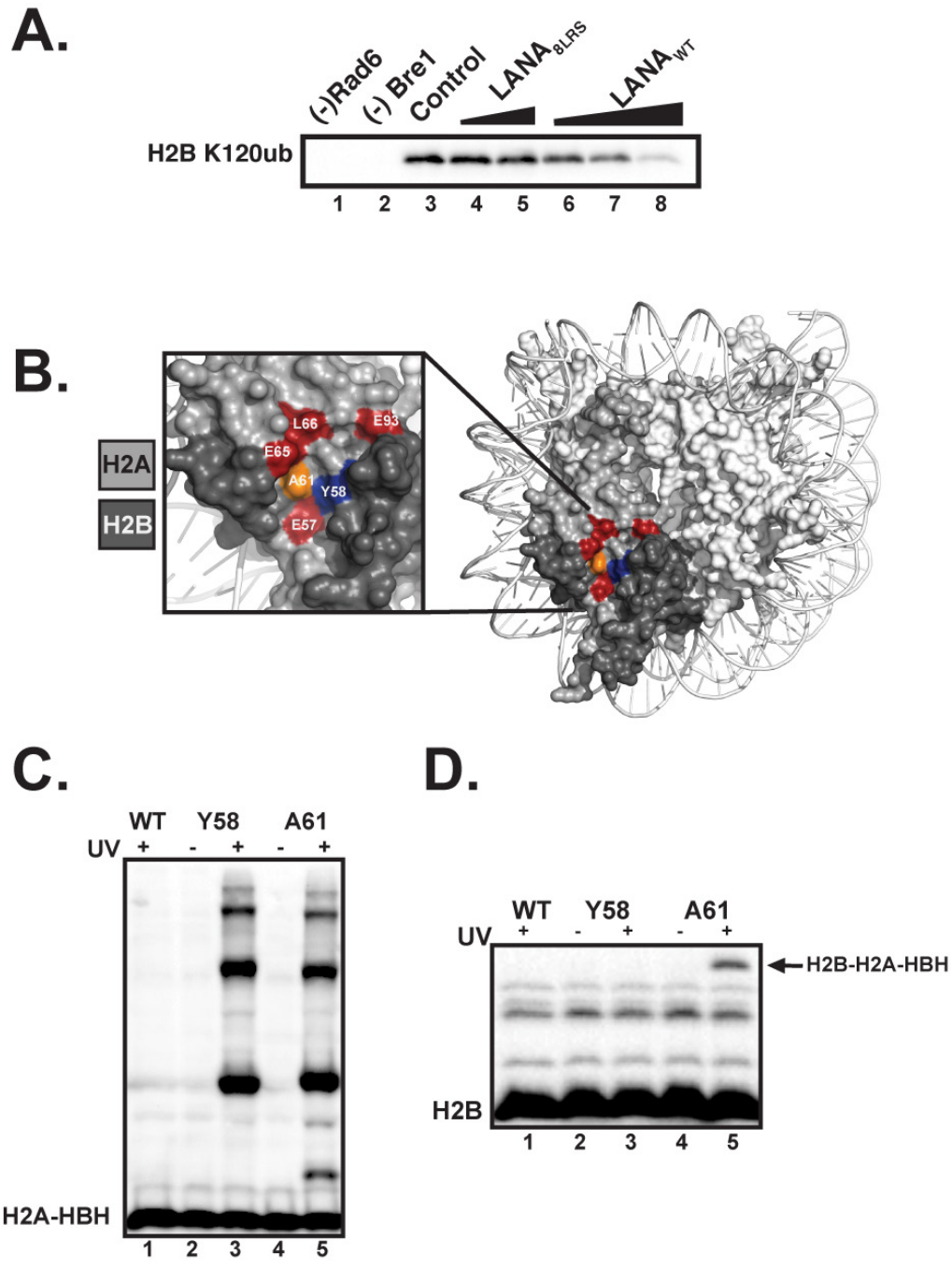

Figure 25. The nucleosome engineered for BPA crosslinking experiments

(A) *In vitro* ubiquitylation assay with increasing concentrations of WT or mutant LANA added to the reaction. Western blot is probed with an antibody against H2B K120ub. **(B)** X-ray

crystal structure indicating amino acids for which BPA was substituted (orange and blue). Residues in red were previously shown to be required for histone modifications in the H2B K123ub cascade (CUCINOTTA *et al.* 2015). This figure was created using Pymol (PDB 1ID3 (WHITE *et al.* 2001)). **(C)** Western blot of UV-crosslinked products. Western blot was probed with an anti-His antibody to detect the HBH tag on the H2A derivatives. Bottom band is uncrosslinked H2A-HBH proteins and upper bands are UV-specific crosslinked species. **(D)** Western blot was probed with anti-H2B antibody. H2A-61BPA interacts with H2B, presumably through the H2A-H2B dimer.

3.3.3 Rtf1 interacts with H2A *in vivo* but the histone modification domain of Rtf1 cannot rescue H2Bub defects in acidic patch mutants *in vitro*

To determine the identity of the different crosslinked species (Fig. 25C), we performed a targeted western blot screen focusing on potential crosslinking between the H2A derivatives and H2B K123ub-associated factors. One key H2B K123ub-promoting factor is Paf1C-member Rtf1, which has been implicated in stabilizing Bre1 protein levels and directly contacts Rad6 *in vivo* (WOZNIAK AND STRAHL 2014; VAN OSS *et al.* 2016). Our previous work showed a marked decrease in Rtf1 occupancy at actively transcribed genes when residues within the acidic patch were substituted with alanine (CUCINOTTA *et al.* 2015). We posited that Rtf1 could directly contact the acidic patch, so we tested crosslinking between the H2A derivatives and 3XHA-Rtf1 (Fig. 26A). Interestingly, we found that cells expressing the H2A-A61BPA derivative exhibited crosslinking between H2A and 3XHA-Rtf1, while cells expressing the H2A-Y58BPA derivative did not (Fig. 26A; lanes 3 and 5). This result suggests that the site of BPA crosslinking is specific, in that a neighboring residue, H2A-Y58BPA, cannot capture the interaction. A61 is situated between two acidic residues, E57 and E65 (Fig. 25B); it is thus possible that this location was more amenable

to capturing certain interactions within the acidic patch compared to the Y58 location. Another possibility is that Y58 itself could be required for the Rtf1-H2A interaction. Likewise, we were able to detect the interaction using an endogenous Rtf1 antibody in an untagged Rtf1 strain (Fig. 26B). However, this crosslinked species was difficult to visualize and reproduce. It is possible that H2A may be binding to a region within the Rtf1 epitope and thus obscuring the detection of the interaction using the Rtf1 antibody. We attempted to visualize crosslinking between H2A and other H2B K123ub-related factors (Bre1 and Rad6); however, we did not reliably detect crosslinking using this method. Further, we did not detect crosslinking between H2A and Paf1 (data not shown), which was previously suggested to interact with H3 (CHU *et al.* 2013). Nevertheless, this result indicates that H2A can directly interact with Rtf1, which corroborates our previous chromatin occupancy data.

The histone modification domain (HMD) of Rtf1 has been shown to enhance H2Bub *in vitro*, and it is necessary and sufficient to stimulate H2B K123ub *in vivo* (PIRO *et al.* 2012; VAN OSS *et al.* 2016). Thus, we tested whether the HMD could rescue H2B K123ub defects caused by alanine substitutions within the acidic patch *in vitro.* We employed the minimal ubiquitylation system using mutant *Xenopus* nucleosomes, where acidic residues E61, E64, D90, and E92 have been substituted with alanine. We added purified HMD to the reaction and observed no stimulation of H2B K123ub by the HMD in this context (Fig. 26C). These results support a previous study that suggested the acidic patch binds to the RING domain of Bre1 to stimulate H2Bub using yeast nucleosomes *in vitro* (GALLEGO *et al.* 2016). Our *in vitro* data here suggest that the acidic patch primarily promotes H2Bub through the Bre1 interaction. The reaction containing wild-type nucleosomes but lacking Bre1 has virtually identical levels of H2B K123ub as reactions containing acidic patch mutant nucleosomes (Fig. 26C; compare lane 1 and lanes 4 and 5). Our previous data

show that the acidic patch is required for recruiting both Bre1 and Rtf1 to chromatin (CUCINOTTA *et al.* 2015). Thus, it is still possible that Rtf1 may be important for the role of the acidic patch in H2Bub *in vivo*, as there are some discrepancies between the *in vitro* ubiquitylation assay and the role of the HMD *in vivo*. For example, a shorter form of the HMD can substitute for full Rtf1 (and even complete Paf1C) to promote H2Bub *in vivo*. However, only a longer form of the HMD can stimulate H2Bub *in vitro* (VAN OSS *et al.* 2016). Furthermore, it is still a possibility that Rtf1 and Bre1 can both bind the acidic patch. However, because the mutant nucleosome disrupts interaction with Bre1, we cannot detect any effect of Rtf1's stimulatory role. The disruption of the Bre1-nucleosome interaction is effectively dominant to the disruption of the HMD interaction.

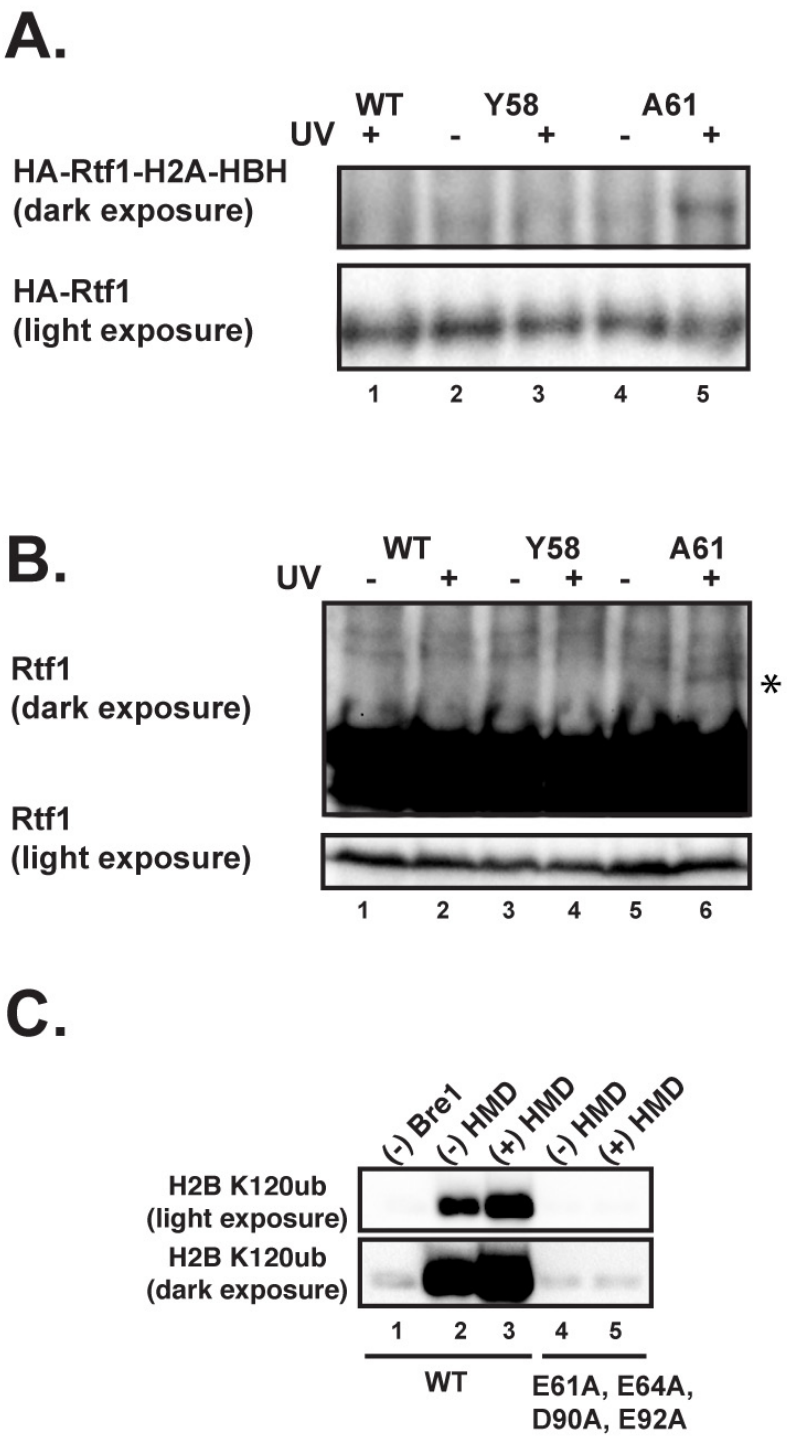

Figure 26. H2A crosslinks with Rtf1 at residue 61 of H2A

(A) Western blot of UV-crosslinked proteins. Upper panel shows the cross-linked species, bottom panel shows non-crosslinked products. Western blots were probed with anti-HA antibodies

to detect HA-tagged Rtf1 species. **(B)** Western blot of UV-crosslinked proteins probed with an anti-Rtf1 antibody. Asterisk denotes putative H2A-Rtf1 interaction. Bottom band is un-crosslinked Rtf1. Top panel is a darker exposure of the bottom panel. **(C)** Western blot of *in vitro* ubiquitylation assay probed with H2B K120ub antibody. Bottom panel is a darker exposure of the upper panel.

3.3.4 The Rtf1-H2A interaction is independent of H2Bub machinery

Due to the interdependent nature of chromatin association among Bre1, Rad6, and Rtf1 (WU *et al.* 2014; VAN OSS *et al.* 2016), we sought to determine whether the H2A-Rtf1 interaction was dependent upon Rad6/Bre1. We previously showed that Rtf1 directly interacts with Rad6 (VAN OSS *et al.* 2016). Thus, we tested if the H2A-Rtf1 interaction would be reduced or lost in strains lacking *BRE1* or *RAD6*. We performed BPA-crosslinking with the A61 derivative and used the Y58 derivative and WT as controls. Interestingly, we observed no decrease in the Rtf1-H2A band in the absence of Bre1 or Rad6, suggesting that the H2A-Rtf1 interaction may occur before Bre1/Rad6 association (Fig. 27A-B). It is possible that there is a very subtle increase in the H2A-A61BPA-Rtf1 crosslink in the *bre1*Δ strain, which could be due to a reduction in competition among proteins binding to the acidic patch (Fig. 27A).

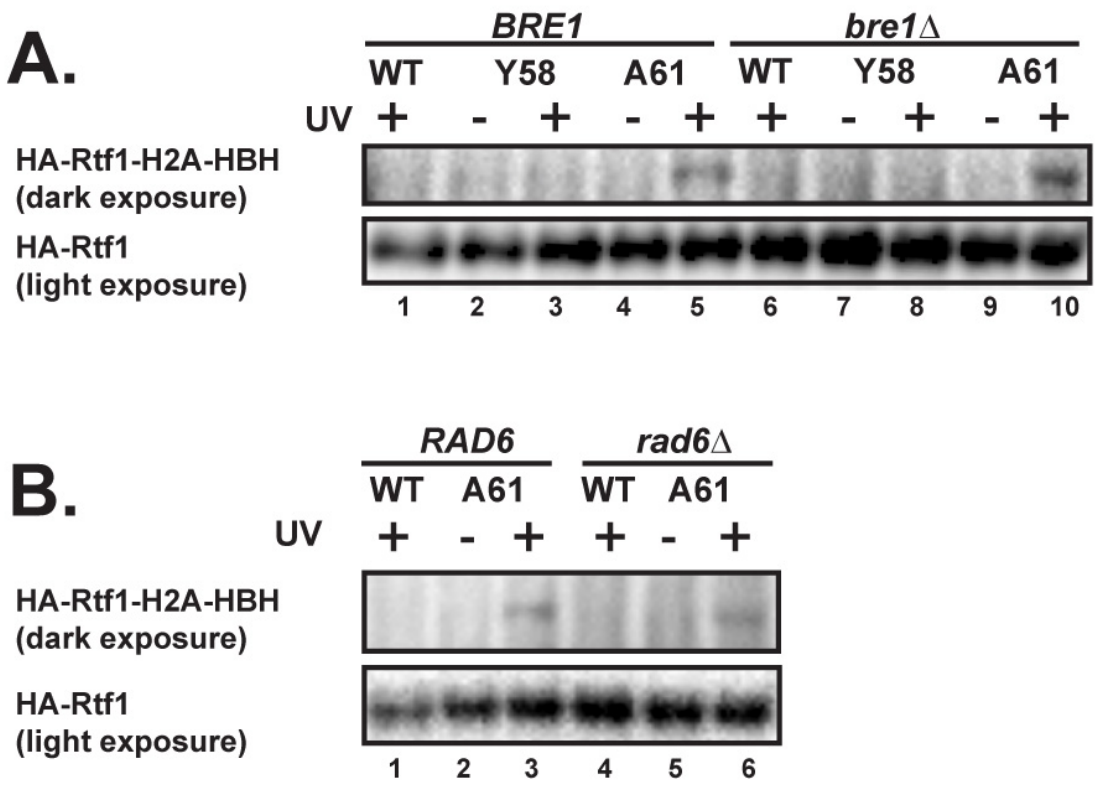

Figure 27. Rtf1 and interact with H2A independently of H2Bub enzymes

Western blots of UV-crosslinked proteins. Upper panel shows the cross-linked species with a longer exposure, bottom panel shows non-crosslinked products with a lighter exposure. Western blots were probed with anti-HA antibodies to detect HA-tagged Rtf1 species.

3.3.5 H2A Residue L66 is not required for the H2A-Rtf1 interaction

We previously showed that substitution of H2A-L66 with alanine eliminates H2B K123ub *in vivo* regardless of the presence or absence of the deubiquitinating enzyme Ubp8. We concluded that the H2A-L66A substitution prevents placement of ubiquitin on H2B K123, rather than increasing removal of ubiquitin by Ubp8 (Chapter 2 (CUCINOTTA *et al.* 2015)). Given Rtf1's role in promoting H2B K123ub, we decided to assess whether the L66A substitution would diminish the H2A-Rtf1 interaction. To do this, we performed UV-crosslinking of the H2A-A61BPA mutant with and without the alanine substitution at H2A L66. The overall pattern of H2A-crosslinked species was unchanged when L66 was substituted with alanine (Fig. 28A). When probing for the H2A-Rtf1 interaction, we did not detect a loss of the Rtf1-H2A crosslinking band when L66 was substituted with alanine (Fig. 28B). It is possible that the L66A substitution increases the level of the H2A-A61BPA-Rtf1 crosslink. This result suggests that the role of L66 in promoting H2B K123ub could be involved in the acidic patch's interaction with Bre1 rather than with Rtf1.

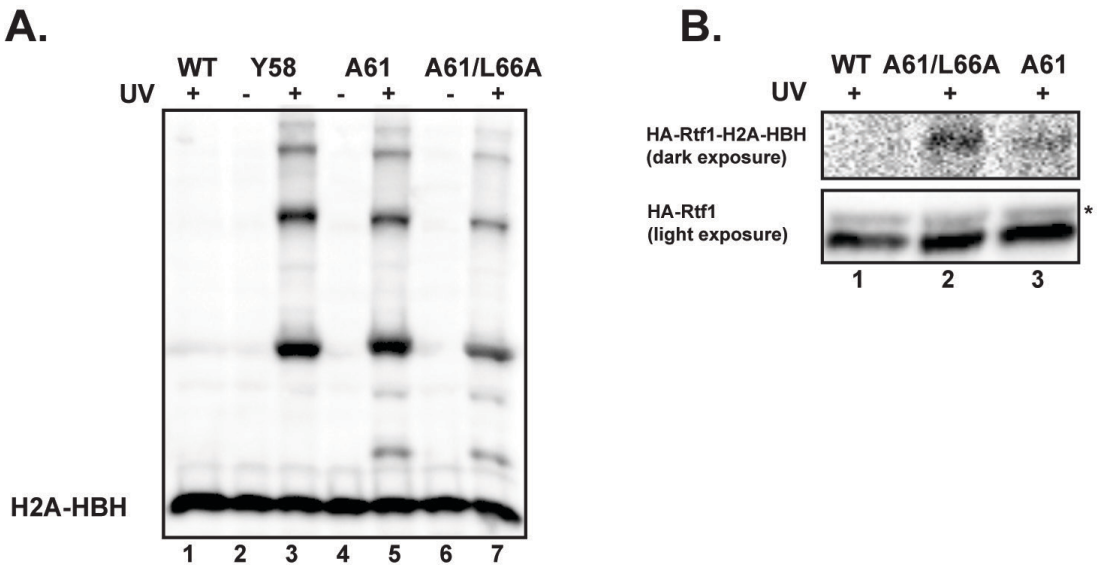

Figure 28. H2A-L66A still interacts with Rtf1 at H2A-A61BPA

(A) Western blot analysis of UV-crosslinking with the indicated H2A derivatives. Immunoblot was probed with an anti-histidine antibody to detect H2A-HBH and its crosslinked species. (B) Western blot analysis of the H2A-Rtf1 interaction of UV-crosslinked samples. WT = no BPA located in the protein, A61/L66A = BPA located at residue 61 and L66 substituted with alanine. A61 = BPA located at residue 61 and no alanine substitution at L66. Asterisk denotes non-specific band.

3.3.6 The amino terminus and a portion of the HMD of Rtf1 are required for the H2A-Rtf1 interaction

Rtf1 is a multifunctional protein with several domains that have been previously characterized and a diagram representing data from these studies is represented in figure 29 (WARNER *et al.* 2007; PIRO *et al.* 2012; MAYEKAR *et al.* 2013; WIER *et al.* 2013; WOZNIAK AND STRAHL 2014; VAN OSS *et al.* 2016). The amino-terminus (region 1) of Rtf1 is required for recruitment of chromatin remodeler Chd1 to chromatin (WARNER *et al.* 2007). The HMD is defined by regions 3 and 4 and is required for H2Bub and downstream modifications (WARNER *et al.* 2007; PIRO *et al.* 2012; VAN OSS *et al.* 2016). Region 5, when deleted exhibits an Spt$^-$ phenotype, though little is known about this region. Region 7 is a part of the Plus-3 domain, or ORF association region (OAR), and it tethers to the phosphorylated C-terminus of Spt5 during transcription elongation. When residues R251, R273, R288, and K299 are substituted with glutamic acid, this function is lost (WARNER *et al.* 2007; MAYEKAR *et al.* 2013; WIER *et al.* 2013). Regions 12 and 13 are required for Rtf1 to associate with the rest of the Paf1C (WARNER *et al.* 2007). Given this knowledge of Rtf1's domain functions, we sought to determine which of these specific domains were required for the H2A-Rtf1 interaction. To test this, we utilized integrated alleles of *3XHA-rtf1* in the BPA cross-linking experiments. As a positive control, we used full-length Rtf1 with the A61$_{BPA}$ substitution and as a negative control we used WT H2A.

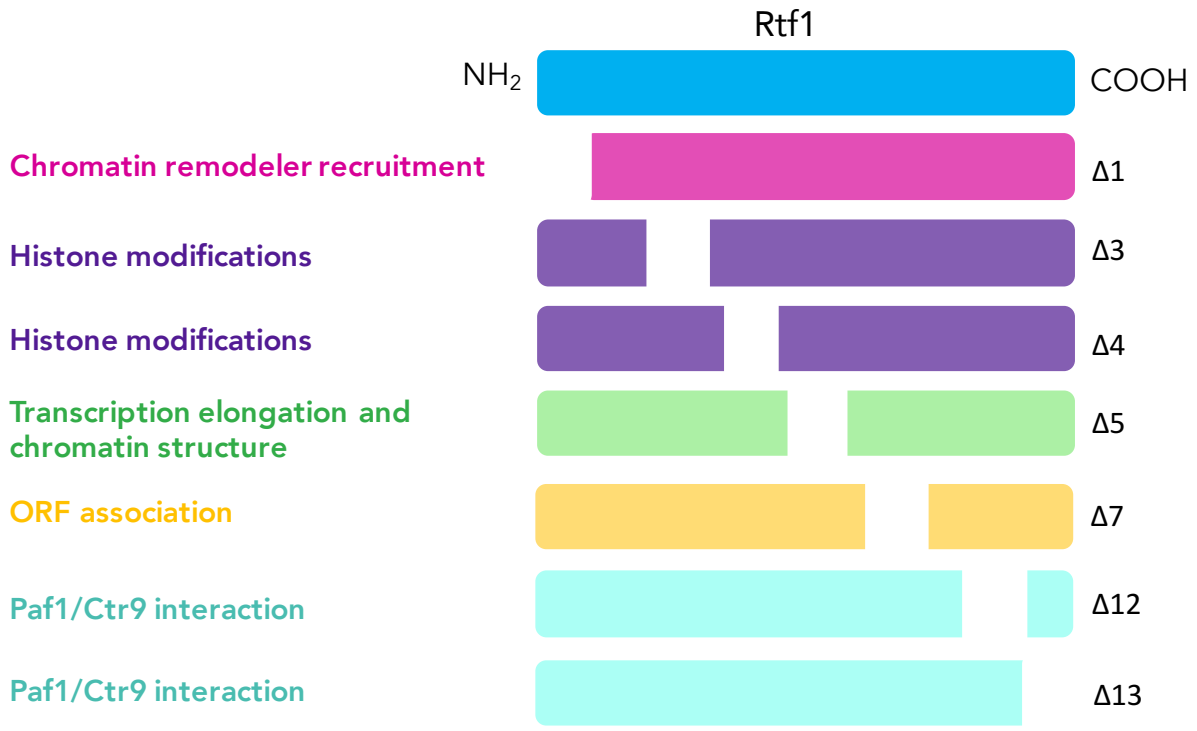

Figure 29. Diagram of Rtf1 internal deletion mutants tested

Adapted from (WARNER *et al.* 2007), regions of Rtf1 have different functions in gene expression.

Figure 30 A-E show the different crosslinking species between Rtf1 mutant proteins and H2A. Notably, we saw a loss of a UV-specific band in the *rtf1Δ1* mutant, which was intriguing to us, as this the region required for Chd1 recruitment (Fig. 30A). Surprisingly, we observed several cross-reacting bands throughout the Rtf1 deletion series, some of which appear to potentially crosslink upon UV-irradiation and some that do not. It is possible that these species could be modified forms of Rtf1. An example of this is in Fig. 30A, where there are two upper bands in lanes 4 and 5 that are present with or without UV exposure. While *rtf1Δ3*, which is the first half of the HMD, still bound to H2A, *rtf1Δ4* showed a reduction in the H2A-Rtf1 crosslinked species. This result suggests that a portion of the HMD is required for the H2A-Rtf1 interaction (Fig. 30B).

Again, minor bands are present in lanes 4-7 and it appears that the minor band no-UV lane of *rtf1*Δ3 mutant may undergo crosslinking, as the band disappears in the UV lane. The *rtf1*Δ*5* mutant did not show a loss for the H2A-Rtf1 interaction (Fig. 30C). The Plus-3 domain mutants did not have a reduction in the H2A-Rtf1 interaction either (Fig. 30D). It is notable that the shift in band sides of the crosslinked species did not change as drastically expected (compare lanes 3 and 5; there is little to no change in band size). However, this is not unique to BPA-crosslinking experiments, as a crosslinked species between Rtf1 and Rad6 did not migrate as expected either (VAN OSS *et al.* 2016). Deletion of regions 12 and 13 did not impact the H2A-Rtf1 interaction (and these crosslinked bands did migrate more quickly compared to WT Rtf1), suggesting that Rtf1 does not need to interact with the rest of the Paf1C to bind H2A (Fig. 30E). Together, these data suggest a specific requirement for regions 1 and 4 for Rtf1 to interact with H2A. There are no arginines located in region 1 and there are several located in region 4. It is thus possible that Rtf1 may interact with H2A through region 4 and Chd1 chromatin binding may be required for the H2A-Rtf1 interaction.

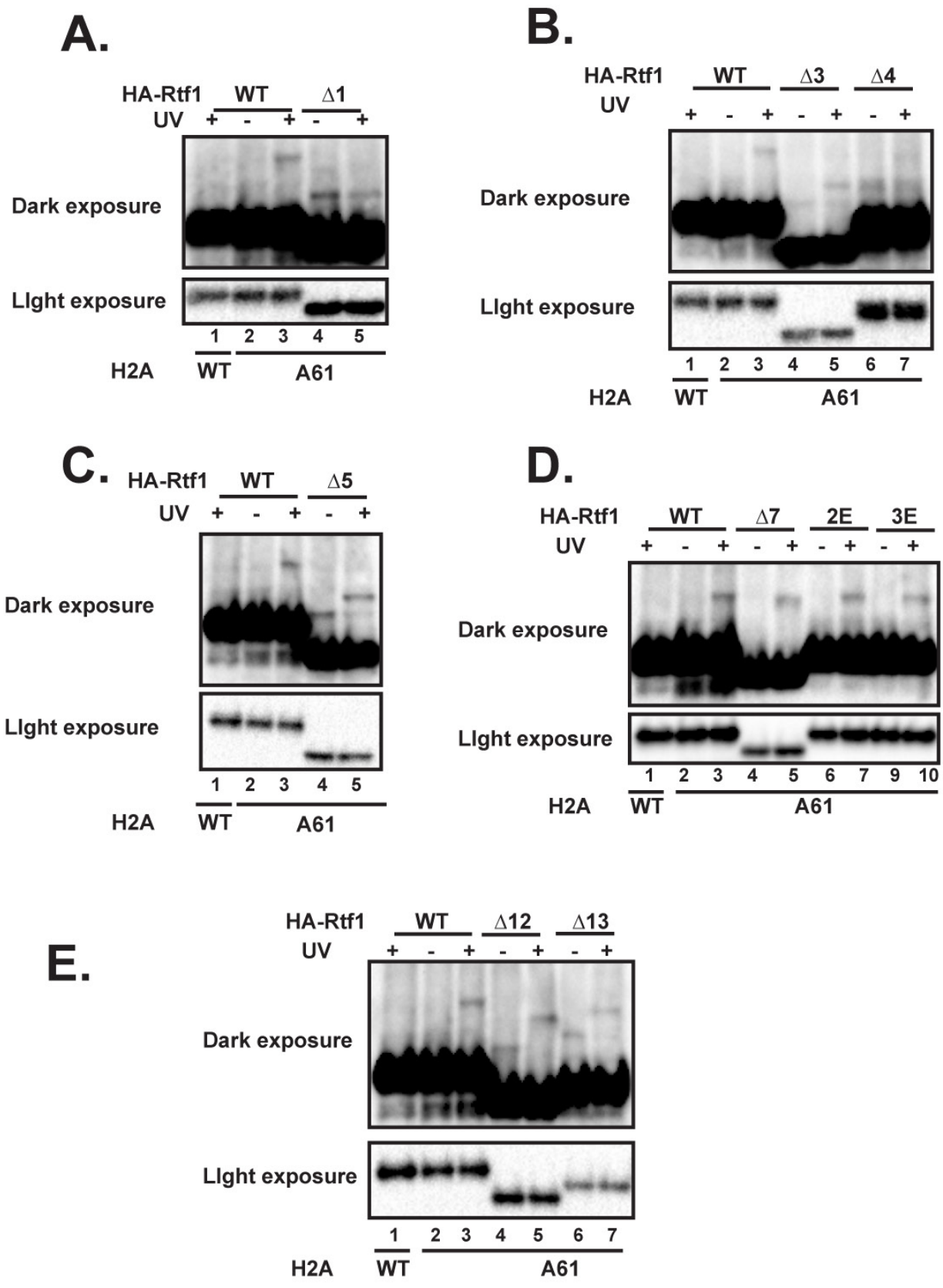
A.
HA-Rtf1
WT
Δ1
UV
+ - + - +
Dark exposure
Light exposure
1 2 3 4 5
H2A
WT
A61
B.
HA-Rtf1
WT
Δ3
Δ4
UV
+ - + - + - +
Dark exposure
Light exposure
1 2 3 4 5 6 7
H2A
WT
A61
C.
HA-Rtf1
WT
Δ5
UV
+ - + - +
Dark exposure
Light exposure
1 2 3 4 5
H2A
WT
A61
D.
HA-Rtf1
WT
Δ7
2E
3E
UV
+ - + - + - + - +
Dark exposure
Light exposure
1 2 3 4 5 6 7 9 10
H2A
WT
A61
E.
HA-Rtf1
WT
Δ12
Δ13
UV
+ - + - + - +
Dark exposure
Light exposure
1 2 3 4 5 6 7
H2A
WT
A61

Figure 30. Internal deletions throughout Rtf1 reveal a role for the amino-terminus and HMD for the Rtf1-H2A interaction.

(A) Western blot analysis using an antibody against the HA-epitope tag on Rtf1 to detect the H2A-Rtf1 interaction with the amino-terminus of Rtf1 deleted. Top panel: a dark exposure of the immunoblot. Bottom panel: a light exposure of the immunoblot to show loading. **(B)** Western blot of the H2A-Rtf1 interaction in strains containing deletions of HMD regions. **(C)** Analysis of the Δ5 region. **(D)** Analysis of the Plus-3 domain. Δ7 is a deletion of the Plus-3 domain and 2E (R273E, R288E) and 3E (R251E, R273E, and K299E) are amino acid substitutions within the Plus-3 domain of Rtf1. **(E)** Analysis of the C-terminus of Rtf1. All westerns were probed with an HA-antibody on PVDF membranes.

3.3.7 BPA-crosslinking followed by mass spectrometry reveals an interaction between H2A and FACT complex member Spt16

The common motif among proteins that bind to the nucleosome acidic patch is a group of three arginines that bind to the glutamic acids on the nucleosome, termed the "arginine anchor." While crystallography has shown a key role for the arginine anchor, it has not yet been possible to predict proteins that bind the acidic patch bioinformatically (McGinty and Tan 2015). Thus, we sought to identify new interacting proteins with the acidic patch using our BPA-crosslinking system followed by affinity purification under denaturing conditions and mass spectrometry.

We utilized the histidine tag on the H2A constructs to perform pull-downs using nickel magnetic beads in the presence of 8M urea (Fig. 31A). Eluates were sent to the Indiana University proteomics core facility for mass spectrometry. This experiment had very high background and few chromatin-associated peptide hits (data not shown). However, we did notice some BPA-specific peptides for Spt16, a member of the FACT histone chaperone complex. This was intriguing to us because we previously published that the acidic patch is required for proper histone occupancy as well as Spt16 occupancy (Chapter 2; (Cucinotta *et al.* 2015)). A recent study also showed a reduction in immunoprecipitation between Spt16 and H2A when acidic patch residues were substituted with alanine, which supported our previous result (Hodges *et al.* 2017). We thus assessed crosslinking between Spt16 and H2A from our IP samples (Fig. 31). Interestingly, we were able to detect an H2A-Spt16 interaction in the eluates from the nickel pull-down experiment suggesting that the nucleosome acidic patch interacts with Spt16 as well as Rtf1(Fig. 31B).

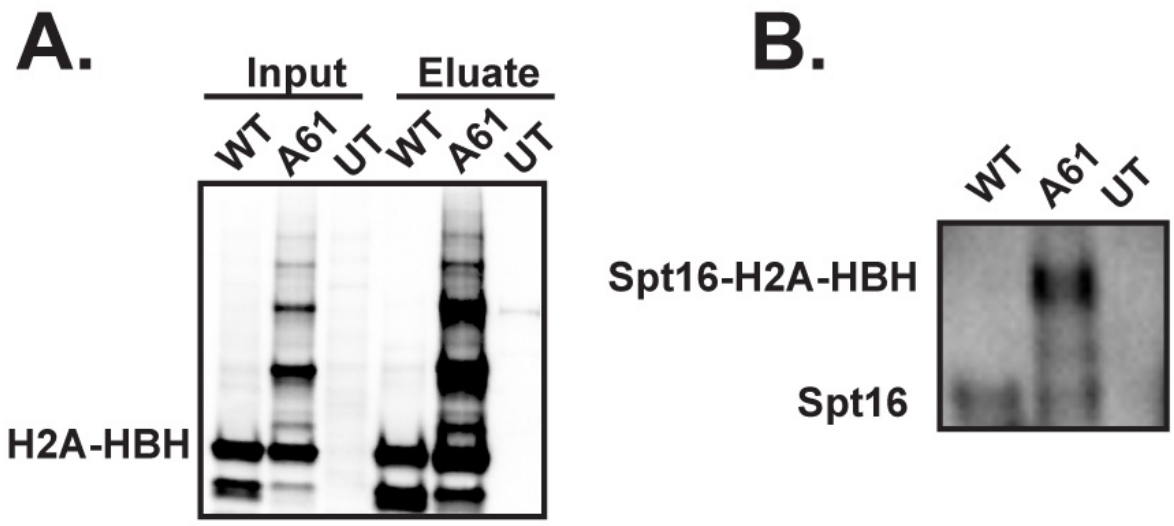

Figure 31. Nickel pull-down following UV-crosslinking of BPA incorporated in H2A at residue 61

(A) Western blot of H2A-HBH probed with an anti-histidine antibody. Samples correspond to WT = wild type, A61 = BPA at residue 61 of H2A, UT = untagged WT H2A. Samples were UV-irradiated, lysed, and purified with magnetic nickel beads. **(B)** Eluate samples probed for Sp16. A crosslinked species is apparent in lane 2.

3.4 DISCUSSION

In this study, we employed site-specific *in vivo* crosslinking to identify previously unknown proteins that interact with the nucleosome acidic patch. Given our previous analysis of the nucleosome acidic patch's role in transcription-coupled histone modifications and transcription elongation (CUCINOTTA *et al.* 2015), we focused our analysis on proteins involved in these pathways. Our efforts yielded interactions with the Paf1C subunit Rtf1 and Spt16. These results were exciting because we had previously showed that the nucleosome acidic patch is required for proper Rtf1 and Spt16 occupancy. However, it was not known whether the acidic patch could be acting directly or indirectly in regulating Rtf1 and Spt16 occupancy. Here we demonstrate that the acidic patch is likely acting directly in transcription elongation, in part through interactions with Rtf1 and Spt16.

In vitro ubiquitylation assays revealed a role for the acidic patch in promoting H2B K120ub. This was previously shown to be through its interaction with the RING domain of Bre1 (GALLEGO *et al.* 2016). We confirmed that the acidic patch is required for H2B K120ub (Fig. 25A). While we were not able to detect crosslinking between the two H2A BPA derivatives and Bre1, we showed that the acidic patch interaction with Bre1 is dominant to the role of the HMD in stimulating ubiquitylation *in vitro*. Levels of H2B K120ub in the context of acidic patch mutant nucleosomes resembled the level of a reaction lacking Bre1(Fig. 26C). It is possible that different BPA locations within the acidic patch may reveal a direct interaction between Bre1 and H2A.

The observation that the Bre1-nucleosome acidic patch interaction is dominant to the HMD *in vitro* does not preclude the possibility that the HMD interacts with the acidic patch. In addition to its interaction with Rad6 (VAN OSS *et al.* 2016), there are other possible roles for the HMD in stimulating H2B K123ub *in vivo.* Our data showing that the H2A-Rtf1 interaction is independent

of Rad6/Bre1 *in vivo* could suggest that Rtf1 could bind to H2A, at least transiently, before Rad6/Bre1 interact with the nucleosome (Fig. 27A-B). It is possible that this function could play a role in the requirement for Rtf1 in H2B K123ub *in vivo*.

We tested an alanine substitution (H2A-L66A) that results in a severe H2B K123ub defect regardless of the presence or absence of the deubiquitylation enzyme Ubp8. We expected to see a reduction in the H2A-Rtf1 interaction in this mutant, however the levels of crosslinking between H2A-and Rtf1 were not reduced, but were potentially increased instead (Fig. 28B). One possibility for this result is that L66 could act primarily in its interaction with Bre1, as the L66A substitution abolishes H2B K123ub in a way that resembles the effect of the acidic patch substitutions in the H2B K120ub reaction.

We exploited a collection of internal deletions within the Rtf1 coding region. These were integrated alleles based on a previous study that characterized the functional regions of Rtf1 (WARNER *et al.* 2007). We focused on a subset that exhibited phenotypes involved in chromatin regulation. We found that the N-terminus and a portion of the HMD were both necessary for the H2A-Rtf1 interaction. The N-terminus had previously been shown to be involved in regulating recruitment of the chromatin remodeling enzyme Chd1 to chromatin (WARNER *et al.* 2007). Althought it is possible that the Rtf1 N-terminus could interact with H2A, there are no arginines in this region of Rtf1. Thus, it is more likely that Chd1 could be required for the H2A-Rtf1 interaction. A previous study suggested that Chd1 could be required for H2B K123ub, thus it could be possible that Chd1 could help promote the H2A-Rtf1 interaction to facilitate H2B K123ub (LEE *et al.* 2012).

Spt16 is important for maintaining nucleosome occupancy and when Spt16 occupancy is diminished, this can cause a loss of histones on chromatin. We previously showed that H2A

mutants have defects in both histone and Spt16 occupancy (CUCINOTTA *et al.* 2015). These two defects are interdependent, however. It was unknown whether the loss of histone occupancy was due to a reduction in Spt16 occupancy or vice versa. Our BPA crosslinking analysis revealed that the nucleosome acidic patch residue A61 can interact directly with Spt16. This result indicates that it is likely the affect on the histone occupancy defect in acidic patch mutants could be due, in part, to the reduction in Spt16 binding to H2A. A recent study confirmed the Spt16-acidic patch interaction *in vivo* using co-immunoprecipitation experiments with acidic patch mutants and Spt16 (HODGES *et al.* 2017). There have been several crystal structures with Spt16 and histones, however so far none of them show an interaction between Spt16 and the nucleosome acidic patch (HAMMOND *et al.* 2017). However, some of the structures indicate that specific Spt16 domains may bind to multiple regions of the nucleosome. Thus, it is possible future structural studies will reveal Spt16 binding to the acidic patch. It could be possible that a co-chaperone or chromatin remodeling enzyme may be required for the Spt16-nucleosome acidic patch interaction.

Together, these data provide two newly identified interactions between the acidic patch and transcription elongation factors *in vivo*. The interactions between the acidic patch and Rtf1 and Spt16 provide a rationale for why the acidic patch is required for H2B K123ub and transcription elongation efficiency. Both Spt16 and Rtf1 are associated with elongating Pol II. Additionally, Spt16 has been shown to be important for H2B K123ub and H2B K123ub is important for Spt16 function (PAVRI *et al.* 2006).

4.0 CONCLUSIONS AND FUTURE DIRECTIONS

When I first embarked on this project, my goal was to characterize how the nucleosome itself interfaces with chromatin binding proteins to control transcription elongation. My work has since led to revealing a pivotal role for the nucleosome itself in mediating histone modifications and transcription elongation. Indeed, the nucleosome is not inert. It not only is dynamically disassembled and reassembled in the wake of transcribing polymerase, but it is an active binding hub for proteins involved in gene expression. My work has revealed that the nucleosome acidic patch interacts with transcription elongation factors to regulate histone modifications and transcription (summarized in Fig. 32).

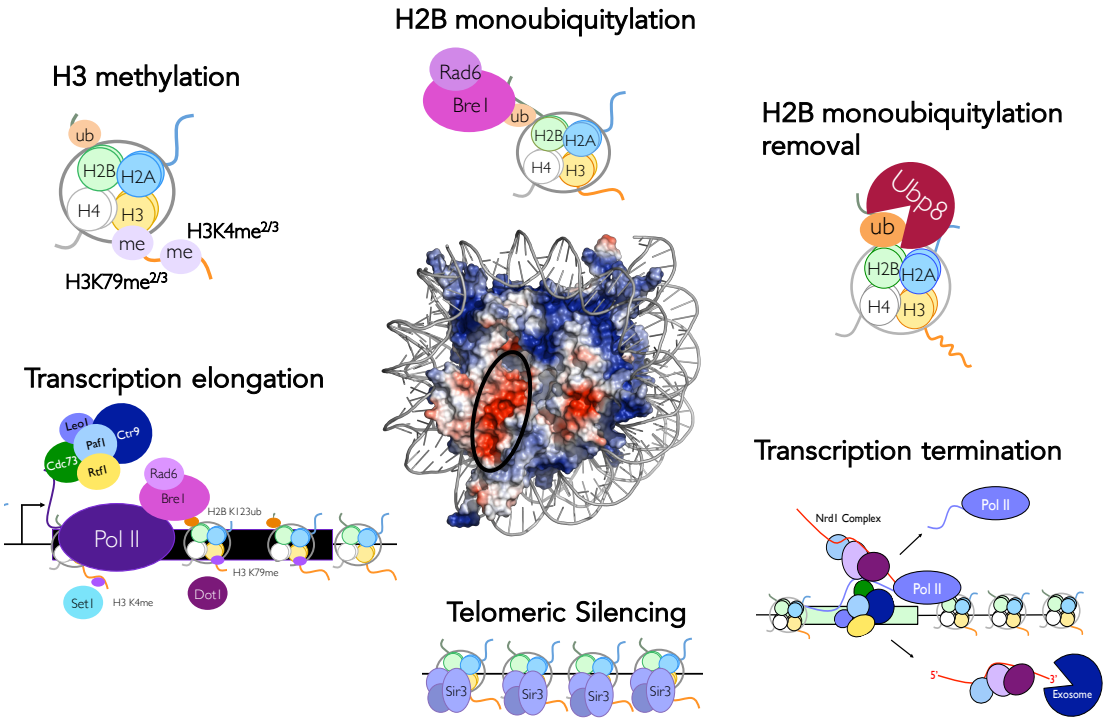

Figure 32. Roles of the nucleosome acidic patch in regulating gene expression as shown in this thesis.

4.1 THE NUCLEOSOME ACIDIC PATCH DIRECTLY REGULATES H2B K123UB

The original genetic screen for mutations synthetically lethal with *rkr1*Δ (Chapter 2, A. Young) yielded a suite of H2A mutants that have diverse phenotypes within the H2B K123ub pathway. Interestingly, while all of the mutants have reduced H2B K123ub levels, there was a range of defects. For example, the H2A-E65A substitution did not cause such a drastic reduction in H2B K123ub as substitution of a neighboring residue, H2A-L66A. The H2A-L66A mutant strain had no detectable level of H2B K123ub and was akin to the H2B-K123R mutant. I would later find out that deletion of the gene coding for the deubiquitylating enzyme Ubp8 would yield some (but not WT levels) recovery of H2B K123ub levels for the H2A-E65A mutant but not for the H2A-L66A mutant. The H2A-L66A mutant exhibited no recovery and still had virtually undetectable H2B K123ub (Chapter 2, Fig. 12). This result suggested the following: 1) the paucity of H2B K123ub in the L66A mutant meant this mutant was defective primarily in placing H2B K123ub, 2) The lack of *complete* recovery (i.e. WT fold-change in H2B K123ub) in the E65A mutant meant that this substitution likely causes a defect in placing H2B K123ub as well as removing it via Ubp8. This notion was solidified by the Wolberger lab when they solved the X-ray crystal structure of Sgf11 (a member of the SAGA complex with Ubp8) bound to the acidic patch of a nucleosome containing H2B K123ub (MORGAN *et al.* 2016). In that structure, the arginine anchor of Sgf11 interacted with E65 as well as other acidic patch residues. This was satisfying, as the genetic and structural studies coalesced to show that indeed the nucleosome acidic patch is required not only for placing ubiquitin on H2B K123 but also in removing it.

I also showed that many of the H2A substitutions caused defects in recruiting the E3 ligase for H2B K123ub, Bre1, to chromatin (Chapter 2, Fig. 18). While the field still eagerly awaits an X-ray crystal structure of Rad6/Bre1 (ideally with the HMD of Paf1C member Rtf1) bound to the

nucleosome, the Köhler lab recently performed *in vitro* crosslinking and mass spectrometry, which showed that the RING domain of Bre1 contacted the nucleosome acidic patch (GALLEGO *et al.* 2016). They also showed that, *in vitro,* the nucleosome acidic patch is required for H2B K123ub. I also showed this using the LANA peptide to block the nucleosome acidic patch as well as with acidic patch mutant nucleosomes (Chapter 3, Fig. 25A, Fig. 26C). I also showed that a nucleosome lacking key acidic patch acidic patch residues was as defective in supporting H2B K123ub as a reaction lacking Bre1 and that this defect was not recoverable by adding the HMD (Chapter 3, Fig. 26C), which typically causes a four-fold increase in H2B K123ub (VAN OSS *et al.* 2016). Together these data suggest that Bre1 must bind to the acidic patch and then the HMD can interact with Rad6 to promote H2B K123ub *in vitro*. The Rad6-HMD interaction was discovered by our lab (VAN OSS *et al.* 2016). Understanding mechanistically how Bre1 interacts with the nucleosome and how the HMD interacts with Rad6 is an exciting area of research that will illuminate the molecular details of how H2B K123ub is catalyzed.

To add an extra layer of complexity to the nucleosome acidic patch's role in transcription elongation, I found that the nucleosome acidic patch also recruits Rtf1 to chromatin (Chapter 2, Fig. 13). Like the initial Bre1 ChIP result, it was unknown at the time whether the acidic patch interacts with Rtf1 directly or through an intermediary protein. My site-specific *in vivo* crosslinking experiments demonstrated that indeed the acidic patch is interacting with Rtf1 directly (Chapter 3, Fig. 26). As the BPA crosslinks are short, we can surmise that any crosslinking detected is through a direct, or extremely close, interaction (DORMAN AND PRESTWICH 1994). Intriguingly, this interaction was independent of Bre1/Rad6, suggesting that the H2A-Rtf1 interaction could occur prior to Bre1/Rad6 recruitment.

Deletion analysis of Rtf1 domains in the H2A-Rtf1 interaction revealed a requirement for the Chd1-interaction region of Rtf1 in stabilizing or promoting the Rtf1-H2A interaction (Chapter 3, Fig. 30A). It is unlikely that this region directly interacts with the acidic patch, however, as there are no arginines in the amino-terminus. It is thus possible that the nucleosome remodeling activity of Chd1 may be required for the Rtf1-H2A interaction. The other region that was found to be important for the H2A-Rtf1 interaction was region 4, which contains a part of the HMD. This was an intriguing result because the HMD is critical for promoting H2B K123ub. *In vivo*, H2B K123ub cannot occur without the HMD, while *in vitro* the HMD stimulates, but is not required for, H2B K123ub. This gives rise to questions regarding the mechanism of H2B K123ub. Does the requirement for the HMD *in vivo* but not *in vitro* have anything to do with its role in binding the acidic patch? Already, *in vitro* data suggest that the nucleosome acidic patch is effectively "epistatic" to the HMD, in that when the nucleosome is mutated there is no effect of adding the HMD to the reaction because the levels are so low. But *in vivo*, there could be different story. One experiment that could address whether the HMD could stimulate H2B K123ub on acidic patch mutant nucleosomes *in vivo* is to overexpress the HMD in acidic patch mutant cells. An undergraduate I mentored, Chelsea Guan, tried to overexpress the HMD on plasmids in acidic patch mutants, however this strategy did not work. Acidic patch mutants, it turns out, have plasmid retention or DNA replication defects, as the HMD was not expressed (data not shown). Given the pleiotropic nature of these histone mutants this was not surprising. As has been the common theme in studies of the nucleosome acidic patch: its involved in everything. In fact, previous work has shown that an acidic patch residue, H2A-E57 is also required for chromosome bi-orientation (KAWASHIMA *et al.* 2011). A different strategy could be employed, such as genomically overexpressing the HMD using an inducible promoter.

4.2 THE ROLE OF THE NUCLEOSOME ACIDIC PATCH IN H3 METHYLATION

It has long-been recognized that H3 K4 and H3 K79 di- and tri-methylation require H2B K123ub (BRIGGS *et al.* 2002; DOVER *et al.* 2002; SUN AND ALLIS 2002). In the case of H3 K4me$^{2/3}$, this is through an interaction with the n-SET domain of Set1 (KIM *et al.* 2013a; THORNTON *et al.* 2014). For Dot1-mediated H3 K79 methylation, Dot1 is stimulated by ubiquitin, and a recent study showed that H2B K123ub "corrals" Dot1 to methylate H3 (MCGINTY *et al.* 2008; MCGINTY *et al.* 2009; CHATTERJEE *et al.* 2010; ZHOU *et al.* 2016). My work in Chapter 2 described how the nucleosome acidic patch may also be playing a direct role in Set1- and Dot1-mediated H3 methylation in addition to its roles in promoting H2B K123ub (Chapter 2 Fig. 15, Fig. 17, Fig. 18). The key result that lends credence to this notion was that while some level of H2B K123ub was recovered, H3 K4me^3 and H3 K79me$^{2/3}$ was not recovered in the H2A-E65A and H2A-E93A mutants, respectively. This suggests that these two residues function not only in promoting H2B K123ub but also that they have separate roles in promoting H3 methylation.

The n-SET domain of Set1 has three arginines that, when mutated, render the protein ineffective at methylating H3 K4 (KIM *et al.* 2013a). Interestingly, the Tan lab recently published a structural model and biochemical analyses of the methyltransferase for H4 K20me1, Set8, that suggested a basic patch in the n-SET domain of Set8 could interact with the acidic patch through an arginine anchor. To speculate, it would be exciting if Set1 could also interact with the nucleosome acidic patch in a similar fashion. Earlier, I showed ChIP data that supports the notion that the acidic patch is required for recruitment of Set1 to chromatin (Chapter 2, Fig. 18). Taken together with the western analysis of *ubp8*Δ strains, these data suggest that the acidic patch could bind Set1. *In vitro* methylation assays as well as binding assays will determine whether this is true. To truly separate the role of H2A-E65 in H3 K4 methylation from its role in H2B K123ub, it would

be critical to use nucleosomes that either have ubiquitin tethered to H2B K123 through intein ligation (DAVID *et al.* 2015) or perform *in vitro* ubiquitylation of the nucleosome prior to the methylation and binding assays.

Dot1 is a non-SET domain containing methyltransferase specific for H3 K79. Dot1 to requires a basic region within the H4 tail to methylate H3 K79 (FINGERMAN *et al.* 2007). The lack of H3 K79me$^{2/3}$ regardless of the presence or absence of *UBP8* in the H2A-E93A mutant is interesting in light of the H4 tail study. This could be an example of a protein interacting with the acidic patch and the H4 tail of a neighboring nucleosome. The scenario would be that Dot1 would bind to the acidic patch and is situated such that it is interacting with the H4 tail of a neighboring nucleosome, the acidic patch, and ubiquitin on H2B K123. Using a cross-linker during the methylation reaction and taking samples over a time course for mass spectrometry analysis could help address this question. We would expect to see crosslinking between Dot1, H2A, ubiquitin, and H4. Mutating the basic patch in the H4 tail, (FINGERMAN *et al.* 2007), acidic patch residues on H2A (CUCINOTTA *et al.* 2015), and residues L71 and L72 on ubiquitin (HOLT *et al.* 2015) should result in a loss of crosslinking and serve as valuable controls.

4.3 THE NUCLEOSOME ACIDIC PATCH MAINTAINS HISTONE OCCUPANCY AND DIRECTLY INTERACTS WITH SPT16

The nucleosome acidic patch is essential for proper histone occupancy (Chapter 2, Fig. 14). While the H2A acidic patch substitutions did not cause a severe defect in cryptic initiation or *SER3* derepression (Chapter 2, Fig. 14), ChIP analyses showed a reduction in occupancy of H2A, H2B, and H3. This result suggests that nucleosome occupancy could be abrogated when the acidic patch

is defective. Performing MNAse-seq on acidic patch mutants would be a follow-up experiment to address this question. To date, there have been no genomic studies on the role of the acidic patch. Thus, it would be an important area to explore. Specifically, I would investigate the effect of H2A-E57A and/or H2A-E93A substitutions on genome-wide nucleosome positioning. These two substitutions caused the strongest defects in Spt16 occupancy (Chapter 2, Fig. 18D).

In Chapter 3, I showed a direct interaction between H2A and Spt16 at the location H2A-A61. This interaction was a fascinating result because I had previously observed a reduction in Spt16 occupancy levels in different *hta1* mutant cells. Additionally, a recent study recapitulated the ChIP result using immunoprecipitation experiments, corroborating the argument that the acidic patch could be required for Spt16 binding (HODGES *et al.* 2017). As these three studies coalesce to show the acidic patch is important for Spt16-nucleosome interactions, it leads to two major questions: 1) where on Spt16 is the acidic patch interaction? 2) What is the purpose of the Spt16 interaction with the acidic patch? Previous work showed a functional interaction between the Spt16 N domain and the docking domain of H2A (VANDEMARK *et al.* 2008). The C-terminal regions of Spt16 and Pob3 have acidic patches that recognize H2A and H2B but not at the nucleosome acidic patch (KEMBLE *et al.* 2015). A recent study however only detected a direct interaction between H2A and the Pob3 C-terminus (HOFFMANN AND NEUMANN 2015). In this study, they used the same photocrosslinking system that I discussed in Chapter 3, but they probed residues in Spt16 and Pob3 for binding to histones. Even though this *in vivo* crosslinking study did not detect an Spt16 interaction, the Pob3 result is in agreement with the structure (KEMBLE *et al.* 2015). These results lead to the question of whether there are other regions in Spt16 that could bind to H2A/H2B. One study showed that the Spt16 M domain recognizes the nucleosome through interaction with the H2A/H2B dimer in a manner that favors binding to H2B (HONDELE *et al.*

2013). *In vitro* binding assays with acidic patch mutant nucleosomes will be critical to determining whether the Spt16-H2A interaction requires the nucleosome acidic patch. As it stands right now, the only evidence for Spt16 interacting with the acidic patch is the *in vivo* data, however, the evidence has been represented by multiple experiments across two different labs (Chapters 2 and 3; (HODGES *et al.* 2017)).

4.4 THE NUCLEOSOME ACIDIC PATCH IS REQUIRED FOR EFFICIENT TRANSCRIPTION ELONGATION AND TERMINATION

In Chapter 2, I showed that nucleosome acidic patch residues are required for efficient transcription elongation and termination of snoRNAs (Fig. 23 and Fig. 18). Taking the results from Chapter 3, where I found that Spt16 interacts with the acidic patch residue A61 and combining them with those in Chapter 2, it is possible that the role of the acidic patch in regulating transcription elongation efficiency could be due to its putative interaction with Spt16. FACT was shown to enhance transcription elongation through nucleosomes and promotes nucleosome recovery *in vitro* (ORPHANIDES *et al.* 1998; HSIEH *et al.* 2013). It will be interesting to see also whether Spt16 is required for transcription termination as well. I showed that the residues E57 and E93 were most important for transcription termination and Spt16 recruitment. Thus, it is possible that these residues could be involved in interacting with Spt16 to promote efficient elongation and termination. There is one major caveat to the transcription elongation efficiency experiment from Chapter 2 (Fig. 23), however, as defects in glucose shut-off can be incorrectly interpreted as a slower elongation efficiency as carbon sources can result in different Pol II profiles due to residual Pol II loading promoter shutoff is incomplete (MALIK *et al.* 2017).

Determining the global levels of transcripts will be crucial to characterizing the role of the acidic patch residues in regulating gene expression. I would recommend performing RNA-seq experiments to determine the genome-wide levels of transcripts. Given that these acidic patch mutants are synthetically lethal in the absence of the protein quality control factor Rkr1, I expect that these histone mutants will have many aberrant transcripts. I expect to see read-through of transcription termination sequences beyond that of snoRNAs as well. One method that would be useful in studying aberrant transcription in these mutants is transient transcriptome sequencing, or TT-seq, which determines levels of RNA synthesis and degradation. This method would be useful in fully characterizing the defects in nascent transcription present in acidic patch mutants (SCHWALB *et al.* 2016). To measure run-on transcription at the genome-wide level, PRO-seq is the latest technology that combines GRO-seq with biotin-tagged nucleotides to obtain single nucleotide resolution of transcripts engaged with polymerase (MAHAT *et al.* 2016).

4.5 REMAINING QUESTIONS

One outstanding question left for the field is: Why do so *many* proteins bind to the nucleosome acidic patch? Is the acidic patch a popular binding hub merely because this region is unique compared to the rest of nucleosome structure? It is the most acidic region on the nucleosome, and it is a cavity amenable to protein binding. Or could this be a regulatory mechanism to prevent chromatin from higher order folding or to help keep chromatin open for gene expression? A remaining experiment left to do is to measure the binding affinities among all the proteins that are known to bind the acidic patch compared to the H4 tail. As the H4 tail

compacts chromatin, one could imagine that the effect of having a suite of proteins that interact with the acidic patch could prevent chromatin compaction at the wrong place and time.

Typically, there are two copies of each of the histones in the nucleosome. However, it has recently come to light that throughout the genome partial nucleosomes exist and that certain histone modifications and histone variants are enriched either proximally or distally to the promoter within the nucleosome (RHEE *et al.* 2014). How the H2A/H2B dimer in hexasomes is oriented, for example, can impact the ability of Chd1 to shift hexasomes (LEVENDOSKY *et al.* 2016). Thus, another key question left is: How are the localization patterns of the proteins that bind to the acidic patch determined across the genome? It is possible that Bre1 and Sgf11 bind to different halves of the nucleosome at the same time or at both halves at different times to place and remove H2B K123ub. One would imagine this could be visualized by performing ChIP-exo analysis of Bre1 and Sgf11 after induction of gene expression (perhaps through a stress response), and in theory, we would be able to see Sgf11 enriched downstream of Bre1. Adding an overexpression construct containing something such as the LANA peptide should render this time-dependent enrichment lost.

Cumulatively, this thesis has thoroughly characterized multiple functions of the nucleosome acidic patch. Some functions, such as its role in H2B K123ub have been mechanistically dissected. For several other functions, such as how the acidic patch is involved in transcription elongation and termination, these data provide a springboard for many projects for years to come.

APPENDIX A

IN VIVO STUDIES WITH PROTEINS KNOWN TO INTERACT WITH THE ACIDIC PATCH

As discussed in Chapter 1, the nucleosome acidic patch binds many different proteins. I wanted to take advantage of this fact to determine whether I could use the idea of competition to manipulate H2B K123ub levels. I hypothesized that I could reduce interactions with the acidic patch to allow for Rad6/Bre1 to bind and increase H2B K123ub and/or overexpress acidic patch interacting proteins and inhibit binding of Rad6/Bre1 to the acidic patch, thereby reducing H2Bub levels.

A.1 H4 TAIL

To determine whether deletion of the H4 N-terminal tail could open up the nucleosome acidic patch for binding by Rad6/Bre1, I tested global H2B K123ub levels in two different H4 tail deletion mutants encompassing the known amino acids that interact with the acidic patch (residues 16-25) (LUGER *et al.* 1997). It was previously identified that the H4 tail is required for H3 K79me$^{2/3}$. The basic patch on the H4 tail stimulates Dot1 methyltransferase activity *in vitro* and is required for H3 K79me$^{2/3}$ levels *in vivo* (FINGERMAN et al. 2007). Thus, as a control I tested H3 K79me$^{2/3}$ as well as H2B K123ub. While H3 K79 methylation was reduced as expected in the

H4Δ1-20 mutant, H2B K123ub levels did not show a corresponding increase in the mutant (Fig. 24). However, it is likely that deletion of the H4 tail alone is not enough to open the acidic patch for binding of Rad6/Bre1. This is likely because the H4 tail binds to the acidic patch for chromatin condensation and therefore visualizing global H2B K123ub changes in an asynchronous culture is possibly refractory to observing any remarkable level of change. One informative future direction is to observe changes in H2B K123ub at the genomic level by performing ChIP-qPCR in lieu of whole cell extracts and western blotting.

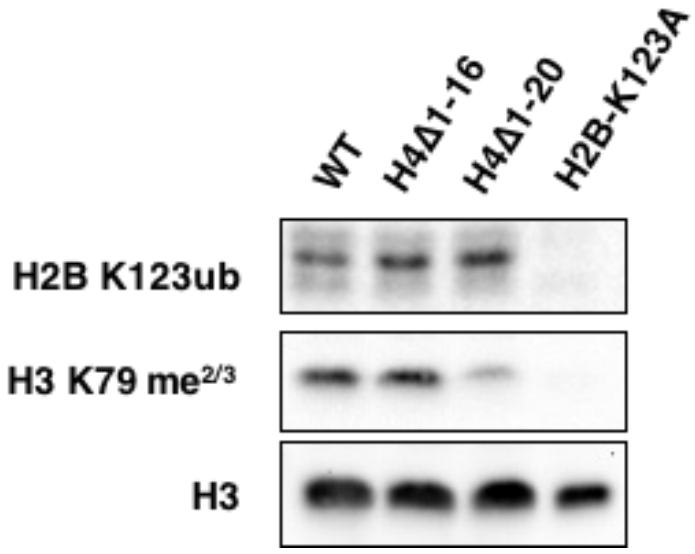

Figure 33. Histone modifications in H4 tail deletion mutants

Western blot analysis of H2B K123ub, H3 K79me$^{2/3}$, and H3. H3 serves as a loading control. This is a representative western of two biological replicates. Strains used were from the Boeke histone mutant collection (DAI *et al.* 2008).

A.2 SIR3

The nucleosome acidic patch is a binding site for the bromo-associated homology (BAH) domain of Sir3, which condenses chromatin and is required for transcriptional silencing of genes at telomeres and the mating type loci in yeast (RUSCHE *et al.* 2003; ARMACHE *et al.* 2011). Thus, I hypothesized that Sir3 could be exploited to study competition to the nucleosome acidic patch between Sir3 and Rad6/Bre1.

A.2.1 Nucleosome acidic patch mutants have defects in telomeric silencing and Sir3 recruitment

I used Sir3 as a model to assess whether the acidic patch mutants abrogated interactions with known proteins. I wanted to test the acidic patch mutants from Chapter 2 to see whether they exhibited telomeric silencing defects. I used RT-qPCR analysis with a *sir3*Δ strain serving as a positive control (Fig. 34A). Indeed, the acidic patch mutants exhibited impaired silencing of telomere-proximal genes *YFR057* and *COS12*. H2A-E65 appears to play the most prominent role in silencing telomeric regions compared to the other acidic patch mutants. H2A-L86, which does not reside in the acidic patch, does not have a telomeric silencing defect at either *YFR057* or *COS12.*

Because the acidic patch mutants lacked silencing of telomeric loci, it was likely that the mutants would have a defect in recruitment of Sir3 to chromatin. Thus, Sir3-TAP ChIPs were performed at three telomeric loci as well as the 5'-end of the actively transcribed gene *PYK1*. Interestingly, all of the mutants displayed a reduction in Sir3-TAP occupancy levels. However, I will note that the relative CT values were rather low and there is relatively high background in the

untagged samples (Fig. 34B). To verify that this result, I would recommend repeating the ChIP with a different tagged strain of Sir3. One striking observation was that the L86A mutant showed a decrease in Sir3 occupancy, however this mutant did not have transcription at its telomeres. One reason for this could be that H2B K123ub is required for expression of telomeric loci. Normally H2B K123ub is absent from telomeric loci (Fig. 35A), however the mutant that had the highest level of telomeric transcripts was H2A-E65A, which was also the H2A mutant that had the highest amount of H2B K123ub among the other H2A mutants. These preliminary data suggest that expression of telomere-proximal genes regulate both alleviation of Sir3-mediated silencing and H2B K123ub.

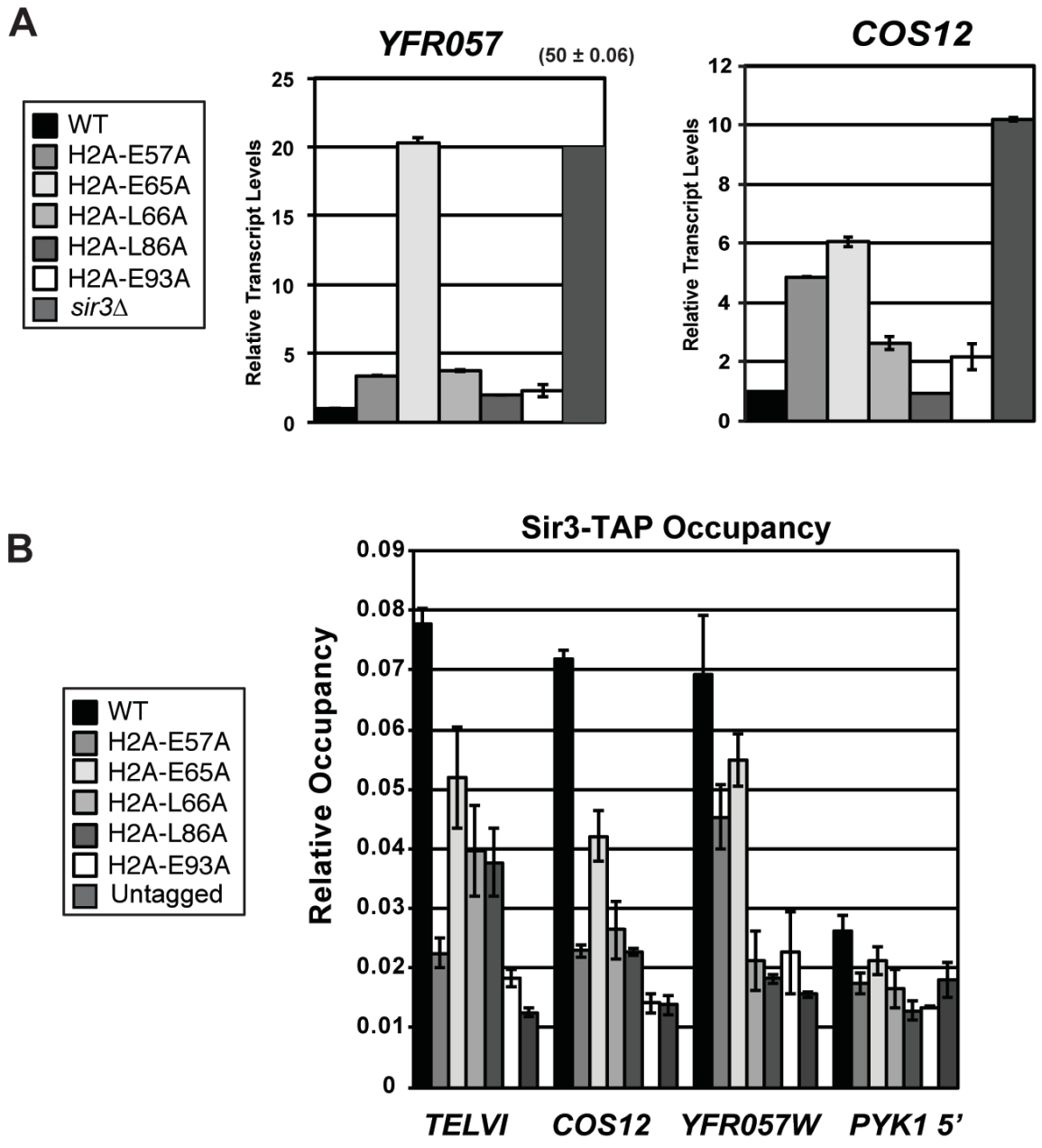

Figure 34. Nucleosome acidic patch mutants have defects in telomeric silencing and Sir3 recruitment

(A) RT-qPCR analysis of RNA levels of telomeric loci in the H2A mutant strains. Transcript levels in the wild-type control strain were set to 1. **(B)** ChIP analysis of Sir3-TAP occupancy at *TELVI, COS12, YFR057W,* and the 5'-end of *PYK1.* The error bars represent SEM of three independent experiments.

A.2.2 Deletion of *SIR3* increases H2B K123ub levels at telomeres

Using a similar rationale to deletion of the H4 tail, I assessed H2B K123ub in a *sir3*Δ mutant. Because Sir3 functions at silent regions, global levels of H2B K123ub would likely be unchanged to a significant degree. Thus, I performed ChIP of H2B K123ub and H2B at telomeric loci and, as a control, at the 5'-end of *PYK1*, which is highly transcribed. At all the telomeric loci tested, the *sir3*Δ strain had increased H2B K123ub levels, suggesting that when the acidic patch is no longer occupied by Sir3, Rad6/Bre1 can ubiquitylate K123 (Fig. 35). As expected, H2B K123ub levels were unchanged at *PYK1*, as the SIR complex is not present at active genes.

One important caveat to note is that while H2B K123ub is increased in the *sir3*Δ mutant at the telomeres, it is possible that this is simply due to increased transcription at this locus. Further studies will have to be done to clarify this result, such as deleting the promoter of a telomere-proximal gene to see if H2B K123ub is increased even in the absence of transcription. We attempted to overexpress the BAH domain of Sir3 to visualize a global decrease in H2B K123ub levels by blocking the acidic patch. However, we did not see a decrease in H2B K123ub levels via western blot analysis (Chelsea Guan, unpublished data). It is possible that a decrease may be discernable by ChIP at a subset of loci.

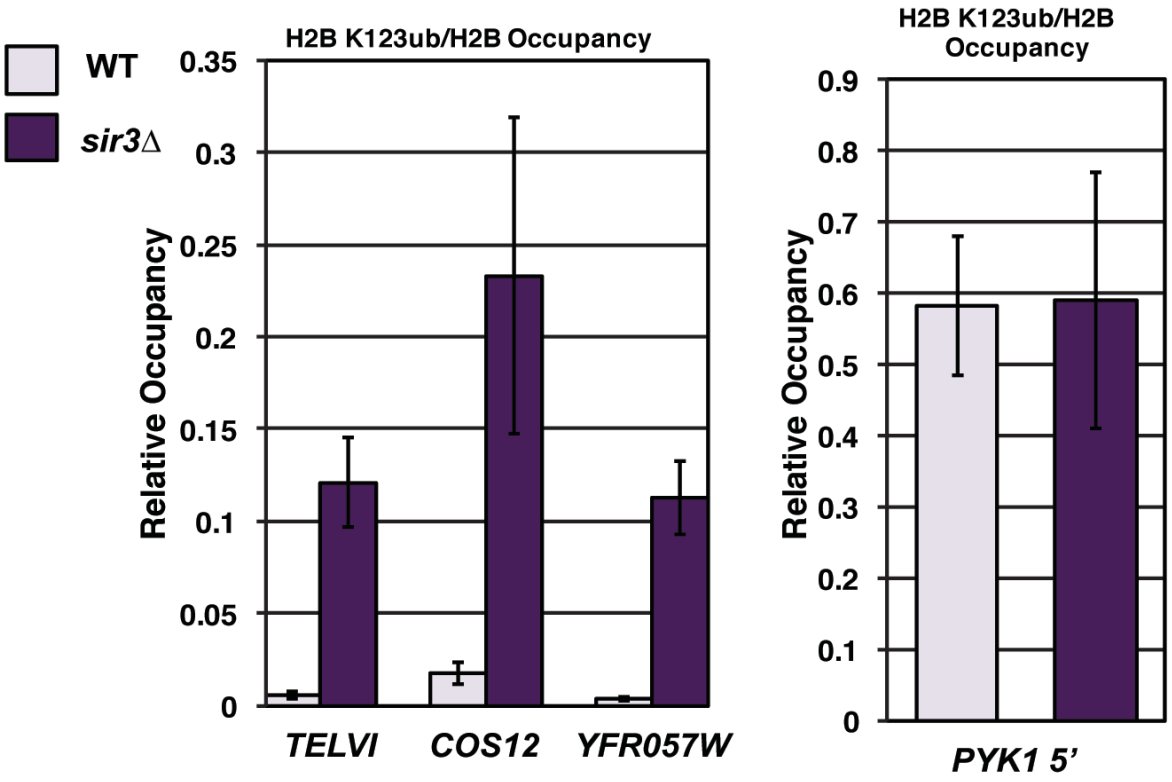

Figure 35. Sir3 represses H2B K123 ubiquitylation at telomeres

ChIP analysis of H2B K123ub occupancy at *TELVI, COS12, YFR057W,* and the 5'-end of *PYK1*. H2B K123ub ChIP values were normalized to total H2B ChIP values. The error bars represent SEM of three independent experiments.

A.3 LANA

The LANA peptide of Kaposi's sarcoma virus binds to the nucleosome acidic patch to tether its genome to host chromatin (BALLESTAS *et al.* 1999). Previous studies have exploited the LANA peptide to block the nucleosome acidic patch inside cells and assess phenotypes associated with specific proteins suspected to bind to the acidic patch. One such study was performed in HEK 293T cells, where GFP-tagged LANA was expressed and H2A/H2AX ubiquitylation by RNF168 was measured (LEUNG *et al.* 2014). Upon expression of GFP-LANA, H2A/H2AX ubiquitylation levels were reduced, but they were not reduced when a mutant form of LANA (8LRS mutant) that cannot bind to the acidic patch was expressed. We received these LANA expression plasmids from the Miller lab and Dr. Annette Chiang from the Brodsky lab kindly transfected the HEK 293 cells with these constructs and made cell lysates for me to assess H2B K120ub when LANA is expressed in HEK 293 cells. Relative to the LANA-8LRS control, expression of GFP-LANA did not decrease H2B K120ub levels in HEK293 cells as measured by western blot analysis (Fig. 36).

While the LANA peptide did not cause a global decrease in H2B K120ub levels in HEK 293 cells, it is possible that at specific loci, LANA might inhibit H2B K120ub. ChIP-qPCR would be a good follow-up method to assess H2B K120ub in these cells. Another possibility for the lack of an effect could be because the nucleosome acidic patch also directly binds to the deubiquitylation module for H2B K120ub, as has been observed in yeast. Therefore, LANA may inhibit removal of ubiquitin from K120 as well as placement of the mark in human cells. Supporting this notion, some of the alanine substitution mutants from Chapter 2 revealed a duel role for the acidic patch in both placing the mark and removing it. To move forward, I would recommend the use of a deubiquitylase inhibitor or, preferably, depletion of the DUB module in

HEK 293 cells. We also attempted to express the LANA peptide in *S. cerevisiae*, however the HA-tagged form of LANA was not expressed (Chelsea Guan, unpublished data).

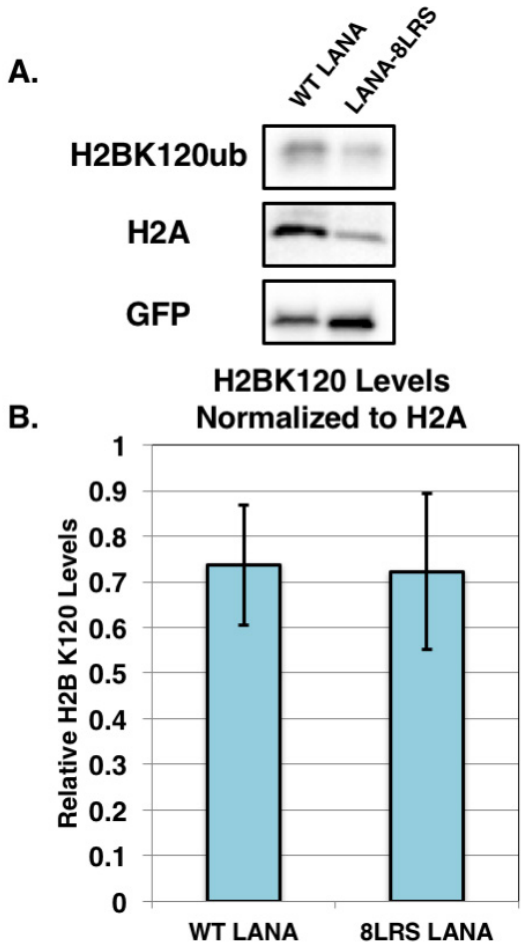

Figure 36. LANA peptide expressed in HEK 293 cells does not reduce H2B K120ub levels

(A.) Western blot analysis of whole cell extracts from HEK 293 cells expressing either WT LANA or the 8LRS mutant. Membranes were probed with antibodies against H2B K120ub, H2A, and GFP. **(B.)** Quantification of H2B K120ub levels relative to total H2A as a loading control. Error bars represent SEM of three biological replicates.

A.4 METHODS

RT-qPCR: Total RNA was isolated as described above and then DNase treated using the Turbo DNA-free kit (Ambion, AM1907) and RNase inhibitor (Ambion, AM2682). cDNA was generated using the RETROscript kit (Ambion, AM1710) with random hexamers and oligo(dT) primers. Quantitative PCRs were performed as described and primers are listed in Table 11. Signals were analyzed using the ΔΔCT method with *ACT1* used as the target gene (LIVAK AND SCHMITTGEN 2001). For controls, reactions lacking reverse transcriptase or template were performed. The graphs show the results of three independent biological replicates.

ChIP-qPCR: Chromatin immunoprecipitation (ChIP) assays were performed with 250 mL of log-phase yeast cultures (1-2 X 10^7 cells/mL) as previously described (SHIRRA *et al.* 2005). For histone ChIPs, sheared chromatin was incubated overnight at 4°C with antibodies specific to H2B, (0.5 µl, Active Motif, 39237), human H2B K120ub (2.5 µl, Cell Signaling 5546). Following incubation with the primary antibodies, chromatin was incubated for 2 hours at 4°C with Protein A-conjugated sepharose for all ChIPs, with the exception of TAP ChIPs, for which chromatin was incubated with Protein G-conjugated sepharose (30 µl, GE Healthcare). DNA was purified (Qiagen) and analyzed by qPCR using Maxima SYBR (Thermo). Occupancy levels were calculated using the primer efficiency raised to the difference between input and immunoprecipitated Ct values. Presented data are an average of two technical replicates for each of three biological replicates. The error bars indicate the standard error of the mean (SEM).

Western blot analysis: For western analyses other than those that measure H2B K123ub, yeast cells were grown to log phase (2-3 X 10^7 cells/mL) and lysed by bead beating in

trichloroacetic acid (TCA), as described previously (COX *et al.* 1997). To make whole cell extracts for H2B K123ub analysis, cells were lysed in SUTEB buffer (10 mM Tris-HCl, pH 8.0, 1% SDS, 8 M urea, 10 mM EDTA, pH 8.0, and 0.01% bromophenol blue) (TOMSON *et al.* 2011). Proteins were resolved on SDS-polyacrylamide gels (15% polyacrylamide) and transferred to nitrocellulose membranes. For H2B K123ub western blot analysis, proteins were transferred to PVDF membranes. Membranes were incubated with primary antibodies and then with anti-mouse or anti-rabbit secondary antibodies (GE Healthcare 1:5,000 dilution). Antibodies that recognize the following proteins or histone modifications were used: total histone H3 (1:30,000 dilution) (TOMSON *et al.* 2011), trimethylated H3 K79me^3 (note: this antibody has been reported by the manufacturer to cross-react with H3 K79me^2, Abcam ab2621, 1:2,000 dilution), H2A (Active Motif, 39235, 1:5,000 dilution), H2B (Active Motif, 39237, 1:5,000 dilution). An antibody against a human H2B K120ub-containing peptide (Cell Signaling 5546, 1:1000 dilution) was used to detect the analogous modification in *S. cerevisiae*, H2B K123ub. Proteins were visualized using enhanced chemiluminescence substrate (PerkinElmer) and either a 440 CF digital imaging station (Kodak) or a ChemiDoc XRS digital imaging station (BioRad).

Primer	Direction	Sequence	Reference
ACT1 qPCR	F R	5'-TGTCACCAACTGGGACGATA-3' 5'-GGCTTCCATCCAAACGTAGA-3'	(TOMSON *et al.* 2013)
COS12 qPCR	F R	5'-CATGGTTACGGTTCCAAACTTCT-3' 5'-AGAACGCAAAGCGTGAATTCA-3'	(DE VOS *et al.* 2011)
YFR057 qPCR	F R	5'-CTAGTGTCTATAGTAAGTGCTCGG-3' 5'-CTCTAACATAACTTTGATCCTTACTCG-3'	(CHANG AND WINSTON 2011)
TELVI qPCR	F R	5'-TGCAAGCGTAACAAAGCCATA-3' 5'-TCCGAACGCTATTCCAGAAAG-3'	(LIU *et al.* 2009)
PYK1 5' qPCR	F R	5'ACGATCTTCTACAATATCGATTCTACCA-3' 5'-TTCTTACGAATACCACAAGTCTGTCA-3'	(LIU *et al.* 2009)
PYK1 3' qPCR	F R	5'-GCAATGGCCAATGGTCTACCT-3' 5'-AACCTCCACCACCGAAACC-3'	(LIU *et al.* 2009)

Table 11. Primers used in this study

APPENDIX B

INITIAL STUDIES OF HISTONE MUTANTS SYNTHETICALLY LETHAL WITH CELLS LACKING RKR1

When I first joined the Arndt lab, I began working on a project that was started by Alexandria N. Young, an undergraduate in the lab at the time. She performed a synthetic lethal screen with histone H2A and H2B mutants from the Shilatifard library (discussed in Chapter 2). As mentioned in Chapter 2, these histone mutant genes are on plasmids carrying a FLAG-tagged H2B, which we later discovered causes a reduction in global H2B K123ub levels (CUCINOTTA *et al.* 2015). However, much work had been done characterizing the mutants carrying a copy of FLAG-tagged H2B, which are documented below. I performed all of the experiments, with the exception of the 5-FOA dilution assay in Figure 31, which was performed by A. Young alone. A. Young and I also worked together for the phenotypic assays in Figures 28 and 29.

B.1 GROWTH PHENOTYPES OF ACIDIC PATCH MUTANTS

To aid in classifying the mutants, we measured the growth of the histone mutant strains on different media that elicit varying stresses (Figure 37). We performed serial dilution assays using media with the following compounds: raffinose, galactose, NaCl, $CdCl_2$, benomyl, LiCl, caffeine, and cycloheximide. As controls, we also performed dilution analyses on a set of gene deletions

consisting of strains with: *dot1Δ*, *set1Δ*, *set2Δ*, *bre1Δ*, *rtf1Δ*, and *rkr1Δ* to assess phenotypic patterns in our isolated histone mutants relative to the phenotypes of strains lacking chromatin modifiers (Figure 29). It appears that most of the histone mutants are sensitive to both cycloheximide and caffeine. Sensitivities to cycloheximide and caffeine can indicate defects in protein translation and altered cell stress response, respectively (Figure 37D). The results from the other growth conditions indicate that the mutants cannot be generally sorted into classes that encompass all the phenotypes tested. However, within phenotypes, certain classes can be observed. For example, strains with the substitution *hta1-F26A* do not appear to be sensitive to benomyl (Figure 37 A-B), a drug that disrupts microtubules, nor do strains with *htb1-K123A* or *rtf1Δ*, whereas the other histone mutants fall into a group that is benomyl sensitive. This same grouping does not occur with respect to $CdCl_2$ sensitivity: *hta1-F26A* is not $CdCl_2$ sensitive, yet *htb1-K123A* and *rtf1Δ* are $CdCl_2$ sensitive. This indicates that while H2B K123 might not be important for benomyl resistance, it might be an important residue for $CdCl_2$ resistance. These data and that of others are summarized in Table 8. The many and varied phenotypes that have emerged from these serial dilution assays suggest possible pleiotropic roles for the nucleosome patch uncovered from this screen, which would indicate that these residues are critical for multiple roles in cell survival.

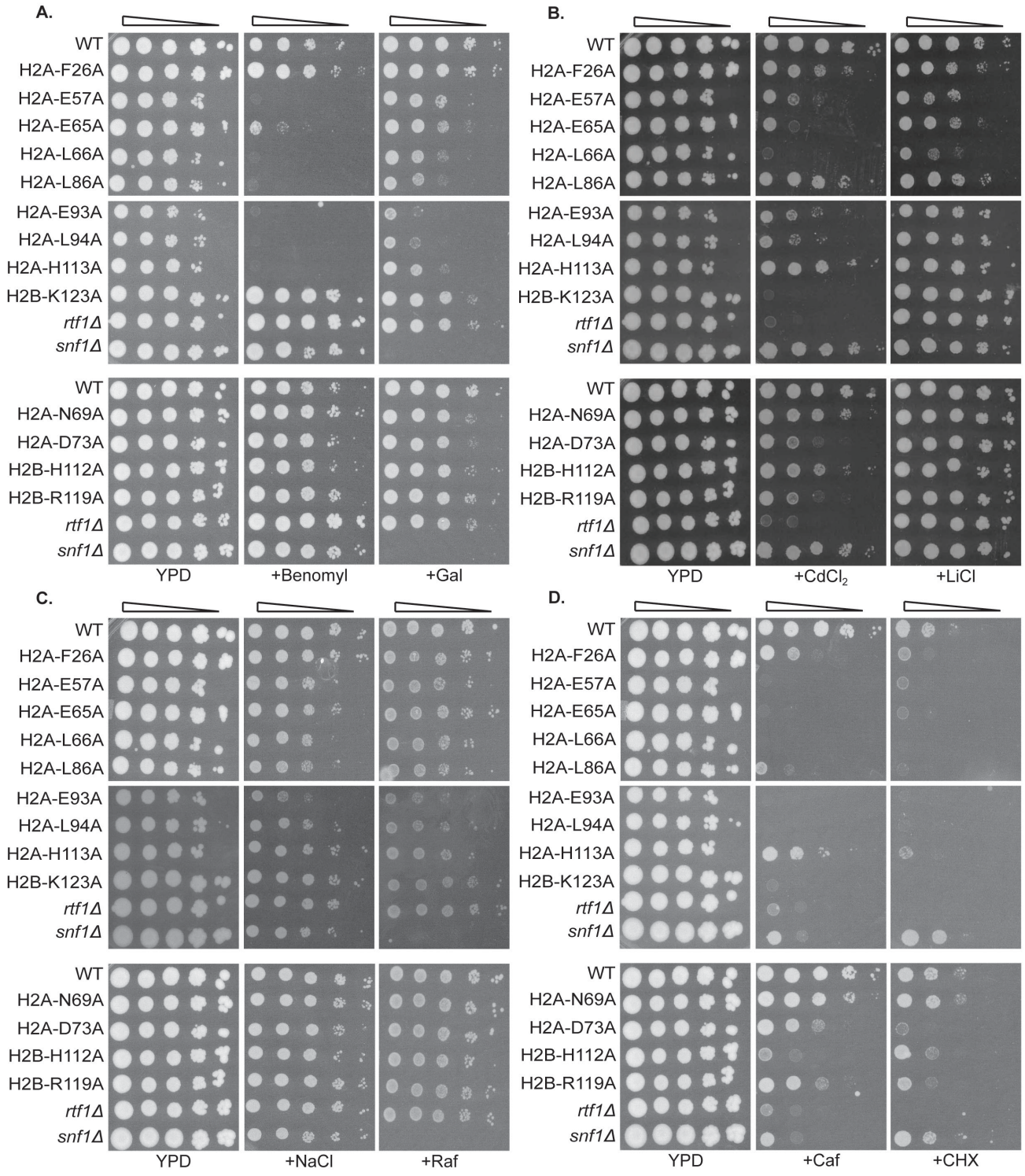

Figure 37. Phenotypic analysis of histone mutants

Ten-fold serial dilution assays starting with 10^8 cells/mL were plated on YPD as a control and YPD + 12.5 mg/mL benomyl (+Benomyl), YP + 2% galactose (+Gal), YPD+ 100 mM LiCl (+LiCl), YPD + 50μM CdCl2 (+CdCl2), YPD + 1 M NaCl (+NaCl), YPD + 15mM caffeine (+Caf), YPD + 0.8 mg/mL cycloheximide (+CHX), YP + 2 % raffinose (+Raf). Plates were incubated for 3 **(A)**, 4 **(B)**, 5 **(C)**, or 6 **(D)** days at 30°C. The *snf1Δ* strain serves as a positive control for +Gal and +Raf plates.

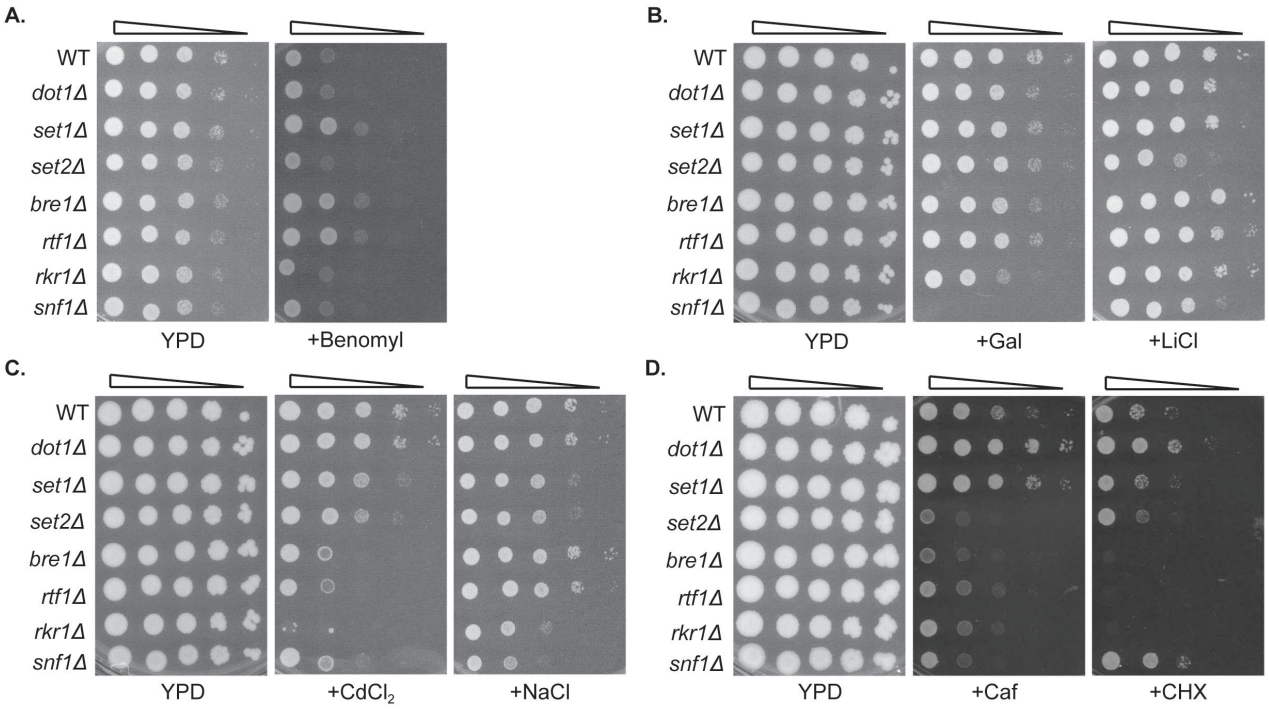

Figure 38. Phenotypic analysis of chromatin modifier deletion mutants

Ten-fold serial dilution assays starting with 10^8 cells/mL were plated on YPD as a control and YPD + 12.5 mg/mL benomyl (+Benomyl), YP + 2% galactose (+Gal), YPD + 100 mM LiCl (+LiCl), YPD + 50μM CdCl2 (+CdCl2), YPD + 1 M NaCl (+NaCl), YPD + 15 mM caffeine (+Caf), YPD + 0.8 mg/mL cycloheximide (+CHX), YP +2% raffinose (+Raf). Plates were incubated for 1 **(A)**, 2 **(B)**, 3 **(C)**, or 5 **(D)** days at 30°C. The *snf1Δ* strain serves as a positive control for +Gal and +Raf plates.

Histone	Residue	Phenotypes
H2A	F26A	Spt[1], Caf[2], Raf[2], Gal[2,] CHX[3]
H2A	E57A	HU[1], MMS[1], MPA[2], Caf[2], Raf[2], Gal[2,3], CHX[3], $CdCl_2$[3], LiCl[3], Benomyl[3,4]
H2A	E65A	6AU[1], HU[1], MMS[1], Caf[2], CHX[3], Gal[3], $CdCl_2$[3], Benomyl[3,4]
H2A	L66A	Spt[1], HU[1], MMS[1], MPA[2], Caf[2], CHX[3], Gal[3], $CdCl_2$[3], LiCl[3], Benomyl[3,4]
H2A	L86A	6AU[1], HU[1], MMS[1], MPA[2], Raf[2], Gal[2,3], NaCl[2], TS[2], CHX[3], Benomyl[3,4]
H2A	E93A	HU[1], MMS[1], MPA[2], Caf[2], Raf[2], Gal[2,3], NaC[2], TS[2], CS[2], CHX[3], Benomyl[3,4]
H2A	L94A	HU[1], MMS[1], MPA[2], Caf[2], Raf[2], Gal[2,3], NaCl[2], CHX[3], $CdCl_2$[3] ,Benomyl[3,4]
H2A	H113A	6AU[1], HU[1], MMS[1], MPA[2], CHX[3], Gal[3], Benomyl[3,4]
H2B	K123A	6AU[1], HU[1], MMS[1], MPA[2], Caf[2], Raf[2], Gal[2], NaCl[2], CHX[3]

Table 12. Summary of phenotypes associated with alanine substitutions in H2A and H2B

Phenotypes are from (MATSUBARA *et al.* 2007)[1], unpublished data by Margaret Shirra and Sarah Hainer[2], unpublished data by Christine Cucinotta and Alexandria Young[3], and (KAWASHIMA *et al.* 2011)[4]. Spt = suppressor of Ty insertion, Caf = caffeine sensitivity, Raf = raffinose sensitivity, Gal = galactose sensitivity, CHX = cycloheximide sensitivity, HU = hydroxyurea sensitivity, MMS = methyl methanosulfonate sensitivity, NaCl = sensitivity to NaCl, $CdCl_2$ = sensitivity to $CdCl_2$, Benomyl = sensitivity to benomyl, 6AU = sensitivity to 6-azauracil, MPA = sensitivity to mycophenolic acid.

B.2 STUDIES OF PREVIOUSLY IDENTIFIED HISTONE MUTANTS THAT ARE NOT SYNTHETICALLY LETHAL WITH RKR1 DELETION

The Shilatifard plasmid library was initially used to screen histone mutants for H3 K4me^3 defects using an immunoblot approach (NAKANISHI *et al.* 2008b). In this study, some residues near the nucleosome acidic patch were found to be required for H3 K4me^3. Alexandria N. Young isolated two of the same mutants from the *rkr1*Δ screen, H2A-E65A and H2A-L66A. However, other amino acids that are not synthetically lethal with *rkr1*Δ (Fig. 40, A. Young) were reported to play a role in promoting H3 K4me^3. Here, I confirmed these results and assessed H3 K79me$^{2/3}$ and H2B K123ub (via the FLAG tag system) in these mutants. Interestingly, the H2B-H112A mutant was defective in H3 K79me$^{2/3}$, H3 K4me^3, but not H3 K4me^2 (Fig. 39). The H2B-H112A mutant also had undetectable levels of H2B K123ub, which was previously reported. It is possible that this mutant may have some very low level of H2B K123ub, as this mutant has H3 K4me$^{2/3}$, albeit very low levels of H3 K4me^3. The undetectable level of H3 K79 methylation is striking, as this is specific to Dot1-mediated methylation. In this way, H2B-H112A behaves similarly to H2A-E93A. Indeed, H2B-H112 and H2A-E93 reside near each other, within a distance of 8.6 Å. Both of these residues are near H3 K79 (Fig. 41). It is therefore possible that Dot1 may contact these amino acids to promote H3 K79 methylation. *In vivo* crosslinking, *in vitro* binding, and methylation assays, (ideally in a system in which ubiquitin is already tethered to H2B K123) would be key to illuminating the role of H2A-E93 and H2B-H112 in promoting H3 K79 methylation.

The H2B-R119A was hyperubiquitylated and had reduced levels of H3 K4 and H3 K79 di- and tri-methylation. Another study revealed a role for H2B-R119A in de-ubiquitylation (CHANDRASEKHARAN *et al.* 2010). This same study also showed that this mutant is defective in recruiting a member of the Set1/COMPASS complex to chromatin.

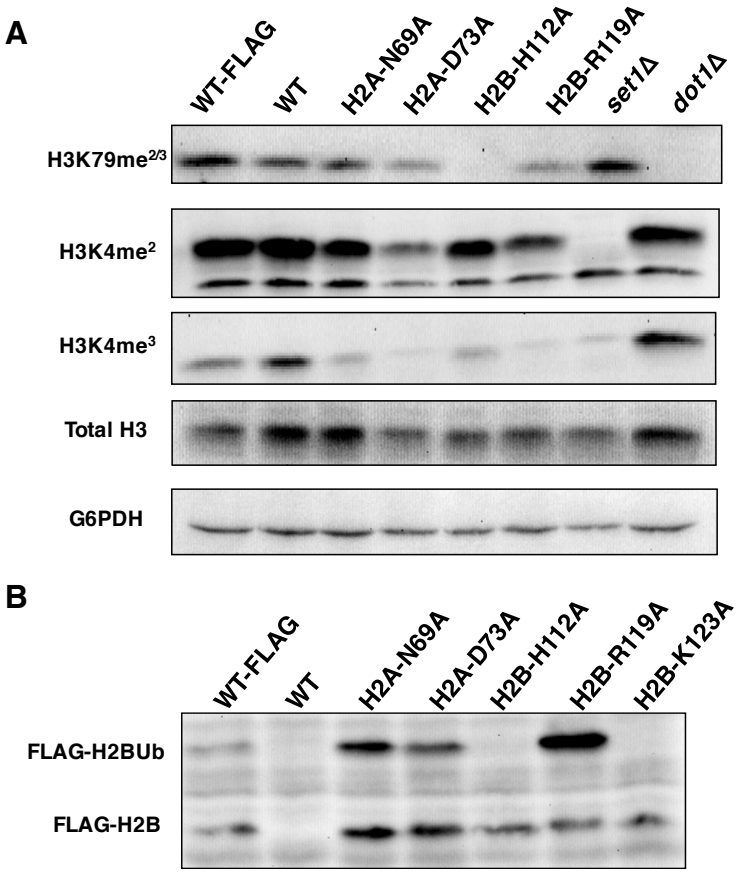

Figure 39. Histone modifications in histone mutants not synthetically lethal with *rkr1*Δ

(A) Western blots were probed with antibodies against the di- and tri-methylation of lysine 4 (K4) on histone H3, the di-/tri-methylation of K79 on H3, and total H3. G6PDH serves as loading control. Representative of three biological replicates. **(B)** Western blots were probed with antibodies against the FLAG epitope tag located on the N-terminus of H2B. Representative western blot of three biological replicates.

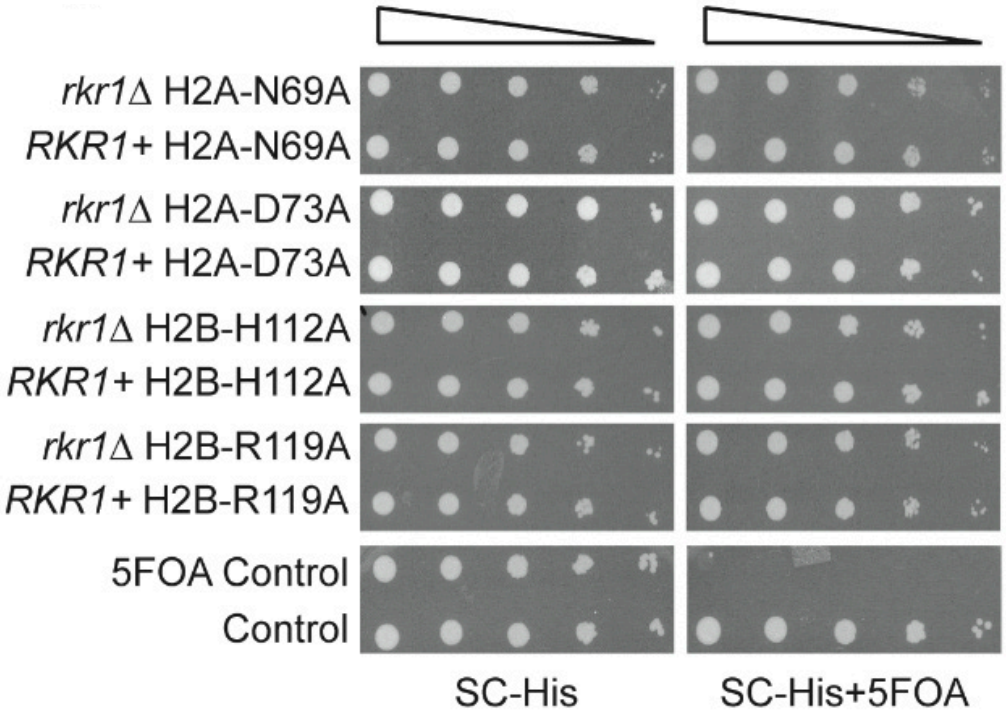

Figure 40. Histone mutants that are defective in H3 K4me3 but not synthetically lethal with *rkr1*Δ

Lack of synthetic lethal/sick phenotypes of *rkr1*Δ *hta1* and *rkr1*Δ *htb1* mutants were assessed through ten-fold serial dilution assays. Double mutant cells, as well as control *RKR1 hta1* and *RKR1 htb1* cells, were plated on SC-His medium as a growth control and on SC-His + 5-FOA medium to select for histone mutant plasmids and against the *URA3*-marked *HTA1-HTB1* plasmid. Library plasmids were transformed into the *rkr1*Δ strain KY981 and wild-type strain KY943. KY2676 and KY2265 were used as respective negative and positive growth controls on 5-FOA plates.

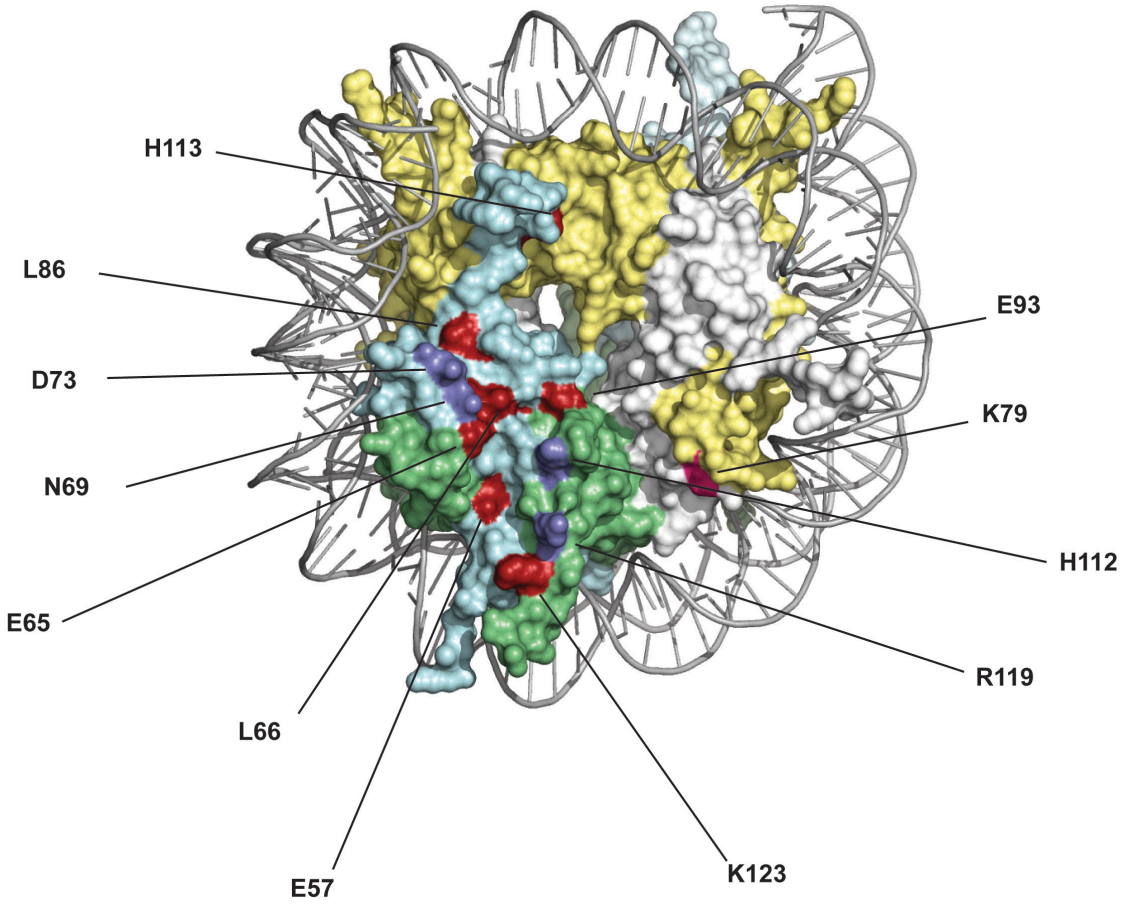

Figure 41. Residues mapped to the structure of the nucleosome

X-ray crystal structure of the nucleosome, denoting histones H2A, H2B, H3, and H4 in cyan, green, yellow, and white, respectively. Red residues are those that when substituted for alanine are synthetically lethal with *rkr1*Δ (CUCINOTTA et al. 2015). Purple residues are those previously identified to be required for H3 K4me^3 (NAKANISHI *et al.* 2008b). H3 K79 is marked in magenta. This figure was created using Pymol (PDB 1ID3 (WHITE *et al.* 2001)).

B.3 ANALYSIS OF HISTONE MODIFICATIONS IN FLAG-TAGGED ACIDIC PATCH MUTANTS

Each plasmid in the histone mutant library contains both *FLAG-HTB1* and *HTA1* (either mutant or wild type version). Each plasmid contains a single amino acid substitution in either *FLAG-HTB1* or *HTA1* (NAKANISHI *et al.* 2008a). The use of the FLAG tag on the N-terminus of H2B is widely used throughout the chromatin field to visualize a shift H2B and shift in gel mobility upon ubiquitylation of H2B. For many years an antibody against H2B K123ub was unavailable. Previous labs have shown that the FLAG tag does not alter levels of H2B K123ub (NAKANISHI *et al.* 2009). However, in our work using the commercial H2Bub antibody against human H2B K120ub from Cell Signaling (#5546), the FLAG tag appears to cause a defect in H2Bub levels in cells containing wild-type histones (Chapter 2, Fig. 12). Additionally, the FLAG tag on H2B causes a strong Spt^- phenotype, a phenotype that is suggestive of a chromatin defect (Celeste Shelton, unpublished data). Therefore, to avoid any mischaracterization of the histone mutants, I performed site-directed mutagenesis on each of the H2A mutant plasmids to remove the FLAG tag. I then reanalyzed all of the phenotypes that I assessed here in this section, which are discussed in Chapter 2. However, the H2B K12ub western blots of the untagged strains show that all H2A mutants have H2B ubiquitylation defects (Chapter 2, Fig. 13), which differed from my results using the tagged strains (Fig. 42). Here, I report that FLAG-tagged E57A and E65A were hyperubiquitylated, however this defect is not apparent in the untagged strains (Chapter 2, Fig. 13). The H3 methylation westerns vary little between the tagged and untagged strains (Fig. 15, Fig. 43, and Fig. 44).

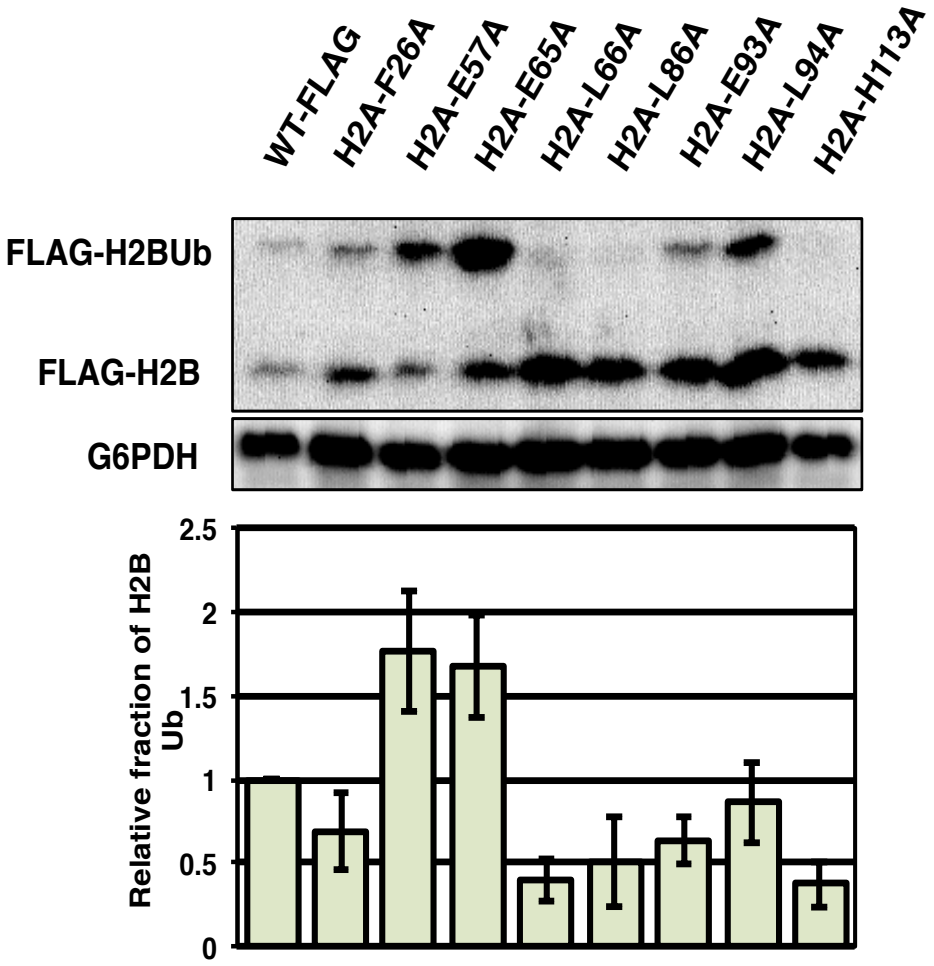

Figure 42. H2B K123ub levels in FLAG-tagged H2A mutants

Western blots were probed with antibodies against the FLAG epitope tag located on the N-terminus of H2B. The relative fraction of modified H2B levels are shown, with H2B-K123A background levels subtracted. The average value of wild type (WT) was set to one. These values represent an average of three biological replicates.

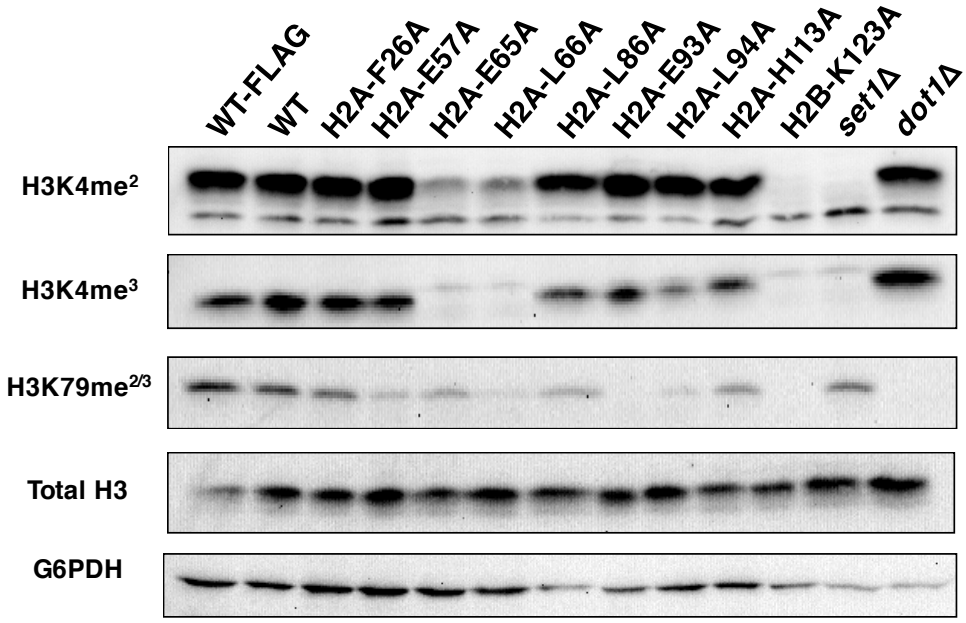

Figure 43. H3 methylation patterns in FLAG-tagged histone mutants

(A) Western blots were probed with antibodies against H3 K4me^2, H3 K4me^3, H3 K79me$^{2/3}$, and total H3. G6PDH serves as loading control. Strains lacking *SET1* and *DOT1* show the specificity of antibodies used.

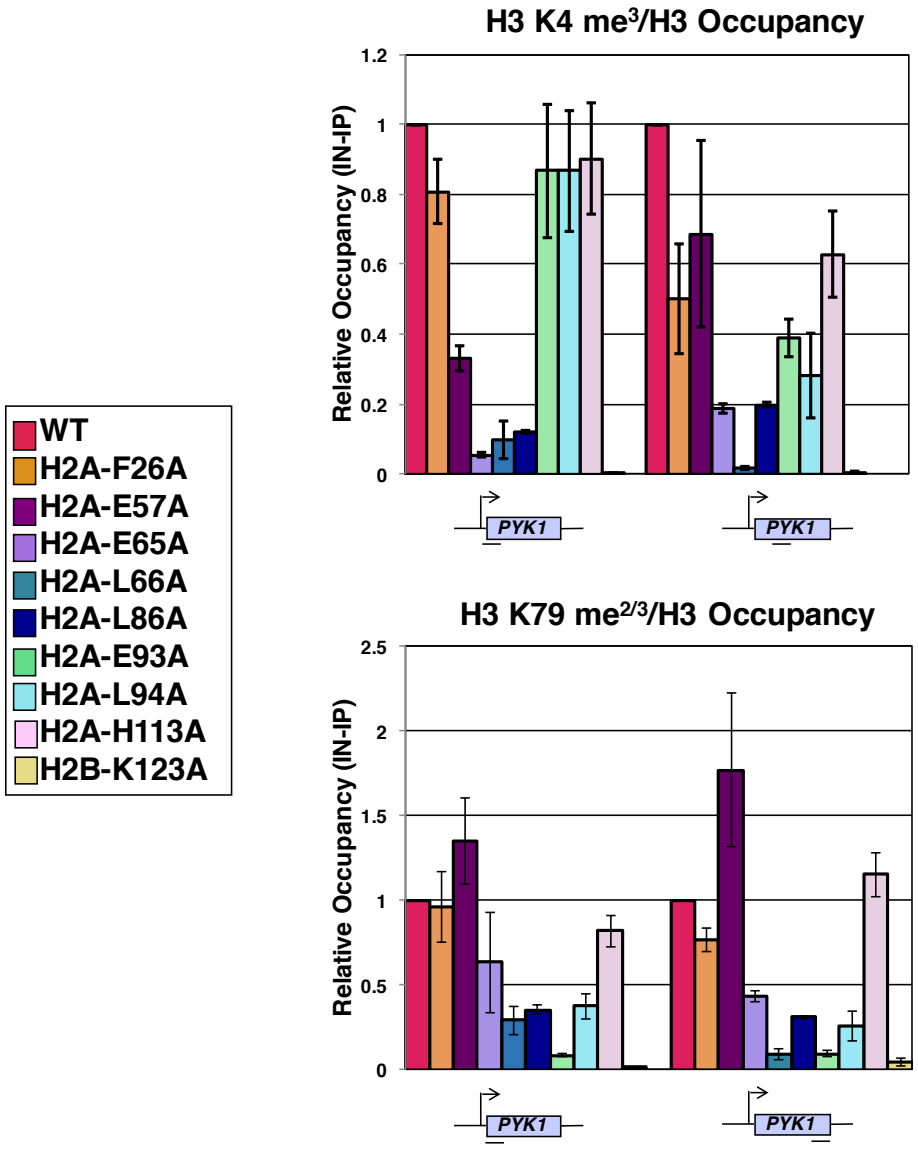

Figure 44. H3 methylation patterns on actively transcribed genes

ChIPs were performed on chromatin isolated from H2A mutant strains. The amount of immunoprecipitated DNA was determined by qPCR as a percentage of input DNA normalized to WT, which was set to one. The error bars represent SEM of three experiments. Below are depictions of loci, where black bars represent regions amplified by qPCR. Levels of methylated H3 were normalized to total H3 levels.

To determine whether the histone mutants had defects in histone modifications specific to the H2B K123ub modification cascade, I performed western blot analysis of H3 K36 di- and tri-methylation. This modification, as discussed in Chapter 2, is promoted independently of H2B K123ub, however it is also promoted by the Paf1C (CHU *et al.* 2007; ZHANG *et al.* 2013). The H2A mutants containing FLAG-tagged H2B did not show any remarkable changes to H3 K36 methylation levels, which falls in line with the untagged version presented in Chapter 2 (Fig. 45, Fig. 15A).

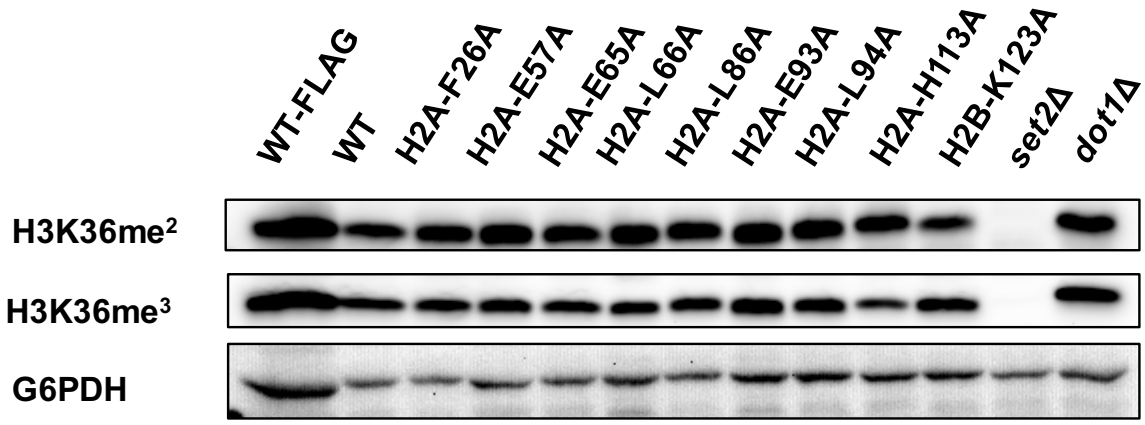

Figure 45. H3 K36 di- and tri-methylation in H2A histone mutants.

Western blots were probed with antibodies against the di- and tri-methylation of lysine 36 on histone H3. G6PDH serves as loading control. Strains lacking *SET2* and *DOT1* show the specificity of antibodies used.

In addition to assessing the effects of mutating residues in this H2A patch on histone modifications, I analyzed occupancy levels of histones H3 and H2B in chromatin. Several of the H2A mutants had decreased levels of H3 by ChIP analysis, though not globally, as visualized by western blot analysis (Fig. 43, Fig. 46, and Fig. 47). Interestingly, global levels of H2B were not decreased in the mutants (Fig. 46). The diminished H3 and H2B occupancy in chromatin may indicate that this H2A patch is required to maintain nucleosome stability. These results are similar to the untagged strains, however the FLAG-tag appears to stabilize nucleosome occupancy to a degree, as the levels of H2B and H3 on chromatin are not as low as they are in the untagged strains (Fig. 47, Chapter 2, Fig. 14).

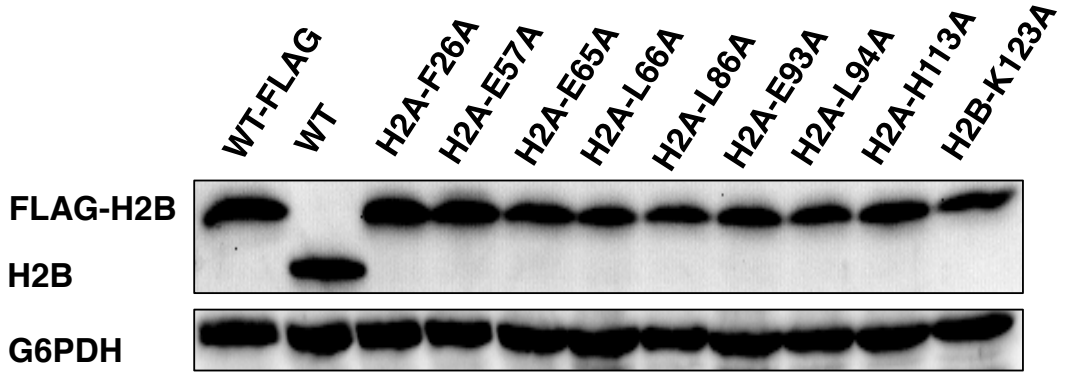

Figure 46. Global H2B levels are unaffected in the FLAG-tagged histone mutants

Western blot was probed with a total H2B antibody and G6PDH, which serves as a loading control.

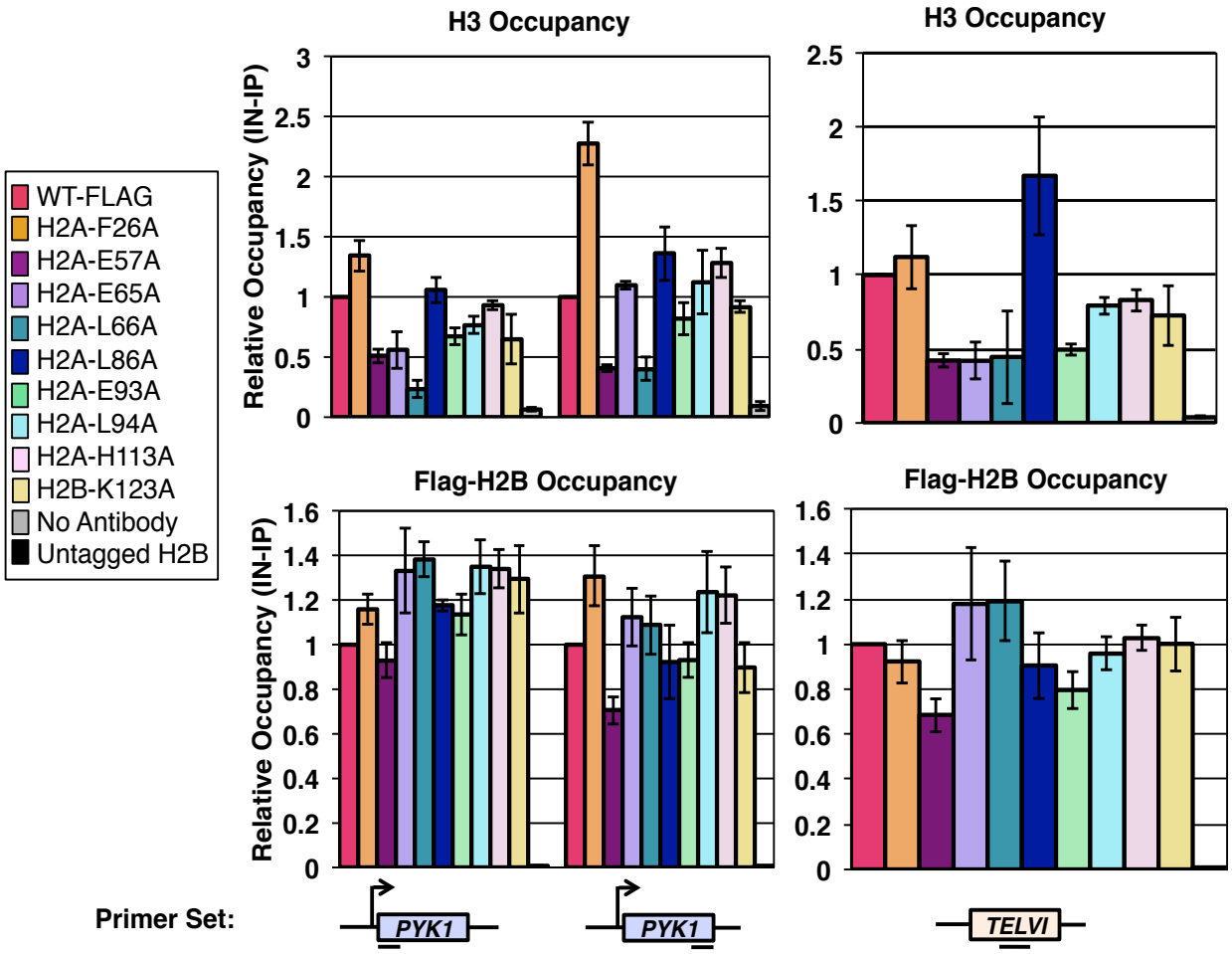

Figure 47. Levels of H3, H2B, and H2A on chromatin in FLAG-tagged strains

Histone ChIPs were performed on chromatin isolated from H2A mutant strains. The amount of immunoprecipitated DNA was determined by qPCR as a percentage of input DNA normalized to WT, which was set to one. The error bars represent SEM of three experiments. Below are depictions of loci, where black bars represent regions amplified by qPCR.

B.4 TRANSCRIPTION TERMINATION DEFECTS IN FLAG-TAGGED HISTONE MUTANTS

Because nucleosome acidic patch mutants exhibit defects in histone modifications involved in transcription, I surmised that there would be transcriptional defects in H2A mutants. Our lab has previously shown that H2B ubiquitylation is required for proper transcription termination of snoRNAs (TOMSON *et al.* 2011). Therefore, the amino acids identified in our screen may be required for proper transcription termination of snoRNA genes. I performed northern blot analysis on two snoRNA genes that are affected differently by histone modifications (TOMSON *et al.* 2013) (Fig. 48)**.** Interestingly, these data suggest that while the mutants have a wide range of histone modification defects, eight of the nine residues were required for proper transcription termination. This result falls in line with my RT-qPCR analyses in Chapter 2 with the untagged versions of the H2A mutant plasmids (Fig. 16).

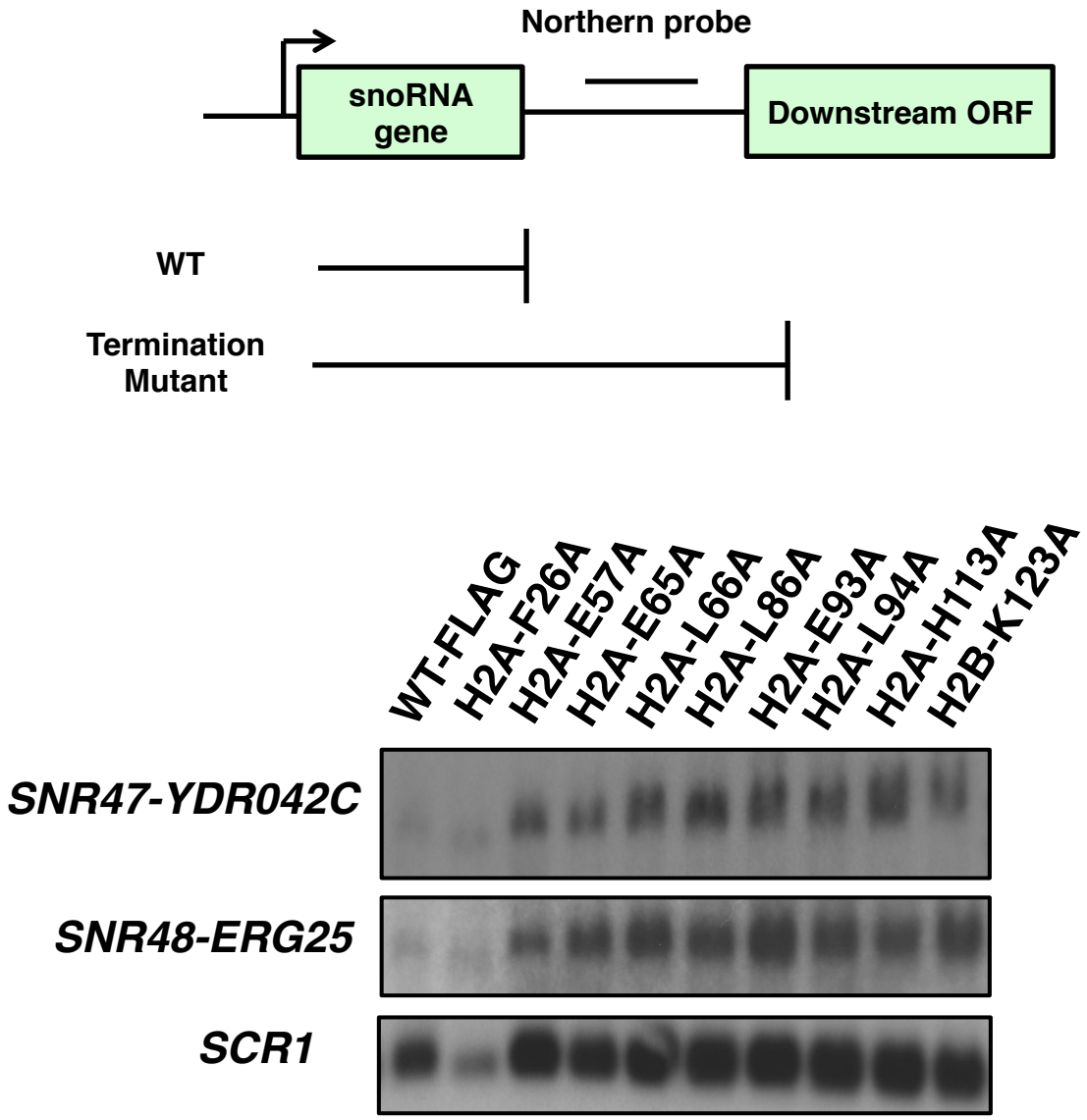

Figure 48. H2A mutants are defective in transcription termination of snoRNAs

Northern blot analysis of transcription read-through of snoRNAs *SNR47* and *SNR48* in the H2A mutants. *SCR1* serves as a loading control.

B.5 METHODS

Dilution growth assays: Cells were grown to saturation at 30°C and washed with sterile water. Beginning with a cell suspension at a concentration of 1 X 108 cells/mL, cells were diluted serially four times by a factor of ten in water. Two microliters of each dilution were spotted on the indicated plates. Plates were incubated at 30°C for three days**,** or as specified.

Western blot analysis: For all westerns aside from the FLAG westerns that measure H2B K123ub, yeast cells were grown to log phase (2-3 X 10^7 cells/mL) and lysed by bead beating in trichloroacetic acid (TCA), as described previously (COX *et al.* 1997). To make whole cell extracts for H2B K123ub analysis, cells were lysed in SUTEB buffer (10 mM Tris-HCl, pH 8.0, 1% SDS, 8 M urea, 10 mM EDTA, pH 8.0, and 0.01% bromophenol blue) (TOMSON *et al.* 2011). Proteins were resolved on SDS-polyacrylamide gels (15% polyacrylamide) and transferred to nitrocellulose membranes, with the exception of the FLAG westerns, which were transferred to PVDF membranes. Membranes were incubated with primary antibodies and then with anti-mouse or anti-rabbit secondary antibodies (GE Healthcare 1:5,000 dilution). Antibodies that recognize the following proteins or histone modifications were used: total histone H3 (1:30,000 dilution) (TOMSON *et al.* 2011), trimethylated H3 K4 (H3 K4me^3) (Active Motif 39159, 1:2,000 dilution), H3 K4me^2 (Millipore 07-030, 1:2000 dilution), H3 K79me^3 (note: this antibody has been reported by the manufacturer to cross-react with H3 K79me^2, Abcam ab2621, 1:2,000 dilution), H3 K36me^2 (Millipore 07-369, 1:1000 dilution), H3 K36me^3 (Abcam ab9050, 1:1000 dilution), H2B (Active Motif, 39237, 1:5,000 dilution), and glucose-6-phosphate dehydrogenase (G6PDH) (Sigma-Aldrich A9521, 1:30,000 dilution). Proteins were visualized using enhanced chemiluminescence substrate (PerkinElmer) and a 440 CF digital imaging station (Kodak). For western blot analysis, signals were quantified using ImageJ software and normalized to the loading control specified in

the figure legend. The relative signal from the wild-type strain was set equal to one. Error bars represent standard error of the mean for three biological replicates (SEM).

ChIP-qPCR: Chromatin immunoprecipitation (ChIP) assays were performed with 250 mL of log-phase yeast cultures (1-2 X 10^7 cells/mL) as previously described (SHIRRA *et al.* 2005). For histone ChIPs, sheared chromatin was incubated overnight at 4°C with antibodies specific to H2B, (0.5 µl, Active Motif, 39237), human H2B K120ub (2.5 µl, Cell Signaling 5546). Following incubation with the primary antibodies, chromatin was incubated for 2 hours at 4°C with Protein A-conjugated sepharose for all ChIPs,aside from the FLAG ChIPs. FLAG-tagged H2B was immunoprecipitated using 30 µl FLAG M2 agarose beads overnight at 4°C (Sigma, A2220). DNA was purified (Qiagen) and analyzed by qPCR using Maxima SYBR (Thermo). Occupancy levels were calculated using the primer efficiency raised to the difference between input and immunoprecipitated Ct values. Presented data are an average of two technical replicates for each of three biological replicates. The error bars indicate the standard error of the mean (SEM).

Northern blot analysis: Total RNA was isolated from log-phase yeast cultures (1-2 X 10^7), and 20 µg of RNA were subjected to northern blot analysis as described previously (SWANSON *et al.* 1991). Radiolabeled DNA probes were generated through random-prime labeling reactions of PCR templates. Membranes (Gene Screen Plus, Perkin Elmer) were incubated with radiolabeled DNA probes from PCR fragments of *SCR1* (amplicon: -163 to +284 relative to the TSS), *SNR47-YDR042C* (amplicon -325 to -33 relative to TSS of *YDR042C*), *SNR48-ERG25* (amplicon: -746 to -191 relative to TSS of *ERG25*).

APPENDIX C

INITIAL SCREEN OF BPA SITES USING HA-TAGGED H2A

When I first began working on the site-specific *in vivo* crosslinking project, I set out to replicate a previous study in which the authors used an HA-tagged form of H2A to detect the direct interaction between the H4 tail and the nucleosome acidic patch *in vivo* (WILKINS et al. 2014). I made C-terminally HA-tagged H2A 2μ constructs with amber codons at the following amino acid sites: Q15, R18, Y58, A61, E62, E65, L66, N69, D91, and E93 (Fig. 49). I chose these sites because they were located within the nucleosome acidic patch, which were the same residues that yielded an interaction with the H4 tail in (WILKINS et al. 2014). I also chose residues Q15 and R18 because they were located within the N-terminal tail region of H2A, which was shown to also play a role in histone modifications (ZHENG *et al.* 2010).

Unfortunately, expression of the H2A constructs in the presence of BPA was low (Fig. 50 and 51). After this, I aimed to perform IPs instead (see Chapter 3). For these experiments, I decided to work with two of the BPA sites from this initial screen that showed the highest levels of expression (Y58 and A61, Fig. 50) and I used Gibson assembly to change the epitope tag to a His-Biotin-His (HBH) tag for use in denaturing IPs (as discussed in chapter 3). Surprisingly, expression of HBH-tagged H2A was much more robust than that of the HA-tagged version, where expression of the BPA derivatives nearly matched the WT. The HA-tagged versions had much less expression compared to WT (Fig. 51). While I chose to focus on the acidic patch residues Y58 and A61, I would recommend a follow-up study on the H2A N-terminus using residues Q15 and R18, as both

of these residues had high levels of UV-crosslinking. R18 also has an additional crosslinked band compared to Q15 (Fig. 50 and Fig. 51). E93 may also be a good candidate for the HBH-tagged construct if expression is increased upon the tag change like it was for the other constructs. Here, the HA-tagged version did not have robust expression but it did display a low level of crosslinking upon UV-irradiation (Fig. 42).

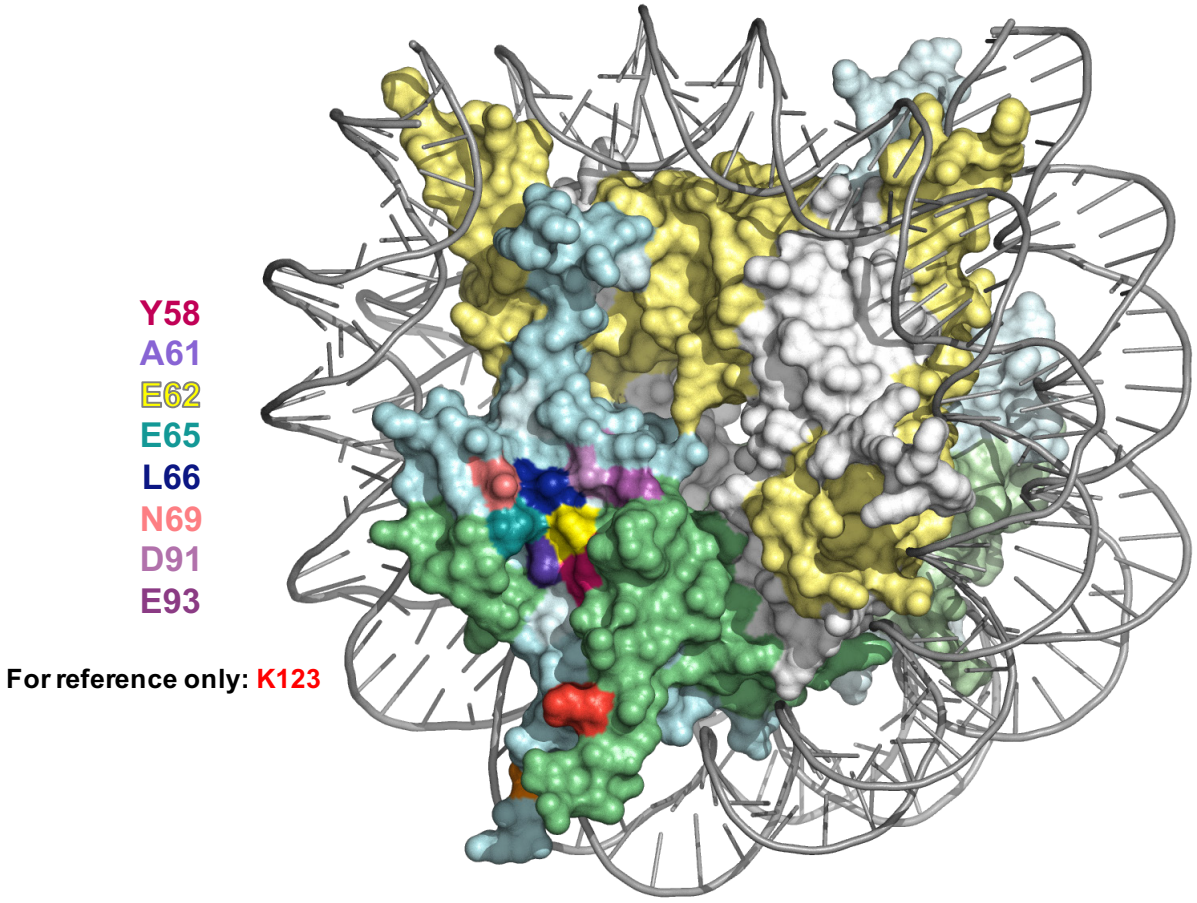

Figure 49. BPA sites mapped to the structure of the nucleosome

X-ray crystal structure of the nucleosome, denoting histones H2A, H2B, H3, and H4 in cyan, green, yellow, and white, respectively. BPA locations are depicted by the colors denoted in the legend to the left of the nucleosome. Not shown are N-terminal tail sites Q15 and R18. This figure was created using Pymol (PDB 1ID3 (WHITE *et al.* 2001)).

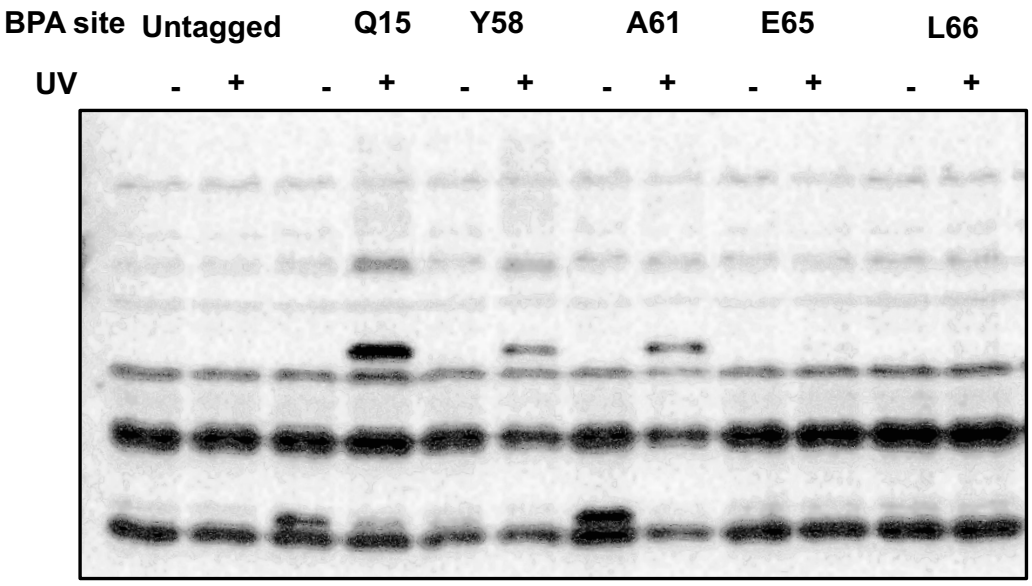

Figure 50. Western blot analysis of UV-crosslinked HA-tagged H2A derivatives

Western blot was probed with an anti-HA antibody. BPA located in place of Q15, Y58, and A61 is expressed and yields cross-linked products upon UV-irradiation. Left-most two lanes are untagged H2A in the presence and absence of UV showing cross-reacting bands with the HA-antibody.

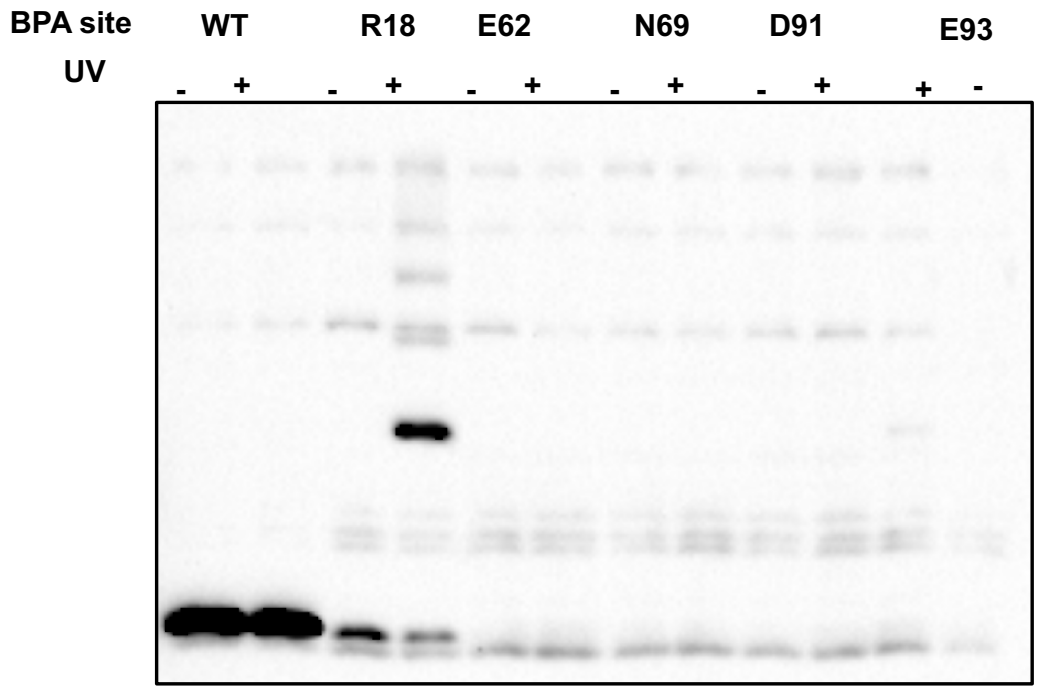

Figure 51. Western blot analysis of UV-crosslinked HA-tagged H2A derivatives

Western blot was probed with an anti-HA antibody. H2A with BPA located in place of R18 and E93 is expressed and yields cross-linked products upon UV-irradiation. Left-most two lanes are HA-tagged WT H2A showing WT levels of H2A-HA in the presence and absence of BPA.

C.1 METHODS

Photocrosslinking: 50 mL of cells (plasmids transformed into KY860) were grown to log phase (between 0.5 and 1.0 OD_{600}) in SC-Leu-Ura + 2% dextrose and 1mM BPA. For each culture, two sets of 12.5 OD units were pelleted and separately resuspended in 1 mL ddH_2O. One half was placed in the center of a 50-mL falcon tube lid 2 cm below a UVGL-55 lamp, which UV-irradiated the cells at 365 nm. Cells were exposed to UV light for 10 minutes. All cells were then subjected to TCA extraction, as described above.

Western blot analysis: For western analyses of whole cell extracts, yeast cells were grown to log phase (0.5-1.0 OD_{600}) and 12.5 OD were lysed by bead beating in trichloroacetic acid (TCA), as described previously (COX *et al.* 1997). Proteins were resolved on SDS-polyacrylamide tris-glycine gels (15% polyacrylamide) for anti-HA westerns and transferred to nitrocellulose membranes. Membranes were incubated with primary antibodies and then with anti-mouse or anti-rabbit secondary antibodies (GE Healthcare 1:5,000 dilution in 5% dry milk and 1X TBST). Proteins were visualized using enhanced chemiluminescence substrate (PerkinElmer) and a ChemiDoc XRS digital imaging station (BioRad).

Plasmid	Purpose	Derivation and reference
pCEC09	Untagged H2A	This study; (WILKINS *et al.* 2014)
pCEC10	WT H2A-HA	Site-directed mutagenesis of pCEC09; (WILKINS *et al.* 2014)
pCEC11	H2A-Q15$_{BPA}$-HA	Site-directed mutagenesis of pCEC10
pCEC12	H2A-R18$_{BPA}$-HA	Site-directed mutagenesis of pCEC10
pCEC13	H2A-Y58$_{BPA}$-HA	Site-directed mutagenesis of pCEC10
pCEC14	H2A-A61$_{BPA}$-HA	Site-directed mutagenesis of pCEC10
pCEC15	H2A-E62$_{BPA}$-HA	Site-directed mutagenesis of pCEC10
pCEC16	H2A-E65$_{BPA}$-HA	Site-directed mutagenesis of pCEC10
pCEC17	H2A-L66$_{BPA}$-HA	Site-directed mutagenesis of pCEC10
pCEC18	H2A-N69$_{BPA}$-HA	Site-directed mutagenesis of pCEC10
pCEC19	H2A-D91$_{BPA}$-HA	Site-directed mutagenesis of pCEC10
pCEC20	H2A-E93$_{BPA}$-HA	Site-directed mutagenesis of pCEC10
pLH157/*LEU2*	tRNA/tRNA synthetase containing plasmid	(VAN OSS *et al.* 2016)

Table 13. Plasmids used in this study

APPENDIX D

ANALYSIS OF PAF1 COMPLEX MEMBERS RTF1 AND CDC73

This section covers some work I did on Paf1C members Rtf1 and Cdc73. I assessed whether over-expression of the HMD could rescue H2B K123ub in cells lacking Bre1 (Fig. 52). I tested whether Rtf1 was required for Rad6 recruitment to chromatin using ChIP-qPCR (Fig. 53). Lastly, I found that the W321 residue in the C-domain of Cdc73 is required for WT levels of Cdc73 occupancy (Fig. 54).

Because the HMD-Rad6 interaction is Bre1 independent (VAN OSS *et al.* 2016), I wanted to determine whether over-expression of the HMD would rescue H2B K123ub in *bre1*Δ cells. As expected, H2B K123ub was completely dependent on Bre1, even though HMD and Rad6 can interact in the absence of Bre1 (Fig. 52).

To determine whether Rtf1 is required for Rad6 occupancy, I performed ChIP analysis of Rad6 in *RTF1, rtf1*Δ*,* and *rtf1-E104K* cells. E104 is a key amino acid that when substituted for lysine, H2B K123ub *in vivo* and the effect of the HMD *in vitro* are abolished (TOMSON *et al.* 2011; VAN OSS *et al.* 2016). The ChIP analysis did not demonstrate a large decrease in recruitment, which differed from ChIP-exo data. This was likely due to the lower sensitivity of conventional ChIP. Rad6-myc levels were not impacted by the loss of function of Rtf1 (Fig. 53).

As described in Chapter 1, the C-domain of Cdc73 is required for its attachment to Pol II (AMRICH *et al.* 2012; QIU *et al.* 2012). To determine whether the amino acid W321 is required for Cdc73 occupancy, I performed ChIP analysis on HA-tagged Cdc73 and the mutant. I found that

when W321 is substituted with alanine, there is a reduction in Cdc73 occupancy on active loci. This result was interesting because it agrees with a result that Ellie Kerr from our lab found that the W321A substitution abolishes Cdc73 crosslinking with Pol II.

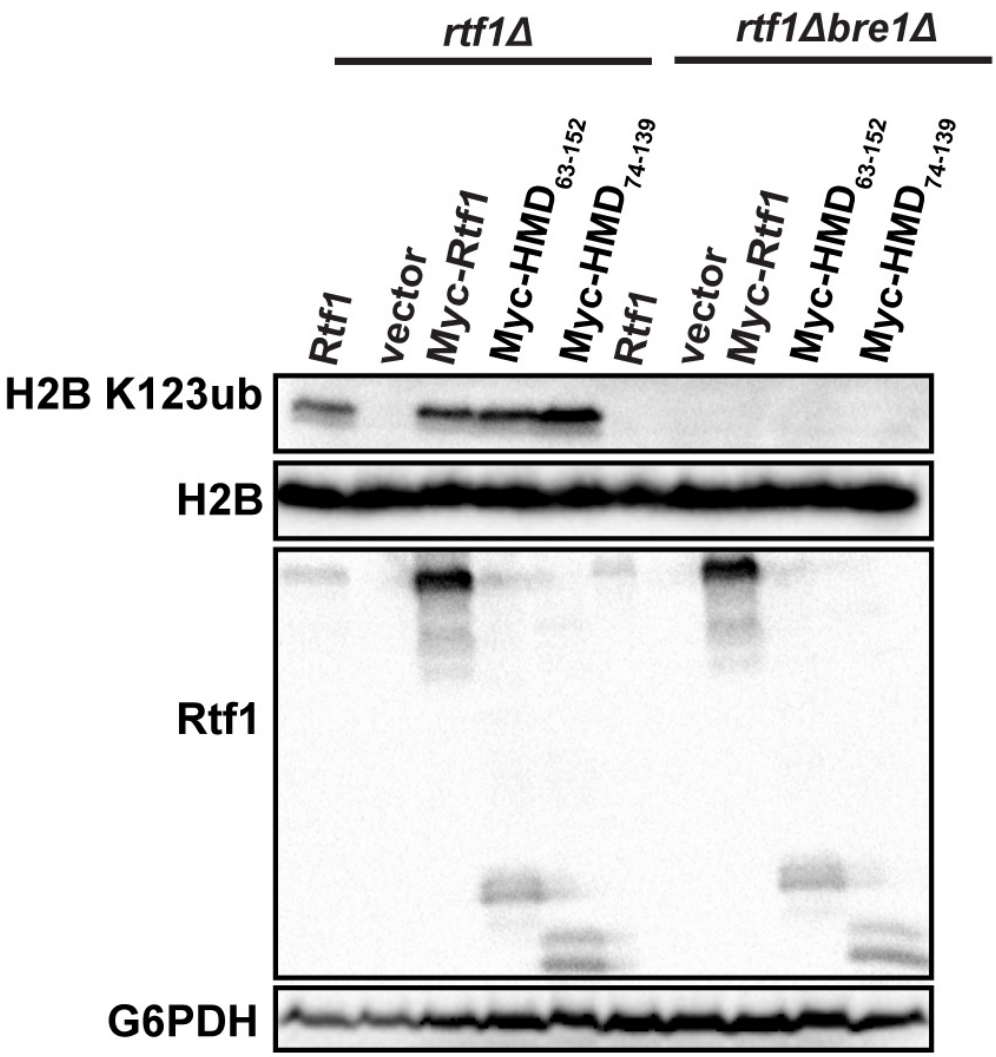

Figure 52. HMD cannot stimulate H2B K123ub in the absence of Bre1 *in vivo*

Western analysis of H2B K123ub, H2B, Rtf1, and G6PDH in the presence and absence of Bre1. G6PDH serves as a loading control. Rtf1 = full length Rtf1 on C/A plasmid, vector = empty vector, Myc-Rtf1 = 3X-myc-tagged full length Rtf1 on a 2μ plasmid, Myc-HMD_{63-152} = 3x-myc-tagged HMD amino acids 63-152, Myc-HMD_{74-139} = 3x-myc-tagged HMD amino acids 74-139. The Rtf1 antibody recognizes the HMD. Upper bands in Rtf1 blot correspond to full-length Rtf1 and lower bands correspond to HMD.

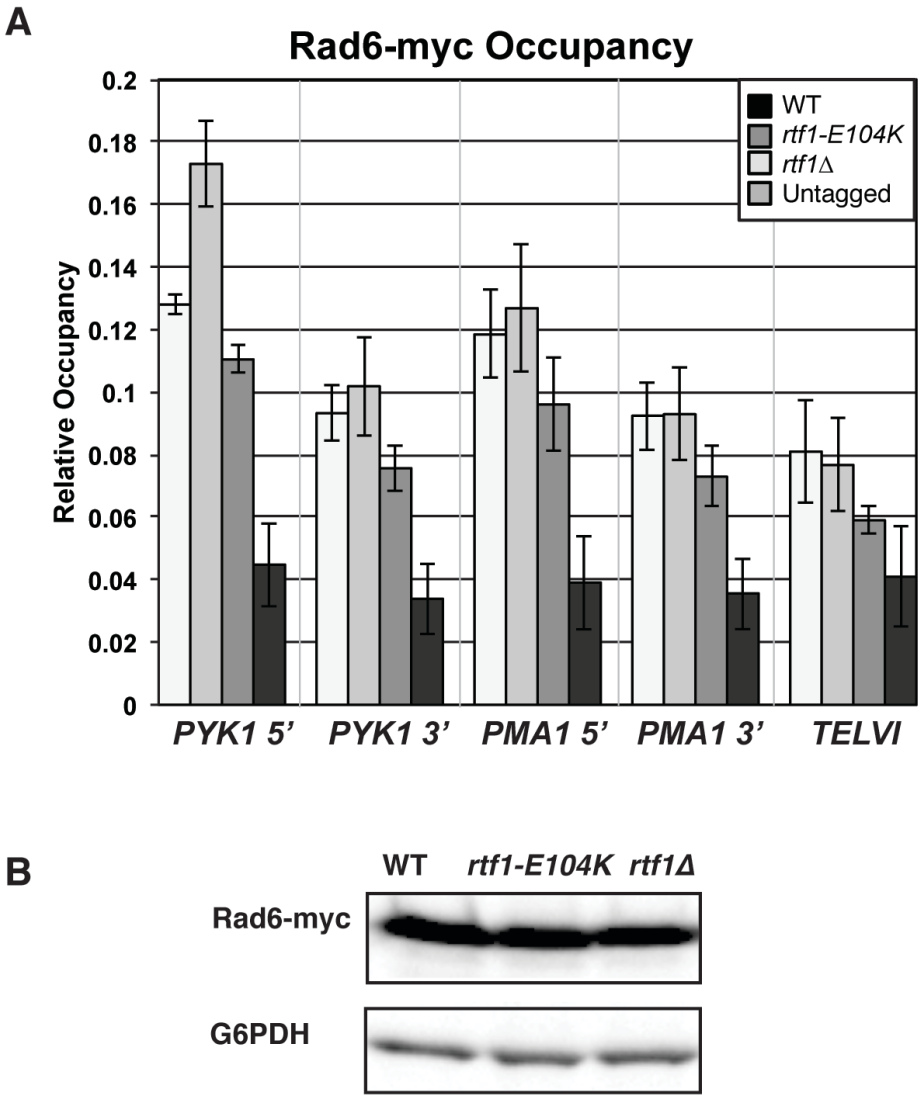

Figure 53. Rad6-myc occupancy and protein levels in the absence of functional Rtf1

(A) ChIPs were performed on chromatin isolated from Rtf1 mutant strains. The amount of immunoprecipitated DNA was determined by qPCR as a percentage of input DNA normalized to WT, which was set to one. The error bars represent SEM of three experiments. **(B)** Western blot analysis of Rad6-myc levels in Rtf1 mutant strains. Westerns were probed with antibodies against the myc epitope and G6PDH for a loading control.

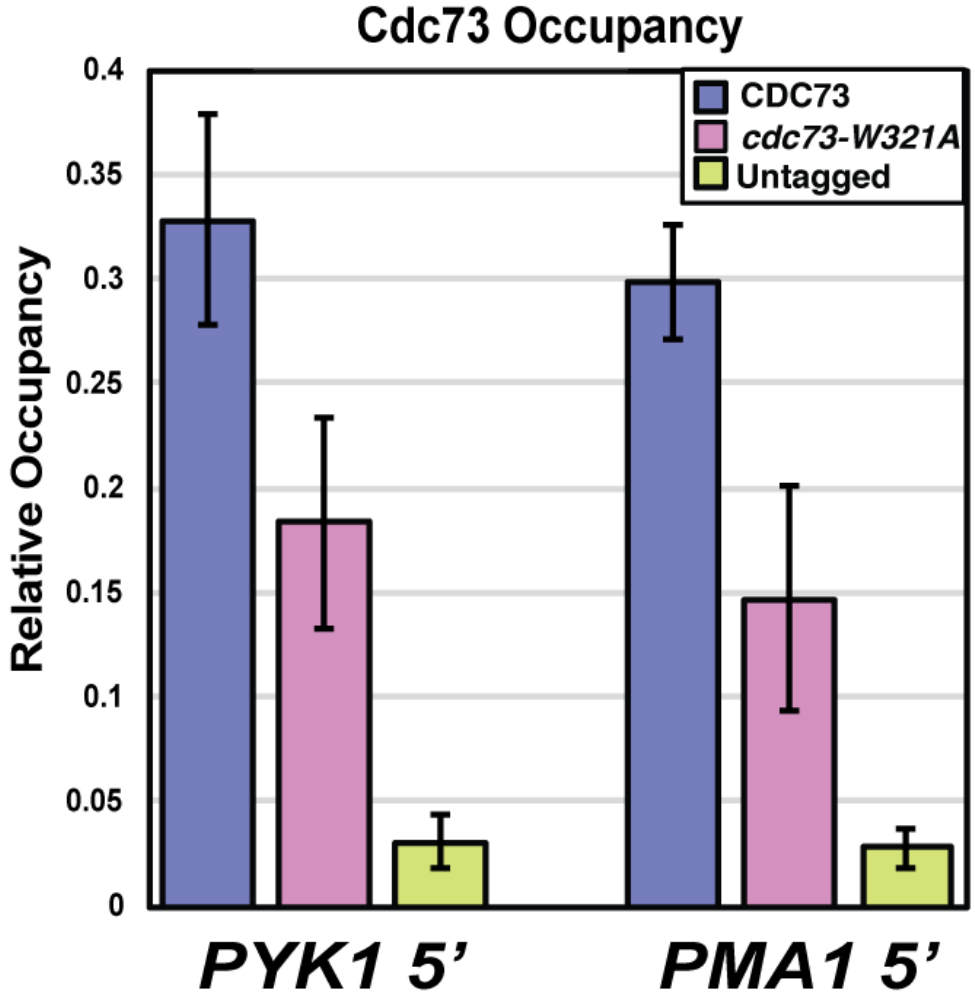

Figure 54. Cdc73 occupancy is reduced when W321 is substituted with alanine

ChIPs were performed on chromatin isolated from Cdc73 mutant strains. The amount of immunoprecipitated DNA was determined by qPCR as a percentage of input DNA normalized to WT, which was set to one. The error bars represent SEM of three experiments.

D.1 METHODS

Western blot analysis: For western analyses of whole cell extracts, yeast cells were grown to log phase (0.5-1.0 OD_{600}) and 10.5 OD were lysed by bead beating in trichloroacetic acid (TCA), as described previously (COX *et al.* 1997). Proteins were resolved on SDS-polyacrylamide tris-glycine gels and transferred to nitrocellulose membranes for all except for the H2B K123ub westerns. Membranes were incubated with primary antibodies: were H2Bub (Cell Signaling #5546; 1:1000 dilution), H2B (Active Motif #39237; 1:3000), Rtf1 (1:2500) (SQUAZZO *et al.* 2002b), α-G6PDH (Sigma #A9521; 1:20000), Myc (Covance) and then with anti-mouse or anti-rabbit secondary antibodies (GE Healthcare 1:5,000 dilution in 5% dry milk and 1X TBST). Proteins were visualized using enhanced chemiluminescence substrate (PerkinElmer) and a ChemiDoc XRS digital imaging station (BioRad).

ChIP-qPCR: Chromatin immunoprecipitation (ChIP) assays were performed with 250 mL of log-phase yeast cultures (1-2 X 10^7 cells/mL) as previously described (SHIRRA *et al.* 2005). For Rad6 ChIPs, sheared chromatin was incubated overnight at 4°C with an antibody against the Myc tag, (4 µl, Abcam ab9132). Following incubation with the primary antibody, chromatin was incubated for 2 hours at 4°C with Protein G-conjugated sepharose (GE healthcare). For the Cdc73 ChIPs, chromatin was incubated with 30µl HA-beads (Santa Cruz sc-7392AC) overnight at 4°C. DNA was purified (Qiagen) and analyzed by qPCR using Maxima SYBR (Thermo). Occupancy levels were calculated using the primer efficiency raised to the difference between input and immunoprecipitated Ct values. Presented data are an average of two technical replicates for each of three biological replicates. The error bars indicate the standard error of the mean (SEM).

BIBLIOGRAPHY

Adelman, K., and J. T. Lis, 2012 Promoter-proximal pausing of RNA polymerase II: emerging roles in metazoans. Nat Rev Genet 13**:** 720-731.

Alen, C., N. A. Kent, H. S. Jones, J. O'Sullivan, A. Aranda *et al.*, 2002 A role for chromatin remodeling in transcriptional termination by RNA polymerase II. Mol Cell 10**:** 1441-1452.

Allen, B. L., and D. J. Taatjes, 2015 The Mediator complex: a central integrator of transcription. Nat Rev Mol Cell Biol 16**:** 155-166.

Amrich, C. G., C. P. Davis, W. P. Rogal, M. K. Shirra, A. Heroux *et al.*, 2012 Cdc73 subunit of Paf1 complex contains C-terminal Ras-like domain that promotes association of Paf1 complex with chromatin. J Biol Chem 287**:** 10863-10875.

Ardehali, M. B., J. Yao, K. Adelman, N. J. Fuda, S. J. Petesch *et al.*, 2009 Spt6 enhances the elongation rate of RNA polymerase II in vivo. EMBO J 28**:** 1067-1077.

Arigo, J. T., K. L. Carroll, J. M. Ames and J. L. Corden, 2006a Regulation of yeast NRD1 expression by premature transcription termination. Mol Cell 21**:** 641-651.

Arigo, J. T., D. E. Eyler, K. L. Carroll and J. L. Corden, 2006b Termination of cryptic unstable transcripts is directed by yeast RNA-binding proteins Nrd1 and Nab3. Mol Cell 23**:** 841-851.

Armache, K. J., J. D. Garlick, D. Canzio, G. J. Narlikar and R. E. Kingston, 2011 Structural basis of silencing: Sir3 BAH domain in complex with a nucleosome at 3.0 A resolution. Science 334**:** 977-982.

Arndt, K. M., and D. Reines, 2015 Termination of Transcription of Short Noncoding RNAs by RNA Polymerase II. Annu Rev Biochem 84**:** 381-404.

Arya, G., and T. Schlick, 2009 A tale of tails: how histone tails mediate chromatin compaction in different salt and linker histone environments. J Phys Chem A 113**:** 4045-4059.

Aso, T., W. S. Lane, J. W. Conaway and R. C. Conaway, 1995 Elongin (SIII): a multisubunit regulator of elongation by RNA polymerase II. Science 269**:** 1439-1443.

Austriaco, N. R., Jr., and L. P. Guarente, 1997 Changes of telomere length cause reciprocal changes in the lifespan of mother cells in Saccharomyces cerevisiae. Proc Natl Acad Sci U S A 94**:** 9768-9772.

Ausubel FM, B. R., Kingston RE, Moore DD, Seidman JG, Smith JA, Struhl K, 1988 *Current protocols in molecular biology.* Wiley-Interscience, New York, NY.

Ayton, P. M., and M. L. Cleary, 2001 Molecular mechanisms of leukemogenesis mediated by MLL fusion proteins. Oncogene 20**:** 5695-5707.

Ballestas, M. E., P. A. Chatis and K. M. Kaye, 1999 Efficient persistence of extrachromosomal KSHV DNA mediated by latency-associated nuclear antigen. Science 284**:** 641-644.

Bannister, A. J., and T. Kouzarides, 2011 Regulation of chromatin by histone modifications. Cell Res 21**:** 381-395.

Barbera, A. J., J. V. Chodaparambil, B. Kelley-Clarke, V. Joukov, J. C. Walter *et al.*, 2006 The nucleosomal surface as a docking station for Kaposi's sarcoma herpesvirus LANA. Science 311**:** 856-861.

Barski, A., S. Cuddapah, K. Cui, T. Y. Roh, D. E. Schones *et al.*, 2007 High-resolution profiling of histone methylations in the human genome. Cell 129**:** 823-837.
Basehoar, A. D., S. J. Zanton and B. F. Pugh, 2004 Identification and distinct regulation of yeast TATA box-containing genes. Cell 116**:** 699-709.
Basnet, H., X. B. Su, Y. Tan, J. Meisenhelder, D. Merkurjev *et al.*, 2014 Tyrosine phosphorylation of histone H2A by CK2 regulates transcriptional elongation. Nature 516**:** 267-271.
Batta, K., Z. Zhang, K. Yen, D. B. Goffman and B. F. Pugh, 2011 Genome-wide function of H2B ubiquitylation in promoter and genic regions. Genes Dev 25**:** 2254-2265.
Battaglia, S., M. Lidschreiber, C. Baejen, P. Torkler, S. M. Vos *et al.*, 2017 RNA-dependent chromatin association of transcription elongation factors and Pol II CTD kinases. Elife 6.
Bednar, J., R. A. Horowitz, J. Dubochet and C. L. Woodcock, 1995 Chromatin conformation and salt-induced compaction: three-dimensional structural information from cryoelectron microscopy. J Cell Biol 131**:** 1365-1376.
Belotserkovskaya, R., S. Oh, V. A. Bondarenko, G. Orphanides, V. M. Studitsky *et al.*, 2003 FACT facilitates transcription-dependent nucleosome alteration. Science 301**:** 1090-1093.
Beltran, M., C. M. Yates, L. Skalska, M. Dawson, F. P. Reis *et al.*, 2016 The interaction of PRC2 with RNA or chromatin is mutually antagonistic. Genome Res 26**:** 896-907.
Bengal, E., O. Flores, A. Krauskopf, D. Reinberg and Y. Aloni, 1991 Role of the mammalian transcription factors IIF, IIS, and IIX during elongation by RNA polymerase II. Mol Cell Biol 11**:** 1195-1206.
Bengtson, M. H., and C. A. Joazeiro, 2010 Role of a ribosome-associated E3 ubiquitin ligase in protein quality control. Nature 467**:** 470-473.
Bernstein, B. E., T. S. Mikkelsen, X. Xie, M. Kamal, D. J. Huebert *et al.*, 2006 A bivalent chromatin structure marks key developmental genes in embryonic stem cells. Cell 125**:** 315-326.
Blythe, A. J., B. Yazar-Klosinski, M. W. Webster, E. Chen, M. Vandevenne *et al.*, 2016 The yeast transcription elongation factor Spt4/5 is a sequence-specific RNA binding protein. Protein Sci 25**:** 1710-1721.
Bonizec, M., L. Herissant, W. Pokrzywa, F. Geng, S. Wenzel *et al.*, 2014 The ubiquitin-selective chaperone Cdc48/p97 associates with Ubx3 to modulate monoubiquitylation of histone H2B. Nucleic Acids Res 42**:** 10975-10986.
Borukhov, S., V. Sagitov and A. Goldfarb, 1993 Transcript cleavage factors from E. coli. Cell 72**:** 459-466.
Bose, D. A., G. Donahue, D. Reinberg, R. Shiekhattar, R. Bonasio *et al.*, 2017 RNA Binding to CBP Stimulates Histone Acetylation and Transcription. Cell 168**:** 135-149 e122.
Brandman, O., J. Stewart-Ornstein, D. Wong, A. Larson, C. C. Williams *et al.*, 2012 A ribosome-bound quality control complex triggers degradation of nascent peptides and signals translation stress. Cell 151**:** 1042-1054.
Braun, M. A., P. J. Costa, E. M. Crisucci and K. M. Arndt, 2007 Identification of Rkr1, a nuclear RING domain protein with functional connections to chromatin modification in Saccharomyces cerevisiae. Mol Cell Biol 27**:** 2800-2811.
Briggs, S. D., T. Xiao, Z. W. Sun, J. A. Caldwell, J. Shabanowitz *et al.*, 2002 Gene silencing: trans-histone regulatory pathway in chromatin. Nature 418**:** 498.

Buratowski, S., S. Hahn, L. Guarente and P. A. Sharp, 1989 Five intermediate complexes in transcription initiation by RNA polymerase II. Cell 56**:** 549-561.
Buratowski, S., and H. Zhou, 1993 Functional domains of transcription factor TFIIB. Proc Natl Acad Sci U S A 90**:** 5633-5637.
Cai, S., Y. Song, C. Chen, J. Shi and L. Gan, 2017 Natural Chromatin Is Heterogeneous And Self Associates In Vitro. bioRxiv.
Cao, Q. F., J. Yamamoto, T. Isobe, S. Tateno, Y. Murase *et al.*, 2015 Characterization of the Human Transcription Elongation Factor Rtf1: Evidence for Nonoverlapping Functions of Rtf1 and the Paf1 Complex. Mol Cell Biol 35**:** 3459-3470.
Carrozza, M. J., B. Li, L. Florens, T. Suganuma, S. K. Swanson *et al.*, 2005 Histone H3 methylation by Set2 directs deacetylation of coding regions by Rpd3S to suppress spurious intragenic transcription. Cell 123**:** 581-592.
Cascon, A., C. V. Huarte-Mendicoa, L. Javier Leandro-Garcia, R. Leton, J. Suela *et al.*, 2011 Detection of the first gross CDC73 germline deletion in an HPT-JT syndrome family. Genes Chromosomes Cancer 50**:** 922-929.
Castelnuovo, M., J. B. Zaugg, E. Guffanti, A. Maffioletti, J. Camblong *et al.*, 2014 Role of histone modifications and early termination in pervasive transcription and antisense-mediated gene silencing in yeast. Nucleic Acids Res 42**:** 4348-4362.
Chandrasekharan, M. B., F. Huang, Y. C. Chen and Z. W. Sun, 2010 Histone H2B C-terminal helix mediates trans-histone H3K4 methylation independent of H2B ubiquitination. Mol Cell Biol 30**:** 3216-3232.
Chandrasekharan, M. B., F. Huang and Z. W. Sun, 2009 Ubiquitination of histone H2B regulates chromatin dynamics by enhancing nucleosome stability. Proc Natl Acad Sci U S A 106**:** 16686-16691.
Chang, J. S., and F. Winston, 2011 Spt10 and Spt21 are required for transcriptional silencing in Saccharomyces cerevisiae. Eukaryot Cell 10**:** 118-129.
Chatterjee, C., R. K. McGinty, B. Fierz and T. W. Muir, 2010 Disulfide-directed histone ubiquitylation reveals plasticity in hDot1L activation. Nat Chem Biol 6**:** 267-269.
Chaudhary, K., S. Deb, N. Moniaux, M. P. Ponnusamy and S. K. Batra, 2007 Human RNA polymerase II-associated factor complex: dysregulation in cancer. Oncogene 26**:** 7499-7507.
Chen, F. X., A. R. Woodfin, A. Gardini, R. A. Rickels, S. A. Marshall *et al.*, 2015 PAF1, a Molecular Regulator of Promoter-Proximal Pausing by RNA Polymerase II. Cell 162**:** 1003-1015.
Cheung, A. C., and P. Cramer, 2011 Structural basis of RNA polymerase II backtracking, arrest and reactivation. Nature 471**:** 249-253.
Cheung, V., G. Chua, N. N. Batada, C. R. Landry, S. W. Michnick *et al.*, 2008 Chromatin- and transcription-related factors repress transcription from within coding regions throughout the Saccharomyces cerevisiae genome. PLoS Biol 6**:** e277.
Chin, J. W., T. A. Cropp, J. C. Anderson, M. Mukherji, Z. Zhang *et al.*, 2003 An expanded eukaryotic genetic code. Science 301**:** 964-967.
Chinchilla, K., J. B. Rodriguez-Molina, D. Ursic, J. S. Finkel, A. Z. Ansari *et al.*, 2012 Interactions of Sen1, Nrd1, and Nab3 with multiple phosphorylated forms of the Rpb1 C-terminal domain in Saccharomyces cerevisiae. Eukaryot Cell 11**:** 417-429.
Cho, E. J., and S. Buratowski, 1999 Evidence that transcription factor IIB is required for a post-assembly step in transcription initiation. J Biol Chem 274**:** 25807-25813.

Chu, X., X. Qin, H. Xu, L. Li, Z. Wang *et al.*, 2013 Structural insights into Paf1 complex assembly and histone binding. Nucleic Acids Res 41**:** 10619-10629.
Chu, Y., R. Simic, M. H. Warner, K. M. Arndt and G. Prelich, 2007 Regulation of histone modification and cryptic transcription by the Bur1 and Paf1 complexes. EMBO J 26**:** 4646-4656.
Clapier, C. R., J. Iwasa, B. R. Cairns and C. L. Peterson, 2017 Mechanisms of action and regulation of ATP-dependent chromatin-remodelling complexes. Nat Rev Mol Cell Biol 18**:** 407-422.
Compe, E., and J. M. Egly, 2012 TFIIH: when transcription met DNA repair. Nat Rev Mol Cell Biol 13**:** 343-354.
Costa, P. J., and K. M. Arndt, 2000 Synthetic lethal interactions suggest a role for the Saccharomyces cerevisiae Rtf1 protein in transcription elongation. Genetics 156**:** 535-547.
Cox, J. S., R. E. Chapman and P. Walter, 1997 The unfolded protein response coordinates the production of endoplasmic reticulum protein and endoplasmic reticulum membrane. Mol Biol Cell 8**:** 1805-1814.
Crickard, J. B., J. Fu and J. C. Reese, 2016 Biochemical Analysis of Yeast Suppressor of Ty 4/5 (Spt4/5) Reveals the Importance of Nucleic Acid Interactions in the Prevention of RNA Polymerase II Arrest. J Biol Chem 291**:** 9853-9870.
Crisucci, E. M., and K. M. Arndt, 2011 The Roles of the Paf1 Complex and Associated Histone Modifications in Regulating Gene Expression. Genet Res Int 2011.
Cucinotta, C. E., and K. M. Arndt, 2016 SnapShot: Transcription Elongation. Cell 166**:** 1058-1058 e1051.
Cucinotta, C. E., A. N. Young, K. M. Klucevsek and K. M. Arndt, 2015 The Nucleosome Acidic Patch Regulates the H2B K123 Monoubiquitylation Cascade and Transcription Elongation in Saccharomyces cerevisiae. PLoS Genet 11**:** e1005420.
D, G. H., D. R. Kelley, D. Tenen, B. Bernstein and J. L. Rinn, 2016 Widespread RNA binding by chromatin-associated proteins. Genome Biol 17**:** 28.
Dai, J., E. M. Hyland, D. S. Yuan, H. Huang, J. S. Bader *et al.*, 2008 Probing nucleosome function: a highly versatile library of synthetic histone H3 and H4 mutants. Cell 134**:** 1066-1078.
Daniel, J. A., M. S. Torok, Z. W. Sun, D. Schieltz, C. D. Allis *et al.*, 2004 Deubiquitination of histone H2B by a yeast acetyltransferase complex regulates transcription. J Biol Chem 279**:** 1867-1871.
David, Y., M. Vila-Perello, S. Verma and T. W. Muir, 2015 Chemical tagging and customizing of cellular chromatin states using ultrafast trans-splicing inteins. Nat Chem 7**:** 394-402.
Davidovich, C., L. Zheng, K. J. Goodrich and T. R. Cech, 2013 Promiscuous RNA binding by Polycomb repressive complex 2. Nat Struct Mol Biol 20**:** 1250-1257.
de la Mata, M., C. R. Alonso, S. Kadener, J. P. Fededa, M. Blaustein *et al.*, 2003 A slow RNA polymerase II affects alternative splicing in vivo. Mol Cell 12**:** 525-532.
De Vos, D., F. Frederiks, M. Terweij, T. van Welsem, K. F. Verzijlbergen *et al.*, 2011 Progressive methylation of ageing histones by Dot1 functions as a timer. EMBO Rep 12**:** 956-962.
Dermody, J. L., and S. Buratowski, 2010 Leo1 subunit of the yeast paf1 complex binds RNA and contributes to complex recruitment. J Biol Chem 285**:** 33671-33679.

Dieci, G., M. Preti and B. Montanini, 2009 Eukaryotic snoRNAs: a paradigm for gene expression flexibility. Genomics 94**:** 83-88.
Dion, M. F., S. J. Altschuler, L. F. Wu and O. J. Rando, 2005 Genomic characterization reveals a simple histone H4 acetylation code. Proc Natl Acad Sci U S A 102**:** 5501-5506.
Dorigo, B., T. Schalch, K. Bystricky and T. J. Richmond, 2003 Chromatin fiber folding: requirement for the histone H4 N-terminal tail. J Mol Biol 327**:** 85-96.
Dorman, G., and G. D. Prestwich, 1994 Benzophenone photophores in biochemistry. Biochemistry 33**:** 5661-5673.
Dover, J., J. Schneider, M. A. Tawiah-Boateng, A. Wood, K. Dean *et al.*, 2002 Methylation of histone H3 by COMPASS requires ubiquitination of histone H2B by Rad6. J Biol Chem 277**:** 28368-28371.
du Preez, L. L., and H. G. Patterton, 2013 Secondary structures of the core histone N-terminal tails: their role in regulating chromatin structure. Subcell Biochem 61**:** 37-55.
Duina, A. A., 2011 Histone Chaperones Spt6 and FACT: Similarities and Differences in Modes of Action at Transcribed Genes. Genet Res Int 2011**:** 625210.
Dujardin, G., C. Lafaille, M. de la Mata, L. E. Marasco, M. J. Munoz *et al.*, 2014 How slow RNA polymerase II elongation favors alternative exon skipping. Mol Cell 54**:** 683-690.
Dvir, A., J. W. Conaway and R. C. Conaway, 2001 Mechanism of transcription initiation and promoter escape by RNA polymerase II. Curr Opin Genet Dev 11**:** 209-214.
Dvir, A., R. C. Conaway and J. W. Conaway, 1997 A role for TFIIH in controlling the activity of early RNA polymerase II elongation complexes. Proc Natl Acad Sci U S A 94**:** 9006-9010.
Emre, N. C., K. Ingvarsdottir, A. Wyce, A. Wood, N. J. Krogan *et al.*, 2005 Maintenance of low histone ubiquitylation by Ubp10 correlates with telomere-proximal Sir2 association and gene silencing. Mol Cell 17**:** 585-594.
Endo, H., Y. Nakabayashi, S. Kawashima, T. Enomoto, M. Seki *et al.*, 2012 Nucleosome surface containing nucleosomal DNA entry/exit site regulates H3-K36me3 via association with RNA polymerase II and Set2. Genes Cells 17**:** 65-81.
England, J. R., J. Huang, M. J. Jennings, R. D. Makde and S. Tan, 2010 RCC1 uses a conformationally diverse loop region to interact with the nucleosome: a model for the RCC1-nucleosome complex. J Mol Biol 398**:** 518-529.
Fang, Q., P. Chen, M. Wang, J. Fang, N. Yang *et al.*, 2016 Human cytomegalovirus IE1 protein alters the higher-order chromatin structure by targeting the acidic patch of the nucleosome. Elife 5.
Fazal, F. M., C. A. Meng, K. Murakami, R. D. Kornberg and S. M. Block, 2015 Real-time observation of the initiation of RNA polymerase II transcription. Nature 525**:** 274-277.
Feng, Q., H. Wang, H. H. Ng, H. Erdjument-Bromage, P. Tempst *et al.*, 2002 Methylation of H3-lysine 79 is mediated by a new family of HMTases without a SET domain. Curr Biol 12**:** 1052-1058.
Ferreira, H., J. Somers, R. Webster, A. Flaus and T. Owen-Hughes, 2007 Histone tails and the H3 alphaN helix regulate nucleosome mobility and stability. Mol Cell Biol 27**:** 4037-4048.
Fierz, B., C. Chatterjee, R. K. McGinty, M. Bar-Dagan, D. P. Raleigh *et al.*, 2011 Histone H2B ubiquitylation disrupts local and higher-order chromatin compaction. Nat Chem Biol 7**:** 113-119.

Finch, J. T., and A. Klug, 1976 Solenoidal model for superstructure in chromatin. Proc Natl Acad Sci U S A 73**:** 1897-1901.
Fingerman, I. M., H. C. Li and S. D. Briggs, 2007 A charge-based interaction between histone H4 and Dot1 is required for H3K79 methylation and telomere silencing: identification of a new trans-histone pathway. Genes Dev 21**:** 2018-2029.
Fischl, H., F. S. Howe, A. Furger and J. Mellor, 2017 Paf1 Has Distinct Roles in Transcription Elongation and Differential Transcript Fate. Mol Cell 65**:** 685-698 e688.
Fischle, W., Y. Wang and C. D. Allis, 2003 Histone and chromatin cross-talk. Curr Opin Cell Biol 15**:** 172-183.
Fleming, A. B., C. F. Kao, C. Hillyer, M. Pikaart and M. A. Osley, 2008 H2B ubiquitylation plays a role in nucleosome dynamics during transcription elongation. Mol Cell 31**:** 57-66.
Fong, N., H. Kim, Y. Zhou, X. Ji, J. Qiu *et al.*, 2014 Pre-mRNA splicing is facilitated by an optimal RNA polymerase II elongation rate. Genes Dev 28**:** 2663-2676.
Formosa, T., 2012 The role of FACT in making and breaking nucleosomes. Biochim Biophys Acta 1819**:** 247-255.
Formosa, T., S. Ruone, M. D. Adams, A. E. Olsen, P. Eriksson *et al.*, 2002 Defects in SPT16 or POB3 (yFACT) in Saccharomyces cerevisiae cause dependence on the Hir/Hpc pathway: polymerase passage may degrade chromatin structure. Genetics 162**:** 1557-1571.
Fuchs, G., D. Hollander, Y. Voichek, G. Ast and M. Oren, 2014 Cotranscriptional histone H2B monoubiquitylation is tightly coupled with RNA polymerase II elongation rate. Genome Res 24**:** 1572-1583.
Fuchs, G., and M. Oren, 2014 Writing and reading H2B monoubiquitylation. Biochim Biophys Acta 1839**:** 694-701.
Fuchs, G., E. Shema, R. Vesterman, E. Kotler, Z. Wolchinsky *et al.*, 2012 RNF20 and USP44 regulate stem cell differentiation by modulating H2B monoubiquitylation. Mol Cell 46**:** 662-673.
Gallego, L. D., M. Ghodgaonkar Steger, A. A. Polyansky, T. Schubert, B. Zagrovic *et al.*, 2016 Structural mechanism for the recognition and ubiquitination of a single nucleosome residue by Rad6-Bre1. Proc Natl Acad Sci U S A 113**:** 10553-10558.
Gangloff, Y. G., S. L. Sanders, C. Romier, D. Kirschner, P. A. Weil *et al.*, 2001 Histone folds mediate selective heterodimerization of yeast TAF(II)25 with TFIID components yTAF(II)47 and yTAF(II)65 and with SAGA component ySPT7. Mol Cell Biol 21**:** 1841-1853.
Gibson, B. A., Y. Zhang, H. Jiang, K. M. Hussey, J. H. Shrimp *et al.*, 2016 Chemical genetic discovery of PARP targets reveals a role for PARP-1 in transcription elongation. Science 353**:** 45-50.
Girish, T. S., R. K. McGinty and S. Tan, 2016 Multivalent Interactions by the Set8 Histone Methyltransferase With Its Nucleosome Substrate. J Mol Biol 428**:** 1531-1543.
Goel, S., S. Krishnamurthy and M. Hampsey, 2012 Mechanism of start site selection by RNA polymerase II: interplay between TFIIB and Ssl2/XPB helicase subunit of TFIIH. J Biol Chem 287**:** 557-567.
Grunberg, S., S. Henikoff, S. Hahn and G. E. Zentner, 2016 Mediator binding to UASs is broadly uncoupled from transcription and cooperative with TFIID recruitment to promoters. EMBO J 35**:** 2435-2446.
Ha, I., W. S. Lane and D. Reinberg, 1991 Cloning of a human gene encoding the general transcription initiation factor IIB. Nature 352**:** 689-695.

Hainer, S. J., and J. A. Martens, 2011 Identification of histone mutants that are defective for transcription-coupled nucleosome occupancy. Mol Cell Biol 31**:** 3557-3568.
Hainer, S. J., J. A. Pruneski, R. D. Mitchell, R. M. Monteverde and J. A. Martens, 2011 Intergenic transcription causes repression by directing nucleosome assembly. Genes Dev 25**:** 29-40.
Hammond, C. M., C. B. Stromme, H. Huang, D. J. Patel and A. Groth, 2017 Histone chaperone networks shaping chromatin function. Nat Rev Mol Cell Biol 18**:** 141-158.
Harlen, K. M., K. L. Trotta, E. E. Smith, M. M. Mosaheb, S. M. Fuchs *et al.*, 2016 Comprehensive RNA Polymerase II Interactomes Reveal Distinct and Varied Roles for Each Phospho-CTD Residue. Cell Rep 15**:** 2147-2158.
Hazelbaker, D. Z., S. Marquardt, W. Wlotzka and S. Buratowski, 2013 Kinetic competition between RNA Polymerase II and Sen1-dependent transcription termination. Mol Cell 49**:** 55-66.
He, C., S. Sidoli, R. Warneford-Thomson, D. C. Tatomer, J. E. Wilusz *et al.*, 2016 High-Resolution Mapping of RNA-Binding Regions in the Nuclear Proteome of Embryonic Stem Cells. Mol Cell 64**:** 416-430.
Henikoff, S., and A. Shilatifard, 2011 Histone modification: cause or cog? Trends Genet 27**:** 389-396.
Henry, K. W., A. Wyce, W. S. Lo, L. J. Duggan, N. C. Emre *et al.*, 2003 Transcriptional activation via sequential histone H2B ubiquitylation and deubiquitylation, mediated by SAGA-associated Ubp8. Genes Dev 17**:** 2648-2663.
Hieb, A. R., A. Gansen, V. Bohm and J. Langowski, 2014 The conformational state of the nucleosome entry-exit site modulates TATA box-specific TBP binding. Nucleic Acids Res 42**:** 7561-7576.
Hirano, M., C. M. Quinzii, H. Mitsumoto, A. P. Hays, J. K. Roberts *et al.*, 2011 Senataxin mutations and amyotrophic lateral sclerosis. Amyotroph Lateral Scler 12**:** 223-227.
Hodges, A. J., L. M. Gloss and J. J. Wyrick, 2017 Residues in the Nucleosome Acidic Patch Regulate Histone Occupancy and Are Important for FACT Binding in Saccharomyces cerevisiae. Genetics.
Hoffmann, C., and H. Neumann, 2015 In Vivo Mapping of FACT-Histone Interactions Identifies a Role of Pob3 C-terminus in H2A-H2B Binding. ACS Chem Biol 10**:** 2753-2763.
Holt, M. T., Y. David, S. Pollock, Z. Tang, J. Jeon *et al.*, 2015 Identification of a functional hotspot on ubiquitin required for stimulation of methyltransferase activity on chromatin. Proc Natl Acad Sci U S A 112**:** 10365-10370.
Hondele, M., T. Stuwe, M. Hassler, F. Halbach, A. Bowman *et al.*, 2013 Structural basis of histone H2A-H2B recognition by the essential chaperone FACT. Nature 499**:** 111-114.
Hsieh, F. K., O. I. Kulaeva, S. S. Patel, P. N. Dyer, K. Luger *et al.*, 2013 Histone chaperone FACT action during transcription through chromatin by RNA polymerase II. Proc Natl Acad Sci U S A 110**:** 7654-7659.
Hsin, J. P., and J. L. Manley, 2012 The RNA polymerase II CTD coordinates transcription and RNA processing. Genes Dev 26**:** 2119-2137.
Huisinga, K. L., and B. F. Pugh, 2004 A genome-wide housekeeping role for TFIID and a highly regulated stress-related role for SAGA in Saccharomyces cerevisiae. Mol Cell 13**:** 573-585.

Hwang, W. W., S. Venkatasubrahmanyam, A. G. Ianculescu, A. Tong, C. Boone *et al.*, 2003 A conserved RING finger protein required for histone H2B monoubiquitination and cell size control. Mol Cell 11**:** 261-266.

Izban, M. G., and D. S. Luse, 1992 The RNA polymerase II ternary complex cleaves the nascent transcript in a 3'----5' direction in the presence of elongation factor SII. Genes Dev 6**:** 1342-1356.

Jeronimo, C., A. R. Bataille and F. Robert, 2013 The writers, readers, and functions of the RNA polymerase II C-terminal domain code. Chem Rev 113**:** 8491-8522.

Joshi, A. A., and K. Struhl, 2005 Eaf3 chromodomain interaction with methylated H3-K36 links histone deacetylation to Pol II elongation. Mol Cell 20**:** 971-978.

Kalashnikova, A. A., M. E. Porter-Goff, U. M. Muthurajan, K. Luger and J. C. Hansen, 2013 The role of the nucleosome acidic patch in modulating higher order chromatin structure. J R Soc Interface 10**:** 20121022.

Kang, J. J., D. T. Auble, J. A. Ranish and S. Hahn, 1995 Analysis of the yeast transcription factor TFIIA: distinct functional regions and a polymerase II-specific role in basal and activated transcription. Mol Cell Biol 15**:** 1234-1243.

Kaplan, C. D., H. Jin, I. L. Zhang and A. Belyanin, 2012 Dissection of Pol II trigger loop function and Pol II activity-dependent control of start site selection in vivo. PLoS Genet 8**:** e1002627.

Kaplan, C. D., L. Laprade and F. Winston, 2003 Transcription elongation factors repress transcription initiation from cryptic sites. Science 301**:** 1096-1099.

Kassabov, S. R., B. Zhang, J. Persinger and B. Bartholomew, 2003 SWI/SNF unwraps, slides, and rewraps the nucleosome. Mol Cell 11**:** 391-403.

Kato, H., J. Jiang, B. R. Zhou, M. Rozendaal, H. Feng *et al.*, 2013 A conserved mechanism for centromeric nucleosome recognition by centromere protein CENP-C. Science 340**:** 1110-1113.

Kato, H., H. van Ingen, B. R. Zhou, H. Feng, M. Bustin *et al.*, 2011 Architecture of the high mobility group nucleosomal protein 2-nucleosome complex as revealed by methyl-based NMR. Proc Natl Acad Sci U S A 108**:** 12283-12288.

Kawashima, S., Y. Nakabayashi, K. Matsubara, N. Sano, T. Enomoto *et al.*, 2011 Global analysis of core histones reveals nucleosomal surfaces required for chromosome bi-orientation. EMBO J 30**:** 3353-3367.

Kemble, D. J., L. L. McCullough, F. G. Whitby, T. Formosa and C. P. Hill, 2015 FACT Disrupts Nucleosome Structure by Binding H2A-H2B with Conserved Peptide Motifs. Mol Cell 60**:** 294-306.

Kettenberger, H., K. J. Armache and P. Cramer, 2003 Architecture of the RNA polymerase II-TFIIS complex and implications for mRNA cleavage. Cell 114**:** 347-357.

Kim, H. D., J. Choe and Y. S. Seo, 1999 The sen1(+) gene of Schizosaccharomyces pombe, a homologue of budding yeast SEN1, encodes an RNA and DNA helicase. Biochemistry 38**:** 14697-14710.

Kim, J., M. Guermah, R. K. McGinty, J. S. Lee, Z. Tang *et al.*, 2009 RAD6-Mediated transcription-coupled H2B ubiquitylation directly stimulates H3K4 methylation in human cells. Cell 137**:** 459-471.

Kim, J., M. Guermah and R. G. Roeder, 2010 The human PAF1 complex acts in chromatin transcription elongation both independently and cooperatively with SII/TFIIS. Cell 140**:** 491-503.

Kim, J., S. B. Hake and R. G. Roeder, 2005 The human homolog of yeast BRE1 functions as a transcriptional coactivator through direct activator interactions. Mol Cell 20**:** 759-770.
Kim, J., J. A. Kim, R. K. McGinty, U. T. Nguyen, T. W. Muir *et al.*, 2013a The n-SET domain of Set1 regulates H2B ubiquitylation-dependent H3K4 methylation. Mol Cell 49**:** 1121-1133.
Kim, J., and R. G. Roeder, 2009 Direct Bre1-Paf1 complex interactions and RING finger-independent Bre1-Rad6 interactions mediate histone H2B ubiquitylation in yeast. J Biol Chem 284**:** 20582-20592.
Kim, J. L., D. B. Nikolov and S. K. Burley, 1993a Co-crystal structure of TBP recognizing the minor groove of a TATA element. Nature 365**:** 520-527.
Kim, K., B. Lee, J. Kim, J. Choi, J. M. Kim *et al.*, 2013b Linker Histone H1.2 cooperates with Cul4A and PAF1 to drive H4K31 ubiquitylation-mediated transactivation. Cell Rep 5**:** 1690-1703.
Kim, M., N. J. Krogan, L. Vasiljeva, O. J. Rando, E. Nedea *et al.*, 2004 The yeast Rat1 exonuclease promotes transcription termination by RNA polymerase II. Nature 432**:** 517-522.
Kim, M., L. Vasiljeva, O. J. Rando, A. Zhelkovsky, C. Moore *et al.*, 2006 Distinct pathways for snoRNA and mRNA termination. Mol Cell 24**:** 723-734.
Kim, Y., J. H. Geiger, S. Hahn and P. B. Sigler, 1993b Crystal structure of a yeast TBP/TATA-box complex. Nature 365**:** 512-520.
Klucevsek, K. M., M. A. Braun and K. M. Arndt, 2012 The Paf1 complex subunit Rtf1 buffers cells against the toxic effects of [PSI+] and defects in Rkr1-dependent protein quality control in Saccharomyces cerevisiae. Genetics 191**:** 1107-1118.
Komissarova, N., and M. Kashlev, 1997 RNA polymerase switches between inactivated and activated states By translocating back and forth along the DNA and the RNA. J Biol Chem 272**:** 15329-15338.
Kornberg, R. D., 1974 Chromatin structure: a repeating unit of histones and DNA. Science 184**:** 868-871.
Korzheva, N., A. Mustaev, E. Nudler, V. Nikiforov and A. Goldfarb, 1998 Mechanistic model of the elongation complex of Escherichia coli RNA polymerase. Cold Spring Harb Symp Quant Biol 63**:** 337-345.
Kostrewa, D., M. E. Zeller, K. J. Armache, M. Seizl, K. Leike *et al.*, 2009 RNA polymerase II-TFIIB structure and mechanism of transcription initiation. Nature 462**:** 323-330.
Kouskouti, A., and I. Talianidis, 2005 Histone modifications defining active genes persist after transcriptional and mitotic inactivation. EMBO J 24**:** 347-357.
Kouzarides, T., 2007 Chromatin modifications and their function. Cell 128**:** 693-705.
Krietenstein, N., M. Wal, S. Watanabe, B. Park, C. L. Peterson *et al.*, 2016 Genomic Nucleosome Organization Reconstituted with Pure Proteins. Cell 167**:** 709-721 e712.
Krogan, N. J., J. Dover, S. Khorrami, J. F. Greenblatt, J. Schneider *et al.*, 2002 COMPASS, a histone H3 (Lysine 4) methyltransferase required for telomeric silencing of gene expression. J Biol Chem 277**:** 10753-10755.
Krogan, N. J., J. Dover, A. Wood, J. Schneider, J. Heidt *et al.*, 2003 The Paf1 complex is required for histone H3 methylation by COMPASS and Dot1p: linking transcriptional elongation to histone methylation. Mol Cell 11**:** 721-729.

Kulaeva, O. I., F. K. Hsieh, H. W. Chang, D. S. Luse and V. M. Studitsky, 2013 Mechanism of transcription through a nucleosome by RNA polymerase II. Biochim Biophys Acta 1829**:** 76-83.
Kwak, H., and J. T. Lis, 2013 Control of transcriptional elongation. Annu Rev Genet 47**:** 483-508.
Lagrange, T., A. N. Kapanidis, H. Tang, D. Reinberg and R. H. Ebright, 1998 New core promoter element in RNA polymerase II-dependent transcription: sequence-specific DNA binding by transcription factor IIB. Genes Dev 12**:** 34-44.
Langenbacher, A. D., C. T. Nguyen, A. M. Cavanaugh, J. Huang, F. Lu *et al.*, 2011 The PAF1 complex differentially regulates cardiomyocyte specification. Dev Biol 353**:** 19-28.
Langmore, J. P., and C. Schutt, 1980 The higher order structure of chicken erythrocyte chromosomes in vivo. Nature 288**:** 620-622.
Laribee, R. N., N. J. Krogan, T. Xiao, Y. Shibata, T. R. Hughes *et al.*, 2005 BUR kinase selectively regulates H3 K4 trimethylation and H2B ubiquitylation through recruitment of the PAF elongation complex. Curr Biol 15**:** 1487-1493.
Larson, A. G., D. Elnatan, M. M. Keenen, M. J. Trnka, J. B. Johnston *et al.*, 2017 Liquid droplet formation by HP1alpha suggests a role for phase separation in heterochromatin. Nature.
Latham, J. A., and S. Y. Dent, 2007 Cross-regulation of histone modifications. Nat Struct Mol Biol 14**:** 1017-1024.
Lee, J. S., A. S. Garrett, K. Yen, Y. H. Takahashi, D. Hu *et al.*, 2012 Codependency of H2B monoubiquitination and nucleosome reassembly on Chd1. Genes Dev 26**:** 914-919.
Lee, K. K., L. Florens, S. K. Swanson, M. P. Washburn and J. L. Workman, 2005 The deubiquitylation activity of Ubp8 is dependent upon Sgf11 and its association with the SAGA complex. Mol Cell Biol 25**:** 1173-1182.
Lee, Y., D. Park and V. R. Iyer, 2017 The ATP-dependent chromatin remodeler Chd1 is recruited by transcription elongation factors and maintains H3K4me3/H3K36me3 domains at actively transcribed and spliced genes. Nucleic Acids Res.
Lesbats, P., E. Serrao, D. P. Maskell, V. E. Pye, N. O'Reilly *et al.*, 2017 Structural basis for spumavirus GAG tethering to chromatin. Proc Natl Acad Sci U S A 114**:** 5509-5514.
Leung, J. W., P. Agarwal, M. D. Canny, F. Gong, A. D. Robison *et al.*, 2014 Nucleosome acidic patch promotes RNF168- and RING1B/BMI1-dependent H2AX and H2A ubiquitination and DNA damage signaling. PLoS Genet 10**:** e1004178.
Leurent, C., S. Sanders, C. Ruhlmann, V. Mallouh, P. A. Weil *et al.*, 2002 Mapping histone fold TAFs within yeast TFIID. EMBO J 21**:** 3424-3433.
Levendosky, R. F., A. Sabantsev, S. Deindl and G. D. Bowman, 2016 The Chd1 chromatin remodeler shifts hexasomes unidirectionally. Elife 5.
Lewis, P. W., M. M. Muller, M. S. Koletsky, F. Cordero, S. Lin *et al.*, 2013 Inhibition of PRC2 activity by a gain-of-function H3 mutation found in pediatric glioblastoma. Science 340**:** 857-861.
Li, X. Y., S. R. Bhaumik and M. R. Green, 2000 Distinct classes of yeast promoters revealed by differential TAF recruitment. Science 288**:** 1242-1244.
Liu, C. L., T. Kaplan, M. Kim, S. Buratowski, S. L. Schreiber *et al.*, 2005 Single-nucleosome mapping of histone modifications in S. cerevisiae. PLoS Biol 3**:** e328.
Liu, X., D. A. Bushnell, D. Wang, G. Calero and R. D. Kornberg, 2010 Structure of an RNA polymerase II-TFIIB complex and the transcription initiation mechanism. Science 327**:** 206-209.

Liu, Y., L. Warfield, C. Zhang, J. Luo, J. Allen *et al.*, 2009 Phosphorylation of the transcription elongation factor Spt5 by yeast Bur1 kinase stimulates recruitment of the PAF complex. Mol Cell Biol 29**:** 4852-4863.

Livak, K. J., and T. D. Schmittgen, 2001 Analysis of relative gene expression data using real-time quantitative PCR and the 2(-Delta Delta C(T)) Method. Methods 25**:** 402-408.

Lu, X., M. D. Simon, J. V. Chodaparambil, J. C. Hansen, K. M. Shokat *et al.*, 2008 The effect of H3K79 dimethylation and H4K20 trimethylation on nucleosome and chromatin structure. Nat Struct Mol Biol 15**:** 1122-1124.

Luger, K., A. W. Mader, R. K. Richmond, D. F. Sargent and T. J. Richmond, 1997 Crystal structure of the nucleosome core particle at 2.8 A resolution. Nature 389**:** 251-260.

Mahat, D. B., H. Kwak, G. T. Booth, I. H. Jonkers, C. G. Danko *et al.*, 2016 Base-pair-resolution genome-wide mapping of active RNA polymerases using precision nuclear run-on (PRO-seq). Nat Protoc 11**:** 1455-1476.

Makde, R. D., J. R. England, H. P. Yennawar and S. Tan, 2010 Structure of RCC1 chromatin factor bound to the nucleosome core particle. Nature 467**:** 562-566.

Malik, I., C. Qiu, T. Snavely and C. D. Kaplan, 2017 Wide-ranging and unexpected consequences of altered Pol II catalytic activity in vivo. Nucleic Acids Res 45**:** 4431-4451.

Marazzi, I., J. S. Ho, J. Kim, B. Manicassamy, S. Dewell *et al.*, 2012 Suppression of the antiviral response by an influenza histone mimic. Nature 483**:** 428-433.

Marfella, C. G., and A. N. Imbalzano, 2007 The Chd family of chromatin remodelers. Mutat Res 618**:** 30-40.

Margueron, R., and D. Reinberg, 2011 The Polycomb complex PRC2 and its mark in life. Nature 469**:** 343-349.

Mason, P. B., and K. Struhl, 2003 The FACT complex travels with elongating RNA polymerase II and is important for the fidelity of transcriptional initiation in vivo. Mol Cell Biol 23**:** 8323-8333.

Mason, P. B., and K. Struhl, 2005 Distinction and relationship between elongation rate and processivity of RNA polymerase II in vivo. Mol Cell 17**:** 831-840.

Matsubara, K., N. Sano, T. Umehara and M. Horikoshi, 2007 Global analysis of functional surfaces of core histones with comprehensive point mutants. Genes Cells 12**:** 13-33.

Mattiroli, F., M. Uckelmann, D. D. Sahtoe, W. J. van Dijk and T. K. Sixma, 2014 The nucleosome acidic patch plays a critical role in RNF168-dependent ubiquitination of histone H2A. Nat Commun 5**:** 3291.

Mayekar, M. K., R. G. Gardner and K. M. Arndt, 2013 The recruitment of the Saccharomyces cerevisiae Paf1 complex to active genes requires a domain of Rtf1 that directly interacts with the Spt4-Spt5 complex. Mol Cell Biol 33**:** 3259-3273.

McGinty, R. K., R. C. Henrici and S. Tan, 2014 Crystal structure of the PRC1 ubiquitylation module bound to the nucleosome. Nature 514**:** 591-596.

McGinty, R. K., J. Kim, C. Chatterjee, R. G. Roeder and T. W. Muir, 2008 Chemically ubiquitylated histone H2B stimulates hDot1L-mediated intranucleosomal methylation. Nature 453**:** 812-816.

McGinty, R. K., M. Kohn, C. Chatterjee, K. P. Chiang, M. R. Pratt *et al.*, 2009 Structure-activity analysis of semisynthetic nucleosomes: mechanistic insights into the stimulation of Dot1L by ubiquitylated histone H2B. ACS Chem Biol 4**:** 958-968.

McGinty, R. K., and S. Tan, 2015 Nucleosome structure and function. Chem Rev 115**:** 2255-2273.
Mischo, H. E., and N. J. Proudfoot, 2013 Disengaging polymerase: terminating RNA polymerase II transcription in budding yeast. Biochim Biophys Acta 1829**:** 174-185.
Missra, A., and D. S. Gilmour, 2010 Interactions between DSIF (DRB sensitivity inducing factor), NELF (negative elongation factor), and the Drosophila RNA polymerase II transcription elongation complex. Proc Natl Acad Sci U S A 107**:** 11301-11306.
Mohan, M., H. M. Herz, Y. H. Takahashi, C. Lin, K. C. Lai *et al.*, 2010 Linking H3K79 trimethylation to Wnt signaling through a novel Dot1-containing complex (DotCom). Genes Dev 24**:** 574-589.
Moqtaderi, Z., and K. Struhl, 2008 Expanding the repertoire of plasmids for PCR-mediated epitope tagging in yeast. Yeast 25**:** 287-292.
Morgan, M. T., M. Haj-Yahya, A. E. Ringel, P. Bandi, A. Brik *et al.*, 2016 Structural basis for histone H2B deubiquitination by the SAGA DUB module. Science 351**:** 725-728.
Morillon, A., N. Karabetsou, J. O'Sullivan, N. Kent, N. Proudfoot *et al.*, 2003 Isw1 chromatin remodeling ATPase coordinates transcription elongation and termination by RNA polymerase II. Cell 115**:** 425-435.
Mueller, C. L., and J. A. Jaehning, 2002 Ctr9, Rtf1, and Leo1 are components of the Paf1/RNA polymerase II complex. Mol Cell Biol 22**:** 1971-1980.
Mueller, C. L., S. E. Porter, M. G. Hoffman and J. A. Jaehning, 2004 The Paf1 complex has functions independent of actively transcribing RNA polymerase II. Mol Cell 14**:** 447-456.
Murawska, M., and A. Brehm, 2011 CHD chromatin remodelers and the transcription cycle. Transcription 2**:** 244-253.
Muse, G. W., D. A. Gilchrist, S. Nechaev, R. Shah, J. S. Parker *et al.*, 2007 RNA polymerase is poised for activation across the genome. Nat Genet 39**:** 1507-1511.
Nagai, S., R. E. Davis, P. J. Mattei, K. P. Eagen and R. D. Kornberg, 2017 Chromatin potentiates transcription. Proc Natl Acad Sci U S A 114**:** 1536-1541.
Nakanishi, S., J. S. Lee, K. E. Gardner, J. M. Gardner, Y. H. Takahashi *et al.*, 2009 Histone H2BK123 monoubiquitination is the critical determinant for H3K4 and H3K79 trimethylation by COMPASS and Dot1. J Cell Biol 186**:** 371-377.
Nakanishi, S., B. W. Sanderson, K. M. Delventhal, W. D. Bradford, K. Staehling-Hampton *et al.*, 2008a A comprehensive library of histone mutants identifies nucleosomal residues required for H3K4 methylation. Nat Struct Mol Biol 15**:** 881-888.
Nakanishi, S., B. W. Sanderson, K. M. Delventhal, W. D. Bradford, K. Staehling-Hampton *et al.*, 2008b A comprehensive library of histone mutants identifies nucleosomal residues required for H3K4 methylation. Nat. Struct. Mol. Biol. 15**:** 881-888.
Nemec, C. M., F. Yang, J. M. Gilmore, C. Hintermair, Y. H. Ho *et al.*, 2017 Different phosphoisoforms of RNA polymerase II engage the Rtt103 termination factor in a structurally analogous manner. Proc Natl Acad Sci U S A 114**:** E3944-E3953.
Newey, P. J., M. R. Bowl and R. V. Thakker, 2009 Parafibromin--functional insights. J Intern Med 266**:** 84-98.
Ng, H. H., S. Dole and K. Struhl, 2003 The Rtf1 component of the Paf1 transcriptional elongation complex is required for ubiquitination of histone H2B. J Biol Chem 278**:** 33625-33628.

Ng, H. H., Q. Feng, H. Wang, H. Erdjument-Bromage, P. Tempst *et al.*, 2002a Lysine methylation within the globular domain of histone H3 by Dot1 is important for telomeric silencing and Sir protein association. Genes Dev 16**:** 1518-1527.

Ng, H. H., R. M. Xu, Y. Zhang and K. Struhl, 2002b Ubiquitination of histone H2B by Rad6 is required for efficient Dot1-mediated methylation of histone H3 lysine 79. J Biol Chem 277**:** 34655-34657.

Nguyen, A. T., B. Xiao, R. L. Neppl, E. M. Kallin, J. Li *et al.*, 2011 DOT1L regulates dystrophin expression and is critical for cardiac function. Genes Dev 25**:** 263-274.

Nguyen, A. T., and Y. Zhang, 2011 The diverse functions of Dot1 and H3K79 methylation. Genes Dev 25**:** 1345-1358.

Nguyen, C. T., A. Langenbacher, M. Hsieh and J. N. Chen, 2010 The PAF1 complex component Leo1 is essential for cardiac and neural crest development in zebrafish. Dev Biol 341**:** 167-175.

Nishino, Y., M. Eltsov, Y. Joti, K. Ito, H. Takata *et al.*, 2012 Human mitotic chromosomes consist predominantly of irregularly folded nucleosome fibres without a 30-nm chromatin structure. EMBO J 31**:** 1644-1653.

Nordick, K., M. G. Hoffman, J. L. Betz and J. A. Jaehning, 2008 Direct interactions between the Paf1 complex and a cleavage and polyadenylation factor are revealed by dissociation of Paf1 from RNA polymerase II. Eukaryot Cell 7**:** 1158-1167.

Nudler, E., 2012 RNA polymerase backtracking in gene regulation and genome instability. Cell 149**:** 1438-1445.

Oh, S., S. Park and S. van Nocker, 2008 Genic and global functions for Paf1C in chromatin modification and gene expression in Arabidopsis. PLoS Genet 4**:** e1000077.

Olins, A. L., and D. E. Olins, 1974 Spheroid chromatin units (v bodies). Science 183**:** 330-332.

Olins, D. E., and A. L. Olins, 2003 Chromatin history: our view from the bridge. Nat Rev Mol Cell Biol 4**:** 809-814.

Orphanides, G., G. LeRoy, C. H. Chang, D. S. Luse and D. Reinberg, 1998 FACT, a factor that facilitates transcript elongation through nucleosomes. Cell 92**:** 105-116.

Owen-Hughes, T., and T. Gkikopoulos, 2012 Making sense of transcribing chromatin. Curr Opin Cell Biol 24**:** 296-304.

Ozer, J., K. Mitsouras, D. Zerby, M. Carey and P. M. Lieberman, 1998 Transcription factor IIA derepresses TATA-binding protein (TBP)-associated factor inhibition of TBP-DNA binding. J Biol Chem 273**:** 14293-14300.

Pavri, R., B. Zhu, G. Li, P. Trojer, S. Mandal *et al.*, 2006 Histone H2B monoubiquitination functions cooperatively with FACT to regulate elongation by RNA polymerase II. Cell 125**:** 703-717.

Penheiter, K. L., T. M. Washburn, S. E. Porter, M. G. Hoffman and J. A. Jaehning, 2005 A posttranscriptional role for the yeast Paf1-RNA polymerase II complex is revealed by identification of primary targets. Mol Cell 20**:** 213-223.

Perales, R., and D. Bentley, 2009 "Cotranscriptionality": the transcription elongation complex as a nexus for nuclear transactions. Mol Cell 36**:** 178-191.

Pinto, P. A., T. Henriques, M. O. Freitas, T. Martins, R. G. Domingues *et al.*, 2011 RNA polymerase II kinetics in polo polyadenylation signal selection. EMBO J 30**:** 2431-2444.

Piro, A. S., M. K. Mayekar, M. H. Warner, C. P. Davis and K. M. Arndt, 2012 Small region of Rtf1 protein can substitute for complete Paf1 complex in facilitating global histone H2B ubiquitylation in yeast. Proc Natl Acad Sci U S A 109**:** 10837-10842.

Pokholok, D. K., C. T. Harbison, S. Levine, M. Cole, N. M. Hannett *et al.*, 2005 Genome-wide map of nucleosome acetylation and methylation in yeast. Cell 122**:** 517-527.
Porrua, O., and D. Libri, 2015 Transcription termination and the control of the transcriptome: why, where and how to stop. Nat Rev Mol Cell Biol 16**:** 190-202.
Portela, A., and M. Esteller, 2010 Epigenetic modifications and human disease. Nat Biotechnol 28**:** 1057-1068.
Portz, B., F. Lu, E. B. Gibbs, J. E. Mayfield, M. Rachel Mehaffey *et al.*, 2017 Structural heterogeneity in the intrinsically disordered RNA polymerase II C-terminal domain. Nat Commun 8**:** 15231.
Powell, D. W., C. M. Weaver, J. L. Jennings, K. J. McAfee, Y. He *et al.*, 2004 Cluster analysis of mass spectrometry data reveals a novel component of SAGA. Mol Cell Biol 24**:** 7249-7259.
Price, D. H., 2000 P-TEFb, a cyclin-dependent kinase controlling elongation by RNA polymerase II. Mol Cell Biol 20**:** 2629-2634.
Pruneski, J. A., S. J. Hainer, K. O. Petrov and J. A. Martens, 2011 The Paf1 complex represses SER3 transcription in Saccharomyces cerevisiae by facilitating intergenic transcription-dependent nucleosome occupancy of the SER3 promoter. Eukaryot Cell 10**:** 1283-1294.
Pugh, B. F., and R. Tjian, 1991 Transcription from a TATA-less promoter requires a multisubunit TFIID complex. Genes Dev 5**:** 1935-1945.
Qiu, H., C. Hu, N. A. Gaur and A. G. Hinnebusch, 2012 Pol II CTD kinases Bur1 and Kin28 promote Spt5 CTR-independent recruitment of Paf1 complex. EMBO J 31**:** 3494-3505.
Ransom, M., B. K. Dennehey and J. K. Tyler, 2010 Chaperoning histones during DNA replication and repair. Cell 140**:** 183-195.
Rhee, H. S., A. R. Bataille, L. Zhang and B. F. Pugh, 2014 Subnucleosomal structures and nucleosome asymmetry across a genome. Cell 159**:** 1377-1388.
Rhee, H. S., and B. F. Pugh, 2011 Comprehensive genome-wide protein-DNA interactions detected at single-nucleotide resolution. Cell 147**:** 1408-1419.
Rhee, H. S., and B. F. Pugh, 2012 Genome-wide structure and organization of eukaryotic pre-initiation complexes. Nature 483**:** 295-301.
Robert, F., M. Douziech, D. Forget, J. M. Egly, J. Greenblatt *et al.*, 1998 Wrapping of promoter DNA around the RNA polymerase II initiation complex induced by TFIIF. Mol Cell 2**:** 341-351.
Robzyk, K., J. Recht and M. A. Osley, 2000 Rad6-dependent ubiquitination of histone H2B in yeast. Science 287**:** 501-504.
Roeder, R. G., and W. J. Rutter, 1969 Multiple forms of DNA-dependent RNA polymerase in eukaryotic organisms. Nature 224**:** 234-237.
Rondon, A. G., M. Gallardo, M. Garcia-Rubio and A. Aguilera, 2004 Molecular evidence indicating that the yeast PAF complex is required for transcription elongation. EMBO Rep 5**:** 47-53.
Rondon, A. G., H. E. Mischo, J. Kawauchi and N. J. Proudfoot, 2009 Fail-safe transcriptional termination for protein-coding genes in S. cerevisiae. Mol Cell 36**:** 88-98.
Rozenblatt-Rosen, O., T. Nagaike, J. M. Francis, S. Kaneko, K. A. Glatt *et al.*, 2009 The tumor suppressor Cdc73 functionally associates with CPSF and CstF 3' mRNA processing factors. Proc Natl Acad Sci U S A 106**:** 755-760.
Rusche, L. N., A. L. Kirchmaier and J. Rine, 2003 The establishment, inheritance, and function of silenced chromatin in *Saccharomyces cerevisiae*. Annu Rev Biochem 72**:** 481-516.

Sainsbury, S., C. Bernecky and P. Cramer, 2015 Structural basis of transcription initiation by RNA polymerase II. Nat Rev Mol Cell Biol 16**:** 129-143.
Santos-Rosa, H., A. Kirmizis, C. Nelson, T. Bartke, N. Saksouk *et al.*, 2009 Histone H3 tail clipping regulates gene expression. Nat Struct Mol Biol 16**:** 17-22.
Sayou, C., G. Millan-Zambrano, H. Santos-Rosa, E. Petfalski, S. Robson *et al.*, 2017 RNA binding by the histone methyltransferases Set1 and Set2. Mol Cell Biol.
Schuller, R., I. Forne, T. Straub, A. Schreieck, Y. Texier *et al.*, 2016 Heptad-Specific Phosphorylation of RNA Polymerase II CTD. Mol Cell 61**:** 305-314.
Schulze, J. M., T. Hentrich, S. Nakanishi, A. Gupta, E. Emberly *et al.*, 2011 Splitting the task: Ubp8 and Ubp10 deubiquitinate different cellular pools of H2BK123. Genes Dev 25**:** 2242-2247.
Schwabish, M. A., and K. Struhl, 2004 Evidence for eviction and rapid deposition of histones upon transcriptional elongation by RNA polymerase II. Mol Cell Biol 24**:** 10111-10117.
Schwalb, B., M. Michel, B. Zacher, K. Fruhauf, C. Demel *et al.*, 2016 TT-seq maps the human transient transcriptome. Science 352**:** 1225-1228.
Schwartzentruber, J., A. Korshunov, X. Y. Liu, D. T. Jones, E. Pfaff *et al.*, 2012 Driver mutations in histone H3.3 and chromatin remodelling genes in paediatric glioblastoma. Nature 482**:** 226-231.
Segala, G., M. A. Bennesch, D. P. Pandey, N. Hulo and D. Picard, 2016 Monoubiquitination of Histone H2B Blocks Eviction of Histone Variant H2A.Z from Inducible Enhancers. Mol Cell 64**:** 334-346.
Shandilya, J., and S. G. Roberts, 2012 The transcription cycle in eukaryotes: from productive initiation to RNA polymerase II recycling. Biochim Biophys Acta 1819**:** 391-400.
Sheldon, K. E., D. M. Mauger and K. M. Arndt, 2005 A Requirement for the Saccharomyces cerevisiae Paf1 complex in snoRNA 3' end formation. Mol Cell 20**:** 225-236.
Shema, E., D. Jones, N. Shoresh, L. Donohue, O. Ram *et al.*, 2016 Single-molecule decoding of combinatorially modified nucleosomes. Science 352**:** 717-721.
Shema, E., I. Tirosh, Y. Aylon, J. Huang, C. Ye *et al.*, 2008 The histone H2B-specific ubiquitin ligase RNF20/hBRE1 acts as a putative tumor suppressor through selective regulation of gene expression. Genes Dev 22**:** 2664-2676.
Shetty, A., S. P. Kallgren, C. Demel, K. C. Maier, D. Spatt *et al.*, 2017 Spt5 Plays Vital Roles in the Control of Sense and Antisense Transcription Elongation. Mol Cell 66**:** 77-88 e75.
Shi, X., A. Finkelstein, A. J. Wolf, P. A. Wade, Z. F. Burton *et al.*, 1996 Paf1p, an RNA polymerase II-associated factor in Saccharomyces cerevisiae, may have both positive and negative roles in transcription. Mol Cell Biol 16**:** 669-676.
Shilatifard, A., W. S. Lane, K. W. Jackson, R. C. Conaway and J. W. Conaway, 1996 An RNA polymerase II elongation factor encoded by the human ELL gene. Science 271**:** 1873-1876.
Shirra, M. K., S. E. Rogers, D. E. Alexander and K. M. Arndt, 2005 The Snf1 protein kinase and Sit4 protein phosphatase have opposing functions in regulating TATA-binding protein association with the *Saccharomyces cerevisiae INO1* promoter. Genetics 169**:** 1957-1972.
Shogren-Knaak, M., H. Ishii, J. M. Sun, M. J. Pazin, J. R. Davie *et al.*, 2006 Histone H4-K16 acetylation controls chromatin structure and protein interactions. Science 311**:** 844-847.

Shukla, M. S., S. H. Syed, D. Goutte-Gattat, J. L. Richard, F. Montel *et al.*, 2011 The docking domain of histone H2A is required for H1 binding and RSC-mediated nucleosome remodeling. Nucleic Acids Res 39**:** 2559-2570.

Simic, R., D. L. Lindstrom, H. G. Tran, K. L. Roinick, P. J. Costa *et al.*, 2003 Chromatin remodeling protein Chd1 interacts with transcription elongation factors and localizes to transcribed genes. EMBO J 22**:** 1846-1856.

Sims, R. J., 3rd, R. Belotserkovskaya and D. Reinberg, 2004 Elongation by RNA polymerase II: the short and long of it. Genes Dev 18**:** 2437-2468.

Sims, R. J., 3rd, C. F. Chen, H. Santos-Rosa, T. Kouzarides, S. S. Patel *et al.*, 2005 Human but not yeast CHD1 binds directly and selectively to histone H3 methylated at lysine 4 via its tandem chromodomains. J Biol Chem 280**:** 41789-41792.

Singer, M. S., A. Kahana, A. J. Wolf, L. L. Meisinger, S. E. Peterson *et al.*, 1998 Identification of high-copy disruptors of telomeric silencing in Saccharomyces cerevisiae. Genetics 150**:** 613-632.

Skalska, L., M. Beltran-Nebot, J. Ule and R. G. Jenner, 2017 Regulatory feedback from nascent RNA to chromatin and transcription. Nat Rev Mol Cell Biol 18**:** 331-337.

Smolle, M., and J. L. Workman, 2013 Transcription-associated histone modifications and cryptic transcription. Biochim Biophys Acta 1829**:** 84-97.

Soares, L. M., M. Radman-Livaja, S. G. Lin, O. J. Rando and S. Buratowski, 2014 Feedback control of Set1 protein levels is important for proper H3K4 methylation patterns. Cell Rep 6**:** 961-972.

Song, F., P. Chen, D. Sun, M. Wang, L. Dong *et al.*, 2014 Cryo-EM study of the chromatin fiber reveals a double helix twisted by tetranucleosomal units. Science 344**:** 376-380.

Song, Y. H., and S. H. Ahn, 2010 A Bre1-associated protein, large 1 (Lge1), promotes H2B ubiquitylation during the early stages of transcription elongation. J Biol Chem 285**:** 2361-2367.

Squazzo, S. L., P. J. Costa, D. L. Lindstrom, K. E. Kumer, R. Simic *et al.*, 2002a The Paf1 complex physically and functionally associates with transcription elongation factors in vivo. EMBO J 21**:** 1764-1774.

Squazzo, S. L., P. J. Costa, D. L. Lindstrom, K. E. Kumer, R. Simic *et al.*, 2002b The Paf1 complex physically and functionally associates with transcription elongation factors in vivo. EMBO J. 21**:** 1764-1774.

Steinmetz, E. J., N. K. Conrad, D. A. Brow and J. L. Corden, 2001 RNA-binding protein Nrd1 directs poly(A)-independent 3'-end formation of RNA polymerase II transcripts. Nature 413**:** 327-331.

Steinmetz, E. J., S. B. Ng, J. P. Cloute and D. A. Brow, 2006a cis- and trans-Acting determinants of transcription termination by yeast RNA polymerase II. Mol Cell Biol 26**:** 2688-2696.

Steinmetz, E. J., C. L. Warren, J. N. Kuehner, B. Panbehi, A. Z. Ansari *et al.*, 2006b Genome-wide distribution of yeast RNA polymerase II and its control by Sen1 helicase. Mol Cell 24**:** 735-746.

Stolinski, L. A., D. M. Eisenmann and K. M. Arndt, 1997 Identification of RTF1, a novel gene important for TATA site selection by TATA box-binding protein in Saccharomyces cerevisiae. Mol Cell Biol 17**:** 4490-4500.

Strahl, B. D., and C. D. Allis, 2000 The language of covalent histone modifications. Nature 403**:** 41-45.

Strom, A. R., A. V. Emelyanov, M. Mir, D. V. Fyodorov, X. Darzacq *et al.*, 2017 Phase separation drives heterochromatin domain formation. Nature.

Struhl, K., and E. Segal, 2013 Determinants of nucleosome positioning. Nat Struct Mol Biol 20**:** 267-273.

Stuwe, T., M. Hothorn, E. Lejeune, V. Rybin, M. Bortfeld *et al.*, 2008 The FACT Spt16 "peptidase" domain is a histone H3-H4 binding module. Proc Natl Acad Sci U S A 105**:** 8884-8889.

Suh, H., S. B. Ficarro, U. B. Kang, Y. Chun, J. A. Marto *et al.*, 2016 Direct Analysis of Phosphorylation Sites on the Rpb1 C-Terminal Domain of RNA Polymerase II. Mol Cell 61**:** 297-304.

Suh, H., D. Z. Hazelbaker, L. M. Soares and S. Buratowski, 2013 The C-terminal domain of Rpb1 functions on other RNA polymerase II subunits. Mol Cell 51**:** 850-858.

Sun, Z. W., and C. D. Allis, 2002 Ubiquitination of histone H2B regulates H3 methylation and gene silencing in yeast. Nature 418**:** 104-108.

Suraweera, A., Y. Lim, R. Woods, G. W. Birrell, T. Nasim *et al.*, 2009 Functional role for senataxin, defective in ataxia oculomotor apraxia type 2, in transcriptional regulation. Hum Mol Genet 18**:** 3384-3396.

Swanson, M. S., E. A. Malone and F. Winston, 1991 *SPT5*, an essential gene important for normal transcription in *Saccharomyces cerevisiae*, encodes an acidic nuclear protein with a carboxy-terminal repeat. Mol Cell Biol 11**:** 4286.

Tan, S., R. C. Conaway and J. W. Conaway, 1995 Dissection of transcription factor TFIIF functional domains required for initiation and elongation. Proc Natl Acad Sci U S A 92**:** 6042-6046.

Taverna, S. D., S. Ilin, R. S. Rogers, J. C. Tanny, H. Lavender *et al.*, 2006 Yng1 PHD finger binding to H3 trimethylated at K4 promotes NuA3 HAT activity at K14 of H3 and transcription at a subset of targeted ORFs. Mol Cell 24**:** 785-796.

Terzi, N., L. S. Churchman, L. Vasiljeva, J. Weissman and S. Buratowski, 2011 H3K4 trimethylation by Set1 promotes efficient termination by the Nrd1-Nab3-Sen1 pathway. Mol Cell Biol 31**:** 3569-3583.

Thorne, A. W., P. Sautiere, G. Briand and C. Crane-Robinson, 1987 The structure of ubiquitinated histone H2B. EMBO J 6**:** 1005-1010.

Thornton, J. L., G. H. Westfield, Y. H. Takahashi, M. Cook, X. Gao *et al.*, 2014 Context dependency of Set1/COMPASS-mediated histone H3 Lys4 trimethylation. Genes Dev 28**:** 115-120.

Tomson, B. N., and K. M. Arndt, 2012 The many roles of the conserved eukaryotic Paf1 complex in regulating transcription, histone modifications, and disease states. Biochim Biophys Acta.

Tomson, B. N., and K. M. Arndt, 2013 The many roles of the conserved eukaryotic Paf1 complex in regulating transcription, histone modifications, and disease states. Biochim Biophys Acta 1829**:** 116-126.

Tomson, B. N., E. M. Crisucci, L. E. Heisler, M. Gebbia, C. Nislow *et al.*, 2013 Effects of the Paf1 complex and histone modifications on snoRNA 3'-end formation reveal broad and locus-specific regulation. Mol Cell Biol 33**:** 170-182.

Tomson, B. N., C. P. Davis, M. H. Warner and K. M. Arndt, 2011 Identification of a role for histone H2B ubiquitylation in noncoding RNA 3'-end formation through mutational analysis of Rtf1 in Saccharomyces cerevisiae. Genetics 188**:** 273-289.

Tsunaka, Y., Y. Fujiwara, T. Oyama, S. Hirose and K. Morikawa, 2016 Integrated molecular mechanism directing nucleosome reorganization by human FACT. Genes Dev 30**:** 673-686.

Turco, E., L. D. Gallego, M. Schneider and A. Kohler, 2015 Monoubiquitination of histone H2B is intrinsic to the Bre1 RING domain-Rad6 interaction and augmented by a second Rad6-binding site on Bre1. J Biol Chem 290**:** 5298-5310.

Ursic, D., K. Chinchilla, J. S. Finkel and M. R. Culbertson, 2004 Multiple protein/protein and protein/RNA interactions suggest roles for yeast DNA/RNA helicase Sen1p in transcription, transcription-coupled DNA repair and RNA processing. Nucleic Acids Res 32**:** 2441-2452.

Van Oss, S. B., M. K. Shirra, A. R. Bataille, A. D. Wier, K. Yen *et al.*, 2016 The Histone Modification Domain of Paf1 Complex Subunit Rtf1 Directly Stimulates H2B Ubiquitylation through an Interaction with Rad6. Mol Cell 64**:** 815-825.

VanDemark, A. P., H. Xin, L. McCullough, R. Rawlins, S. Bentley *et al.*, 2008 Structural and functional analysis of the Spt16p N-terminal domain reveals overlapping roles of yFACT subunits. J Biol Chem 283**:** 5058-5068.

Vasiljeva, L., M. Kim, H. Mutschler, S. Buratowski and A. Meinhart, 2008 The Nrd1-Nab3-Sen1 termination complex interacts with the Ser5-phosphorylated RNA polymerase II C-terminal domain. Nat Struct Mol Biol 15**:** 795-804.

Veloso, A., K. S. Kirkconnell, B. Magnuson, B. Biewen, M. T. Paulsen *et al.*, 2014 Rate of elongation by RNA polymerase II is associated with specific gene features and epigenetic modifications. Genome Res 24**:** 896-905.

Viktorovskaya, O. V., F. D. Appling and D. A. Schneider, 2011 Yeast transcription elongation factor Spt5 associates with RNA polymerase I and RNA polymerase II directly. J Biol Chem 286**:** 18825-18833.

Vogler, C., C. Huber, T. Waldmann, R. Ettig, L. Braun *et al.*, 2010 Histone H2A C-terminus regulates chromatin dynamics, remodeling, and histone H1 binding. PLoS Genet 6**:** e1001234.

Voigt, P., G. LeRoy, W. J. Drury, 3rd, B. M. Zee, J. Son *et al.*, 2012 Asymmetrically modified nucleosomes. Cell 151**:** 181-193.

Wada, T., T. Takagi, Y. Yamaguchi, A. Ferdous, T. Imai *et al.*, 1998 DSIF, a novel transcription elongation factor that regulates RNA polymerase II processivity, is composed of human Spt4 and Spt5 homologs. Genes Dev 12**:** 343-356.

Warner, M. H., K. L. Roinick and K. M. Arndt, 2007 Rtf1 is a multifunctional component of the Paf1 complex that regulates gene expression by directing cotranscriptional histone modification. Mol Cell Biol 27**:** 6103-6115.

White, C. L., R. K. Suto and K. Luger, 2001 Structure of the yeast nucleosome core particle reveals fundamental changes in internucleosome interactions. EMBO J 20**:** 5207-5218.

Wier, A. D., M. K. Mayekar, A. Heroux, K. M. Arndt and A. P. VanDemark, 2013 Structural basis for Spt5-mediated recruitment of the Paf1 complex to chromatin. Proc Natl Acad Sci U S A 110**:** 17290-17295.

Wilkins, B. J., N. A. Rall, Y. Ostwal, T. Kruitwagen, K. Hiragami-Hamada *et al.*, 2014 A cascade of histone modifications induces chromatin condensation in mitosis. Science 343**:** 77-80.

Winkler, D. D., and K. Luger, 2011 The histone chaperone FACT: structural insights and mechanisms for nucleosome reorganization. J Biol Chem 286**:** 18369-18374.

Winston, F., C. Dollard and S. L. Ricupero-Hovasse, 1995 Construction of a set of convenient Saccharomyces cerevisiae strains that are isogenic to S288C. Yeast 11**:** 53-55.
Wood, A., N. J. Krogan, J. Dover, J. Schneider, J. Heidt *et al.*, 2003a Bre1, an E3 ubiquitin ligase required for recruitment and substrate selection of Rad6 at a promoter. Mol Cell 11**:** 267-274.
Wood, A., J. Schneider, J. Dover, M. Johnston and A. Shilatifard, 2003b The Paf1 complex is essential for histone monoubiquitination by the Rad6-Bre1 complex, which signals for histone methylation by COMPASS and Dot1p. J Biol Chem 278**:** 34739-34742.
Wood, A., J. Schneider, J. Dover, M. Johnston and A. Shilatifard, 2005 The Bur1/Bur2 complex is required for histone H2B monoubiquitination by Rad6/Bre1 and histone methylation by COMPASS. Mol Cell 20**:** 589-599.
Wozniak, G. G., and B. D. Strahl, 2014 Catalysis-dependent stabilization of Bre1 fine-tunes histone H2B ubiquitylation to regulate gene transcription. Genes Dev 28**:** 1647-1652.
Wu, L., L. Li, B. Zhou, Z. Qin and Y. Dou, 2014 H2B ubiquitylation promotes RNA Pol II processivity via PAF1 and pTEFb. Mol Cell 54**:** 920-931.
Wu, L., B. M. Zee, Y. Wang, B. A. Garcia and Y. Dou, 2011 The RING finger protein MSL2 in the MOF complex is an E3 ubiquitin ligase for H2B K34 and is involved in crosstalk with H3 K4 and K79 methylation. Mol Cell 43**:** 132-144.
Wyrick, J. J., M. N. Kyriss and W. B. Davis, 2012 Ascending the nucleosome face: recognition and function of structured domains in the histone H2A-H2B dimer. Biochim Biophys Acta 1819**:** 892-901.
Xiao, T., C. F. Kao, N. J. Krogan, Z. W. Sun, J. F. Greenblatt *et al.*, 2005 Histone H2B ubiquitylation is associated with elongating RNA polymerase II. Mol Cell Biol 25**:** 637-651.
Xie, X., T. Kokubo, S. L. Cohen, U. A. Mirza, A. Hoffmann *et al.*, 1996 Structural similarity between TAFs and the heterotetrameric core of the histone octamer. Nature 380**:** 316-322.
Xin, H., S. Takahata, M. Blanksma, L. McCullough, D. J. Stillman *et al.*, 2009 yFACT induces global accessibility of nucleosomal DNA without H2A-H2B displacement. Mol Cell 35**:** 365-376.
Yang, C., and A. S. Ponticelli, 2012 Evidence that RNA polymerase II and not TFIIB is responsible for the difference in transcription initiation patterns between Saccharomyces cerevisiae and Schizosaccharomyces pombe. Nucleic Acids Res 40**:** 6495-6507.
Yang, J., X. Zhang, J. Feng, H. Leng, S. Li *et al.*, 2016a The Histone Chaperone FACT Contributes to DNA Replication-Coupled Nucleosome Assembly. Cell Rep 14**:** 1128-1141.
Yang, Y., W. Li, M. Hoque, L. Hou, S. Shen *et al.*, 2016b PAF Complex Plays Novel Subunit-Specific Roles in Alternative Cleavage and Polyadenylation. PLoS Genet 12**:** e1005794.
Yu, M., W. Yang, T. Ni, Z. Tang, T. Nakadai *et al.*, 2015 RNA polymerase II-associated factor 1 regulates the release and phosphorylation of paused RNA polymerase II. Science 350**:** 1383-1386.
Yuen, B. T., and P. S. Knoepfler, 2013 Histone H3.3 mutations: a variant path to cancer. Cancer Cell 24**:** 567-574.
Yuryev, A., M. Patturajan, Y. Litingtung, R. V. Joshi, C. Gentile *et al.*, 1996 The C-terminal domain of the largest subunit of RNA polymerase II interacts with a novel set of serine/arginine-rich proteins. Proc Natl Acad Sci U S A 93**:** 6975-6980.

Zaborowska, J., S. Egloff and S. Murphy, 2016 The pol II CTD: new twists in the tail. Nat Struct Mol Biol 23**:** 771-777.
Zentner, G. E., and S. Henikoff, 2013 Regulation of nucleosome dynamics by histone modifications. Nat Struct Mol Biol 20**:** 259-266.
Zentner, G. E., T. Tsukiyama and S. Henikoff, 2013 ISWI and CHD chromatin remodelers bind promoters but act in gene bodies. PLoS Genet 9**:** e1003317.
Zhang, F., and X. Yu, 2011 WAC, a functional partner of RNF20/40, regulates histone H2B ubiquitination and gene transcription. Mol Cell 41**:** 384-397.
Zhang, K., J. M. Haversat and J. Mager, 2013 CTR9/PAF1c regulates molecular lineage identity, histone H3K36 trimethylation and genomic imprinting during preimplantation development. Dev Biol 383**:** 15-27.
Zheng, S., J. J. Wyrick and J. C. Reese, 2010 Novel trans-tail regulation of H2B ubiquitylation and H3K4 methylation by the N terminus of histone H2A. Mol Cell Biol 30**:** 3635-3645.
Zhou, K., W. H. Kuo, J. Fillingham and J. F. Greenblatt, 2009 Control of transcriptional elongation and cotranscriptional histone modification by the yeast BUR kinase substrate Spt5. Proc Natl Acad Sci U S A 106**:** 6956-6961.
Zhou, L., M. T. Holt, N. Ohashi, A. Zhao, M. M. Muller *et al.*, 2016 Evidence that ubiquitylated H2B corrals hDot1L on the nucleosomal surface to induce H3K79 methylation. Nat Commun 7**:** 10589.
Zhu, B., S. S. Mandal, A. D. Pham, Y. Zheng, H. Erdjument-Bromage *et al.*, 2005 The human PAF complex coordinates transcription with events downstream of RNA synthesis. Genes Dev 19**:** 1668-1673.